Natural Environment Research Council

BRITISH GEOLOGICAL SURVEY

Mineral Reconnaissance Programme Report

D. Slater
Programme Manager
Mineral Reconnaissance Programme
British Geological Survey
154 Clerkenwell Road
London EC1R 5DU

No. 78

Exploration for porphyry-style copper mineralisation near Llandeloy, southwest Dyfed

BRITISH GEOLOGICAL SURVEY
Natural Environment Research Council

BRITISH GEOLOGICAL SURVEY
Natural Environment Research Council

Mineral Reconnaissance Programme

Report No. 78

Exploration for porphyry-style copper mineralisation near Llandeloy, southwest Dyfed

Geology
P. M. Allen, BSc, PhD

Geochemistry
D. C. Cooper, BSc, PhD
P. Bide, BSc
D. G. Cameron, BSc

Geophysics
M. E. Parker, BSc

Mineralogy
H. W. Haslam, MA, PhD, MIMM
G. D. Easterbrook, BSc
I. R. Basham, BSc, PhD, MIMM

A report prepared for the Department of Trade and Industry

Keyworth, Nottinghamshire . 1985

Mineral Reconnaissance Programme Reports

33 Mineral investigations at Carrock Fell, Cumbria. Part 1—Geophysical survey

34 Results of a gravity survey of the south-west margin of Dartmoor, Devon

35 Geophysical investigation of chromite-bearing ultrabasic rocks in the Baltasound–Hagdale area, Unst, Shetland Islands

36 An appraisal of the VLF ground resistivity technique as an aid to mineral exploration

37 Compilation of stratabound mineralisation in the Scottish Caledonides

38 Geophysical evidence for a concealed eastern extension of the Tanygrisiau microgranite and its possible relationship, to mineralisation

39 Copper-bearing intrusive rocks at Cairngarroch Bay, south-west Scotland

40 Stratabound barium-zinc mineralisation in Dalradian schist near Aberfeldy, Scotland; Final report

41 Metalliferous mineralisation near Lutton, Ivybridge, Devon

42 Mineral exploration in the area around Culvennan Fell, Kirkcowan, south-western Scotland

43 Disseminated copper-molybdenum mineralisation near Ballachulish, Highland Region

44 Reconnaissance geochemical maps of parts of south Devon and Cornwall

45 Mineral investigations near Bodmin, Cornwall. Part 2—New uranium, tin and copper occurrence in the Tremayne area of St Columb Major

46 Gold mineralisation at the southern margin of the Loch Doon granitoid complex, south-west Scotland

47 An airborne geophysical survey of the Whin Sill between Haltwhistle and Scots' Gap, south Northumberland

48 Mineral investigations near Bodmin, Cornwall. Part 3—The Mulberry and Wheal Prosper area

49 Seismic and gravity surveys over the concealed granite ridge at Bosworgy, Cornwall

50 Geochemical drainage survey of central Argyll, Scotland

51 A reconnaissance geochemical survey of Anglesey

52 Miscellaneous investigations on mineralisation in sedimentary rocks

53 Investigation of polymetallic mineralisation in Lower Devonian volcanics near Alva, central Scotland

54 Copper mineralisation near Middleton Tyas, North Yorkshire

55 Mineral exploration in the area of the Fore Burn igneous complex, south-western Scotland

56 Geophysical and geochemical investigations over the Long Rake, Haddon Fields, Derbyshire

57 Mineral exploration in the Ravenstonedale area, Cumbria

58 Investigation of small intrusions in southern Scotland

59 Stratabound arsenic and vein antimony mineralisation in Silurian greywackes at Glendinning, south Scotland

60 Mineral investigations at Carrock Fell, Cumbria. Part 2—Geochemical investigations

61 Mineral reconnaissance at the Highland Boundary with special reference to the Loch Lomond and Aberfoyle areas

62 Mineral reconnaissance in the Northumberland Trough

63 Exploration for volcanogenic sulphide mineralisation at Benglog, North Wales

64 A mineral reconnaissance of the Dent–Ingleton area of the Askrigg Block, northern England

65 Geophysical investigations in Swaledale, North Yorkshire

66 Mineral reconnaissance surveys in the Craven Basin

67 Baryte and copper mineralisation in the Renfrewshire Hills, central Scotland

68 Polymetallic mineralisation in Carboniferous rocks at Hilderston, near Bathgate, central Scotland

69 Base metal mineralisation associated with Ordovician shales in south-west Scotland

70 Regional geochemical and geophysical surveys in the Berwyn Dome and adjacent areas, North Wales

71 A regional geochemical soil investigation of the Carboniferous Limestone areas south of Kendal (south Cumbria and north Lancashire)

72 A geochemical drainage survey of the Preseli Hills, south-west Dyfed, Wales

73 Platinum-group element mineralisation in the Unst ophiolite, Shetland

74 A reconnaissance geochemical drainage survey of the Harlech Dome, North Wales

75 Geophysical surveys in part of the Halkyn–Minera mining district, north-east Wales

76 Disseminated molybdenum mineralisation in the Etive plutonic complex in the western Highlands of Scotland

77 Follow-up mineral reconnaissance investigations in the Northumberland Trough

78 Exploration for porphyry-style copper mineralisation near Llandeloy, southwest Dyfed

On 1 January 1984 the Institute of Geological Sciences was renamed the British Geological Survey. It continues to carry out the geological survey of Great Britain and Northern Ireland (the latter as an agency service for the government of Northern Ireland), and of the surrounding continental shelf, as well as its basic research projects; it also undertakes programmes of British technical aid in geology in developing countries as arranged by the Overseas Development Administration.

The British Geological Survey is a component body of the Natural Environment Research Council.

Bibliographic reference
Allen, P. M., Cooper, D. C., and **others.** 1985. Exploration for porphyry-style copper mineralisation near Llandeloy, southwest Dyfed. *Mineral Reconnaissance Programme Rep. Br. Geol. Surv.*, No. 78.

CONTENTS

TABLES

SUMMARY

Geological, geochemical and geophysical surveys followed by drilling in the area around Llandeloy, south-west Dyfed, have located disseminated copper mineralisation of porphyry type associated with intermediate intrusive rocks masked by thick overburden.

Intermediate intrusive rocks in the area were selected for investigation as potential hosts for disseminated copper mineralisation on the basis of the known geology and tectonic setting. An initial assessment of the area involved revising the geological maps, analysing rocks from surface exposures, studying available geophysical data and carrying out a stream sediment survey in the catchment of the River Solfach. This work revealed the presence of weak polymetallic sulphide mineralisation associated with the margin of a tonalitic intrusion at Middle Mill. In view of the very poor exposure, more detailed geochemical and geophysical surveys were carried out across the two areas underlain by intrusive rocks of dioritic or tonalitic composition.

At Middle Mill six traverse lines, spaced 300 m apart and totalling 10.5 km in length, were surveyed by IP, VLF-EM and magnetic methods. Soil samples, subsequently analysed for Cu, Pb and Zn were collected at 25 m intervals. Few anomalies were located. Most of those found could be ascribed to artificial sources and it was concluded that no substantial body of disseminated copper mineralisation was present at or near the surface in the area. The mineralisation found in Middle Mill quarry is thought to be minor, epigenetic mineralisation, associated with the intrusion.

At Llandeloy 13 traverse lines spaced 600 m apart and covering an area of 12 km^2 were surveyed by IP, VLF-EM, magnetic and radiometric methods. Soil samples were collected along these lines at 50 m intervals and analysed for Cu, Pb and Zn. In about 4 km^2 around Treffynnon additional lines were sampled and measured to close the spacing to 200 m. Gravity data were also collected from some traverses and sites to supplement the National Gravity Survey. Several strong copper-in-soil and geophysical anomalies were identified. Nine boreholes were drilled to investigate the causes.

Disseminated copper mineralisation was intersected in the boreholes. It occurs principally within a concordant or semiconcordant sheeted complex of dioritic and tonalitic rocks, believed to be uppermost Cambrian or low Arenig in age, whose composition is consistent with emplacement within a volcanic arc setting. The intrusions and their host rocks have suffered a two phase, pervasive, hydrothermal alteration which is inseparable from the sulphide mineralisation and recorded in boreholes over an area of 1 km^2. The alteration shows features common to porphyry copper systems, consisting of an early patchy and irregularly developed propylitic and potassic alteration, overprinted by a widespread and locally intense late propylitic alteration. The potassic alteration is only well preserved locally and is divisible into K-feldspar and biotite types. When intense, the potassic alteration is characterised by substantial changes to the bulk chemistry of the rocks involving increases in K, K/Na, K/Rb, Rb/Sr, Cu/S and, erratically Ba and losses of Na, Sr and Ca. In the most altered rocks so called 'immobile' elements such as Y and Nb are redistributed. The late propylitic alteration affected rocks in all boreholes except one and gave rise to the dominant alteration assemblage of sericite, chlorite, epidote, albite, pyrite and magnetite. Introduction of Fe and S appears to have accompanied this event but any other bulk chemical changes are confused by host rock variation. Retrograde effects on potassic alteration, such as the lowering of Rb/Sr, K/Na and Cu/S are probable but not clearly defined.

Mineralisation, involving the introduction of Cu, Fe and S, accompanied the first phase and ?Cu, Fe and S the second phase of alteration. Cu levels are generally modest, the best intersection being 0.1% over 3.4 m in borehole 2. Cu and particularly the Cu/S ratio are generally highest in the most altered (potassic) rocks but locally high levels of Cu may be found in weakly altered rocks. There is only weak and erratic enrichment in Mo, and high levels of Cu and Mo show only a weak correlation. There are localised very weak enrichments of As, Pb and Zn. Au was not determined.

It is suggested that the present erosion level cuts a deep section through a copper porphyry deposit, this explaining the imperfectly developed zonation, low Cu content and abundant magnetite. The part of the system most likely to have contained ore grade material has, therefore, been eroded away and some of the material is found in the overlying lacustrine sediments which contain abundant magnetite, clay, feldspar and up to 640 ppm Cu. The style of mineralisation, chemistry of the rocks and geological setting all suggest that mineralisation took place in conditions consistent with an island arc setting. The detailed geology of the area is, however, imperfectly understood because of the extremely poor exposure, and the possibility exists that, because of downfaulting and tilting, parts of the deposits may be preserved and concealed to the north and east of the area drilled.

The case history shows that in such areas of low relief and thick overburden drainage sampling can be an ineffective mineral exploration technique. Surface rock sampling also failed to indicate the presence of the deposit, partly because of poor exposure and partly because of the patchy, multi-phase alteration pattern. The locally thick sequence of interbedded sands and clays containing copper and magnetite overlying the deposit confused to varying degrees all the geochemical and geophysical survey results except lithogeochemistry. If the sands and clays had not contained anomalous copper the deposit would probably not have been located. Borehole results suggest that Cu, S and the Cu/S ratio provide the best lithogeochemical targets.

INTRODUCTION

Two adjoining prospects, one centred on Middle Mill near Solva, the other a broad belt of country north of Llandeloy (Fig. 1), both in the catchment of the River Solfach, were covered by reconnaissance geochemical and geophysical surveys. The results of the work around Middle Mill were not encouraging and the area was abandoned. In the Llandeloy prospect, however, the geochemical and geophysical results were of sufficient interest to justify further investigation. Detailed geophysical surveys were made and soil samples collected for chemical analysis along 200 metre spaced traverse lines across a target area around Treffynnon. Anomalies were identified and nine boreholes were drilled to investigate their cause.

The surface of both areas is a peneplain incised deeply by the lower reaches of the River Solfach. All the land is farmed and outcrop of any kind is rare. Many of the quarries recorded by early workers have now been filled in and grassed over.

In both prospects the target was disseminated copper mineralisation. Intermediate intrusions within the Cambrian and Precambrian of this region are similar to those in the eastern part of the Harlech dome - a comparison made by Cox and others (1930). While their age is not known for certain, the possibility exists that the intrusions were co-magmatic with the andesites at Treffgarne (Thomas and Cox, 1924) which are either late Tremadoc or early Arenig in age. In the Harlech dome the intermediate intrusions and the associated Coed y Brenin porphyry copper mineralisation (Rice and Sharp, 1976) are believed to be derivatives of the late Tremadoc magmatism that gave rise to the Rhobell Volcanic Group. Furthermore, it has been suggested that the andesitic Rhobell Fawr volcanism formed part of an

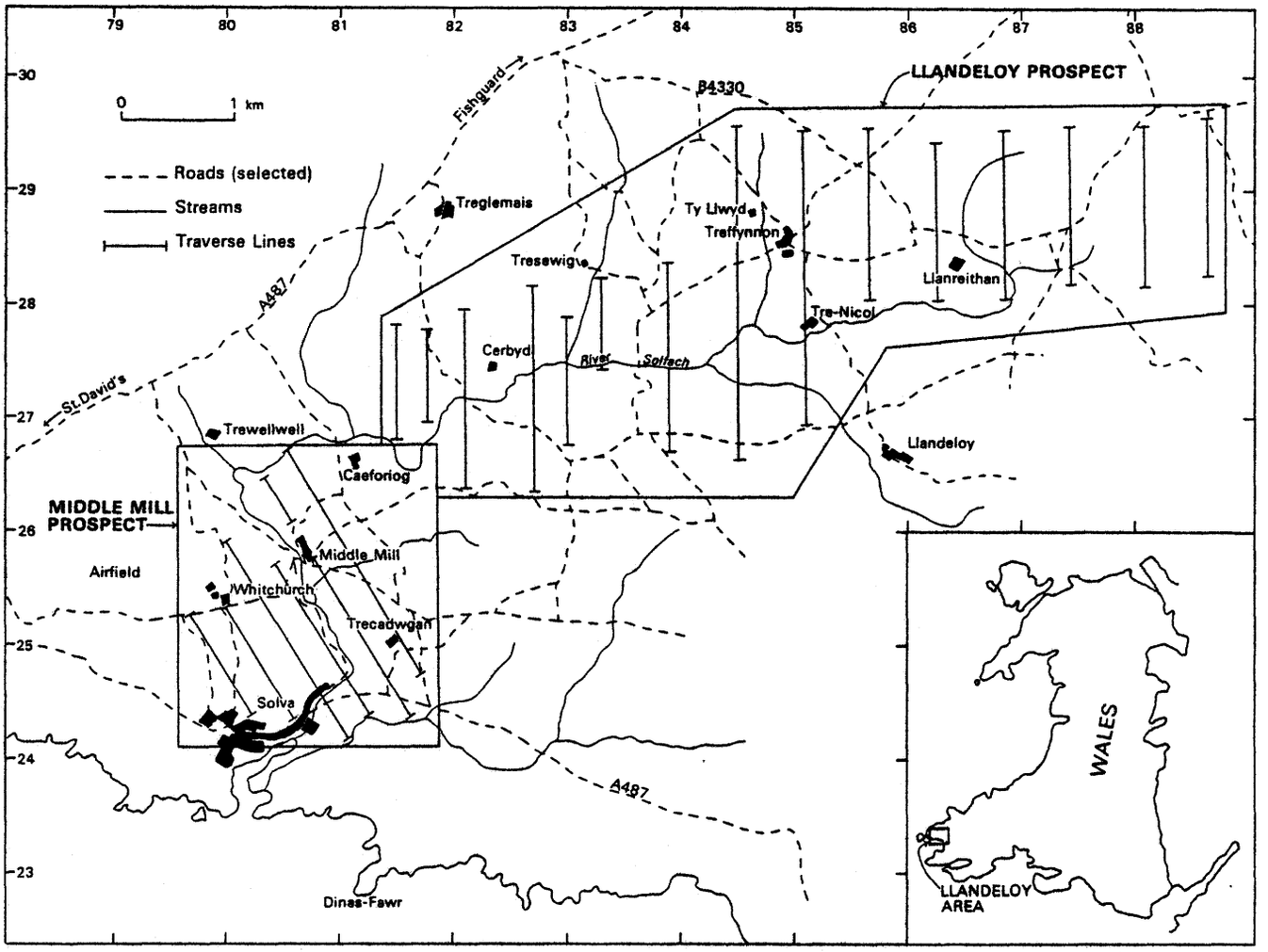

Figure 1 The Middle Mill and Llandeloy prospects showing the traverse lines followed during the reconnaissance surveys

island arc volcanic episode whereas the succeeding, Llanvirn to Caradoc, volcanic rocks in Wales relate to bimodal, dominantly tholeiitic, volcanism in a back arc extensional setting (Kokelaar, 1979; Kokelaar and others, 1984). Because it is known that disseminated copper mineralisation is associated with the end Cambrian subduction event, any area in which there is some evidence for the existence of volcanic rocks and subvolcanic intrusions derived from it is worth investigating.

The Treffgarne Andesites have not been recorded around Middle Mill and Llandeloy, but Williams (1933) noted that the lowest component of the Llandeloy Ashes, which are early Arenig in age, is richly pyritic locally. The traverse lines, set mainly to cover the intrusions within the Cambrian and Precambrian, therefore were extended near Llandeloy to cover the earliest of the Ordovician volcanic rocks.

Previous work

The part of the area around Llandeloy was mapped by T. G. Williams (1933) and later all the area was remapped by A. C. Wilcox and H. H. Thomas, the latter responsible for the Solfach valley. Their maps were not published, but were lodged with the Geological Survey in 1952. The linework on them has been used in conjunction with that on the published work of T. G. Williams (1933) to draw Fig. 2. However any map showing solid geology in this area must be largely speculative. A comparison of the Geological Survey map (Sheet 40) of 1857 with those of Cox and others (1930), Williams (1933) and manuscript maps of Cox and Thomas shows several different ways of interpreting essentially the same data.

Twentieth century written accounts of the area are limited to Williams (1933) for the part north of Llandeloy, Cox and others (1930) for a general account of the area between Ramsey Island and Newgale, and Stead and Williams (1971) who have described excursions in the area. Rushton (1974) has reviewed all the literature on the stratigraphy.

The drift of the area has never been properly examined. No attempt has been made here to reinterpret the work of Williams (1933) and Cox and Thomas except around Treffynnon where the boreholes yielded previously unavailable information. Some minor adjustments have been made to boundaries around intrusions that have been re-examined.

Very little geochemical work has taken place in the area. U-Pb zircon age determinations have been carried out on the St David's granophyre and the Johnston diorite, both just outside the area (Patchett and Jocelyn, 1979), and Thorpe (1970, 1972) has discussed chemical analyses of the Johnston intrusions. The only geochemical drainage survey data available is that included in the Wolfson geochemical atlas of England and Wales (Imperial College, 1978). No outstanding features are shown in this area except for moderately high levels of iron and manganese. The Soil Survey of Great Britain has published a general account of the soils across the whole of west and central Pembrokeshire (Rudeforth and Bradley, 1972). More pertinent to this work Bradley, Rudeforth and Wilkins (1978) published the results of analyses for 12 elements on alternate soil profiles collected at 1 km intervals across the same area. They

concluded that except for Zn the results showed similar spatial patterns to those obtained from the analysis of stream sediment reported in the Wolfson atlas (Imperial College, 1978), though careful inspection of the soil results indicate copper enrichment in soil over this area not evident on the published stream sediment maps.

REGIONAL STUDIES

The work and results described here are common to both the Middle Mill and Llandeloy areas. Most was undertaken during initial studies of the area.

Stratigraphy

The area is underlain by sedimentary and volcanic rocks of Precambrian, Cambrian and Ordovician age. The rocks are folded, probably as a result of Caledonian deformation, but this area lies on the edge of the Hercynian front and it is possible that early structures have been modified by this event. Most rocks examined contain chlorite and sericite, and at Solva the manganiferous sedimentary rocks contain spessartine. There is not a strongly developed cleavage. The metamorphism is low grade, possibly low greenschist facies. In several places spotting was observed in mudstone not adjacent to exposed intrusions which suggests the presence of a widespread thermal event separate from the regional metamorphism.

The stratigraphic succession is shown in Table 1. No attempt has been made to modernise the terminology except where following Rushton (1974). The brief descriptions that follow are taken mainly from Williams (1933).

Table 1 Stratigraphic subdivisions

8	Tetagraptus Shales		
7	Brunel Beds including Llandeloy Ashes	Arenig	Ordovician
6	Lingula Flags	Merioneth Series	
5	Menevian Group	St. David's	
4	Solva Group	Series	Cambrian
3	Caerfai Group	Comley Series	
2	Treffynnon Group	Pebidian	Precambrian
1	Treglemais Group		

1. Treglemais Group: variously coloured conglomeratic tuffs with interbedded banded porcellanites and halleflintas, and less common coarse crystal tuff and rhyolitic tuff. According to Williams (1933) pyrite and, in less abundance, chalcopyrite, galena and arsenopyrite occur in all the rock types.
2. Treffynnon Group: well-bedded, fine-grained, green to brown rhyolitic tuff thinly interbedded with quartzite.
3. Caerfai Group: thinly bedded, green or purple, argillaceous, quartz-feldspar sandstones with minor horizons of purplish mudstone.
4. Solva Group: green, coarse, pebbly sandstone, overlain in turn by feldspathic sandstone, purple and green thinly interbedded mudstone and sandstone, and green and grey flaggy sandstone and mudstone. In Solva harbour there are thin beds, laminae and disconnected nodules of spessartine rock.
5. Menevian Group: dark and light grey laminated mudstone with silty and sandy lenses and, in places, ashy beds. Thickly bedded dark grey sandstone occurs at the top in places.
6. Lingula Flags: thinly interbedded pale grey, siliceous, coarse siltstone and greenish-grey micaceous mudstone.
7. Brunel Beds: dark blue to grey sandy slate and mudstone with interbedded ashy, pebbly sandstone. The Llandeloy Ashes comprise lithic and crystal tuff of intermediate composition, tuffite, sandstone and mudstone.
8. Tetragraptus Shales: blue to blue-black cleaved mudstone with thin, pale ashy beds.

Intrusive rocks

Classification of Williams (1933)

The many intrusions in this area were divided by Williams (1933) into two groups of different ages. The Dimetian group intruded the Precambrian volcanic rocks and was believed to be Precambrian in age; whereas a younger group intruded Cambrian rocks. The nomenclature he adopted for these rock types reflected this division into age groupings: hornblende porphyry is found only among the Dimetian rocks intruding the Treffynnon Group; hornblende-diorite porphyrite intrudes only the Cambrian; quartz porphyry intrudes the Treglemais Group.

Hornblende porphyry Williams (1933) commented on the diversity in the texture, in the proportions of hornblende and feldspar, and in the alteration in these intrusions. He recognised potash feldspar in the rocks and from his descriptions they appear to be granodioritic in composition. The largest of the intrusions, exposed in a quarry near Hollybush, is bordered by diorite but separated from it by a thin wall of tuff. Intrusions of this rock are cut by pegmatite veins and thin basic dykes. Williams (op. cit.) observed chilled contacts against tuff at the margin of the Ty-llwyd intrusion and found intense pyritisation locally. He compared these rocks with similar bodies believed to be Dimetian in age within the Precambrian in neighbouring areas.

Hornblende-diorite porphyrite Williams (op. cit.) recorded several laccoliths and sills of this rock type within the Cambrian strata southwest of Treffynnon. They show a diversity in character similar to the hornblende porphyries intruding the Treffynnon Group and, except for the absence of K-feldspar in these rocks, they resemble them petrographically. Intrusions of this type were reported to be numerous by Cox and others (1930) around Solva.

Quartz porphyry Williams (op. cit.) recorded that the only intrusion within the Treglemais Group is quartz porphyry near Llanhowel. The relative proportions of quartz, plagioclase and potash feldspar phenocrysts vary considerably as does the overall grain size. The rock is always heavily altered, chiefly to sericite and chlorite. Williams (op. cit.) classified this rock among the Dimetian intrusives.

Reclassification of the igneous rocks

Despite the poor exposure all the major intrusions and some minor bodies in the survey area were re-examined; samples from some were analysed for major and trace elements. Considerable textural variation was observed even among compositionally similar rock types, and the rock types themselves were gradational into each other.

Nevertheless taking into account only rocks exposed at surface four petrographic types were identified. They are:

Quartz-feldspar porphyry
Porphyritic microtonalite
Quartz-diorite
Porphyritic quartz-microdiorite

The quartz-feldspar porphyry and the quartz-diorite are limited in distribution, but both the other types occur within the Dimetian and post-Cambrian suites. In addition they were found to intrude Cambrian rocks in an area mapped by Williams as Precambrian. There is also no petrographic evidence to justify Williams's (1933) subdivision of the intrusions into two groups of different ages. Furthermore the potash feldspar identified by Williams (1933) in the Dimetian rocks, though confirmed in slides of rocks from boreholes, is considered to be secondary.

To test further Williams' classification the chemical analyses of rocks in the two age groups were compared. Because of the small number of samples in each group their unequal size and the presence of weathered float samples a rigorous comparison is not possible. A visual examination of the results, however, shows that the two quartz-feldspar porphyry samples are of markedly different composition from all the other samples, but that otherwise it is not possible to recognise any meaningful differences between the two groups. It was concluded, therefore, and later supported by boreholes data, that the microtonalite, quartz-diorite and quartz-microdiorite intrusions most likely form a consanguineous suite which is younger than the Cambrian, whilst the quartz-feldspar porphyry is a distinct perhaps unrelated lithology.

Petrography

Quartz-feldspar porphyry This rock is present only around Llanhowel. Exposures known to Williams (1933) were not found and the two samples analysed (RPR 23, 24*) are both float. The rock contains a sparse scattering of euhedral sodic plagioclase phenocrysts (possibly some potash feldspar) and embayed quartz with clusters of muscovite flakes in a groundmass of flow-oriented plagioclase laths, abundant sericite and equant quartz crystals.

Porphyritic microtonalite The rocks are uniformly strongly porphyritic with phenocrysts up to 2-3 mm and a groundmass grain size of about 0.05 mm. They show textural and compositional variation, ranging from varieties transitional to quartz-microdiorite to relatively siliceous types, in addition to commonly intense alteration to calcite, sericite and chlorite.

The most basic variety occurs around Ty-llwyd, though the sample (RPR 31 in Table 2) is from float. The rock contains euhedral phenocrysts of altered plagioclase and very pale greenish-brown ?amphibole. Quartz forms large irregular-shaped ophitic patches. The groundmass is composed of subhedral feldspar crystals and interstitial quartz with abundant ?tremolite/actinolite. The most coarse-grained variety, from a locality [SM 8438 2772] south of Trescaw Farm, is composed of sparse altered plagioclase phenocrysts in a groundmass of plagioclase, euhedral quartz and pseudomorphs after ferromagnesian minerals (LA 729). The grain size median for the groundmass is about 0.25 mm. A typical example of the more common fine-grained type intrudes the coarse-grained rock in this outcrop. The finer grained variety contains subhedral to euhedral altered plagioclase and chloritised amphibole phenocrysts 1-2 mm long in a groundmass comprising equant grains of feldspar and quartz about 0.05 mm in diameter. There are several occurrences of this type of rock, differing mainly in degrees of alteration and the amount of quartz in the groundmass. Several of them also contain chlorite pseudomorphs after biotite in addition to amphibole. One such intrusion (LA 624, RPR 7) forms a 60 m thick sill, xenolithic in parts, exposed in the sea cliffs near Dinas-fawr [SM 8143 2311]. The top of the intrusion is concordant but the base is markedly discordant here. Another major body of this type is the main intrusion of Middle Mill [SM 804 259] which is concordant. The rock (LA 625, RPR 12-14, 17, 36) contains more amphibole pseudomorphs than at Dinas-fawr and one or two quartz phenocrysts. Phenocrysts of quartz also occur in the highly altered variety from within Upper Cambrian near Pont y Cerbyd (LA 617). In the intrusion at Trinity Quay, Solva [SM 8024 2412], the groundmass contains patchy chlorite and the feldspar commonly forms laths (LA 626, RPR 8).

Other intrusions of this rock include the large Parke body (LA 629, RPR 4) around SM 8754 2928; the main Hollybush body (LA 619, RPR 3); the Olmarch intrusion (RPR 30), now unexposed and represented only by float, and the body north of Llanddynog (RPR 27), also represented only by float. Another type which has abundant, locally closely spaced phenocrysts (LA 621, RPR 5, 28, 29), forms a large intrusion southwest of Trenichol.

Quartz-diorite The rock (LA 618) from Hollybush quarry [SM 8600 2895] described as diorite by Williams (1933) is the most coarse-grained rock in the area. It consists of euhedral and subhedral altered plagioclase up to 2 mm, chloritic pseudomorphs after ?biotite, greenish-brown hornblende and interstitial quartz.

Porphyritic quartz-microdiorite The distinction between this rock type and quartz-poor microtonalite is difficult to make and the main petrographic characteristics of the two rock types are shared. A variety from a sill on the east side of Solva Harbour [SM 8024 2399] has a strongly flow textured feldspathic groundmass (LA 733). The specimen (RPR 15) from a dyke in Middle Mill quarry is intensely altered.

Alteration

Only the two specimens of quartz-feldspar porphyry from west of Cerbyd contained fresh feldspar, though there was alteration to sericite and chlorite in the groundmass. In all the rocks in the series microtonalite to quartz-microdiorite and quartz diorite the primary minerals show various degrees of alteration.

There are two main alteration assemblages: the more common is sericite-epidote-chlorite ± magnetite ± pyrite; the less common is sericite-chlorite-pyrite. Carbonate is present with both assemblages, but in very few localities.

In the sericite-epidote-chlorite assemblage the feldspar is replaced by sericite and either epidote or clinozoisite with rare, small amounts of chlorite. Alteration is by no means uniform in each rock and there may co-exist feldspars which are fresh, slightly sericitised and totally altered to clinozoisite in one sample. Amphibole is replaced totally by chlorite and epidote, with quartz and magnetite in some rocks. Biotite is commonly replaced by chlorite, in places with magnetite. In a number of rocks there are veinlets of epidote or quartz and in some rocks sericite with chlorite or pyrite.

The sericite-chlorite-pyrite assemblage is characterised by rocks in which the feldspar has been altered to sericite, rarely with chlorite and quartz; biotite is chloritised and amphibole is pseudomorphed by chlorite with sericite and possibly pyrite. Chlorite, sericite and pyrite veinlets are present.

*Refers to BGS sample number.

The only rock containing evidence of secondary minerals of a higher pressure-temperature stability range than the minerals in these assemblages is the quartz diorite from Hollybush (RPR 2). In this rock there is abundant chlorite after biotite, much of it forming a rough network through the rock. It also appears that these chlorite pseudomorphs occur in chlorite pseudomorphs after amphibole. It is possible, therefore, that the biotite was a secondary mineral in part replacing amphibole and both minerals have undergone retrograde alteration.

There is no regional pattern to the relative distribution of the two alteration types. Both may occur in close proximity, e.g. both are present in Middle Mill quarry, also in neighbouring intrusions at Solva and parts of the same intrusion south of Tre-nichol. Highly altered rocks occur in all parts of the area and there is no obvious pattern to their distribution. The most intensely sericitised rocks occur around Solva harbour where hydrothermal breccias are particularly common and at Dinas Fawr, south of St. Elvis, where mineral veins have been worked.

Mineralisation

The quartz-sulphide veins near St. Elvis, said by Hall (1971) to have been worked for lead and copper in the sixteenth century, and the sulphide minerals found in Middle Mill quarry (see below) are the only occurrences of base metal mineralisation known in this area. The alteration styles resembling the propylitic, phyllic and, at Hollybush, possibly potassic (biotite) types around porphyry copper systems, give a hint that hydrothermal activity was associated with igneous intrusion in the area. Outcrop is too poor, however, for any firm conclusions to be made other than that the area around Hollybush appears to contain signs of high temperature alteration assemblages consistent with porphyry copper mineralisation.

Geochemistry

All available exposures of intrusive rocks around Llandeloy together with selected exposures in the general area were sampled. In addition, because of the absence of any exposure over three of the mapped intrusives around Llandeloy, some samples of float were collected (Fig. 2). Samples weighing about 2 kg were crushed, and a split ground in a 'tema' mill with 'elvacite' binder prior to pelletising and analysis for a range of elements by XRFS. Major elements were determined on intrusive rock samples by β-probe. The results and detection limits are given in Tables 2, 3 and 4.

The majority of sedimentary rock samples are mineralised siltstones and sandstones of the Solva Group from Middle Mill quarry. These are discussed in more detail in the section describing that area. Two samples of laminated siltstone collected from quarries in the Brunel Beds have compositions very similar to Beaufont Group siltstones and world averages for shales compiled by Beeson (1980) except for a very low Ca content and less pronounced lower levels of Sr, Zn and Ni (Table 3). There is no indication of any concentration of siderophile or chalcophile elements despite the presence of pyrite both disseminated and on joints in one sample. Comparisons of tuffaceous rocks are more difficult because of their extremely variable composition, but no exceptionally high levels of any of the elements determined are present in the three samples from the Treglemais Group. The relatively high Fe level in the sample from a fault zone may be caused by pyritisation, but if so, no accompanying enrichment in other chalcophile elements is evident.

Representatives of all four groups of intrusive rocks distinguished petrographically were analysed. Two of the groups, however, are only represented by a single sample and a third group by two samples whilst the remaining twenty samples are all of porphyritic microtonalite (Table 2). This imbalance and the small total number of samples precluded rigorous statistical treatment of the results.

As a guide to the most likely differences in chemistry between samples of float and bedrock samples, samples of fresh and weathered porphyritic microtonalite were collected from one quarry. The results (Table 2, nos. 1 and 26) suggest that weathered samples may be relatively enriched in SiO_2, Al_2O_3, Nb, Y, Cu and As and depleted severely in CaO, but a high degree of uncertainty must exist in a single sample comparison of this type.

Although the quartz feldspar porphyry group is only represented by two float samples it is clear that chemically it forms a distinct group. The samples may be separated solely on their high SiO_2 content, though K_2O, Rb, Pb and Nb are also high whilst total iron, MgO, TiO_2, Mn, Ni, Zn and Y are lower than in the other intrusive rocks (Table 2). A highly altered rock sample collected from the faulted margin of the quartz feldspar porphyry intrusive (Table 2, no. 25) has a composition more similar to the porphyritic microtonalites and is included in that group. However it is uncertain whether the rock represents highly altered quartz porphyry, or whether there is a slice or small body of microtonalite in the fault zone at this point.

The compositional range within the porphyritic microtonalite group is produced by a combination of primary geochemical variation, patchy and variable alteration and weathering. For example, the most acid rock in the group (Table 2, no. 42) which also contains the lowest TiO_2 and MgO is quartz veined, whilst the second lowest level of CaO and highest Al_2O_3 and Y are recorded in a deeply weathered sample (no. 26). The highest K_2O, Na_2O and Rb and lowest K_2O and Ba results are all in samples taken from a small part of a variably altered intrusion exposed in Middle Mill quarry. Perhaps the sample with the most extreme composition is that of a pyritised microtonalite from an intrusion exposed by Solva harbour (Table 2, No. 8): it contains the lowest Na_2O, Al_2O_3 and Rb and highest As, Cu, CaO and K/Rb in the group. Another feature which is taken as indicative of the variable alteration is the absence of a clear pattern of inter-element correlations. The only two closely correlated groups of elements are a 'mafic' group, probably concentrated in amphiboles and chlorite, characterised by Ti-Fe-Ni-Mg-Zn-Y, and a 'potash group' of K-Rb-Ba-?Pb. Several elements show no close ties whilst others, such as Mo and Pb, generate positive correlations which may be spurious, because the bulk of the results are close to or below the analytical detection limit and appear as near constant values in the data matrix.

The sample representative of the quartz diorite group can be readily distinguished from the porphyritic microtonalites by its low SiO_2 content and high TiO_2, total iron, MgO, Cu and Sr levels (Table 2, no. 2). The porphyritic quartz microdiorite sample, which came from a small intrusion separate from the main body in Middle Mill quarry has a composition which falls between the quartz diorite and porphyritic microtonalites (Table 2, no. 15). Further samples of these two lithologies were obtained from boreholes at Llandeloy and their chemistry is discussed in that section.

The overall composition of the intermediate rocks collected at surface suggests a calc-alkaline parentage and comparison with analyses from elsewhere indicate that low TiO_2 and Nb contents are particular features of these rocks.

There are no clear indications of nearby disseminated copper mineralisation in the chemistry of these rocks. No Cu result is above the expected background level for these lithologies whilst Pb and Zn show lithophile rather than chalcophile affinities in their inter-element relationships. Only one sample, collected near a fault

Table 2 Analyses of intrusive rock samples collected from exposures in the Llandeloy - Middle Mill area

No	Rock Type	Grid Reference SM		SiO_2	Al_2O_3	TiO_2	Fe_2O_3	MgO	CaO	Na_2O	K_2O
2	Quartz-diorite	8600	2895	54.97	16.78	0.92	9.05	4.89	6.58	3.92	0.86
15	Porph. qtz.m.diorite	8035	2595	55.13	16.44	0.49	6.88	4.67	5.29	5.13	1.33
3		8542	2888	63.52	17.25	0.41	5.19	2.01	4.65	5.89	0.64
4		8754	2928	65.13	17.04	0.38	4.57	1.93	3.13	6.91	0.55
30F		8348	2764	60.51	17.93	0.44	6.92	2.93	3.17	4.74	1.69
42F		8623	2843	65.21	16.62	0.34	5.13	1.78	2.75	6.75	0.65
8		8024	2412	59.30	15.86	0.43	6.02	3.26	9.74	2.21	0.52
27F		8301	2712	64.91	17.61	0.36	5.73	2.10	1.08	6.44	1.11
12		8040	2590	59.56	16.81	0.35	5.23	2.77	4.80	3.85	2.60
13	Porphyritic	8040	2590	61.76	16.43	0.41	5.46	3.05	4.44	6.33	0.72
14	microtonalite	8040	2590	61.84	16.65	0.37	5.63	2.69	2.58	7.98	0.52
17		8040	2590	62.34	15.97	0.42	5.06	2.98	5.32	5.24	0.89
40		8083	2506	62.38	16.78	0.46	5.77	3.70	4.18	4.87	1.26
41		8083	2506	60.89	16.43	0.44	6.17	3.17	4.66	4.61	1.21
1		8213	2712	58.01	16.55	0.41	6.18	3.30	4.71	5.24	1.27
26		8216	2715	62.07	18.62	0.42	6.59	3.02	0.36	4.90	1.74
29		8489	2737	58.89	17.85	0.52	7.63	4.18	1.97	4.70	1.43
5		8496	2741	58.82	17.29	0.51	7.51	4.79	2.20	5.62	0.78
28F		8492	2757	62.55	17.10	0.46	6.66	3.53	1.18	5.78	1.14
31F		8452	2891	57.98	17.24	0.62	7.36	3.89	5.85	3.87	1.33
43F		8710	2910	60.97	17.85	0.50	6.87	3.88	0.46	5.75	1.60
25		8189	2720	65.15	16.94	0.36	6.43	3.57	0.29	3.50	2.50
23F	Quartz-feldspar	8169	2725	73.01	16.53	<0.01	1.35	0.50	0.38	5.51	2.26
24F	porphyry	8183	2709	73.39	16.60	<0.01	1.35	0.48	0.31	5.49	2.32

No	P_2O_5	Cu	Pb	Zn	As	Mo	Ni	Mn	Ba	Rb	Sr	Zr	Th	Ce	Y	Nb	K /Rb
2	0.15	46	<13	62	<2	4	16	1,200	196	20	500	82	<4	34	18	<2	356
15	0.12	<6	<13	68	<2	<2	22	960	321	47	355	75	<4	21	14	3	234
3	0.17	<6	<13	19	<2	<2	<5	320	140	21	473	100	<4	<21	14	7	253
4	0.16	<6	<13	73	3	<2	<5	810	158	15	346	89	<4	<21	14	6	304
30F	0.17	26	<13	78	3	<2	7	930	430	37	390	99	<4	21	16	6	379
42F	0.15	32	<13	47	<2	<2	<5	640	244	18	384	90	4	<21	15	3	300
8	0.14	42	<13	57	16	<2	11	1,050	131	11	124	87	<4	<21	13	4	392
27F	0.16	15	34	71	6	<2	<5	690	212	39	296	118	5	26	13	6	236
12	0.13	<6	<13	54	<2	<2	6	1,130	546	91	222	94	<4	<21	12	3	239
13	0.14	7	<13	54	3	5	12	810	270	16	491	100	<4	<21	13	<2	373
14	0.14	6	<13	49	<2	<2	6	770	100	18	226	98	<4	33	13	6	239
17	0.14	19	<13	60	3	<2	13	790	355	21	473	104	5	<21	12	4	351
40	0.15	23	<13	68	3	<2	15	790	211	34	419	101	<4	<21	14	5	307
41	0.14	34	<13	56	<2	<2	10	2,120	893	35	356	99	<4	<21	13	4	286
1	0.13	10	<13	68	3	<2	8	850	323	41	260	96	<4	<21	12	3	257
26	0.14	23	<13	77	7	<2	14	1,000	472	60	187	106	<4	<21	23	6	240
29	0.15	<6	<13	99	10	<2	13	1,170	237	40	280	97	<4	26	15	3	296
5	0.13	16	16	111	9	<2	13	1,190	242	19	295	93	<4	22	15	6	340
28F	0.14	15	<13	74	<2	<2	7	920	229	33	264	102	<4	<21	13	4	286
31F	0.16	10	<13	52	<2	<2	19	1,150	466	33	421	107	<4	27	19	6	334
43F	0.13	31	<13	99	<2	<2	15	1,030	501	46	157	94	<4	25	13	4	288
25	0.12	36	61	66	8	25	10	1,160	383	70	133	80	<4	<21	16	3	296
23F	0.16	8	40	36	<2	<2	<5	380	743	70	184	68	4	30	9	11	268
24F	0.14	<6	16	32	<2	<2	<5	340	729	70	169	70	4	26	8	10	295

F denotes float sample

Also determined: Sn <9ppm, Sb <11ppm, F <0.05%, U <3ppm

Total iron reported as Fe_2O_3

Major elements reported as % oxide, trace elements in ppm

Table 3 Analyses of miscellaneous rocks from the Llandeloy - Middle Mill area

No.	10	22	34	32	33	6
Ti%	0.22	0.41	0.53	0.61	0.64	0.01
Mn%	0.04	0.11	0.16	0.03	0.08	0.22
Fe%	2.11	4.16	8.81	6.63	6.22	3.72
Ni	<5	<5	13	36	27	<5
Cu	10	7	<6	44	28	>10,000
Pb	<13	<13	<13	<13	23	<13
Zn	47	120	133	76	56	-
As	<2	4	5	9	10	<2
Mo	<2	2	2	2	3	3
Sn	<9	<9	<9	<9	<9	<9
Ba	55	165	222	851	439	38
Rb	3	42	44	194	135	3
Sr	76	171	97	26	137	15
Ca%	0.26	0.91	0.51	0.03	0.03	6.68
Y	29	44	30	22	38	48
Ce	<21	22	60	38	71	27
Zr	135	137	355	165	204	<2
Th	5	4	10	13	13	<2
U	<2	<2	3	4	3	3

Results in ppm except where indicated

10 Siliceous, fine grain, grey-green tuffs with minor pyrite, Treglemais Group [SM 8164 2812]
22 Siliceous, medium grained, grey-green tuffs, Treglemais Group [SM 8147 2756]
34 Grey-green, pyritic tuffs, brecciated and quartz veined, Treglemais Group [SM 8096 2694]
32 Banded, ashy siltstones with weathered ?pyrite, Brunel beds [SM 8395 2710]
33 Thinly bedded siltstones, Brunel beds [SM 8320 2625]
6 Vein material from old working, Ramsey Head [SM 7153 2352]

Table 4 Analyses of sedimentary rock samples from Middle Mill quarry

No.	11	16	18	21	20	35	37	38	39
Ti%	0.19	0.45	0.31	0.37	0.69	0.56	0.39	0.28	0.34
Mn%	0.06	0.17	0.19	0.23	0.23	2.40	0.15	0.17	0.16
Fe%	1.98	5.92	6.15	7.54	6.20	7.43	7.65	5.73	6.14
Ni	<5	10	12	15	34	39	12	12	15
Cu	<6	13	<6	95	33	52	345	1,010	884
Pb	<13	<13	<13	<13	43	24	67	155	93
Zn	20	53	77	104	74	102	227	1,195	423
As	9	8	8	13	41	41	18	18	19
Mo	<2	2	<2	<2	3	<2	5	4	6
Ba	163	564	293	274	403	289	489	295	375
Rb	15	79	59	58	197	32	96	52	66
Sr	29	21	27	37	51	297	30	30	29
Ca%	0.51	0.51	0.65	0.57	0.54	2.00	0.22	0.59	0.71
Y	9	21	17	22	27	30	18	24	28
Ce	25	59	45	51	62	72	42	77	71
Zr	99	347	145	207	304	206	163	115	131
Th	6	10	8	9	12	10	9	8	11
U	<2	2	<2	3	5	2	3	3	2

Sn also determined, all results <9ppm
Results in ppm except where indicated

11 Quartzitic sandstone
16 Quartzitic sandstone cross cut by abundant pyrite veinlets
18 Sandstone with disseminated pyrite modified by ?contact metamorphism
21 Quartzitic sandstone with disseminated sulphides modified by ?contact metamorphism
20 Banded siltstone/grit with disseminated pyrite dominantly in grit bands
35 Laminated, ?siliceous siltstone with disseminated pyrite
37 Altered quartzitic grit with pyrite and chalcopyrite
38 & 39 Brecciated quartzitic grit and siltstone with sulphides disseminated and in veinlets

(Table 2, no. 25), contains elevated levels of some chalcophile elements (Pb, Mo, As) which are perhaps indicative of weak epigenetic mineralisation. The erratic level of alkalis is considered to reflect alteration seen in thin section, but no regional pattern could be discerned with variation within one outcrop as great as across the whole area.

Rock geochemistry, based on available outcrop sampling therefore failed to give any clear indication of the presence of disseminated mineralisation, a conclusion which agreed with the stream sediment sampling, but was in distinct contrast to the findings of a soil sampling survey and subsequent drilling.

Stream sediment survey

A stream sediment survey was carried out in the catchment of the Solfach, partly to look for indications of mineralisation and partly as an orientation study, to test the effectiveness of drainage sampling as a mineral exploration technique in this area of low relief with incised drainage, thick drift cover, sluggish streams and extensive contamination.

Sampling and analysis

Thirty five sites (Figs. 3, 4) were sampled for water stream sediment and panned concentrates. Stream sediment was wet-sieved at site to pass 100 mesh BSS (0.15 mm) using a minimum of water to retain the clay fraction. Samples were dried in the laboratory prior to grinding in a ball mill for 30 minutes. A 0.5 g split was analysed for Cu, Pb and Zn by atomic absorption spectro-photometry (AAS) following digestion in hot concentrated nitric acid for one hour. As was determined by X-ray fluorescence spectrometry (XRF) following grinding of a 12 g subsample in a 'tema' mill with 'elvacite' binder and pelletising. A further range of elements was determined by optical emission spectroscopy (OES). Detection limits were approximately 1 ppm for Be; 2 ppm for As; 3 ppm for Cu; 5 ppm for Pb, B, Zn, Y and Sn; 10 ppm for V, Cr, Co and Ni; 20 ppm for Zr; 50 ppm for Mn; 100 ppm for Ba and 0.5% for Fe.

Constant volume panned concentrates of about 50 g were made at site from about 4 kg of -8 mesh BSS (2 mm) stream sediment. Following drying, a 12 g subsample was ground in a 'tema' mill with 3 g of 'elvacite' binder for five minutes prior to pelletising and analysis by XRF for a range of elements. Detection limits were 2 ppm for Mo and As; 3 ppm for Th and Zn; 5 ppm for Ni; 6 ppm for Mn and Cu; 9 ppm for Sn; 11 ppm for Sb; 13 ppm for Pb; 21 ppm for Ce and 27 ppm for Ba.

A 30 ml water sample was collected in a plastic screw top bottle and acidified in the field with 0.3 ml perchloric acid. The sample was subsequently analysed by AAS for Cu and Zn without further sample preparation. Detection limits were approximately 0.02 ppm.

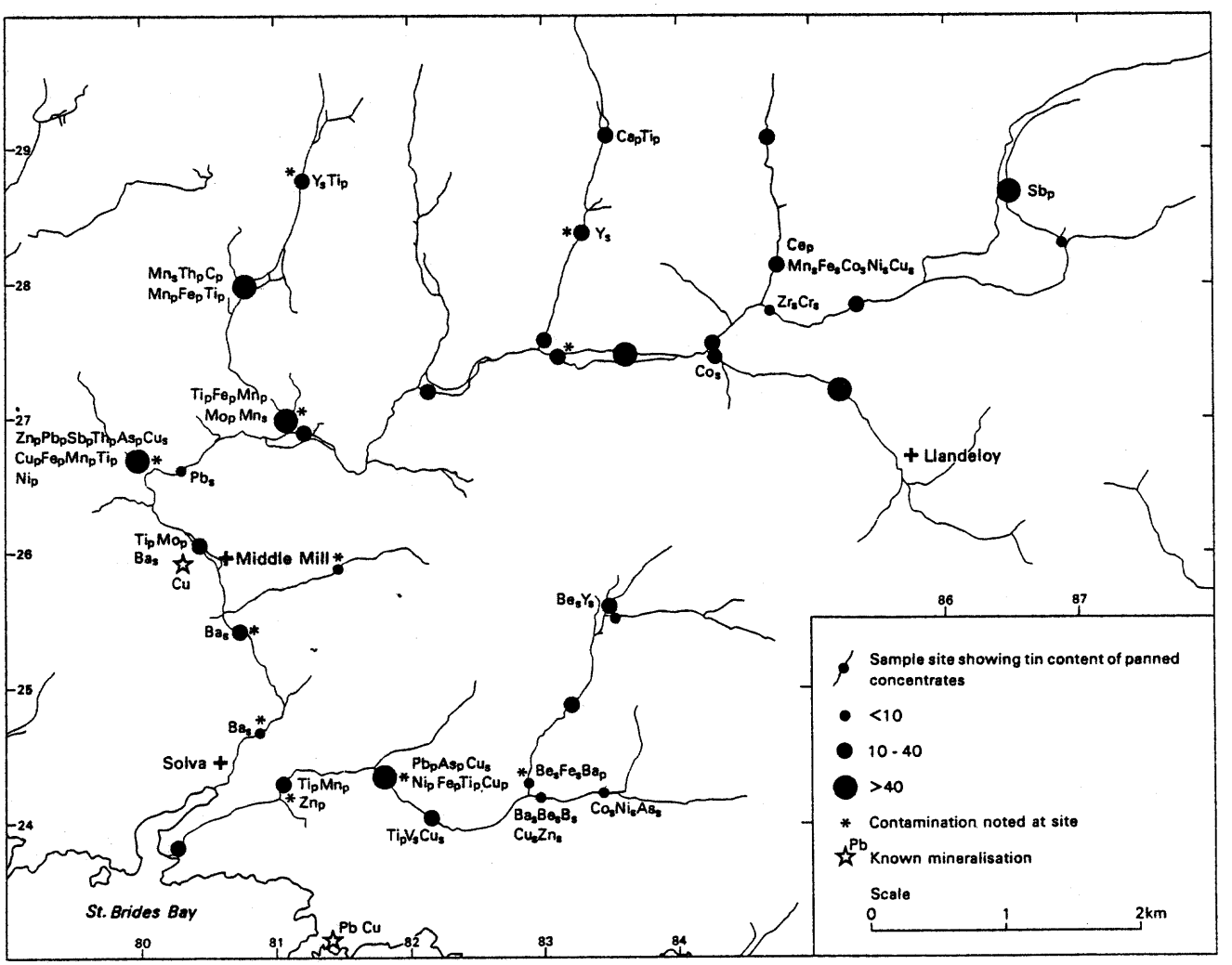

Figure 3 Location of drainage survey anomalies

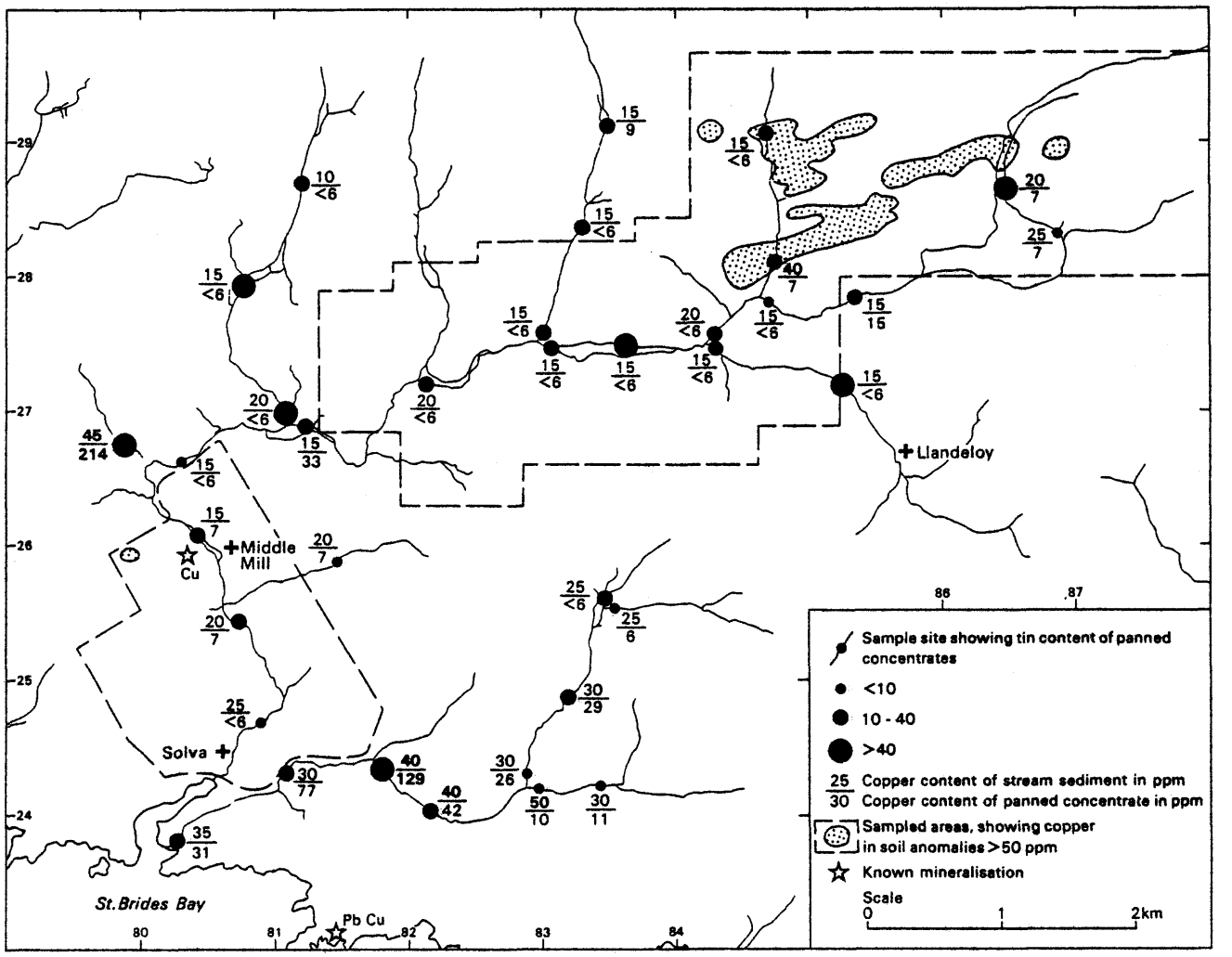

Figure 4 Drainage survey results for copper in stream sediments and panned concentrates

Results and interpretation

A complete set of results is given in Appendix 8 and summary in Table 5. Cumulative frequency curves and histograms were plotted to examine element distributions and determine threshold levels. The small number of samples resulted in some ambiguous plots from which distribution type and threshold levels proved difficult to determine. A large group of element distributions (B, V, Cr and Pb in sediment, Ni Cu, Zn, Ba, Ca and Th in panned concentrate) have approximately lognormal form, but the majority (Be, Ni, Ba, Cu Co, Mn, Y and Zr in sediments, Ti, Mn, Fe and Sn in panned concentrate) give sigmoidal or 'dogleg' plots on logscale probability paper indicating a bimodal form (Parslow, 1974; Sinclair, 1976). Fe in sediment has a normal distribution and other variables have either a complex or uncertain form; the latter caused by 'stepping' in the results and bottom-censoring of the data by analytical detection limits.

Threshold levels for elements with lognormal distributions were set at the 97.5 percentile level, equal to the geometric mean plus two geometric deviations for a perfect distribution, as a 'safety level', though, apparently, no anomalous populations, which might be related to mineralisation or other cause, are present. As no better criteria were available this level was also arbitrarily chosen for elements of uncertain and apparently complex distribution which may represent incomplete lognormal forms. Strictly, the 97.5% level yields only one result as anomalous but, because of the small number of samples, if there is a distinct break below the top two values both were considered anomalous.

Threshold levels for 'dogleg' plots on logscale probability paper were set at the point of significant departure of the lower (background) population from a straight line (Sinclair, 1976). For sigmoidal plots lines describing the upper and lower populations were constructed but in all cases, with the possible exception of Fe in panned concentrate, the median level and standard deviations of the upper populations suggested that they were related to background lithologies rather than bedrock mineralisation. Thresholds for this group were arbitrarily set to include the upper 10% of the upper population as a 'safety net'. For Fe in stream sediment the 95.5% percentile level, equivalent to the mean plus two standard deviations for a normal distribution, was chosen as threshold.

Mineralogical examination of the three panned concentrate samples containing the highest levels of base metals, tin, and elements concentrated in basic rocks (Appendix 8: nos. 16, 23, and 35) indicated that high levels of Sn in the samples were caused by contamination. High levels of other elements in the samples were related to the presence of Fe-Ti minerals (garnet, chromite, magnetite) or contaminants such as metallic fragments and yellow-glaze. No sulphides were seen except for minor pyrite and pyrrhotite in sample 35, suggesting that the principal base metal anomalies are not related to sulphide minerals in the samples.

Table 5 Summary of analytical results for drainage samples from the Solfach catchment

Element	Mean	Median	Maximum	Minimum	Geo. Mean	Geo. Mean +2 x Geo. Dev.	Threshold
Stream Sediments:							
Be	4.0	3.0	8.7	1.3	3.5	9.8	7.0
B	82	78.4	138	48.7	79.4	130	130
V	123	119	171	85	121	170	165
Cr	144	121	285	80	137	252	250
Ni	28.7	27	77	15	27	51	39
Co	24.1	19	104	6	19	36	50
Mn	4,654	3,638	20,550	867	3,706	13,397	6,500
Fe	46,500	44,100	69,800	23,500	45,186	74,989	6,700
Cu	23.1	20	50	10	21	48	38
Pb	34.8	30	60	20	34	55	54
Zn	140	140	250	70	133	252	220
As	10.6	10	26	<2	8	52	25
Ba	547	508	880	323	532	859	700
Y	37.3	36	78	19	36	59	50
Zr	433	441	791	231	414	771	780
Panned Concentrates:							
Ti	17,326	8,090	161,990	2,580	9,226	59,020	10,000
Ni	13.6	10	44	5	11.5	36	34
Mn	1,863	890	17,180	180	1,069	6,012	2,000
Fe	45,685	32,240	131,500	19,610	38,726	115,345	95,000
Cu	20.6	7	214	<6	8	89	100
Pb	206	16	5,877	<13	21.4	396.3	350
Zn	60.8	42	181	18	51	169	155
As	25.7	23	57	18	25	42	47
Mo	3.3	3	7	<1	3	12	6.5
Sb	-	<11	58	<11			?30
Sn	61.8	16	689	<9	20	270	40
Ba	148	126	426	34	124	429	420
Ca	4,395	3,190	19,040	860	3,572	13,062	12,000
Ce	520	394	1,490	26	316	3,334	1,400
Th	14.3	12	37	2	12	45	35
Streamwater:							
Cu		0.01	0.02	<0.01			
Zn		0.01	0.37	<0.01			?0.06

All results in ppm

Although not rigorous, because of the bimodal or complex and truncated form of many distributions, very highly significant (>99.95%) Pearson product correlations were considered to a useful guide to inter-element relationships and these are summarised in Fig. 5. Mineralogical and field evidence indicates that positive correlations and most variation within the data matrix can be related to basic igneous rocks (Mn_p*-Ti_p-Fe_p-Ni_p-?Ca_p-?Mn_s), clays and hydrous oxide precipitates (Co_s-Ni_s-Fe_s-Zn_s), detrital sedimentary rocks (B_s-Be_s-Ba_s-Cr_s) and heavy resistate minerals (Th_p-Ce_p-Sn_p-?Zr_s). There is also a suggestion of sulphide mineralisation in the presence of an ill-defined Cu_s-Cu_p-As_p-Pb_p-Zn_p-Fe_p group, though this could be generated by pyritiferous dark shales. Both Sn and Pb appear to be strongly associated with elements concentrated in basic rocks; a relationship which is considered to be spurious and caused by some of the most contaminated sites having basic rocks in their catchments.

*Subscript s denotes in stream sdiment, p in panned concentrate.

The spatial distribution of anomalies with respect to observed contamination, the Sn content of panned concentrates (used as an indicator of contamination on the basis of the mineralogical results) and known mineralisation are shown in Fig. 3. The two Sb anomalies both occur in samples containing high Sn and it is suspected that they are also caused by contamination. The only metal anomalies found in the catchment which could be related to sulphide mineralisation occur in the tributary running through St. Elvis. The element associations, bedrock geology and mineralogy all suggest that the high metal levels here are caused by basic intrusives and/or dark pyritiferous shales, but the presence of exploited base-metal vein mineralisation in the vicinity suggests another possible source.

Fig. 4 shows the distribution of copper in stream sediments and concentrates with respect to contamination, known mineralisation and copper anomalies in soil overlying bedrock mineralisation found subsequently. It can be seen that the pattern of drainage anomalies bears little relationship to the known mineralisation and that there is no well developed

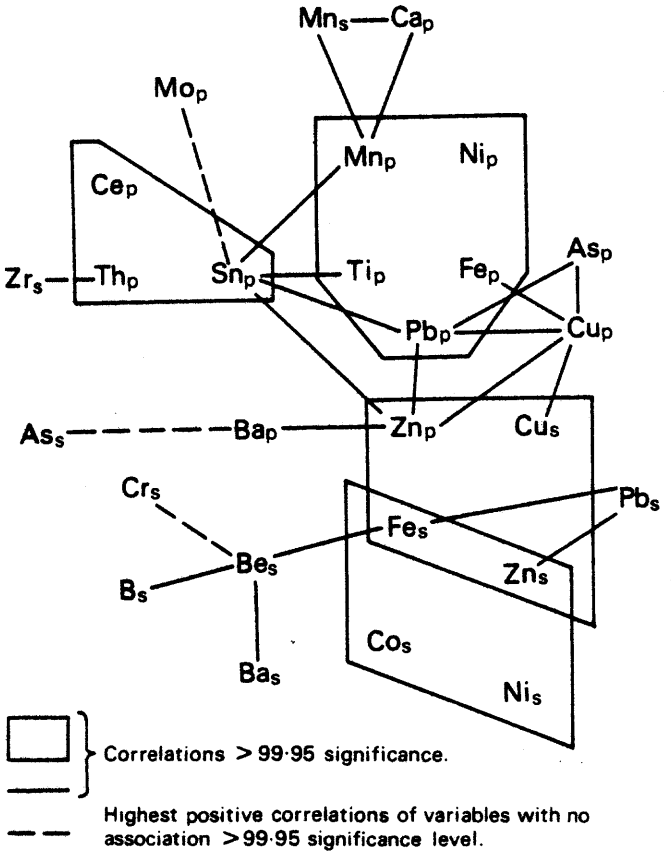

Figure 5 Diagrammatic illustration of highly significant positive correlations within the drainage survey data

dispersion train of anomalies downstream of the copper mineralisation located by soil sampling. One marginally anomalous copper in stream sediment result is the only indication of the mineralisation about Treffynnon. The isolated position, small magnitude and absence of an anomaly in concentrate, but association with anomalous levels of elements concentrated in hydrous oxide precipitates, are reasons to suggest that this weak Cu anomaly would not have been followed up during a routine survey.

The failure of the drainage survey to outline the area of hidden copper mineralisation about Treffynnon indicates the ineffectiveness of the technique for mineral exploration in geographically similar terrains.

Regional geophysics

The Llandeloy and Middle Mill areas are covered by the national aeromagnetic and gravity surveys and by a recent helicopter-borne magnetic and very low frequency electromagnetic (VLF-EM) survey of part of west Dyfed. Mean terrain clearance was 60 m for the magnetic and 75 m for the VLF-EM sensors (Cornwell and Cave, in press). Extra gravity stations, including two detailed traverses, were occupied to supplement existing data in the area.

Magnetic surveys

The national aeromagnetic map (IGS, 1980) shows the survey areas lying at the eastern end of a NE-SW elongated magnetic high (Fig. 6), one of a series of similar features extending along the south Welsh coast from Ramsey Island to the Vale of Neath. These may be fragments of an original single linear feature which has been broken up by postulated NE-SW transform faults active intermittently during the Caledonian and

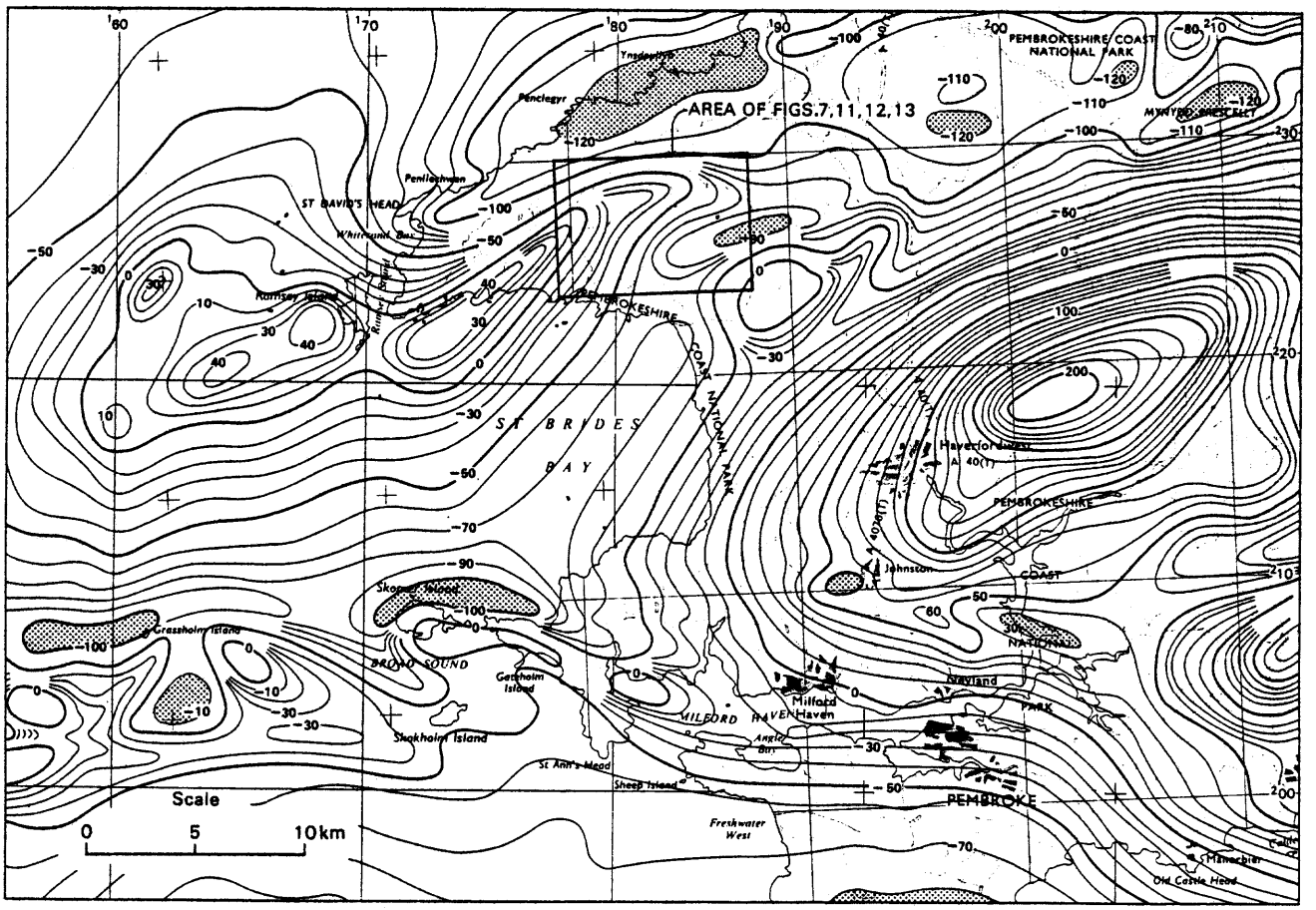

Figure 6 Aeromagnetic anomaly map of west Wales (IGS 1980). Contours at 10 nT intervals with magnetic lows stippled

Hercynian orogenies (M. J. Arthur, private communication, 1982). The related suggestion that the south Wales magnetic anomalies have been displaced by 140 km dextral transcurrent motion along the precursor to the Bala Fault, from an original position adjacent to the Harlech Dome magnetic anomaly, is of particular interest to this investigation. Dextral transcurrent movement of the same order has also been proposed for the Menai Fault (Nutt and Smith, 1981).

On the more detailed airborne magnetic survey map (Fig. 7) the broad Llandeloy/St. David's high has numerous short-wavelength features superimposed on it indicating that the magnetic rocks reach the surface. Near the coast, west of the present survey area, the anomalies can be seen to be due to Precambrian rocks of the Pebidian Volcanic Series and perhaps also to intrusions within them. The pattern of small, short features is ascribed to the disruption of magnetic horizons by the numerous faults in the area. With the exception of the Ramsey Sound Group, most of the Pebidian rocks are more or less magnetic. The Pebidian forms the core of a horst running the length of the St. David's Peninsula, and the breadth of the main anomaly shows that the sides of this block must extend to some depth. Numerical modelling of the three profiles shown on Fig. 7 indicates sides dipping away at 40–60° to a depth of about 3 km (Figs. 8–10). Gradients indicate that the dip of the southern margin lessens to the west. To effect this interpretation some sweeping assumptions had to be made, namely: a block uniformly magnetised by induction with a value of susceptibility typical of acid igneous rocks. Consequently the models should be regarded only as order-of-magnitude indications of the true shape of the block. (See Appendix 5 for details of the interpretation.)

Two groups of ill-defined magnetic anomalies indicate that the porphyry intrusions around Middle Mill, and the Ordovician Brunel Beds are also weakly magnetic.

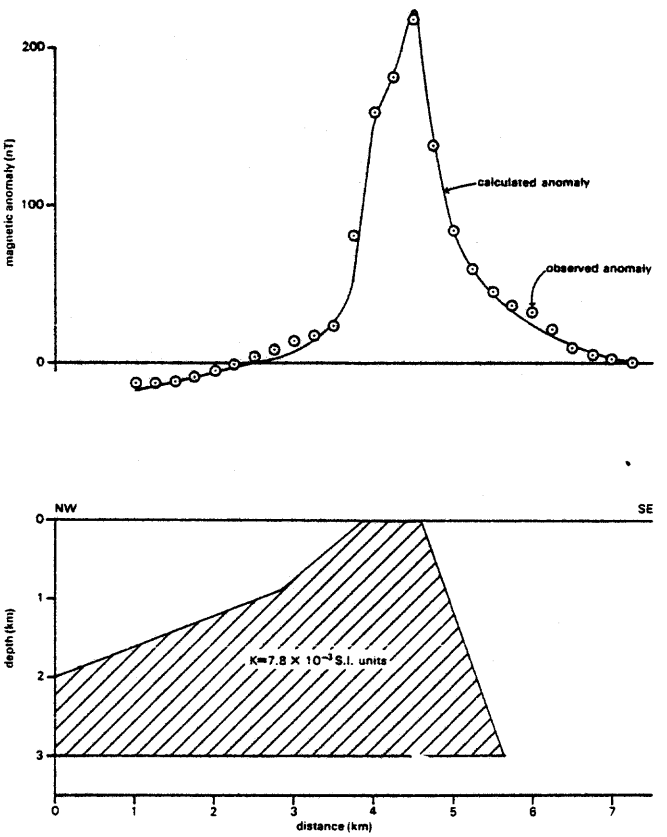

Figure 8 Interpretation of aeromagnetic profile 1

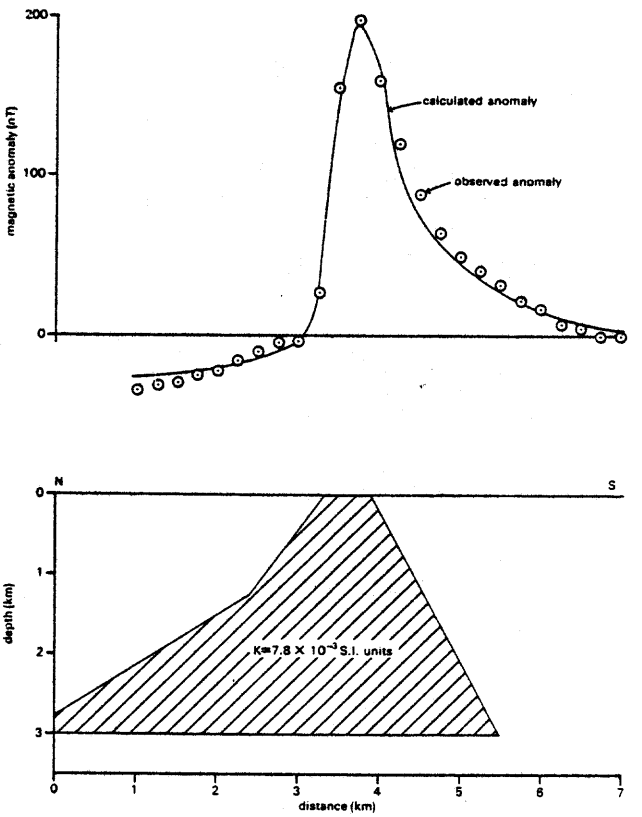

Figure 9 Interpretation of aeromagnetic profile 2

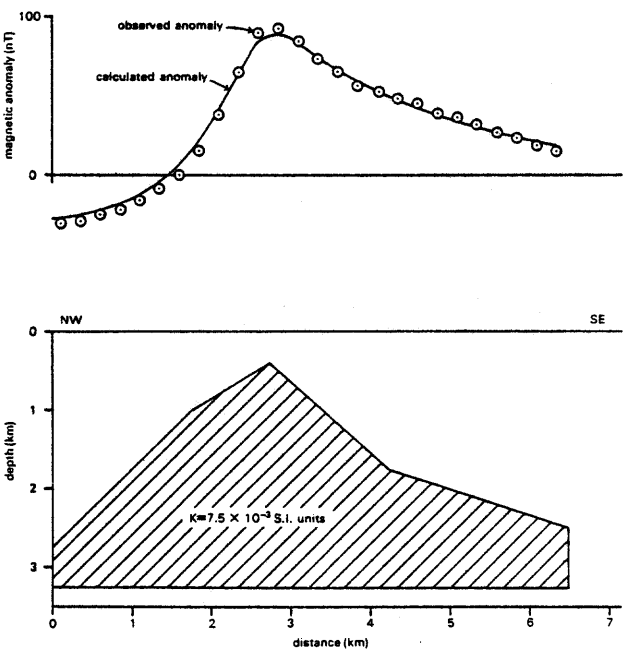

Figure 10 Interpretation of aeromagnetic profile 3

Gravity survey

The Middle Mill intrusions correspond to a slight low in the Bouguer gravity anomaly field (Fig. 11), implying a density slightly lower than the surrounding rocks. A Bouguer anomaly gradient of about 1 mGal km^{-1} crosses the survey area, values increasing northwards from a low associated with intrusions into the Hayscastle Anticline to the south, towards a high which lies offshore along the coast of Cardigan Bay. There is no gravity anomaly associated with the magnetic feature interpreted above.

Electromagnetic survey

The airborne VLF-EM survey allows some geological structures to be recognised in areas where exposure is very poor (Fig. 12). High horizontal intensity values imply conductive rocks, faults or overburden, while low values indicate electrically resistive rocks. A compilation of the ground resistivity results is given for comparison (Fig. 13). The main features which can be interpreted from the regional geophysical maps have also been marked on Fig. 13. The fault forming the northern edge of the horst is particularly clearly defined by all geophysical methods. It divides denser, non-magnetic rocks from the magnetic rocks which form a discontinuous arc to its south. A second discontinuity, less well defined, runs NE-SW through both ground survey areas. It divides VLF-EM anomalies striking predominantly E-W from those striking NE-SW, and could be the southern fault of the horst. Several other faults can be inferred from the VLF-EM map, but only those which can be supported by other geophysical evidence have been marked on Fig. 13.

MIDDLE MILL

Introduction

The area comprises a gently undulating peneplain, mostly between 60 m and 90 m above O.D., and deeply incised by the Solfach valley. There is very little exposure, but a reconnaissance visit to a large quarry [SM 8045 2590] in microtonalite and adjacent sedimentary rocks at Middle Mill revealed the presence of sulphide mineralisation. Consequently, soil samples were collected and geophysical measurements taken along six traverse lines trending 330°, spaced 300 m apart and totalling about 10.5 km in length set up across intrusions emplaced within the Solva Group.

Geology

The Solva Group here is composed of purplish-blue siltstone and mudstone with thin beds of pale grey mudstone and plentiful coarse-grained, graded, locally pebbly, quartzose sandstone beds 60 to 90 cm thick. The sedimentary rocks north of the quarry at Middle Mill are folded into gentle NE-trending folds. In the quarry the sedimentary rocks overlie a concordant intrusion of porphyritic microtonalite, the base of which is not exposed. The intrusion appears to terminate at a NE-trending fault on the south side. A dyke of porphyritic quartz-microdiorite cuts sedimentary rocks on the north side of the quarry. Apart from an outcrop of altered microtonalite about 1 km to the south [SM 8083 2506] no other rocks are exposed in the area.

Mineralisation and alteration

There are plentiful signs of mineralisation in Middle Mill quarry and several samples were collected for detailed mineralogical examination and chemical analysis. Among the sedimentary rocks sulphides occur most abundantly in the coarse-grained sandstones. These rocks consist mostly of quartz grains with some feldspar and muscovite in an altered muddy matrix now comprising sericite, chlorite, which is commonly spherulitic, opaque minerals and rare carbonate. Among the opaque minerals are fine-grained crystals of ?magnetite and large, commonly euhedral, porphyroblasts of pyrite. Chalcopyrite and rare bornite, both altering to covellite and malachite, are present locally. Sphalerite and galena were observed in one rock only. Pyrite commonly occurs on joint surfaces and in veinlets.

The mineral composition and texture of these rocks suggest that they have been modified by thermal metamorphism. Laminae and thin beds of siltstone and mudstone associated with them show obvious signs of hornfelsing. Sulphides are commonly enriched in these layers, which contain small amounts of carbonaceous material. In the one banded sample examined that contains galena and sphalerite these minerals were preferentially concentrated in the mudstone bands.

The intrusive rocks in the quarry are intensely altered both to sericite-epidote-chlorite and sericite-chlorite assemblages, both with late carbonate in places. Chlorite-epidote pseudomorphs after amphibole commonly contain magnetite. Disseminated pyrite is relatively rare in the intrusive rocks, though it is present on joint surfaces and in veinlets.

Some of the sulphide in the sedimentary rocks may be syngenetic in origin, but most of it is either remobilised or introduced. Sulphides are most abundant in rocks showing the strongest signs of contact metamorphism and it is suggested that they were introduced during the late hydrothermal stages of intrusion.

Geochemistry

Rock geochemistry

The majority of intrusive rock samples collected in this area came from Middle Mill quarry because of the poor exposure elsewhere. All the samples from the larger intrusions (Table 2; no. 8, Solva; nos. 40, 41 NNE of Solva; nos. 12-14 and 17, Middle Mill quarry) are of porphyritic microtonalite. A single sample taken from a small dyke-like intrusion at the north end of the Middle Mill quarry is of porphyritic quartz-microdiorite. The porphyritic microtonalite samples display many of the extreme results reported in the general account for the group as a whole: a feature attributed to the strong alteration observed in thin section. None of the intrusive rocks contains high levels of chalcophile elements and variations in chalcophile elements do not show close correlation, despite the presence of abundant pyrite on joints in several samples.

Analyses of Solva Group sandstones and siltstones from Middle Mill quarry are shown in Table 4. The only sandstone sample free of sulphides (no. 11) has a composition broadly similar to that of an average sandstone (Turekian and Wedepohl, 1961) except for a relatively high level of Th and low Ce and Y, features also shared by the pyritised sandstones which probably relate to the provenance of the rocks. The pyritised sandstones (Table 4) all contain high levels of Fe, Ni and Zn compared with the average sandstone and the pyrite-free sample. The banded siltstone-grit sample contains relatively high levels of Pb and As even compared with the average slate or shale (Turekian and Wedepohl, 1961; Wedepohl, 1969). Mineralogical examination of this rock indicated that Pb and As are concentrated in mudstone layers and organic lenses, whilst pyrite is concentrated in the coarse bands. The more highly mineralised samples show, as would be expected, notable discrepancies when compared with average analyses of sandstones and siltstones. Differences in some chalcophile elements are very clear with high levels of Cu, Pb, Zn and Mo reported.

In contrast to the intrusive rocks there is a strong (99% confidence level) positive rank correlation between the chalcophile elements Cu, Pb, Zn and Mo in the sedimentary rocks. Highest levels of these elements are found in the brecciated rocks and they are related to epigenetic sulphide mineralisation. This chalcophile group is not significantly correlated with a second positive inter-correlated group consisting of As, Ni, Ti, Fe and Mn. High levels of these elements are

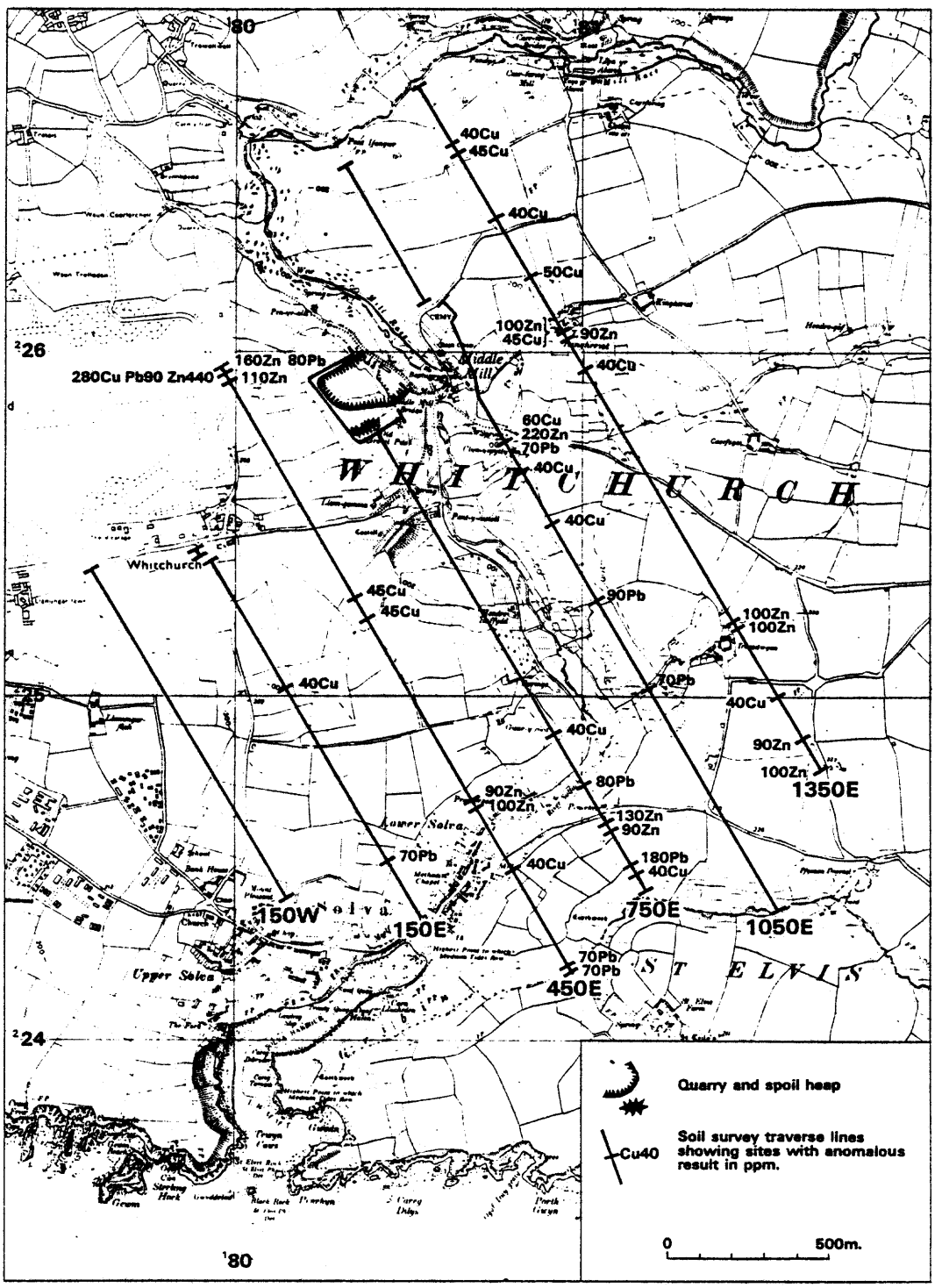

Figure 14 Location of soil anomalies in the Middle Mill area

related to the presence of mafic silicate minerals, magnetite and pyrite in the rocks. In the epigenetic sulphide group Cu shows the greatest contrast to background: high levels are related to the presence of chalcopyrite (samples 21, 35, 37, 38 and 39), bornite (sample 37), covellite and malachite (sample 38). Paradoxically sphalerite was noted in sample 21 which shows only the weakest indications of Zn enrichment whilst no discrete Zn minerals were observed in the sections of other samples containing much higher Zn levels. These discrepancies are attributed to the poor sample represented by a thin section when the rocks are grossly inhomogenous.

There is no obvious relationship between elements concentrated in sulphides and those which may be related to alteration. Ba, Rb, Sr and Ca yield high levels in individual samples but, as in the intrusive rocks, there is no regular pattern which can related to observed alteration.

It is concluded that both weak syngenetic and epigenetic mineralisation may be present in the sedimentary rocks at Middle Mill, with the high levels of Cu, Pb and Zn in some of the rocks concentrated by the latter process. The epigenetic mineralisation may be connected with the intrusive episode but the lack of disseminated sulphide and any enrichment of chalcophile elements in the intrusive rocks suggest that the mineralisation exposed in the quarry is not of porphyry type.

Soil sampling survey

Four hundred and thirty one soil samples of about 200 g were collected at 25 m intervals along the traverse lines from two or more holes driven as deeply as possible using a 120 cm hand auger (Fig. 14). In addition, as an orientation exercise, 23 samples were collected at the same interval and by the same method from around the margin of Middle Mill quarry. Samples consisted mainly of unconsolidated material derived from glacial or periglacial deposits and weathered bedrock from below the organic-rich topsoil. A few samples collected in the floor of the Solfach valley contained recent alluvium. All samples were dried, sieved and the -85 mesh BSS (0.15 mm) fraction analysed for copper, lead and zinc by atomic absorption spectrophotometry following dissolution in hot concentrated nitric acid for one hour.

Analytical results are summarised in Table 6. Threshold levels were determined from cumulative frequency plots (Fig. 15) following the methods of Lepeltier (1969) and Sinclair (1976). Copper shows an approximately lognormal distribution whilst lead has a binormal or truncated sigmoidal form. Minor deviations in both plots are attributed to stepping in the analytical data. Zinc shows a more complex form suggesting the presence of a background normal population and a higher lognormally distributed group. Threshold for all three elements was set at the 97.5 percentile level, equivalent to the mean plus twice the standard deviation for a perfect lognormal distribution. For lead and zinc the 97.5 percentile level coincided approximately with the departure of the background population from a straight line.

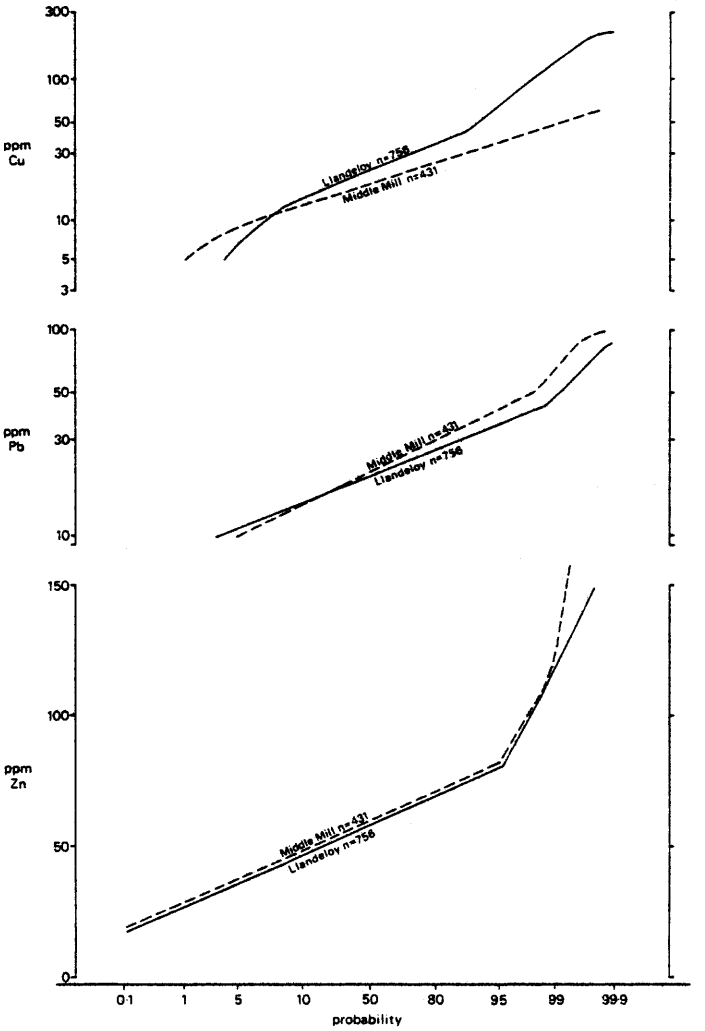

Figure 15 Cumulative frequency plots for Cu, Pb and Zn in soil samples from Middle Mill and Llandeloy

The threshold levels (Cu 38 ppm, Pb 53 ppm, Zn 81 ppm) were applied to the results of the 23 samples collected around the margin of the Middle Mill quarry. None of the results was anomalous. All the results fall in the central part of the sample populations for the whole area: Cu 10-25 ppm, median 15 ppm; Pb 20-40 ppm, median 30 ppm; zinc 50-70 ppm, median 60 ppm. The lack of anomalous results in samples collected from as closely as possible to bedrock mineralisation was unexpected. The lack of response cannot be accounted for by thick drift deposits (they appear to be generally <3 m thick in the vicinity of the sample sites), or to leaching related to deep weathering, for there is no evidence for this in the quarry. Very limited mobility,

Table 6 Summary of copper, lead and zinc results in ppm for 431 soil samples from the Middle Mill area

Element	Mean	Geometric mean	Geo. mean + 2 x geo. dev.	Median (background)	Maximum	Second highest result	Minimum	Threshold
Cu	22	20	41	20	280	60	5	38
Pb	23	26	55	20	180	90	10	53
Zn	56	53	99	50	440	220	10	81

producing a very limited dispersion halo, is a possible cause of the discrepancy, but the most likely explanation is that the base-metal mineralisation sampled in the quarry is very localised in extent. The high base-metal levels are confined to thin brecciated zones and no soil samples were collected closer than 20 m from the quarry face because of topsoil stripping. Pyritisation, though more widespread, would not be detected in the soil results unless accompanied by base-metal enrichment.

The position of anomalous samples collected along the traverse lines is shown on Fig. 14. They are very scattered, mostly of low magnitude, and form no clear spatial pattern. All three element distributions are dominated by one or two high results which are concentrated in a three site anomaly at the northen end of traverse 450E [SM 7996 2593]. The middle site of this group contains the highest levels of Cu and Zn in the area as well as being one of only two sites to be anomalous for all three elements determined (Fig. 14). The anomalies are thought to be caused by contamination as the soil was found to contain metal and glass fragments and the sites lie close to the eastern end of St. David's airfield. The second site anomalous for all three elements is found on line 1050E [SM 8077 2573]. It contains an outlying high level of Zn, is situated at the base of a steep slope by a stream and is close to a spring at Clyn-yspytty. The location suggests that this is a seepage anomaly, but whether the high metal levels are derived from background sources or hidden mineralisation is uncertain. The cause of the only other distinctly anomalous result, for Pb at SM 8114 2450 on line 750E, is uncertain. Other anomalies are all weak and close to the threshold levels; a few can be related to contamination or seepage but the cause of most is uncertain.

None of the anomalous results or variation in background levels along traverse lines could be related to the known geology, but exposure is very poor and available geological maps so uncertain that it does not necessarily mean that a relationship does not exist.

Unless glacial deposits are exerting a very strong masking effect, or dispersion halos are extremely restricted, then the soil results suggest that there is no substantial hidden mineralisation close to surface in this area. The results from around the quarry suggest that dispersion is limited and that consequently small-scale and deeply buried mineralisation may have escaped detection.

Geophysics

Induced polarisation (IP) measurements were made along the traverse lines, using the dipole-dipole array with a dipole length (a) of 50 m. To provide some depth information, readings were taken at dipole separations n = 2 to n = 6, where n x a is the separation between the dipole centres. All lines were surveyed by proton magnetometer, and some very low frequency electromagnetic (VLF-EM) measurements were also made, though the latter were so strongly affected by man-made interference that they are not presented here. Detailed airborne magnetic and VLF-EM data were also available for the area.

The results are summarised on Figs. 16 and 17 and described in detail in Appendix 3. Severe problems of artificial noise were encountered, and most of the anomalies can be ascribed to man-made sources.

The chargeability anomalies measured are marked on the magnetic anomaly map from the airborne survey (Fig. 16). The porphyry intrusions in the area seem to be weakly magnetic and coincidence of high chargeabilities with a magnetic anomaly may indicate a mineralised intrusion. Three such locations occur, marked A, B and C (Fig. 16). The IP effects at B, and both IP and magnetic anomalies at C, however, almost certainly have man-made sources, namely water-mains. Anomaly A extends westwards from the Middle Mill quarry (where mineralisation is exposed), to the airfield boundary, and has no visible artificial origin. The forms in pseudosection of the IP anomaly on lines 450E and 650E are, however, indicative of a narrow near surface source, most likely be to a water pipe. At D, minor IP and magnetic anomalies coincide with a small porphyry body, but powerlines also cross the traverse at this point. Several IP anomalies occur unaccompanied by magnetic features, but in almost all cases are due to artificial sources, as detailed in Appendix 3.

The resistivity results (omitting the strongest man-made effects) are superimposed for comparison upon the contour map of VLF horizontal intensity from the airborne survey (Fig. 17). There is a general inverse correlation between the two quantities, except where strong topographic VLF effects occur along the Solfach gorge, and where superficial low resistivity material was observed. The broad pattern of bedrock resistivity has NE-SW (060°E) grain, but exposure is so poor that it is not possible to see clearly the relationship to geology. A linear conductive feature with this orientation runs about 200 m south of the baseline. It marks the southern edge of several magnetic features and could be a fault. Another possible fault, running at 035° across the northwest corner of the area forms the southern edge of high resistivity weakly magnetic rock, probably the porphyry exposed in the quarry.

In summary the geophysical surveys at Middle Mill did not suggest the presence of substantial mineralised intrusions at or near the surface. Small mineralised structures may occur to the west and south of Middle Mill quarry, but no geophysical anomaly was completely free of man-made interference.

Assessment

No indications of near-surface disseminated copper mineralisation were revealed either by the soil survey or by geophysical measurements. The copper with minor lead and zinc mineralisation in sedimentary rocks from Middle Mill quarry is thought to represent minor epigenetic mineralisation associated with an intrusion of microtonalite. Some metalliferous concentrations in the sedimentary rocks may be of syngenetic origin, remobilised by the igneous event. The intrusive rock itself is highly altered, probably by late-stage hydrothermal activity, but except for pyrite, which occurs commonly on joint surfaces and sparsely in disseminated form, the intrusion is not mineralised in the quarry.

Exposure in the area is very poor. The little outcrop that is available for examination reveals a complex tectonic history. It cannot be concluded from this survey that the intrusion exposed in the quarry is not associated with mineralisation at depth.

LLANDELOY

Introduction

Reconnaissance survey lines for soil geochemistry and geophysical measurements were laid out to cover the eight intrusions shown by Williams (1933) to have been emplaced within the Cambrian and Precambrian rocks. Thirteen N-trending lines at 600 m spacing with two intermediate lines at 300 m spacing at the western end of the area, covering about 12.5 km^2, were surveyed first. The results indicated an area of special interest covering about 4 km^2 around Treffynnon, in which additional traverse lines were placed to close the traverse spacing to 200 m (Fig. 30). Radiometric, IP and magnetic measurements were made and soil samples were collected along all the lines. Several geochemical

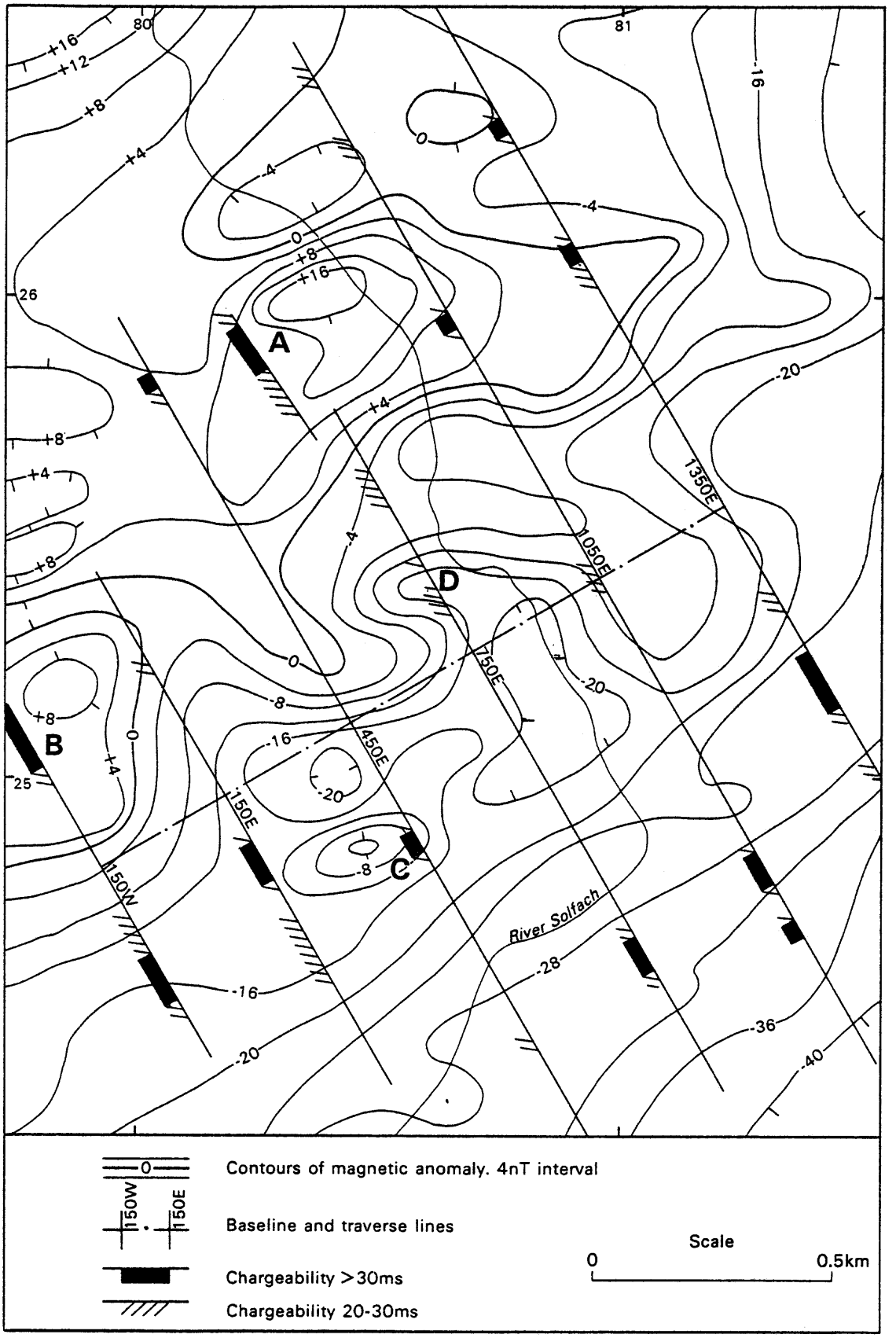

Figure 16 Magnetic anomaly and chargeability map, Middle Mill

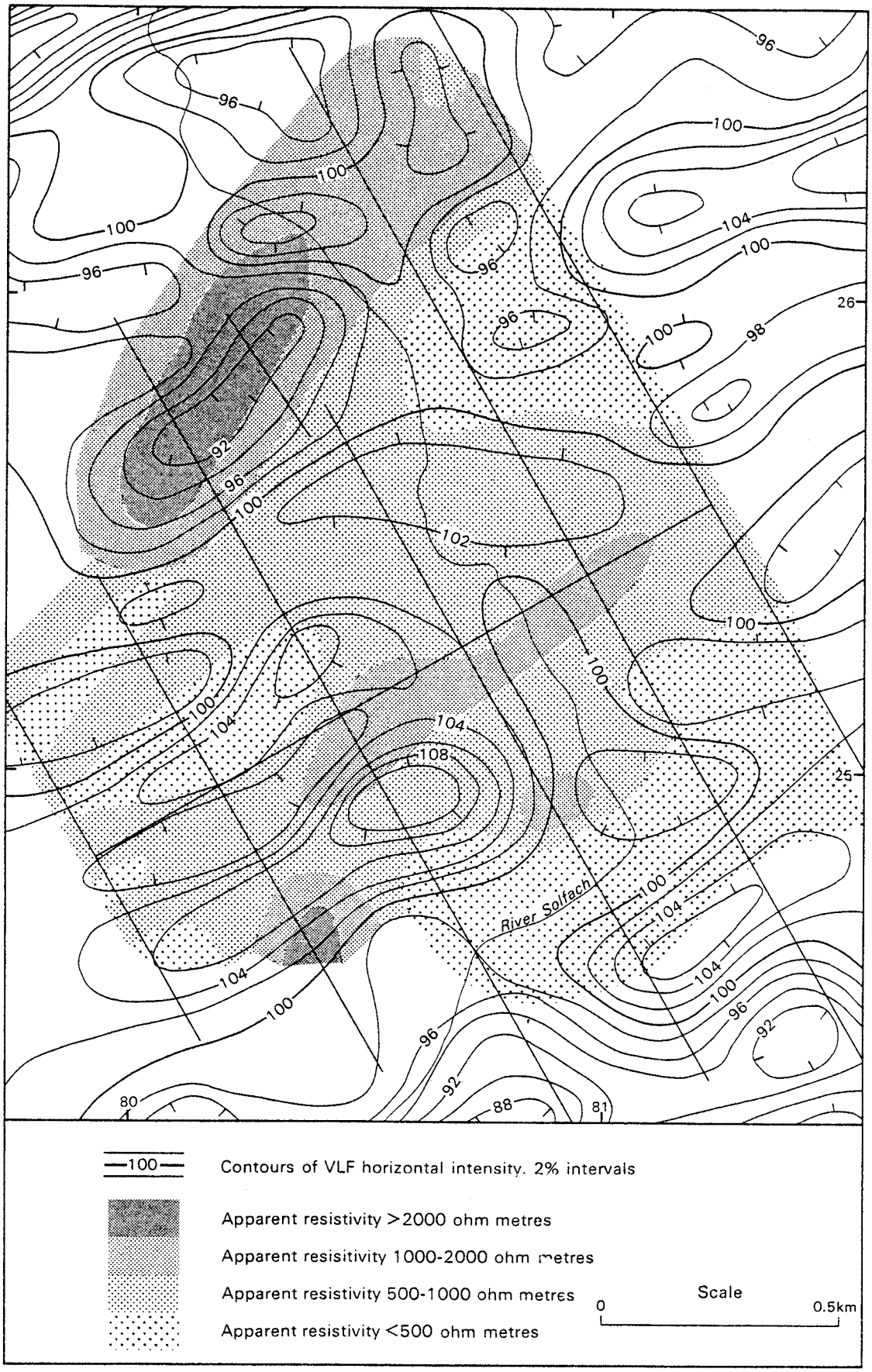

Figure 17 VLF-EM and apparent resistivity map of the Middle Mill area

and geophysical anomalies were identified. Explanations for them were not evident from the examination of surface exposures and nine boreholes were drilled to find their causes. In addition, a gravity survey was carried out in an attempt to find another method for refining the setting of the mineralised zone. Down-hole geophysical measurements were taken in five of the boreholes.

All the boreholes were drilled using the B.G.S.JKS 300 rig. Eight vertical holes were drilled to between 21.45 and 45.72 m; the ninth, an inclined hole, was stopped at 124.12 m. BQ core was retrieved from all holes above the depth of 72.26 m; and AQ below that in the ninth hole.

In boreholes 1 and 8 no samples were collected until the first solid core was retrieved. In all the other holes samples of the superficial deposits were taken while the casing was being driven.

While drilling it was discovered that much of the area was underlain by a previously unrecorded, locally thick succession of superficial deposits. The third borehole (3A) was stopped at 26.83 m and re-sited in an attempt to avoid this deposit, but on the second attempt this borehole (3B) penetrated the same thick deposit and collapsed before solid was reached.

Detailed logs of all nine holes have been lodged with the Aberystwyth office of B.G.S. Abbreviated logs are presented in Appendix 1 and graphic logs in Figs. 20 to 28.

Geology

Introduction

The map showing the solid geology for the area around Treffynnon (Fig. 18) was constructed using data from the few outcrops still accessible, the map of H. H. Thomas, the geophysical surveys, the boreholes and the distribution of float. Measurements of the dip and strike of stratified rocks were possible at only two localities and the exposures were such that modification of the orientation by hillcreep or other agencies could not be ruled out. Information on the superficial deposits was gained mainly by hand augering during the soil survey, and from the boreholes.

Table 7 The stratigraphic succession in the Treffynnon area

Sedimentary and volcanic rocks	Drift deposits	Pleistocene
	Lacustrine deposits	?Tertiary
	Tetragraptus Shales Brunel Beds	Ordovician
	Treffynnon Group volcanic rocks	?Cambro/Ordovician
	Solva Group quartz-wacke and siltstone	Cambrian
Igneous rocks	Intermediate and acid intrusions	Post-Cambrian

In this section account is taken only of the small area of the detailed survey carried out around Treffynnon. Notes on the whole of the reconnaissance area are in the regional account.

The succession (Table 7) consists of sedimentary and volcanic rocks of possible Cambrian and Ordovician age into part of which is emplaced a complex of intermediate and acid intrusive rocks. Lacustrine sediments of probable Tertiary age occur in much of the

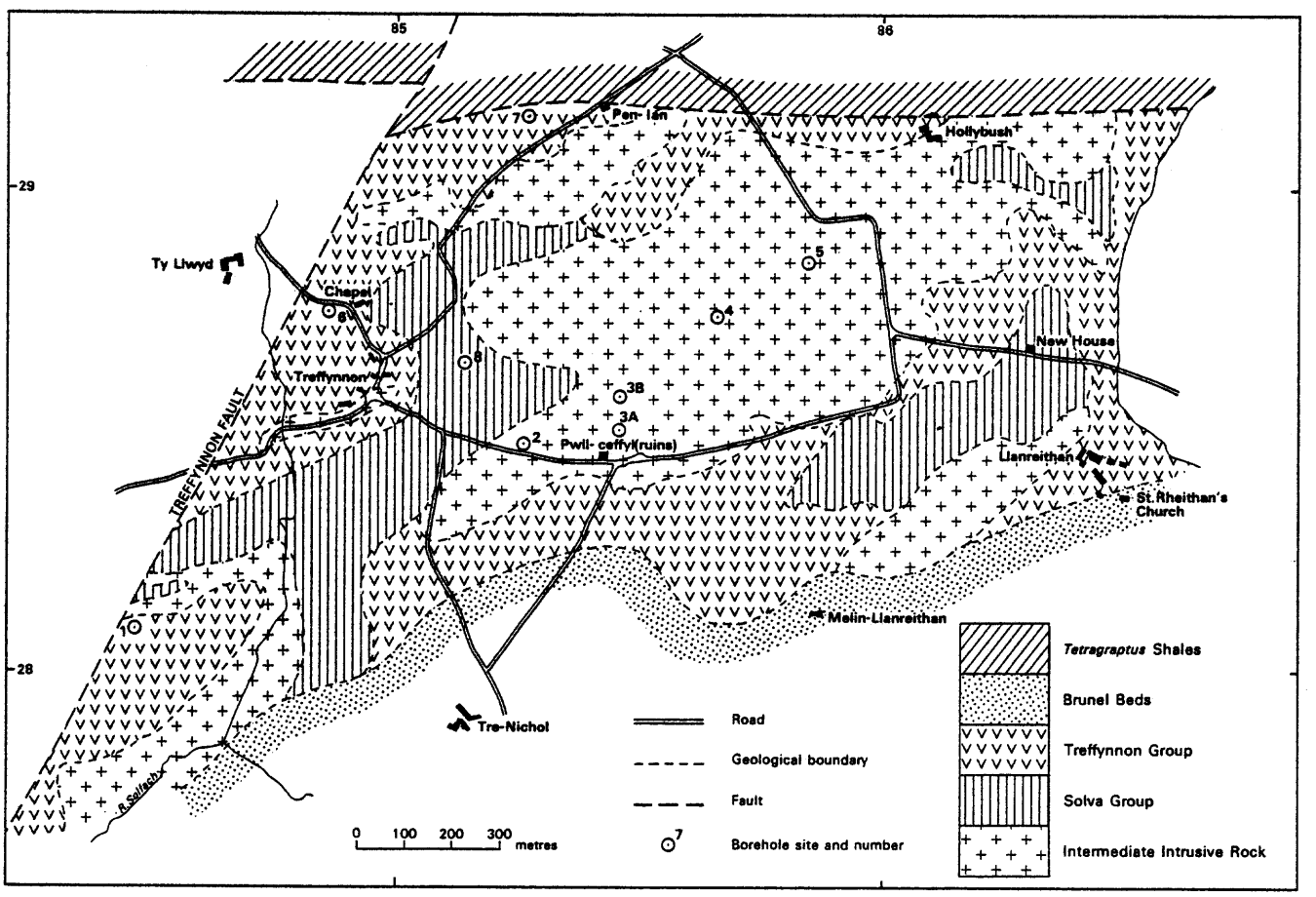

Figure 18 The solid geology of the area around the boreholes

area and periglacial and glacial deposits form blanket deposits masking them and the older solid rocks.

Stratigraphy

Solva Group According to Williams' (1933) interpretation, the intrusive rocks in this area are emplaced entirely within the Treffynnon Group. Borehole 8, however, penetrated a thick succession of sedimentary rocks which showed strong affinities to the Solva Group. Nowhere here are similar rocks exposed, but the rock types encountered in the borehole are dominant in float in several places.

The succession in borehole 8 (Fig. 28) consists of northward-dipping, mainly thinly bedded, green, fine or medium-grained quartz wacke sandstone with wisps and laminae of mudstone in places. In the top ten metres and at intervals below, the quartz wacke is thinly interbedded with up to an equal proportion of silty mudstone and siltstone. Beds of coarse-grained arkosic and quartzose sandstone were recorded at only three levels.

Between 45 and 72 m depth, but mostly between 62 and 72 m, there are several thin laminae of tuffaceous mudstone. The laminae tend to be graded, with a concentration near the base of crystals, angular and subangular fragments of feldspar, minor quartz and oval (?bomb-shaped) quartzo-feldspathic lithic fragments set in a dense, sericite matrix. These laminae are usually closely associated with laminae of silty, sandy mudstone and a distinctive spotted mudstone. Some of the spots, which are most likely to be due to thermal metamorphism, have an amorphous ferruginous core and a clear sericite rim; others are slightly richer in chlorite than the host rock.

At seven levels thin beds of black magnetite sandstone were recognised. They are usually less than 1 cm thick and they are always associated with a heterogeneous assemblage of sedimentary rock types in units no more than 12 cm thick, which contrast markedly with the rock above and below. Among the interbedded rock types are greenish-grey fine sandstone, white quartzite, purple or bluish-grey massive sandstone and spotted mudstone. There is usually some epidotisation either along beds or fractures. These heterogeneous units occur elsewhere in the core without associated magnetite sandstone.

The fine-grained clastic component in the rocks has been recrystallised to green mica, sericite, chlorite and microcrystalline quartz and some rocks possess a good sericite-defined schistosity. It is probable that these rocks have undergone a regional metamorphism, but there is a suggestion also (see later) of pervasive hydrothermal alteration. The spotting noted in the mudstones indicates that there has been a thermal metamorphic overprint, which has possibly led to some recrystallisation, especially of the green mica.

The sedimentary structures seem to indicate deposition in a turbulent shallow water environment. The sandstone beds are either massive of thinly laminated; the coarse-grained beds are graded. Evidence of slumping is present in convoluted units between planar bedded units and there is abundant soft sediment deformation: load casts, downward sandy flames, sandballs and microfaults are common. Flaser bedding is characteristic of the thinly interbedded sandstone and mudstone units and washouts characterise the base of some sandstone beds.

The succession bears no resemblance to the Treffynnon Group described by Williams (1933), but shows similarities to parts of his middle Cambrian. It compares with the middle Cambrian Solva Group as exposed at Solva except that no manganiferous beds are known at Treffynnon and no magnetite-bearing beds at Solva. At Porth y Rhaw, about 1.5 km west of Solva, Price (1963) recorded ashy bands in the middle Menevian, which overlies the Solva Group. In North Wales tuffaceous beds are present in the Gamlan Formation, which correlates with the Solva Group. Whether or not the succession encountered in the borehole is the Solva Group, it is considered most likely to be middle Cambrian in age.

Treffynnon Group Only two of the several outcrops of volcanic rocks recorded by Williams (1933) are still accessible. The deeply weathered exposure in a quarry near Treyscaw Farm [SH 8464 2810] consists of thinly bedded brownish yellow siltstone overlying brecciated massive rock. In thin section the bedded rock is composed of very fine-grained sericite and quartz with quartz-rich silty laminae and lenses and is obviously of volcanic origin. The other occurrence is a poor exposure of weathered light grey siltstone with thin quartzose siltstone beds in an old quarry near Llanreithan [SM 8645 2865]. There are no volcanic rocks in the quarry. Williams (1933) commented that parts of this group had been mapped as Lingula Flags by the Geological Survey, and the rocks in this exposure certainly show similarities with the Cambrian rocks, but the quality of the exposure is too poor to be definite about their affinity.

Volcanic rocks were encountered in borehole 1, which is about 180 m west of this locality, and in boreholes 6 and 7 (Figs. 20, 26 and 27). In borehole 1 the volcanic rocks are intruded by thin sills of porphyritic microtonalite in the top 12 m. The rocks are deeply weathered and the core is badly broken, but it appears that a faulted stratified succession of volcanic breccias, crystal tuff, porphyritic acid lava and thinly interbedded muddy quartzose sandstone, tuff, lapillistone and mudstone was penetrated. The breccia is typically polymict with the majority of the angular fragments composed of quartzose sandstone and laminated silty mudstone; the remainder include highly altered porphyritic acid volcanic rock and aggregates of quartz and heavily altered feldspar crystals. The matrix, of indeterminate origin, is structureless, fine-grained quartz, feldspar, sericite and minor chlorite.

The top 15.10 m below rockhead in borehole 6 consists of two thick units of porphyritic acid volcanic rock, separated by a bed, 37 cm thick, of poorly sorted recrystallised quartzite. The volcanic rock is uniformly porphyritic with locally well-orientated sericitic pseudomorphs after feldspar phenocrysts up to 3 mm long and small recrystallised quartz phenocrysts, in a matrix of equant, platy feldspar, minor quartz, sericite and chlorite. The rock is brecciated in parts and contains some lithic inclusions. The uppermost few centimetres of the unit below the quartzite bed display contorted banding. The texture of the rock is most likely to be that of an acid lava. Rock similar to this was encountered near the top of borehole 7, apparently intruded by quartz-microdiorite.

The evidence gathered here suggests that the Treffynnon Group consists of acid pyroclastic and extrusive rocks interbedded with shallow water sedimentary rocks. The rocks are highly altered, locally to sericite, and the quartzose sandstones have undergone secondary silicification. The age of the rocks is not known for certain. Williams (1933) regarded them as being Precambrian and he surrounded their area of outcrop with faults. The presence of probable Cambrian in the area around borehole 8 and distribution of other possible areas of Cambrian sedimentary rocks with respect to the known occurrences of the Treffynnon Group suggest that the volcanic rocks may unconformably overlie the Cambrian rather than be faulted against it. If this is the case the volcanic rocks, which are intruded by the same rocks that penetrate the Cambrian, could well be equivalent in age to the Treffgarne andesites.

Brunel Beds Dark grey or nearly black cleaved mudstones are exposed in ditches beneath drift deposits in a few localities in the north of the area. The mudstones lie within the westernmost limit of a belt of

sedimentary rocks, which, though unfossiliferous, Williams (1933) attributed to the Tetragraptus Shales of Arenig age.

Tertiary deposits Apart from sedimentary infill in solution cavities in limestone south of Milford Haven no deposits of Tertiary age have previously been found in southwestern Dyfed. However, in seven of the boreholes a succession of lacustrine sediments 2.44-20.0 m thick was encountered, which Allen (1981) has argued is most likely to be Tertiary in age. The sediments consist of deeply weathered thinly interbedded feldspar sand and clay, with some thick beds of clay, silt and sandy gravel. The deposits were probably laid down in the marginal parts of a lake in a landscape of deeply rotted rock now substantially reduced by erosion. The extent of the thickest part of the deposit was defined by resistivity measurements (Fig. 19), but it is likely that remnants of an originally extensive cover of lake sediments could be found in many parts of this district.

Drift deposits The approximate distribution of drift deposits was determined during the soil survey (Fig. 19). Details of the deposits were obtained from drillhole samples.

The most extensive deposit is a variously coloured silty or sandy pebbly clay. The pebbles (or cobbles) are mostly subangular or subrounded and their composition tends to reflect the underlying bedrock: thus large pebbles of black or dark grey mudstone are abundant only in the north of the area and occur no more than two hundred metres beyond the faulted margin of the Tetragraptus Shales. This lithology, however, is an important constituent of the sand-size fraction in drift deposits over much of this area.

In four of the boreholes (3A, 3B, 6 and 7) structureless clay with pebbles (0.12-1.77 m thick) was found to overlie pebbly silty clay (0.21-0.94 m thick) with thin beds, laminae and lenses of clay, silt, coarse sandy clay and gravel. It is not known whether the two units together represent an undermelt drift sequence or whether they are a complex of water-lain deposits and geliflucted till, laid down under periglacial conditions. Whichever is the case the material in the deposits is locally derived and ice-related.

Locally filling hollows in this drift deposit and occupying the bottom of most of the valleys is grey, sticky clay, in places containing rounded pebbles. The clay overlies alluvial gravels in one locality and itself is covered in places by alluvium. The origin of the clay is unknown, but it may be late-glacial, alluvial or lacustrine.

Intrusive rocks

One major intrusive complex, penetrated by five of the boreholes, and several smaller ones which may be connected to it at depth, are present in this area. Using textural and compositional criteria seven rock types may be named, among which are equivalents of all the intrusive rocks exposed at surface. They include microdiorite, porphyritic microdiorite (0-5% quartz), quartz-microdiorite, porphyritic quartz-microdiorite, quartz diorite (5-10% quartz), tonalite and porphyritic microtonalite (>10% quartz). Intrusive contacts were observed against rocks of the Solva Group and the Treffynnon Group. Xenoliths found in the intrusive rocks include basic rock types, diorite and sedimentary and volcanic rocks from these groups. There is no evidence to show that any intrusions were emplaced into either

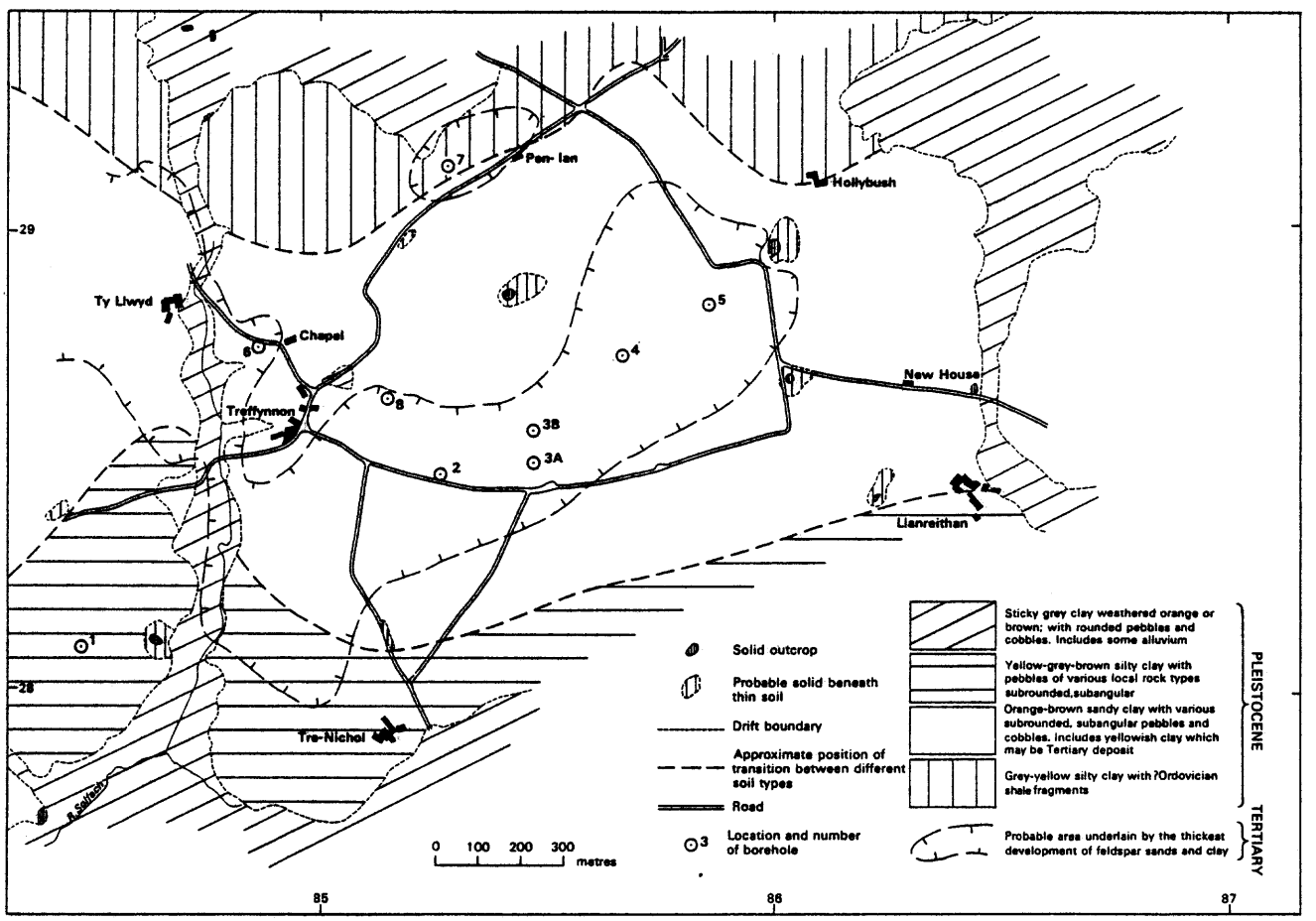

Figure 19 Distribution of outcrop and superficial deposits in the area around the boreholes

the Brunel Beds or the Tetragraptus Shales. The intrusive episode can be dated, therefore, as being pre-Arenig and later than middle Cambrian.

The form of both the individual intrusions and complexes is difficult to resolve. Porphyritic microdiorite intersected in borehole 8 shows markedly discordant relationships with the Solva Group and in other boreholes the porphyritic microdiorite appears to form veins intersecting other intrusive rocks. Porphyritic quartz-microdiorite and microtonalite in borehole 8, however, form concordant sheets. There is evidence of repeated injection of sheet-like bodies of the same rock; in borehole 7, for example, four sheets of quartz-microdiorite were intersected showing intrusive contacts against each other. It is not uncommon to find cognate xenoliths in quartz-microdiorite and porphyritic microtonalite. Where both the top and bottom of a sheet were located none exceeded 16.5 m in thickness. The intrusive complexes are unlikely to be stocklike. It is most probable that they are concordant or semi-concordant laccolithic bodies, the results of repeated injection of thin sheets of magma, with, perhaps the porphyritic microdiorite forming a late dyke phase.

Relative orders of intrusion among some of the rock types can be established by the examination of contacts and identification of xenoliths in some boreholes. Extrapolation between them, however, is not easy and no order of intrusion applicable to all boreholes can be devised for all the rock types. This particular problem is compounded by the considerable amount of variation within some rock types and among transitional types: thus, though distinct rock names are given it is conceivable that differently named rocks could belong to the same intrusive phase and vice versa.

Petrography of the intrusive rocks

The seven distinct rock types, each of which is described below, can be grouped into three broader divisions which may be more meaningful when considering magma genesis. These are:

a) Porphyritic microdiorite
b) Microdiorite
   Quartz-microdiorite
   Porphyritic quartz-microdiorite
   Quartz diorite
c) Tonalite
   Porphyritic microtonalite

The porphyritic microdiorite, though displaying some textural variation is outstanding in being quartz-free or containing a very low content of it.

The second group, with the exception of the porphyritic quartz-microdiorite, which is of restricted occurrence, is texturally homogeneous. The principal variations are in the quartz content and grain size. The quartz, however, is unevenly distributed even within a single slide and the microdiorite and quartz-microdiorite may comprise a single series.

The third group is consistently quartz-rich and texturally distinct. All the microtonalites are strongly porphyritic and the tonalites, though differently named, may be regarded as densely porphyritic microtonalites.

Among the rocks sampled at surface no equivalent was found of the porphyritic microdiorite or of the microdiorite to quartz-microdiorite series. The Hollybush quartz diorite compares with the quartz diorite in borehole 3A. The porphyritic quartz-microdiorites found at surface are similar to and as uncommon as among the borehole rocks. Most of the surface rocks are porphyritic microtonalite and, though no textural equivalents of the tonalites were found, they may be compared directly with the tonalite-porphyritic microtonalite group in the boreholes.

Microdiorite This rock (E 53249-53) is sparsely porphyritic with phenocrysts of plagioclase and amphibole up to 5 mm long. The bulk of the rock is composed of stubby plagioclase crystals with a median size of 0.5 mm patchily altered, mostly at the crystal centres, to sericite, epidote and minor chlorite. Small amounts of (?)exsolved K-feldspar occurs within the plagioclase. Relict zoning shows through the alteration. Hornblende, when fresh is pale green and forms poikilitic crystals, but mostly it is replaced by chlorite and calcite. Quartz is interstitial, locally recrystallised and comprises no more then 4% of the rock, though it is irregularly distributed. Accessory minerals include magnetite and sphene.

Three sheets of this rock occur in borehole 4 (Fig. 24). In all cases, there is a fine-grained porphyritic margin, containing euhedral amphibole and plagioclase phenocrysts, which passes into coarse-grained only sparsely porphyritic rock. In the upper sheet this rock shows little variation through over 14 m of core. In the middle sheet, only 0.58 m thick, the porphyritic variety reappears in the middle; but in the lower sheet, 4.44 m thick, there is complete mixing of the two types with irregular transitions between them. Patches of medium-grained uniform feldspar and amphibole rock merge into rock containing feldspar crystals from 0.25-2.5 mm long dispersed in irregular concentrations through fine-grained feldspar, hornblende and quartz.

Porphyritic microdiorite In borehole 4 a sheet of porphyritic microdiorite beneath the lower microdiorite sheet passes inperceptibly into it and, like it, it displays some textural heterogeneity. Plagioclase phenocrysts (E 53254) up to 2 mm long, showing sutured margins, are altered to sericite and epidote. Some phenocrysts of greenish brown, poikilitic, euhedral hornblende are slightly smaller. The groundmass comprises plagioclase, hornblende, minor quartz with abundant chlorite and epidote, but is partly recrystallised.

In boreholes 1 and 5 porphyritic microdiorite forms irregular, discordant veins and minor intrusions no more than 1.48 m thick. They display sharp, chilled contacts with flames and lobes penetrating the wall rock. The rock (E 53169, 53244-5, 53248) is texturally quite different from the type in borehole 4. It is stongly porphyritic with euhedral and subhedral amphibole phenocrysts commonly up to 5 mm long, rarely up to 1 cm long and abundant somewhat smaller plagioclase phenocrysts. The pseudomorphs after amphibole are composed of chlorite and ?magnetite; in places containing plagioclase inclusions. The feldspar phenocrysts are altered to sericite and albite, but display relict twinning and zoning. Typically, the groundmass consists of feldspar laths about 0.05 mm long with variable amounts of chlorite and opaque dust. The texture, however, is obscured by alteration. One rock only has a fine-grained recrystallised matrix. Quartz is very rare. Accessory minerals include apatite, sphene and hematite.

The two-metre thick discordant intrusion intersected in borehole 8 (E 53846) differs from the others in being fine-grained and having closely packed phenocrysts. The rock is chlorite rich and it is veined by slightly more acid, uniformly fine-grained feldspar-quartz rock.

Quartz-microdiorite Two large complexes of this rock were intersected; one in borehole 2, the other in borehole 7. The rock bears a strong resemblance texturally to the non-porphyritic microdiorite in borehole 4, but the quartz content is higher, ranging from 6.5 to over 10%. Quartz is irregularly distributed through this rock giving concentrations as high as 12.5% in parts, but the overall content is below 10%.

Four units of this rock were drilled in borehole 2. They ranged from 0.91 to 8.32 m thick. Each of the top three units has a richly xenolithic basal zone, the inclusions all being of quartz-microdiorite. The rock in borehole 2

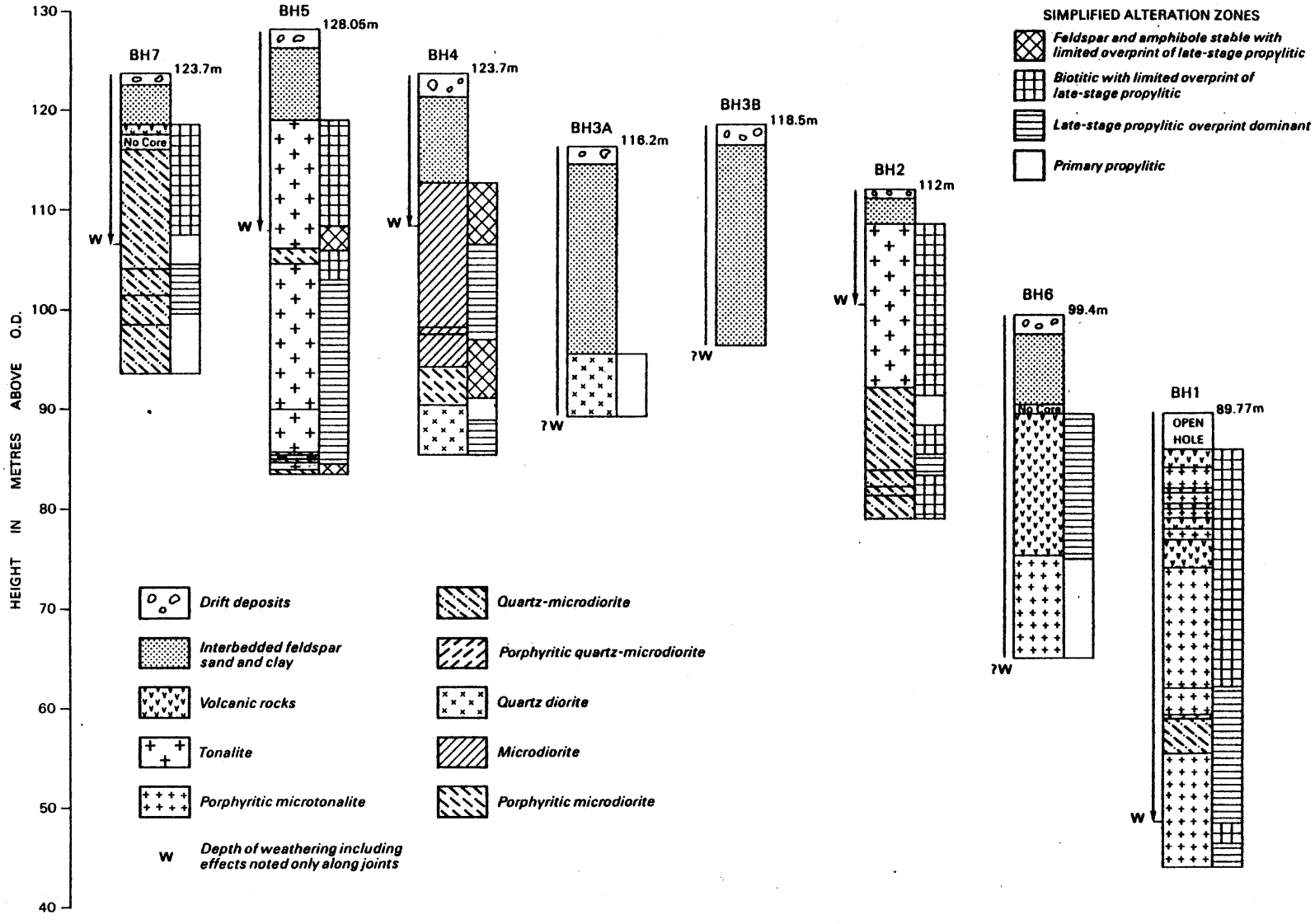

Fig.29. SIMPLIFIED GRAPHIC LOGS OF BOREHOLES 1-7, PLOTTED AGAINST O.D.

contains sparse subhedral plagioclase phenocrysts (E 53235-41), reaching 2 mm long, and 3 mm long poikilitic hornblende crystals. Most of the rock is composed of stubby plagioclase crystals roughly 0.5 mm long, which are strongly altered though they often retain a clear rim of albite. Brownish-green hornblende forms anhedral poikilitic crystals and is usually partly replaced by tremolite or chlorite, calcite and magnetite. Quartz is interstitial to feldspar.

Four units of this rock were also intersected in borehole 7; the top two separated by a fault whereas the lower two show intrusive relationships. A generation of large pseudomorphs after amphibole, in places with remnants of green hornblende, is common to all the specimens (E 53295-9, E 53300-1) and there are some phenocrysts of plagioclase in the 2 mm size range. Most of the rock contains closely packed subhedral to anhedral feldspar crystals 0.25-1.00 mm long between which is a generation of small crystals not exceeding 0.15 mm with quartz, pale brown mica, epidote and chlorite. Chloritised biotite is present in some specimens. All the feldspars are altered, though relict zoning is visible. Magnetite is present in this rock as a primary magmatic phase, partly altered to hematite, and also as a secondary mineral. Ilmenite, partly leucoxenized, is the main accessory mineral.

A rock similar to this (E 53170-1) forms a sheet 3.50 m thick in borehole 1 within the thick composite body of porphyritic microtonalite.

Porphyritic quartz-microdiorite A sill of this rock just over a metre thick intrudes sedimentary rocks in borehole 8. The rock (E 53848) contains plentiful subhedral and euhedral phenocrysts, up to 2 mm long, of zoned plagioclase which is usually altered to sericite. Relict fresh crystals are oligioclase, but are possibly albitised. Pseudomorphs of chlorite and magnetite, some with pyrite, are probably after amphibole. There are a few recrystallized quartz phenocrysts no more than 0.25 mm in size. The groundmass, median grain size about 0.5 mm, consists of subhedral altered feldspar, with chlorite and some quartz. There is abundant pyrite in this rock.

Quartz diorite In borehole 4 this rock intrudes the overlying microdiorite complex and shows an irregular sharp contact with it. No other rock was in contact with it in borehole 3A. The rock (E 53242, 53255-6) is composed of euhedral and subhedral, normally zoned, plagioclase crystals up to 2.5 mm long and plentiful brownish-green hornblende, which varies from euhedral to poikilitic anhedral. In places the hornblende may form 5 mm long phenocrysts. The plagioclase is usually lightly altered whilst some hornblende is completely altered. Chlorite and epidote pseudomorphs are suspected to be after biotite. There is a little interstitial microperthite in the samples from borehole 4. Quartz, which is also interstitial, comprises about 10% of the rock and is unevenly distributed.

Tonalite Textually, this rock (53246-7, 53257) is difficult to classify. It consists mainly of subhedral to euhedral crystals of plagioclase ranging in size from 0.25 to 3 mm, but with a median size of about 1 mm. The feldspar crystals, which in places are closely packed and elsewhere form an open framework, are set in a matrix of equant grains of quartz, rarely more than 0.15 mm in size, and small plagioclase crystals. The plagioclase, though strongly altered in some rocks, shows excellent relict zoning. Many crystals have clear albite rims. There are large pseudomorphs of chlorite and epidote, or chlorite with pale brown biotite and tremolite, after amphibole and some chloritised biotite. Where unaltered the hornblende is brownish-green. The quartz content ranges from a little over 10% to 25%. Rutile occurs as an accessory mineral.

Porphyritic microtonalite This rock is present in boreholes 1, 2, 6 and 8. It is always porphyritic, locally glomeroporphyritic, containing abundant euhedral or subhedral phenocrysts of plagioclase, 0.4-3 mm long, less abundant pseudomorphs after biotite and amphibole and small phenocrysts of quartz in a groundmass of equant grains of quartz, subhedral or euhedral feldspar and chlorite with a grain-size range 0.02 to 0.2 mm (E 53165-8, 53172-5, 53233-4, 53294, 53857, 53860-1). The feldspar phenocrysts are altered mostly to sericite and albite, some with chlorite, or to saussurite. Relict zoning and twinning is commonly visible. Fresh crystals in borehole 6 display cores of labradorite, and in a sill in borehole 8 they show oscillatory zoning. Exsolved or replacement K-feldspar is present in samples from borehole 1. Euhedral pseudomorphs of chlorite, biotite and magnetite after amphibole, in some slides enclosing plagioclase, fall in the same size range as feldspar phenocrysts. Most rocks contain chlorite and magnetite pseudomorphs after biotite. Quartz phenocrysts are not common. They rarely exceed 0.5 mm in size. They are euhedral or irregularly embayed, clear and locally slightly strained. Ilmenite is a common accessory mineral. The total quartz content ranges up to 25%, most of which is in the groundmass.

Weathering

Pervasive weathering was observed in boreholes 1 to 7 down to depths ranging from 8 to over 23 m and below these depths down to over 40 m in zones adjacent to joints. In borehole 8 weathering only along joints was observed immediately at rockhead.

Most intersections through the uppermost glacial deposits revealed oxidised clay throughout, though in places lengths of residual grey clay were evident. The underlying Tertiary lacustrine sediments are uniformly deeply weathered. Feldspar crystals in the feldspar sands are almost completely kaolinised. At all depths there are ferruginous or manganese-lined fractures. At certain levels pebbles in gravel beds have been completely pseudomorphed by manganese minerals.

The weathered zone beneath rockhead varies from 4 to >37 m in thickness. The complete profile consists of an upper zone of deeply weathered rock, a middle zone in which deeply weathered rock alternates with less weathered or even fresh rock, and a lower zone in which weathering is confined to rock immediately adjacent to joints. This full profile was recorded even in the borehole with the thinnest weathered zone, but it is not always complete. Intrusive rocks are preferentially weathered and in borehole 8 weathering in the sedimentary rocks, which extended only to 18 m depth was along joints only. The volcanic rocks in boreholes 1, 6 and 7 all weather less readily than the intrusive rocks, which in the upper part of borehole 1 are reduced to orange-brown crumbly clay with white kaolinite pseudomorphs after feldspar phenocrysts adjacent to much less intensely weathered volcanic rock.

Common to the weathered zones in all rocks are ferruginous or manganese-filled joints and fractures, manganese-lined cavities and hematite-altered pyrite.

Brecciation, alteration and mineralisation

Brecciation

Rocks in all the boreholes are brecciated and fractured. Zones of closely spaced, planar fractures or irregular intersecting fractures are commonplace. There are, however, many examples of network hair fracturing and crackle breccia also in zones, and in places these are associated with clearly defined veins of intrusive breccia. Brecciation is not confined to any one rock though it is confined to zones within them: all the

intrusive rocks are affected, as are the volcanic and sedimentary rocks they intrude (see Figs. 20 to 29).

Discrete veinlets of intrusive breccia occur in porphyritic microtonalite in borehole 1 (7.28 m) and a 5 cm vein is present within porphyritic microdiorite (22.74 m) in borehole 5. In the latter example the breccia is composed of angular fragments no more than 8 mm long of porphyritic microdiorite in a matrix predominantly of epidote, but with some small angular fragments of feldspar. A 4 cm thick vein intersects volcanic rocks in borehole 6 (22.45 m).

Intrusive breccia is most common within the succession of Solva Group sedimentary rocks encountered in borehole 8. At several levels lengths of core as much as four metres long display intense crackle breccias, through which are threaded either several veins of breccia containing rotated and in some parts subrounded fragments, or a single breccia vein in the middle. No truely exotic fragments were observed in these breccias, but the fragments were not always the same as the immediately adjacent wall rock. In one vein (E 53837) fragments of mudstone with aligned sericite were rotated after the formation of the schistosity. Elsewhere, clearly defined breccia veins penetrated unbroken rock. In some the fragments are set in quartz cement, or less commonly, epidote. Usually, however, the matrix consists of a small portion of finely comminuted rock and sand-size quartz with abundant chlorite and, in some rocks, associated sulphides. The chlorite fills most voids and penetrates fractures in fragments.

Alteration

All the rocks encountered show evidence of alteration though it is irregularly developed. Veining, sulphide mineralisation and brecciation are all spatially related to the alteration and together appear to reflect the effects of a hydrothermal system comparable to that associated with classic porphyry copper deposits. Four principal types of alteration are present, two of which are essentially potassic and two propylitic. The potassic alteration is represented by a high temperature form in which K-feldspar and amphibole are stable, and a presumed lower temperature form in which biotite is the main alteration mineral and K-feldspar minor or absent. A primary propylitic alteration is recognisable locally, but the most widespread alteration is late-stage propylitic. This has been imposed on all other alterations and local epidotisation is related to it. Widespread, but localised alteration to carbonate is the last event.

K-feldspar alteration Despite the widespread late-stage propylitic alteration relict mineral assemblages of earlier, high temperature events are preserved and in boreholes 4 and 5 there are minerals and textures characteristic of the high temperature potassic alteration. The characteristic minerals are K-feldspar, pale green amphibole and biotite. In both boreholes there are zones of recrystallisation consisting of an aggregate of sutured equant grains in veins forming a network through the rock. Veins may cross large feldspar phenocrysts. The recrystallised veins contain euhedral crystals of potash feldspar, the amount of which varies from minimal (E 53250) to moderately abundant (E 53252). Potash feldspar also is present, derived from recrystallized plagioclase, in the walls adjacent to mineralized fractures. Some of the potash feldspar is introduced in veins, for example, in microdiorite in borehole 4 (E 53253). The slightly microperthitic potash feldspar is associated in recrystallized areas with pale green amphibole and pyrite and in veins with pale green amphibole, epidote, sphene and pyrite, in places with late calcite. Pale green amphibole replaces the magmatic hornblende and itself is chloritised or replaced by secondary brown mica. Fine-grained pale green mica is present in some rocks in both of these boreholes and this also is chloritised.

In borehole 4, near the top, no K-feldspar was identified in the rock, but primary brown-green hornblende is replaced by pale green amphibole which also forms veins traversing the rock. In all of these rocks the plagioclase is albitised and altered mainly to sericite but both may be a result of the late-stage propylitisation. Magmatic amphibole and biotite has been replaced mostly by secondary biotite which is now chloritised.

The original extent of this type of alteration is difficult to determine but veinlets containing K-feldspar occur in boreholes 1 and 2 where the rocks are dominated by low temperature, presumably retrograde, mineral assemblages.

Biotite alteration Alteration to biotite is evident in all boreholes except 3A and 6, though little of the biotite is preserved in borehole 4. The effect of retrograde propylitic alteration, which generally masks this alteration, are least visible in borehole 5. In the tonalite from this borehole fresh brownish-green biotite replaces both primary hornblende and biotite. Relict crystals of pale green amphibole, similar to the variety which characterises the potassic zone, remains in parts of the rock and there are tiny exsolution blebs or replacement patches of K-feldspar in plagioclase. Original zoning is visible through the alteration in these rocks and in another lightly altered rock from a thin sill of porphyritic microtonalite (E 53856) containing biotite pseudomorphs after amphibole in borehole 8; suggesting that the original plagioclase is stable in the biotite zone. Strictly speaking this alteration is potassic, but it is a slightly lower temperature form. In most rocks the partly chloritised biotite is dusty brown and besides replacing original ferromagnesian minerals it forms clusters of small crystals, stringers, network veinlets and disseminations through the body of the rock.

The characteristic assemblage of minerals replacing the argillaceous matrix in the quartz wacke and siltstones encountered in borehole 8 contains greenish-brown or brownish-green biotite and sericite, in places with disseminated fine pyrite and a little chlorite. The micas are fine-grained and not strongly foliated. Veinlets of biotite and chlorite with pyrite are present, in places forming a network. The sills within the succession contain biotite pseudomorphs after amphibole or contain chloritised secondary biotite and it is considered that both the sills and sedimentary rocks have been subjected to biotite alteration.

Primary propylitic alteration Common characteristics of the rocks showing this type of alteration are an alteration assemblage of clinozoisite, epidote, chlorite, sericite and tremolite; the common, but not necessarily total preservation of primary brownish-green hornblende, and the presence of the original, though mildly altered, zoned plagioclase.

The least altered rock in all the boreholes is quartz diorite in borehole 3A. Zoned plagioclase is patchily altered to clinozoisite and minor sericite. Poikilitic brownish-green hornblende is fresh, though clumps of small crystals of brown biotite show selective chloritisation. This alteration may be late stage deuteric or even metamorphic, but it differs only by degree from that in other boreholes (for example in borehole 7) which is probably hydrothermal. Quartz-microdiorite in borehole 7 contains saussuritised zoned plagioclase, chloritised biotite and pseudomorphs of fibrous amphibole, chlorite, yellow epidote and quartz after amphibole. Rosettes of fibrous amphibole occur throughout the rock (E 53296). There is some disseminated pyrite. Veins of fibrous amphibole, minor quartz and chlorite with pyrite and some chalcopyrite are also present.

There is some variation in the alteration of primary amphibole. One rock from near the bottom of borehole 7 contains pseudomorphs after amphibole with lath-like tremolite crystals among the other replacement minerals (E 53300). In another (E 53301) the pseudomorphs consist entirely of aggregates of small crystals of pale green tremolite-actinolite.

The amount of sericite alteration of plagioclase, in addition to clinozosite, is locally high in boreholes 2, 4 and 6. The associated amphibole may be only mildly chloritised (E 53235, 53255) or replaced by chlorite and epidote (E 53294). Pseudomorphs of these two minerals replace magmatic biotite and there are veins of epidote, chlorite, pyrite and minor quartz. This alteration is typical of the late stage propylitic assemblage, but in these rocks the plagioclase has not been albitized. It is considered possible therefore that a mild version of the late stage propylitic alteration might have been imposed on the earlier event here.

Late-stage propylitic alteration The full assemblage of minerals in this alteration includes albite, sericite, chlorite, epidote (and clinozoisite), magnetite, pyrite and chalcopyrite. It is the dominant alteration in the area and appears to have been imposed on all others. The alteration is pervasive, but there is a widespread development of veins with it.

Typically plagioclase is altered to albite and sericite, the latter varying from a light peppering to a dense mass totally replacing plagioclase. Muscovite is commonly present as well. In some rocks a rim of clear albite may be preserved around a mica pseudomorph and it is not unusual for original zoning to be represented by zones of alteration minerals. Minor chlorite and clinozoisite may be present with the sericite and in some rocks chlorite forms a partial rim around sericitised feldspar.

Original amphibole phenocrysts are most commonly replaced by pale green chlorite, usually with magnetite and less commonly with sericite. Primary biotite is replaced by chlorite with lenticles of sphene or ilmenite or magnetite.

Veinlets of chlorite and chlorite with sericite, commonly with a little pyrite and magnetite, are widespread. Larger veins of quartz, albite, epidote, minor chlorite and pyrite are common as are veins of quartz alone (up to 58 cm thick) or quartz with pyrite and chalcopyrite. Disseminated and veinlet pyrite, alone or with sericite and epidote, in places with chalcopyrite, is ubiquitous. Pyrite is commonly concentrated in pseudomorphs after amphibole. Magnetite is present in veins with pyrite and disseminated.

This alteration is both prograde and retrograde in its effects. Quartz diorite at the bottom of borehole 4 contains an alteration assemblage characteristic of primary propylitic alteration in its upper part and late-stage propylitic below. In the latter rock there is no textural or other evidence of an earlier higher temperature alteration assemblage. This is also true of the volcanic rocks in borehole 6 in which there is abundant sericite, in places with only minor chlorite, pervading the rock and totally replacing feldspar crystals. The rocks are riddled with veins and veinlets of quartz, some of which contain opaque dust. Veinlets of chlorite or quartz-chlorite are uncommon. Disseminated cubes of pyrite are rarely present. Pyrite also occurs sparsely in veins and in a network fracture system in borehole 1. The alteration assemblage in the volcanic rocks has been determined largely by their original acid composition.

Evidence of earlier biotite alteration is present in borehole 7 where the quartz-diorite at around 22 m depth contains plentiful green or brown chlorite (E 53297) in diffuse veins, patches and forming a close network, all of which appears to be after secondary biotite. In other rocks, for example in borehole 5, pale brown and green chlorite in pseudomorphs after amphibole also appears to be after secondary biotite.

In borehole 1 thin veinlets of quartz and K-feldspar occur in rocks with propylitic alteration suggesting earlier potassic alteration. In borehole 4 there is chloritised pale green amphibole with relict cores of brownish-green hornblende and abundant chloritised secondary biotite. In one of the rocks containing unaltered secondary biotite (E 53233) a vein of epidote, chlorite and quartz has a chlorite envelope where it crosses a biotite pseudomorph after an amphibole phenocryst, providing clear evidence of the retrograde effect of this alteration.

Rocks least effected by the retrograde propylitic alteration are the sedimentary and intrusive rocks in borehole 8. It is reflected in the intrusions, but the effect, particularly the alteration of plagioclase, is mild and the feldspar does not appear to have been albitised.

In the sedimentary rocks the late-stage alteration is most evident in zones of brecciation and fracturing within which there is abundant veining, wall rock alteration and sulphide mineralisation. Most common is a fine network of chlorite and chlorite-quartz veinlets with pyrite. Veins of quartz-albite-pyrite are less common. The quartz in them may be strained and such veins are intersected by others carrying unstrained quartz. The wallrock adjacent to these early veins is sericitised locally. Sulphides may be evenly disseminated or form a network of irregular trains of euhedral to subhedral crystals throughout the rock, in places associated with some chlorite enrichment. Pyrite also occurs in quartz-chlorite veinlets and in veins intersecting them.

The quartz-chlorite-sericite-pyrite assemblage also dominates the breccias. These minerals fill the voids in the intrusive breccias and comprise the veins in the "crackle" breccia. Pyrite usually concentrates at the rim of breccia fragments. Sericitisation of fragments is locally intense.

Epidote-bearing veins, which may be intersected by chlorite-sulphide veins, are characteristic of the late-stage propylitic alteration and it is not likely that epidotisation is a separate event. There are, however, many places in both intrusive and sedimentary rocks where epidote veining is intense and adjacent wallrock is patchily or totally replaced by yellow epidote. Indeed, throughout the rocks affected by the late-stage event yellow epidote is confined to parts of the rock near epidote veins. Specular hematite occurs locally with epidote in epidotised breccias.

Carbonate alteration Veins of carbonate are consistently the last event recorded in these rocks. They are widespread and associated with patchy replacement of the host rock; carbonate, therefore, occurs as an additional mineral in most types of pseudomorph. It is present additionally in veins of all types and commonly shows replacement texture with other minerals in the veins.

Mineralisation

Because of the widespread effect of the late-stage propylitic alteration it is difficult to determine the extent of earlier phases of sulphide mineralistion. The main sulphide minerals identified are pyrite and chalcopyrite and both occur in veins with epidote, quartz and other minerals associated with the late event. It is likely, therefore, that this is a mineralising event, but geochemical evidence (see later) shows that rocks little effected by the retrograde alteration are copper rich and an earlier mineralisation, probably during the potassic alteration, seems likely.

Pyrite is the most abundant sulphide reaching levels of up to 4% in borehole 2. It is more or less altered to hematite within the weathered zone. The pyrite is evenly or patchily disseminated, in places forming cubes up to 1 cm wide, and it occurs in veins, veinlets and concentrated in network fracture systems. Veins of solid

pyrite do not usually exceed 1 cm in width. Veins of euhedral crystals occur in some rocks, not obviously related to a fracture system. Pyrite is a common additional mineral in veins of quartz, chlorite, epidote and calcite.

Chalcopyrite very rarely occurs as disseminated anhedra. It was observed mostly as blebs within pyrite, in veins, or associated with magnetite in bands. These bands are intersected by late epidote-carbonate veins carrying interstitial chalcopyrite and, in places, pyrite. It is also present with pyrite in chlorite lenticles and veinlets. Chalcopyrite, therefore, was formed in at least two phases, but both appear to have been within the late-stage propylitic event.

Magnetite, though probably a primary mineral in some rocks, is mainly a secondary mineral and is locally abundant. It forms subhedral, disseminated crystals marginally altered to hematite or partly surrounded by leucoxene, but there is a preferential association with chlorite either in pseudomorphs after ferromagnesian minerals or as a pervasive alteration product. Large anhedral crystals occur with quartz in veins and, rarely, in late carbonate veins.

Apart from hematite and leucoxene, the only secondary minerals recorded include malachite and rare covellite.

Finally, fluid inclusions in quartz were examined in a number of specimens from boreholes 4 and 5 by T.J. Shepherd (B.G.S.) and though the state of preservation was poor, three phase inclusions (with halite) of a type common in the Coed y Brenin porphyry copper deposit (Allen and others, 1979) were found in four samples.

Geochemistry

Soil sampling survey

Sampling and analysis 756 soil samples, each weighing about 200 g, were collected from as deeply as possible using a 120 cm long hand auger from two or more holes at sites spaced at 50 m intervals along the traverse lines. The samples were analysed for Cu, Pb and Zn by AAS following the same sample preparation and acid digestion used for the Middle Mill samples. Total gamma radiometric measurements were made at all sample sites using an AERE 1597A ratemeter in an attempt to detect contrasting lithologies and alteration zones.

Results The analytical results are summarised in Table 8 and all the copper results together with anomalous lead and zinc results are plotted on Fig. 30. Distributions and threshold levels were determined by cumulative frequency curve analysis (Lepeltier, 1969; Sinclair, 1976). Copper and lead give sigmoidal plots on logscale probability graphs, which in the case of lead tends towards binormal form as the upper population is poorly defined and only represents a small percentage of the total sample population. The copper distribution assumes a normal form at low levels, a feature which may be of natural origin, but could be produced by sampling or analysis. Zinc shows a binormal form on a true-scale probability plot indicating the presence of a background normal population and an upper population of uncertain form (Fig. 15).

Threshold levels for all three elements were set where the main background population deviated significantly (95% confidence level, Sinclair, 1976) from a straight line. Consequently the anomalous sample populations contain a percentage of samples belonging to the background populations, but few samples from the upper populations have been excluded. The near 'dog-leg' (bi-normal) form of the lead and zinc plots did not allow the parameters of the upper populations to be defined, but the small range of the results and low overall metal content of the upper lead and zinc populations suggests that they are not related to substantial near surface mineralisation. The upper copper population has a median value of 85 ppm, a 2.5% level of 45 ppm and a 97.5% level of 155 ppm. Only 0.5% of samples from the lower population have copper contents greater than the median of the upper population.

Copper and zinc show a highly significant (>99.95% confidence level) positive correlation ($\rho 0.56$) by the Spearman-rank method. Lead and zinc show a much weaker but still significant positive correlation ($\rho 0.24$) whilst copper and lead show no significant relationship. Pearson product-moment correlations on log transformed data yield closely similar results.

The correlation between copper and zinc is thought to be generated by similar background variation and enhanced levels of both elements related to mineralisation. Chalcopyrite is found in the mineralisation but sphalerite is not recorded and, in view of the low overall levels of zinc, it is suspected that the anomalous levels of zinc are generated from pyrite and magnetite associated with copper mineralisation.

Interpretation Soil sample lithologies, which consisted largely of weathered till or periglacial deposits, showed a broad relationship to the regional geology and were used to construct Fig. 19. The distribution of samples containing shale fragments with respect to the southern boundary of the Ordovician Tetragraptus Shales suggests that displacement from bedrock source does not normally exceed 300 m. The distribution of geochemical anomalies shows no relation to soil type apart from possible secondary concentrations in the grey gley.

Anomalous results can be contoured but the rectangular sample spacing tends to generate east-west trends which may be unrealistic. The majority of Cu anomalies, including all those greater than 80 ppm, were subsequently proved to be related to sulphide mineralisation. Weak copper anomalies have at least two other causes which may also contribute to some of the larger anomalies. Firstly, contamination may have caused a combined lead anomaly and threshold level copper result close to a field boundary and road at SM 8565 2935 and a similarly sited anomaly at SM 8804 2956. Secondly, copper anomalies which occur in marshy ground may be enhanced by hydromorphic processes; examples are located on line 2900E at SM 8466 2935 and in the Solfach valley on line 4700E.

Table 8 Summary of copper, lead and zinc results in ppm for 756 soil samples from the Llandeloy area

Element	Mean	Standard deviation	Geometric mean	Geo. mean + 2 x geo. dev.	Median (background)	Maximum	Minimum	Threshold
Cu	30	23.5	25	82	20	215	5	45
Pb	25	7.9	24	44	30	90	10	42
Zn	55	16.1	53	96	50	150	<10	81

The cause of other isolated weak Cu anomalies is uncertain. All Cu anomalies greater than 70 ppm occur over Treffynnon Group rocks and intrusions into them.

Background levels of Cu are dominated by the change at 2100°E, with much lower levels characteristic of the area to the west of this line. Allowing for some inaccuracy in the geological boundaries and glacial redistribution, this may be interpreted as reflecting low Cu levels in the Precambrian Treglemais Group and Cambrian sedimentary rocks compared with the Treffynnon Group and Ordovician rocks. The pattern may, however, also be influenced by the presence of Cu rich lacustrine deposits proved by subsequent drilling.

A few of the lead anomalies may be enhanced or caused by contamination (eg at SM 8565 2935) but the majority occur in samples collected from poorly drained, marshy ground by the Solfach and its tributaries, for example on line 4500E at SM 8625 2936, line 900E at SM 8266 2750, line 4900E at SM 8666 2910 and line 3300E at SM 8506 2740. The cause of the remaining lead anomalies is less certain, but all are weak and not thought to be related to mineralisation. The background level of lead apparently increases to the east of Llanreithan with a higher proportion of results greater than 30 ppm, but there is no clear relationship to the geological map.

Several zinc anomalies are associated with high levels of copper, for example at SM 8525 2850 and SM 8545 2841. These, together with some others such as at Hollybush [SM 8605 2915], are probably caused by mineralisation. The majority of other zinc anomalies coincide with marshy ground and may, therefore, be cuased or enhanced by hydromorphic processes. These include the anomalies at SM 8296 2750, SM 8467 2935, SM 8646 2940 and SM 8666 2920. The reasons for the remaining anomalies are unclear. Background levels of Zn are noisy within a small overall range, probably because of local secondary redistribution. Ordovician rocks appear to be characterised by a relatively high background and this may at least in part be responsible for two weak anomalies on line 6900E and that near the south end of line 3300E.

Subsequent drilling showed that many of the soil anomalies were located in thin drift deposits overlying substantial thicknesses of lacustrine sands and clays. Therefore many of the soil anomalies, notably those about boreholes 3 to 7, are not derived directly from underlying bedrock; they are transported anomalies and it may be considered fortuitous that mineralised bedrock was intersected at depth beneath them.

Radiometric results were uniformly low with a range of 3-9 μ R/h and a mode of 7 μ R/h. No pattern could be discerned in the results. This is attributed to a low relatively uniform radioelement content in the rocks, a lack of any substantial potassic alteration halo at surface and the homogenising effect of the extensive till and lacustrine deposits.

Comparison of Llandeloy and Middle Mill soil survey results Levels of copper and particularly lead and zinc in the soil samples from the two areas are very similar (Fig. 15). The higher maximum values recorded in the Middle Mill area are caused by one or two outlying high values attributed to contamination. The form of the lead and zinc distributions is very similar in both areas, but the copper graph shows the presence of an upper population in the Llandeloy data which is absent in the Middle Mill results (Fig. 15). This upper population is related to the presence of mineralisation at Llandeloy and infers the absence of similar mineralisation in the Middle Mill samples. Differences in the zinc distributions at high levels are attributed to contaminated samples in the Middle Mill batch and a contribution from the high background generated by extensive pyritisation and Ordovician rocks at Llandeloy.

Despite the lack of mineralisation at Middle Mill inter-element relationships are very similar in both areas, with Cu and Zn showing the closest correlation and Pb and Zn showing a weakly significant correlation. This suggests similar geochemical behaviour of these elements in both areas independent of mineralisation.

Superficial deposits

Core samples of the unconsolidated deposits were collected for analysis at intervals in boreholes 2-7. In borehole 2 a complete cored section was collected, in other holes interval core sampling was supplemented by drill sludge sampling. Cu, Pb, Zn and Fe were determined in both sludge and sediment samples by AAS following digestion of a subsample in hot concentrated nitric acid for one hour. Results are shown on the graphic logs (Figs. 20-28).

Allowing for the different depth ranges covered by the samples, the hand auger soil sample results are closely comparable to those obtained on cores of the drift deposits collected some months later. For example, the highest Cu result in core (310 ppm from borehole two) comes from the same site as the largest soil anomaly (215 ppm).

There is no consistent relationship between depth and metal content in the two boreholes (3A and 5) where more than two samples were collected from the drift deposits. Reduced Cu and higher Pb levels are found in the organic rich topsoil of these profiles.

In all boreholes, except six, Cu levels rise sharply at the contact with the lacustrine sands and clays. These deposits are characterised by high levels of Cu, reaching a maximum of 640 ppm in borehole four. Metal levels show less variation within a hole, i.e. with depth, than between holes. There is no pronounced relationship to depth and, in the only two holes where sampling of bedrock and overlying sands and clays is near continuous, Cu levels in the lacustrine deposits are higher than in the immediately underlying bedrock. An unexplained feature, bearing in mind the proposed origin of these deposits, is the apparent correlation of the most Cu rich lacustrine deposit profiles with the more highly mineralised and altered underlying bedrock. It would appear, if not a coincidence, to suggest a very local source for these deposits.

Panned heavy mineral concentrates made from drill sludges showed that magnetite and occasional pyrite were the principal heavy minerals in the sands and clays; the Cu bearing phases were not identified.

Rock geochemistry

Introduction In this section only borehole results are considered. Analyses from the few surface exposures are described in the regional account and compared with the borehole results below.

Analysed borehole rock samples consist of igneous rocks except for quartz wackes with and without tuffaceous bands and magnetite sandstones from borehole 8. Samples were collected by taking half of the core over 5 cm lengths at 30 cm intervals along a 10 foot (3.04 m) length unless a geological feature was encountered. Shorter lengths were than sampled by taking half of the core. All borehole samples were crushed, mixed, split and ground in a 'tema' mill with 'elvacite' binder prior to analysis for a range of elements by XRF. These were, with detection limits in ppm bracketed: Cu (6), Pb (13), Zn (3), Ba (27), As (2), Mo (2), Ni (5), Mn (6), Rb (1), Sr (2), Zr (3), Th (4), Nb (2), Y (2), Ce (21), W (3), Fe, Ti and Ca. Unweathered samples of igneous rocks from boreholes 1-7 were also analysed for major elements by β-probe. A total of 111 samples were analysed by XRF and 39 by β-probe. Results for selected elements are shown on the borehole logs, and all are contained in Appendices 6 and 7. Results are summarised in Tables 9, 12 and 13.

Igneous rocks Distribution of analysis of SiO_2, TiO_2, Fe_2O_3, MgO, CaO, P_2O_5 and Zr indicated the presence of a multipopulation sample whose multimodel distribution patterns are determined largely by the relative proportion of the petrographically defined sub-groups present in the sample population. The distribution plots of the remaining elements determined tended to normal (Al_2O_3, Na_2O, Zn, Sr, Y, Nb) or lognormal (K_2O, S, Cu, As, Mo, Ni, Mn, Ba, Rb) form and were wholly or partly independent of the petrographic groupings. In some cases, such as Al_2O_3, this was attributed to highly overlapping populations perhaps little modified by alteration but some distributions, such as Cu, S, As and Mo were clearly governed by mineralisation whilst others (K_2O, Na_2O, Rb, Ba, Sr) are highly modified by alteration processes (Fig. 31).

Classifying analyses on the basis of the petrographic groups shows that the two major divisions of tonalites/microtonalites and quartz diorites/diorites are chemically distinct (Table 9). Despite the altered and mineralised nature of the rocks there is no overlap in SiO_2, TiO_2 or MgO content, allowing unknown samples to be classified with confidence and suggesting a discontinuity which may be of genetic significance. The porphyritic microdiorite group is chemically indistinguishable from the quartz diorite/diorite group. Classification into petrographic sub-groups and statistical analysis using, firstly, all elements and, secondly, elements believed to be substantially unaffected by alteration showed that none of the sub-groups displayed distinctive chemical features. This suggests that differences in the petrographic sub-groups, largely defined on the basis of texture, are not fundamental but related to intrusion and crystallisation history.

Chemically distinct sub-groups unrelated to petrography can be discerned. Quartz microdiorites from borehole 7 have a more acid composition and contain distinctly higher concentrations of P_2O_5, Ce, Zr and Th and lower Zn than those from borehole 2 (Table 10). The relatively high levels of these elements, generally considered to be some of the least affected by alteration processes, allow borehole 7 quartz microdiorites to be distinguished from all other intrusive rocks. Tonalites and microtonalites may be divisible on the basis of their chemistry into a more acid group of porphyritic microtonalites (>63% SiO_2) and a more basic variety of tonalites and microtonalites (<62% SiO_2). Because of the absence of major element analysis for many samples in this group and discrimination on trace elements alone is imperfect, these two sub-groups are ill defined.

The bulk chemistry of the rocks, therefore, shows the presence of two major groups with distinctive mineralogy (tonalites and diorites), and a sub-division of diorites into P, Ce, Th and Zr rich and poor diorites and of tonalites into an acid porphyritic variety and others.

The small number of analysed samples in each sub-group, coupled with the effects of mineralisation and alteration, prevented detailed study of the primary rock geochemistry.

Plots of element concentration against silica content show typical igneous differentiation trends. With the exception of Zr, the degree of scatter shows a marked relationship to the suspected redistribution of elements during alteration and mineralisation processes (Fig. 32). Multivariate statistical analysis suggested that, despite intense alteration and mineralisation, primary acid-basic variation was the major source of variation in the data set and that petrographic groupings were most clearly discriminated by a combination of SiO_2, MgO or TiO_2 and Zr. Hence igneous trends and these groupings are clearly displayed on Ti/Zr v SiO_2 and Mg/Zr v SiO_2 (Fig. 33) plots which are very similar. On these plots, scatter in the microtonalite samples collected from surface exposure is attributed to weathering, which tends to

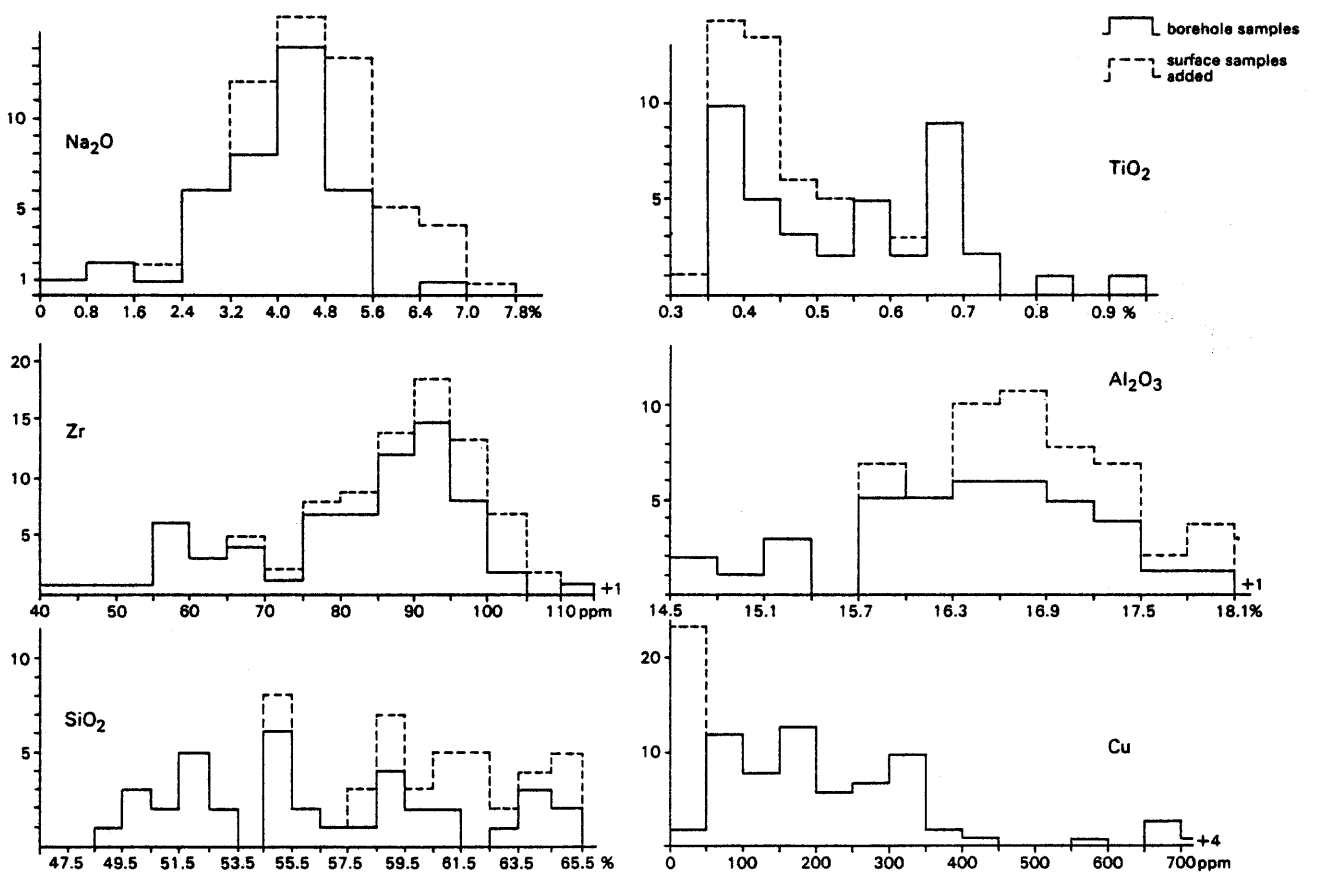

Figure 31 Distribution of selected elements in igneous rock samples

Table 9 Summary of analyses of intrusive rocks from boreholes

	All Intrusive Rocks					Tonalite and Microtonalite Group					Quartz Diorite and Microdiorite Group				
	Mean	Median	Std. Dev.	Max.	Min.	Mean	Median	Std. Dev.	Max.	Min.	Mean	Median	Std. Dev.	Max.	Min.
SiO_2	55.79	55.22	5.40	65.04	42.79	61.11	60.46	2.64	65.04	57.49	52.20	52.06	3.49	56.33	42.79
Al_2O_3	16.38	16.40	0.80	17.99	14.69	16.54	16.50	0.49	17.33	15.79	16.12	16.30	0.91	17.55	14.69
TiO_2	0.53	0.54	0.13	0.83	0.35	0.40	0.39	0.04	0.47	0.35	0.61	0.64	0.07	0.72	0.49
Fe_2O_3	8.10	8.42	2.30	17.75	4.85	6.14	6.46	0.60	7.06	4.85	9.51	9.04	2.17	17.75	7.02
MnO	0.15	0.14	0.05	0.31	0.07	0.12	0.12	0.02	0.14	0.06	0.18	0.18	0.05	0.31	0.10
MgO	3.95	3.98	1.17	6.24	2.00	2.71	2.75	0.28	3.17	2.00	4.75	4.89	0.68	6.24	3.96
CaO	4.49	4.20	2.49	12.00	0.51	2.81	3.44	1.81	6.03	0.51	5.91	6.24	2.07	12.00	1.57
Na_2O	3.82	4.01	1.22	6.43	0.39	4.48	4.35	0.80	6.43	3.13	3.30	3.44	1.27	5.31	0.39
K_2O	1.76	1.39	1.15	5.96	0.41	1.65	1.43	0.55	2.80	0.93	1.70	1.35	1.20	4.94	0.41
P_2O_5	0.14	0.13	0.03	0.21	0.10	0.14	0.14	0.02	0.16	0.12	0.15	0.13	0.04	0.21	0.10
S	0.57	0.32	0.72	3.23	0.10	0.27	0.22	0.19	0.76	<0.01	0.82	0.53	0.92	3.23	<0.01
Cu	293	194	445	3515	18	191	156	135	716	36	436	258	643	3515	56
Pb	24	<13	56.6	375	<13	41	<13	77	376	<13	<13	<13	-	<13	<13
Zn	80	78	30.3	196	32	68	68	23	116	32	87	82	34	196	48
As	6	<2	16.3	92	<2	9	<2	21	92	<2	<2	<2	-	3	<2
Mo	6	3	14.5	91	<2	3	2	3	18	<2	11	4	21	91	<2
Ni	16	16	9.7	41	<5	9	7	5	19	<5	24	22	8	41	11
Ba	449	373	255	1840	67	490	424	285	1840	229	418	333	226	973	67
Rb	42	39	16.7	101	10	47	46	17	101	25	34	33	12	56	10
Sr	273	279	136	580	32	258	279	120	458	65	309	298	151	579	32
Zr	81	87	14.7	114	42	89	90	7	114	65	73	75	16	102	42
Th	4	<4	-	5	<4	<4	<4	-	4	<4	<4	<4	-	5	<4
Nb	4	4	1.4	7	<2	4	4	0.9	7	4	3	4	1.5	6	<2
Y	14	14	2.6	20	7	13	13	1.9	16	7	15	15	2	18	7
Ce	<21	<21	-	35	<21	<21	<21	-	23	<21	<21	<21	-	35	<21
W	<3	<3	-	6	<3	<3	<3	-	5	<3	<3	<3	-	6	<3
Sample	Major elements 39; trace elements 71					Major elements 16; trace elements 35					Major elements 20; trace elements 30				

Major elements quoted in % oxide, S in %, trace elements in ppm.

Table 10 Mean analyses of main intrusive rock types in boreholes

	1	2	3	4	5	6	7	8
SiO_2	63.34	59.89	55.00	54.36	49.92	-	52.11	51.94
Al_2O_3	16.55	16.55	16.89	16.81	15.77	-	15.39	17.06
TiO_2	0.37	0.43	0.52	0.64	0.65	0.62	0.55	0.74
Fe as Fe_2O_3	5.77	6.52	7.72	8.82	10.50	8.97	9.45	9.48
MgO	2.59	2.83	3.97	4.54	5.28	-	4.39	5.30
CaO	1.36	4.26	5.10	5.19	6.57	2.12	6.05	4.50
Na_2O	4.49	4.45	3.95	3.08	2.52	-	4.86	4.59
K_2O	1.90	1.40	1.57	1.44	2.38	-	0.80	1.09
P_2O_5	0.13	0.15	0.15	0.20	0.12	-	0.13	0.14
S	0.17	0.36	0.61	0.87	0.62	-	1.29	0.20
Cu	165	279	166	219	795	194	342	250
Pb	36	62	<13	<13	<13	<13	<13	14
Zn	63	89	111	58	82	56	110	98
As	11	<2	<2	<2	<2	<2	<2	<2
Mo	3	3.7	2	5	12	<2	4	3
Ni	10	6	27	27	21	12	24	20
Mn	720	1020	1080	975	1700	1100	1350	1450
Ba	529	360	452	314	469	337	442	340
Rb	52	33	36	38	40	35	21	33
Sr	226	365	360	456	193	212	310	260
Zr	91	85	72	93	55	89	70	74
Nb	5	4	3	3	3	5	4	5
Y	12	14	15	16	14	18	14	18
Ce	<21	<21	<21	25	<21	30	<21	<21
Th	<4	<4	<4	4	<4	<4	<4	<4
n majors	8	8	2	6	8	1	4	2
n traces	27	8	4	17	10	1	8	3

Major elements quoted in % oxide, S in %, trace elements in ppm.

1 Porphyritic microtonalite
2 Tonalite
3 Quartz diorite
4 Quartz microdiorite, borehole 7
5 Quartz microdiorite, borehole 2
6 Porphyritic quartz microdiorite
7 Microdiorite
8 Porphyritic microdiorite

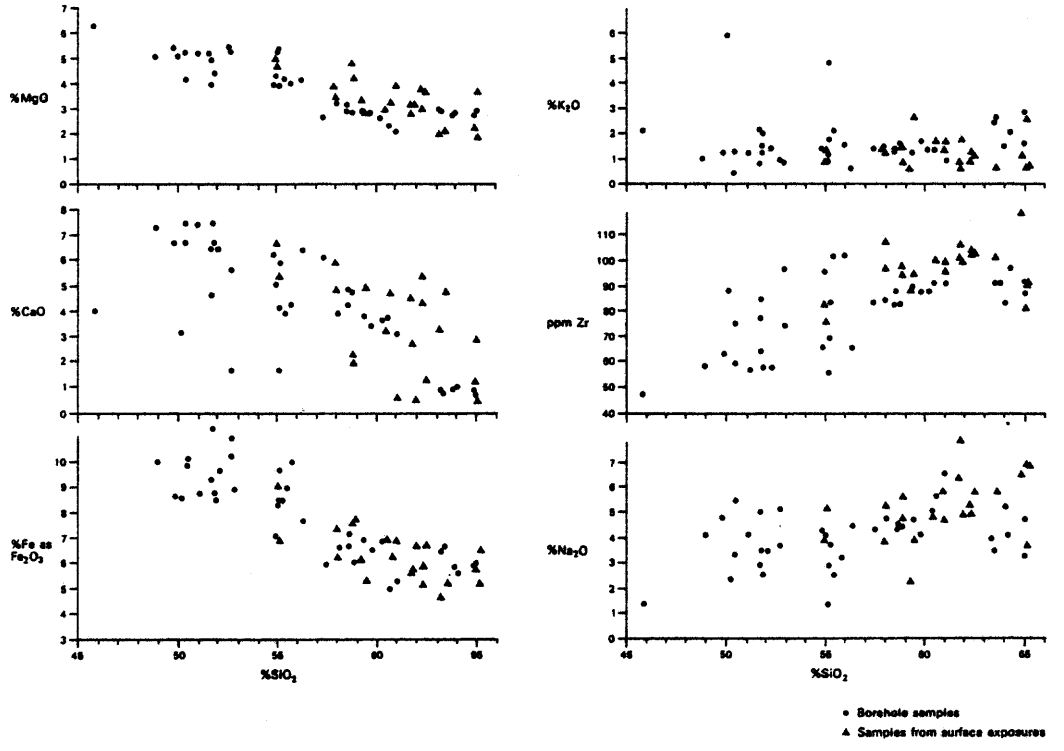

Figure 32 Plots of SiO_2 v MgO, CaO, iron as Fe_2O_3, K_2O, Na_2O and Zr for all igneous rock samples

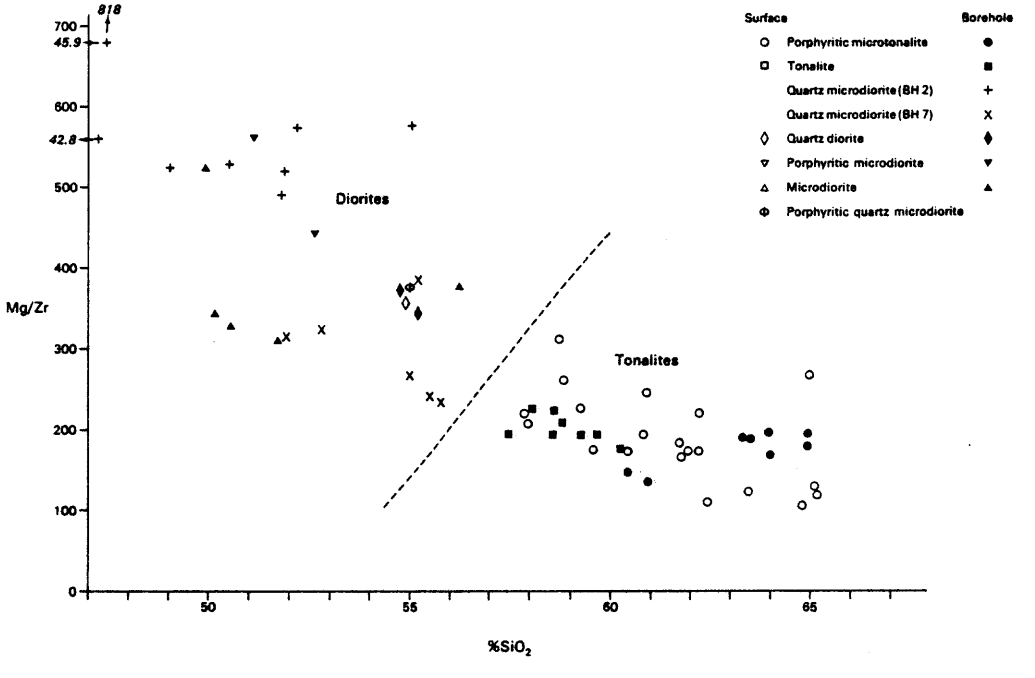

Figure 33 Plot of Mg/Zr v SiO_2 for igneous rock samples

increase the Zr content. The division between tonalites and diorites is clearly defined and two trends are evident in the diorites which merge in the tonalite field. One trend, characterised by low Mg/Zr and Ti/Zr is formed by the microdiorite and quartz microdiorite samples from borehole 7 (Fig. 33). The higher trend is followed by all other diorite samples and these contain distinctly higher Mg/Zr and Ti/Zr ratios. The only samples which fall off-line are highly mineralised and contain a high proportion of quartz or carbonate vein material. The distinctive 'immobile' element content of the lower Mg/Zr group, particularly the quartz microdiorites from borehole 7, suggests a genetic difference but in borehole 4 quartz diorite from the high Mg/Zr group intrudes a microdiorite complex that contains rocks from both trends, porphyritic microdiorite passing imperceptibly into microdiorite. Another feature, and an apparent paradox of the intrusives, is that the sequence of intrusion based on contact relationships is almost the reverse of that which might be predicted on a simplistic igneous differentiation model. It is not thought possible to resolve these problems with the data available and it is simply concluded that the petrogenesis of these intrusives is probably a complex multiphase event.

The chemical composition of the intrusive rocks indicates their affinity with intrusions emplaced in an island arc setting. Examination of the least altered rocks suggests that CaO = Na_2O + K_2O at 56-57% SiO_2, giving them a calc-alkali composition. Very low Nb contents, maximum 7 ppm, suggest an island arc rather than continental margin setting. All samples plot in the low-Rb volcanic-arc field of the Nb v SiO_2 plot of Pearce and Gale (1977). The low K, Rb, Ba, Sr, Th and Zr content of the least altered rocks and high K/Rb ratios (mean = 383 for 39 intrusives) compared with comparative lithologies emplaced in a continental margin setting (e.g. Saunders, Tarney and Weaver, 1979) is consistent with this conclusion.

Alteration associated with disseminated copper mineralisation Chemical changes accompanying alteration proved difficult to study because of the variety of rock types, the lack of unaltered rocks for comparison and the complex series of alteration events. Only major chemical changes accompanying alteration have been determined in this study, and a more rigerous investigation is required involving further careful sampling, analysis and mineralogical studies to clarify the chemical signatures of the various alteration events.

For the purpose of this study four major alteration episodes are distinguished: (i) weathering, (ii) alteration and metasomatism on a regional scale, possibly associated with low grade metamorphism, (iii) alteration associated with disseminated copper mineralisation and (iv) localised alteration associated with vein mineralisation. Any regional metasomatism can be expected to affect all the samples whilst weathering effects are evident in surface and near surface samples. The process dominant in the borehole samples is alteration associated with the targeted disseminated copper mineralisation. Here only alteration affecting borehole samples is considered and, because major elements were only determined on fresh igneous rock samples, principally alteration affecting the intrusive rocks.

Chemical studies about well documented porphyry copper deposits such as Highland Valley, British Columbia (Olade and Fletcher, 1976; Olade, 1977), Bougainville (Ford, 1978) and northern Turkey (Taylor and Fryer, 1980) have indicated that most elements can be at least locally redistributed in the alteration zones formed by a copper porphyry system. It is not surprising, therefore, that compatible element ratios, plots of so-called immobile elements and mobile/immobile element ratios in igneous rocks against well documented igneous rock trends (e.g. Beswick and Soucie, 1978; Davies and others, 1979), show that nearly all the elements determined in Llandeloy borehole samples show some evidence of at least limited redistribution attributable to alteration processes. At Llandeloy the situation is complicated by the late stage propylitic overprinting of earlier alteration and only rocks containing remnant K-feldspar alteration yield a distinctive geochemical signature.

Few analysed samples contain remnant K-feldspar but in boreholes 2 (quartz microdiorite) and 5 (tonalite) this and weaker forms of alteration are present within the same lithology, allowing a comparison to be made without the complication of major host rock variation. The comparison shows that K-feldspar alteration is characterised by great increases in K_2O and small increases in Rb (Fig. 34). CaO, Sr and Na decrease whilst Ba shows erratic behaviour decreasing in K-feldspar bearing rocks in these two boreholes but elsewhere

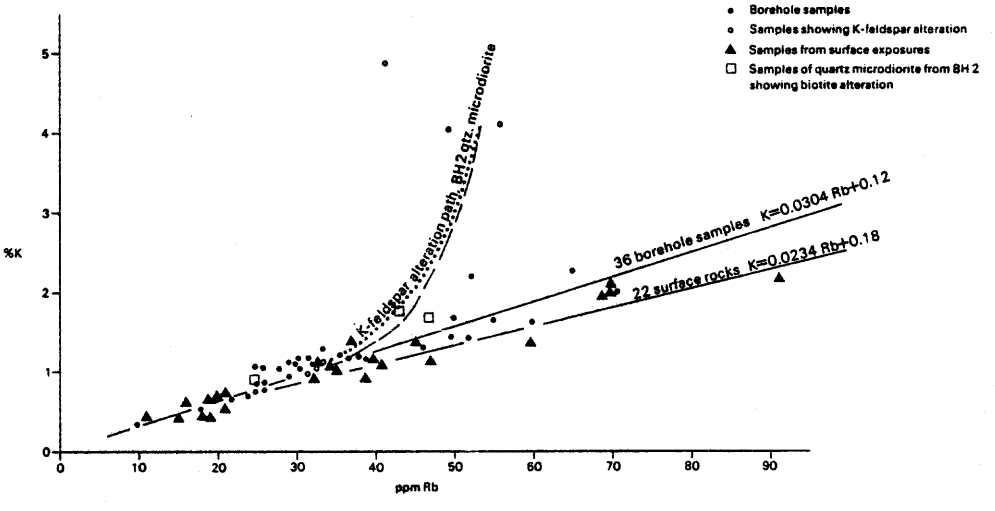

Figure 34 Plot of K v Rb, showing the effects of potassic alteration

showing a possible increase. Consequently, high K_2O/Na_2O, K/Rb and Rb/Sr ratios are characteristic of the potash alteration and K/Rb correlates closely with K but not Rb. The K/Rb pattern is atypical of porphyry copper systems. In the general case K and Rb both increase so that K/Rb decreases with Rb anomalies extending into the propylitic zone (e.g. Armbrust, 1977; Ford, 1978), though examples of Rb decreasing as K increases are also recorded (Davies, 1980). Two possible explanations for the Llandeloy pattern are suggested: (i) as argued by Armbrust and Gannicott (1980), the altering fluids may have been characterised by very high K/Rb ratios, suggesting the presence of seawater or primitive magmatic water in the hydrothermal system; (ii) a mechanism similar to that proposed by Davies (1980) may have operated. This involved the strong partitioning of Rb relative to K into the escaping vapour phase, brought about by rapidly decreasing temperature and pressure in the veinlets where K-feldspar was deposited, with K-feldspar being a selective carrier of K with respect to Rb. A third possibility, that Rb loss accompanied the late stage propylitic overprint, is considered unlikely because K/Rb ratios do not decrease noticeably in the rocks least affected by late stage propylitic alteration.

Examination of the results of all samples thought to have sustained K-feldspar alteration and the results of multivariate statistical analyses indicates some other chemical features of the zone. Though erratic, Cu and Cu/S increase whilst there is a loss of Nb and Y in some samples. Pb may also be depleted but results are confused by detection limit truncation. Other apparent changes, such as increases in Zn and Mn, were more probably related to host rock variation. More dioritic (particularly porphyritic microdiorites) than tonalitic rocks appear to be affected by K-feldspar alteration. It is not certain whether this is significant or simply coincidental.

Biotite alteration is not so clearly defined chemically. This may be partly due to retrograde overprinting and inadequate sampling. It apparently shows a weaker chemical signature transitional to, and in most respects similar to, the K-feldspar type. In the quartz microdiorites of borehole 2 element concentrations suggest that biotite alteration involves increases in K and Rb with respect to propylitic alteration and that, in contrast to the K-feldspar type, K/Rb is little changed (Fig. 34). In concert with the small K and Rb increases, Ca, Nb, Na and Sr generally decrease and Ba increases. In borehole 7 Mo increases in rocks displaying biotite alteration but elsewhere there is no such correlation. Pb is also high in more rocks with biotite alteration than might be expected by chance. Other chalcophile elements show no obvious relationships to biotite alteration. In common with K-feldspar alteration the 'stable' elements Ti, Zr and Y show apparent decreases in a few samples but in all cases this is associated with extensive veining and may simply be a dilution effect.

Most chemical features of the potash alteration at Llandeloy are similar to those reported from other porphyry deposits, namely the increase in Cu, K, Rb, K_2O/Na_2O, Rb/Sr and Cu/S, decrease in Na, Sr, Ca and Y and low Pb (e.g. Olade, 1977; Chaffee, 1976; Ford, 1978; Olade and Fletcher, 1976). Some differences from commonly reported patterns are found at Llandeloy, notably the lack of Mo enrichment in most rocks and the increase of the K/Rb ratio in rocks with K-feldspar alteration.

The absence of unaltered rocks precludes study of bulk chemical changes accompanying the primary propylitic alteration. The differing intensity of the late stage propylitic overprint indicates that, as seen in the quartz diorite and microdiorite of borehole 4, it is accompanied by an increase in Fe, S and possibly Mn and Zn. Pyrite is probably the main sulphide as Fe and S appear to increase at the expense of Cu, resulting in low Cu/S ratios in these rocks. This is well seen in borehole 1 where a dramatic decrease in Cu content at 27.13 m is coincident with a change from biotite to late stage propylitic alteration. Changes in borehole 7 appear to be distinct, with no change or a reduction in Mn and Zn and increase in Na accompanying late propylitic alteration. This difference may be caused by the distinct host rock composition and/or superposition on earlier K-feldspar alteration. The retrograde effect of late propylitic alteration may be expressed chemically by a reduction in K, Ba, Rb and Rb/Sr in rocks which had already undergone K-feldspar alteration, but data and sampling are insufficient to be certain. Factor analysis models using unweathered rock data show a well defined Al_2O_3-Zr-P_2O_5 v CaO source of variation which may be caused by late stage carbonate veining.

The elements most affected by the porphyry style alteration are the alkalis (K, Na, Rb), alkaline earths (Ba, Sr, Ca) and chalcophile elements (Cu, Pb, Zn, Mo, Fe, As, S). Of these elements Ba, Pb, Mo and As show independent behaviour: they are not closely correlated with other elements or observed alteration patterns (Fig. 35). This suggests that other factors may have contributed to their present distribution patterns. For example a Ba v Rb scattergram or a Ba v Rb v Sr triangular plot (El Bouseily and El Sokkary, 1976) shows that the majority of samples enriched in Ba are those which have suffered potash metasomatism, but that a group of porphyritic microtonalites from borehole 2 have very high Ba contents without corresponding increases in K. This appears to be the only occurrence in the boreholes, but one surface rock from south of Middle Mill (Table 2, no. 41) shows a similar pattern.

Because of the similar style of alteration the mineralised rocks at Llandeloy show compositional similarities with those from other porphyry style deposits (Table 11). For example, the tonalite group (Table 9) are closely similar to the Bougainville quartz diorites showing propylitic and potassic alteration. Principal differences of the Llandeloy rocks are the relatively low Cu and Mo content of all rocks and more basic composition of the diorite group (Table 9), with depressed silica levels a particular feature of some of the rocks showing potassic alteration. The low chalcophile element content is perhaps related to the deep section of the deposit thought to be intersected at Llandeloy, but the relatively basic composition appears to be a perculiar feature of this deposit.

The two stage alteration pattern or later metasomatic events may have nullified some of the prospecting criteria recommended for porphyry copper deposits. For example alkali and alkaline earth elements and ratios only show readily discernible differences from host rock variation in the potash alteration zone. Consequently changes in these elements and their ratios do not form the wide halos about the mineralisation recorded about many copper porphyries (e.g. Armbrust 1977; Ford, 1978). Here the best indicators of mineralisation are the elements principally involved: Cu and S. Both show appreciable enrichment in even weakly altered rocks and the Cu/S ratio may allow discrimination between the late stage propylitic and earlier potassic alteration.

'Stable' elements Evidence from several authors suggests that incompatible high field strength elements such as Zr, Ti and Nb often remain immobile during the alteration of volcanic rocks by processes such as hydrothermal activity, low grade metamorphism and weathering (e.g. Davies and others, 1979; Floyd and Winchester, 1978). Analyses of rocks from volcanogenic massive sulphide deposits showed, however, that during the formation of these deposits Y, Sc and Nb could be extremely mobile but that Zr, Ti and Ce remained immobile (Finlow-Bates and Stumpfl, 1981). The evidence from Llandeloy allows a similar conclusion to be reached: it indicates that under conditions of

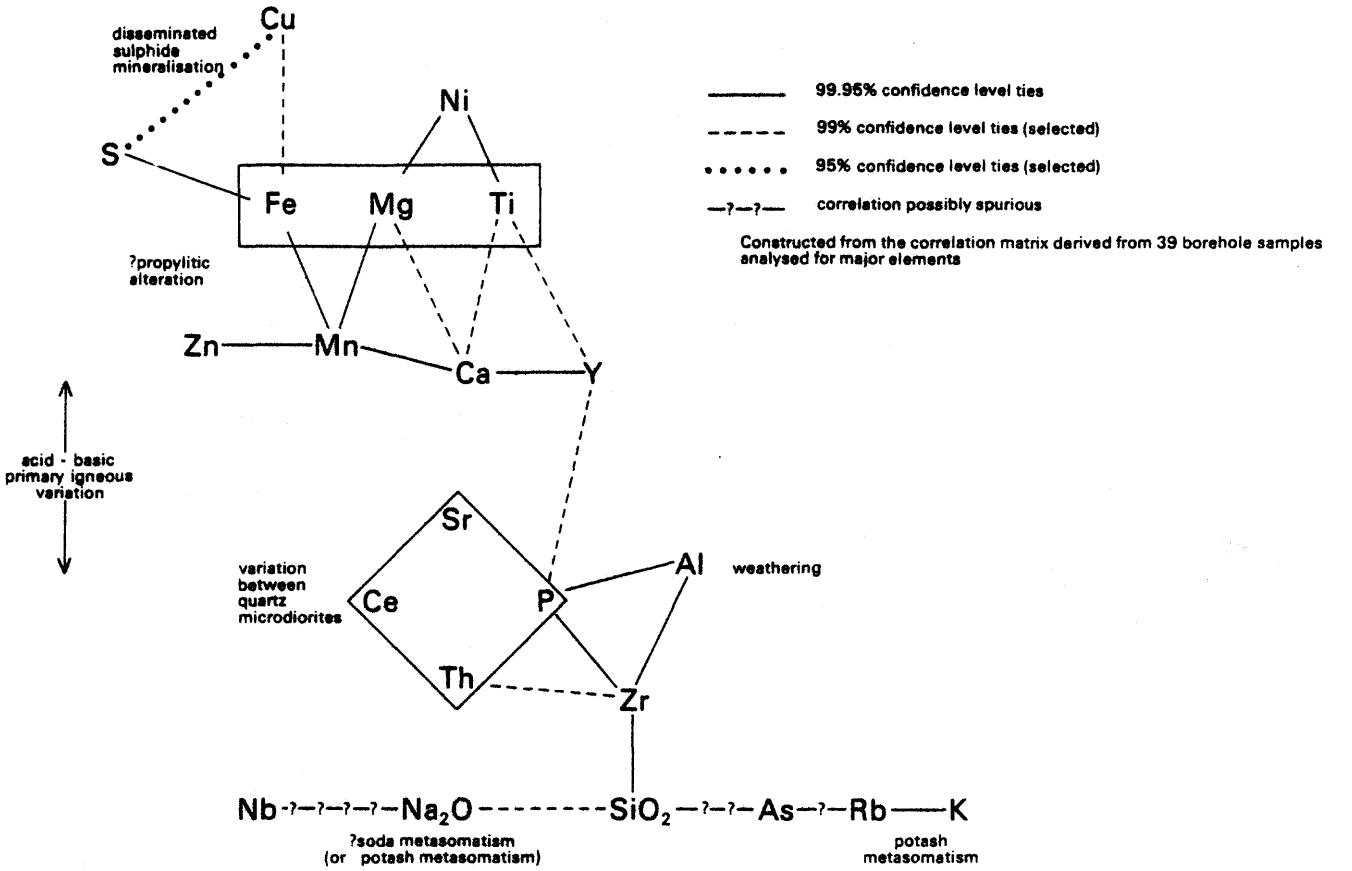

Figure 35 Diagrammatic summary of positive inter- element correlations in igneous rock samples from boreholes and their possible causes

Table 11 Selected analyses of mineralised rocks from porphyry copper deposits

	1				2	3	4	5
	Mean	Median	Max.	Min.				
SiO_2	57.88	57.85	63.40	51.80	61.68	64.22	61.05	65.08
Al_2O_3	16.04	15.90	19.10	13.50	16.92	15.19	-	-
TiO_2	0.43	0.42	0.67	0.23	0.53	0.33	-	-
Fe as Fe_2O_3	5.61	5.46	7.55	3.82	5.66	5.81	4.09	1.86
MgO	3.93	3.86	5.68	1.77	2.08	1.36	1.97	0.74
CaO	3.58	3.67	3.62	2.00	4.08	1.93	3.17	1.48
Na_2O	2.27	2.26	4.52	0.50	4.13	4.95	4.42	2.91
K_2O	2.31	2.38	3.89	1.12	1.79	2.76	1.77	3.84
P_2O_5	0.13	0.13	0.18	0.11	0.20	0.12	-	-
S	-	-	-	-	6100	3300	-	-
Cu	1450	740	7400	17	1500	4100	-	-
Pb	-	-	-	-	5	2	-	-
Zn	36	37	70	17	49	34	25*	10*
Ni	-	-	-	-	6	4	-	-
Mn	1200	1200	2100	700	400	200	205*	133*
Ba	-	-	-	-	236	134	510*	560*
Rb	-	-	-	-	43	35	41*	81*
Sr	-	-	-	-	638	566	686*	235*
Zr	-	-	-	-	109	91	-	-

Major elements quoted as percent of oxide, trace elements as ppm.

1 Coed y Brenin, dioritic rocks, phyllic zone, n=20 (Allen and others, 1976).
2 Panguna, Bougainville, average quartz diorite, propylitic and potash alteration, n=17 (Ford, 1978).
3 Panguna, Bougainville, average leucocratic quartz diorite, propylitic and potash alteration, n=15 (Ford, 1978)
4 Bethlehem-Ja, British Columbia, mean granodiorite and quartz diorite, propylitic zone, n=16 (Olade and Fletcher, 1976 ; Olade, 1977) * indicates geometric mean.
5 Bethlehem-Ja, British Columbia, mean granodiorite and porphyry, potassic zone, n=6 (Olade and Fletcher, 1976; Olade, 1977) * indicates geometric mean.

propylitic alteration all these elements are immobile, whilst under the more extreme conditions of potassic alteration Nb and Y show irregular mobility. No data are available for Sc whilst Ce and Th results above the detection limit are insufficient to reach a conclusion.

Ratio plots of the type suggested by Beswick and Soucie (1978) permit an evaluation of the effects of metasomatism in remobilising and redistributing elements in varied lithologies provided that the unaltered rocks follow common igneous trends. Plots of this type (Fig. 36) together with simple 'stable' element scattergrams (Fig. 37) of the type used by several authors (e.g. Pearce and Norry, 1979), indicate that whilst both Ti and Zr are depleted in a few samples (e.g. borehole 2, 25.25-26.82 m and 27.80-29.56 m) their ratio only shows moderate variation within a given rock type. As the silica content of these samples is heavily depressed compared with less altered rocks of similar type (due to extensive carbonate veining) it is suspected that the decrease in Ti and Zr is largely due to dilution. Y shows more erratic behaviour (Fig. 37) with two samples from borehole 2 depleted whilst one from borehole 5 is apparently enriched with respect to Zr or Ti, suggesting Y mobility in rocks which have suffered potassic alteration.

Statistics and elemental levels suggest that P and Al may also have remained relatively immobile during alteration though small changes in P may be hidden by the relative imprecision of the analyses with respect to the total variation in the rocks. The Nb content of all rocks is low but is below the detection limit in a greater proportion of the rocks which have suffered K-feldspar alteration than can be readily attributed to chance, and it is believed that depletion during potash alteration may have taken place. These observations are supported by multivariate statistical analysis of the borehole data which show negative associations of the type Cu, S, Fe v Y and K_2O, Ba, Rb v Nb, Sr, Na_2O.

Mobile/stable element plots of the type shown in Figure 36 can be useful indicators of the degree of

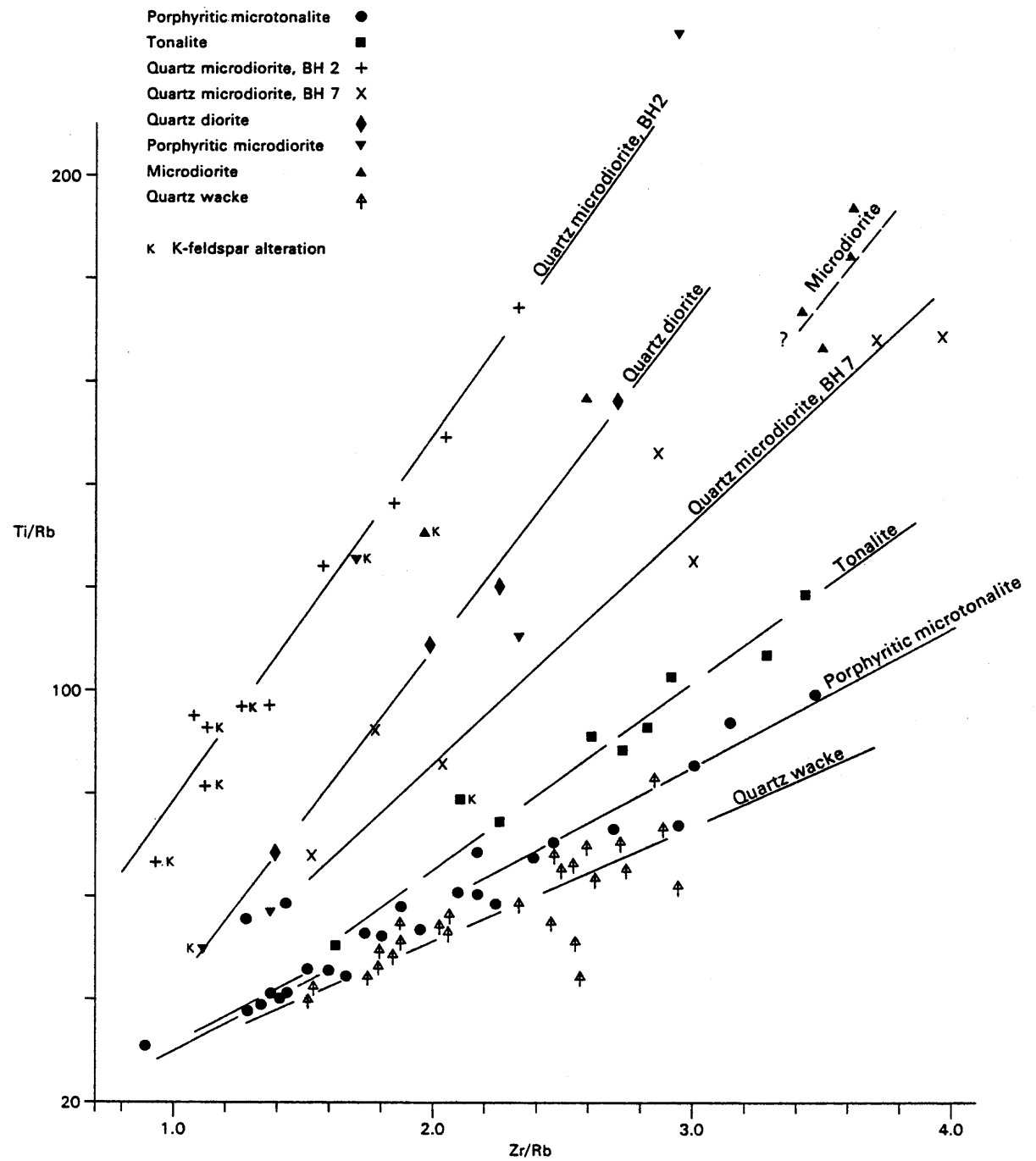

Figure 36 Ratio plot of Ti/Rb v Zr/Rb for igneous rock samples

	Thickness m
Limestone; coalesced nodules in unlaminated siltstone	c.5
LOWER LUDLOW SHALE	
Siltstone, tough, calcareous, flaggy, with abundant limestone nodules and some coquinal limestone beds; large strophomenids	c.4

7. Cutting [7258 4102–7254 4094] below Hope End House exposes about 6 m of the lower part of the formation. Poorly fossiliferous, tough, olive-grey, calcareous siltstones contain abundant limestone nodules coalesced into thin beds; the limestones occupy about 30 per cent of the rock. The basal 2 m are laminated, with *Favosites* sp., *Atrypa reticularis*, *Gypidula lata*, *S. euglypha* and *P. globosa*. Solitary corals, *Howellella elegans*, *L. depressa*, *P. ludloviensis* and *S. wilsoni* occur in the higher beds.

8. Disused quarry [7276 4093] opposite Lavanger Coppice exposing about 6m of poorly fossiliferous, massive, open-jointed limestone consisting of nodules coalesced into thin beds in a brown-grey to red-brown calcareous siltstone matrix.

9. Track exposures [7209 4004–7228 4021] on Godwins Rise in which up to 3 m of Aymestry Limestone are exposed (Penn and French, 1971, pp.20–21).

10. Disused quarry [7453 4027] north of Chance's Pitch exposing the highest part of the Aymestry Limestone; about 5 m of brown-grey tough calcareous poorly laminated siltstone contain numerous limestone nodules and layers; *A. reticularis*, *L. depressa*, *M. nucula*, *S. wilsoni*, *S. euglypha* and *D. myops* were collected.

Upper Ludlow Shale

The Upper Ludlow Shale consists mainly of olive-grey calcareous siltstones and mudstones. Thickness is generally 50 to 60 m, but increases to a maximum of about 100 m in the south around Coddington. Phillips (1848) recorded 18.3 m (60 feet) at Knightwick, but the section may be faulted (p.33). Limestone nodules and layers are

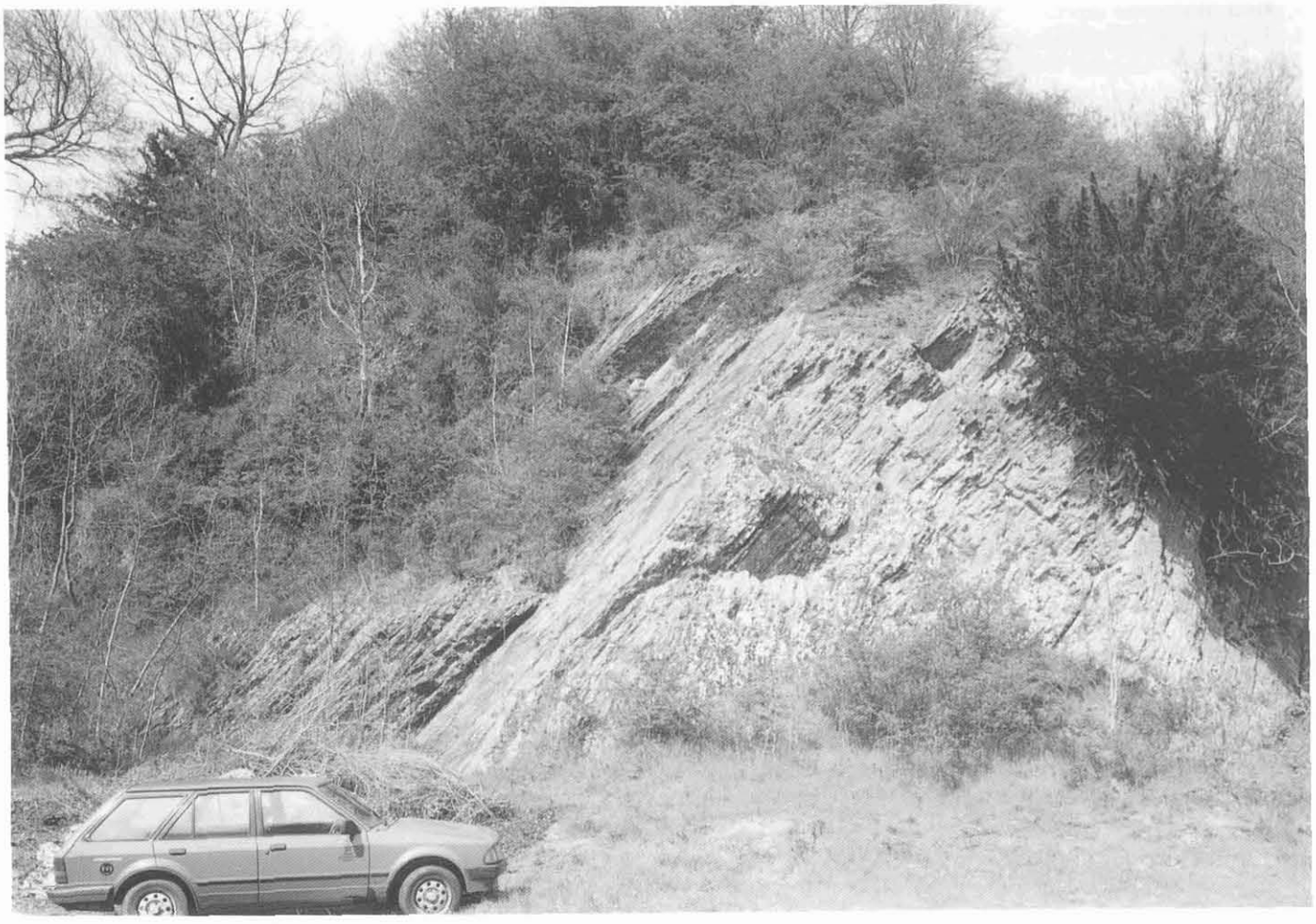

Plate 4 Ludlow Series rocks, Halesend Quarry [7378 4866]. Calcareous siltstones of the Upper Ludlow Shale overlie thinly bedded limestones of the Aymestry Limestone Formation. The junction is placed at the prominent bedding plane above the car bonnet. A 15081.

Zinc levels are broadly similar to those recorded in unmineralised rocks of similar type and, together with strong positive correlations with Ni, Mn and Ti and lack of sphalerite or other zinc minerals, suggest that most of this element is held in silicate and oxide phases. Contrary to most models zinc is not depleted in the highly altered rocks. There is some evidence for weak enrichment associated with pyritisation and late stage propylitic alteration. The highest levels of Zn occur in weathered rocks at the top of boreholes 1, 3A and 4 and it is probable that these are the product of secondary concentration processes. High levels of Pb and Cu accompany high Zn levels in the upper part of borehole 1, suggesting perhaps the presence of very weak but distinctive polymetallic mineralisation at this locality.

Molybdenum shows very patchy enrichment up to a maximum of 91 ppm over 1.1 m in borehole 2. High levels are most consistent in the quartz microdiorite intersected in borehole 7. The reasons for this association are obscure, but may be related to the distinctive composition of this intrusion. There is a relationship between Cu and Mo levels to the extent that in all samples with greater than 8 ppm Mo there is greater than 100 ppm Cu, but the overall correlation is not close and many rocks with high Cu contain only background levels of Mo. The Cu/Mo ratio is high and erratic. It does not, therefore, support the idea that a porphyry root zone is intersected at Llandeloy, for on a typical porphyry model high Mo and low Cu/Mo would be expected in the root zone (e.g. Hawkes and Littlefair, 1981). Mo displays independent behaviour, it shows no strong correlation with any other element determined. There is an apparent correlation of the highest values with propylitic alteration, but this may be spurious as it is generated by the association with quartz microdiorite in borehole 7 and one other sample.

Arsenic only shows increases above background levels in borehole one. Enrichment is weak with a maximum concentration of 92 ppm over 1.5 m and shows no correlation with any other element determined. Arsenopyrite was not recorded and As at these levels is probably held in pyrite particularly as high As coincides with the zone of highest chargeability recorded in this borehole. The analytical results provide no evidence for W mineralisation.

Very high levels of iron (>10%) are associated with abundant pyrite and with high levels of Cu, and preferentially occur in rocks with potassic (K-feldspar and biotite) alteration. Detailed examination within a single lithology allows an association with late stage propylitic alteration to be discerned, but Fe variation is primarily governed by host rock lithology and is confused by redistribution in weathered rocks and partition into many mineral phases.

It may be concluded that mineralisation involving Cu, Fe and S was pervasive and associated with propylitic and potassic alteration. It was either enhanced or redistributed during late stage propylitic alteration but never reaches economic levels in the rocks examined. Pb, Zn, As and Mo all show unrelated local enrichments but any mineralisation is very weak and the apparent distribution patterns do not conform to those of a typical porphyry model.

Sedimentary rocks A summary of analyses of the main sedimentary rock types intersected in borehole 8 is given in Tables 12 and 13. The division into three groups is somewhat arbitrary to the extent that some quartz wacke analyses cover lengths of core which contain either a very thin magnetite sandstone layer or minor tuffaceous material.

Comparison of the quartz wacke analyses with those of greywackes from elsewhere (Table 14) indicates that the Llandeloy rocks are characterised by unusually high levels of Ti, Fe, Mn and Cu. The mineralogy of the rocks suggest that the high levels of Cu and perhaps Fe are caused by sulphide mineralisation but, as in some other areas (e.g. Condie and Snansieng, 1971), the Ti content is related to provenance. Other chemical characteristics of the Llandeloy quartz wackes are their low Sr and Ca levels. The constant Sr/Ti ratios (Fig. 38) suggest that low Sr is not caused by metasomatism unless it is an unusually uniform depletion. A comparison with sedimentary rocks from Central Wales (Read, 1983) indicates that low Ca and Sr may be common features of Welsh Basin greywackes. Quartz wackes with tuffaceous bands (Table 13) show few chemical differences from those without volcanic material. The tuffaceous rocks contain higher levels of Ce, Y, Zr and possibly As.

Table 12 Summary statistics for 21 quartz wacke samples from borehole eight

	Mean	Median	Standard deviation	Maximum	Minimum
Cu	62 (95)	54	42 (161)	222 (794)	21
Pb	<13	<13	-	15	<13
Zn	56	53	11	79	39
Fe	66900	66360	7000	86500	57000
As	<2	<2	-	7	<2
Mo	2.2	2	1.3	5	<2
Ni	31	31	2.8	36	25
Mn	1100	1100	266	1900	740
Ti	6300	6360	330	6800	5300
Ba	450	461	90	610	280
Rb	111	114	26	149	46
Sr	104	97	32	168	65
Zr	236	236	11	256	215
Ca	7700	7560	2600	13400	3640
Th	10	10	1.6	13	7
Nb	14	14	1.4	17	11
Y	27	26	2.7	32	22
Ce	54	53	10.3	74	32
W	5	5	2.5	9	<3

Values in brackets refer to recalculated values including a highly mineralised sample where significantly different.

All results in ppm.

The magnetite sandstone samples, all of which are from sections less than 30 cm thick, have a very variable composition. Two of the samples contain appreciable sulphide mineralisation in veinlets. One of the mineralised samples contains the highest Cu and Pb and lowest Fe and Mn of the group, suggesting that slight Pb enrichment accompanied mineralisation. The low Fe and Mn are not thought to be caused by replacement but are due to poor sampling (the sample included a large amount of mineralised vein material outside of the boundary of the magnetite sandstone band). Both mineralised samples contain higher Rb and lower Sr than the unmineralised rocks, a feature attributed to alteration accompanying mineralisation. All four samples contain high levels of Ca, Sr, Ti, Cu, Mn and Fe compared with the quartz wacke. It is not certain whether these are all primary differences or whether, because of their composition, they have proved particularly susceptible to alteration.

The bulk chemistry of the rocks in borehole 8 appears to be largely unaffected by alteration processes despite the presence of biotite alteration. For example, Sr/Ti shows very little scatter compared with igneous rocks (Fig. 38). More predictably Zr/Ti and Ce/Y ratios also show little variation. Ba/Sr and Rb/Sr indicate that there may be a relative depletion in Ba and Rb in the more intensely brecciated rocks but Ba/Rb remains almost constant (3.7-4.2) showing only small changes related to increased proportions of mudstone (3.0-3.6). Late

Table 13 Summary statistics for sedimentary rocks containing tuffaceous and magnetite horizons

	Magnetite sandstones n=4					Quartz wackes with tuffaceous mudstone laminae n=6				
Element	Mean	Median	Standard deviation	Maximum	Minimum	Mean	Median	Standard deviation	Maximum	Minimum
Cu	104	94	36	154	75	53	52	18	79	29
Pb	16	<13	20	45	<13	<13	<13	-	<13	<13
Zn	48	48	4	54	45	59	59	5	67	54
Fe	90700	90900	26000	122000	59000	64000	64070	2300	66800	60000
As	<2	<2	-	2	<2	3.5	4	2.5	7	<2
Mo	4	2.5	4	11	<2	<2	<2	-	3	<2
Ni	27	28	3	30	24	29	30	2.5	32	25
Mn	1260	1290	256	1490	970	1080	1075	40	1130	1020
Ti	4900	5150	836	5610	3810	6170	6205	350	6550	5630
Ba	320	318	14	338	305	482	488	46	551	414
Rb	75	78	38	108	37	115	112	13	136	99
Sr	229	235	74	301	145	103	104	17	124	83
Zr	190	192	31	219	159	286	280	41	350	235
Ca	35000	35100	5700	41000	27500	6070	6350	1420	7590	4110
Th	7.7	7.5	1.0	9	7	11	12	1.1	13	10
Nb	12	12	1.5	13	10	15	15	1.9	18	13
Y	26	25	5	33	22	32	31	6	39	23
Ce	57	58	14	70	42	62	64	10	73	43
W	3	3	2.5	7	<3	6	6	1.4	9	5

All results in ppm.

Table 14 Greywacke analyses

	Quartz Wackes (this study)	Central Wales Greywackes[1]	North American Greywackes[2]	Culvennan Sandstone[3]	Vosges Greywackes[4]	North American Greywackes[5]	Cairngarroch Mineralised Greywacke[6]
SiO_2		63.21	70.60		63.54		62.33
Al_2O_3		17.74	12.59		15.51		14.04
TiO_2	1.05	0.88	0.64		0.77		0.83
Fe as Fe_2O_3	9.58	7.48	4.97		8.98	0.85	6.93
MgO		1.67	1.51		3.63	1.99	3.30
CaO	1.08	0.47	1.61		2.71		3.02
Na_2O		1.16	2.76		3.01		1.28
K_2O		2.83	2.20		1.80		2.58
P_2O_5		0.14			0.08		0.16
Cu	62		14	12	37	33	73
Pb	<13			<13			<13
Zn	56			54			43
As	<2			57			188
Mo	2.2			<2		<DL	5
Ni	31		8	29	85	43	93
Mn	1100	750	770	366	830	600	483
V		125	79		120	67	
Ba	450	616	403	265	399	380	201
Rb	111			58			101
Sr	104	102	110	95	232	260	176
Zr	236	221	413	331	182	400	200
Th	10			9			8
Nb	14						
Y	27	34	37	25		<DL	21
Ce	54	67		50			42

1 Read, 1983. n=80
2 Rensselaer Greywacke, Troy, New York (Ondrick and Griffiths, 1969). n=119
3 Allen and others, 1981. n=5
4 Rivalenti and Sighinolfi, 1969. n=35
5 Normanskill Formation (Weber and Middleton, 1961). n=31
6 Allen and others, 1981.

Major elements quoted in % oxide, trace elements in ppm.

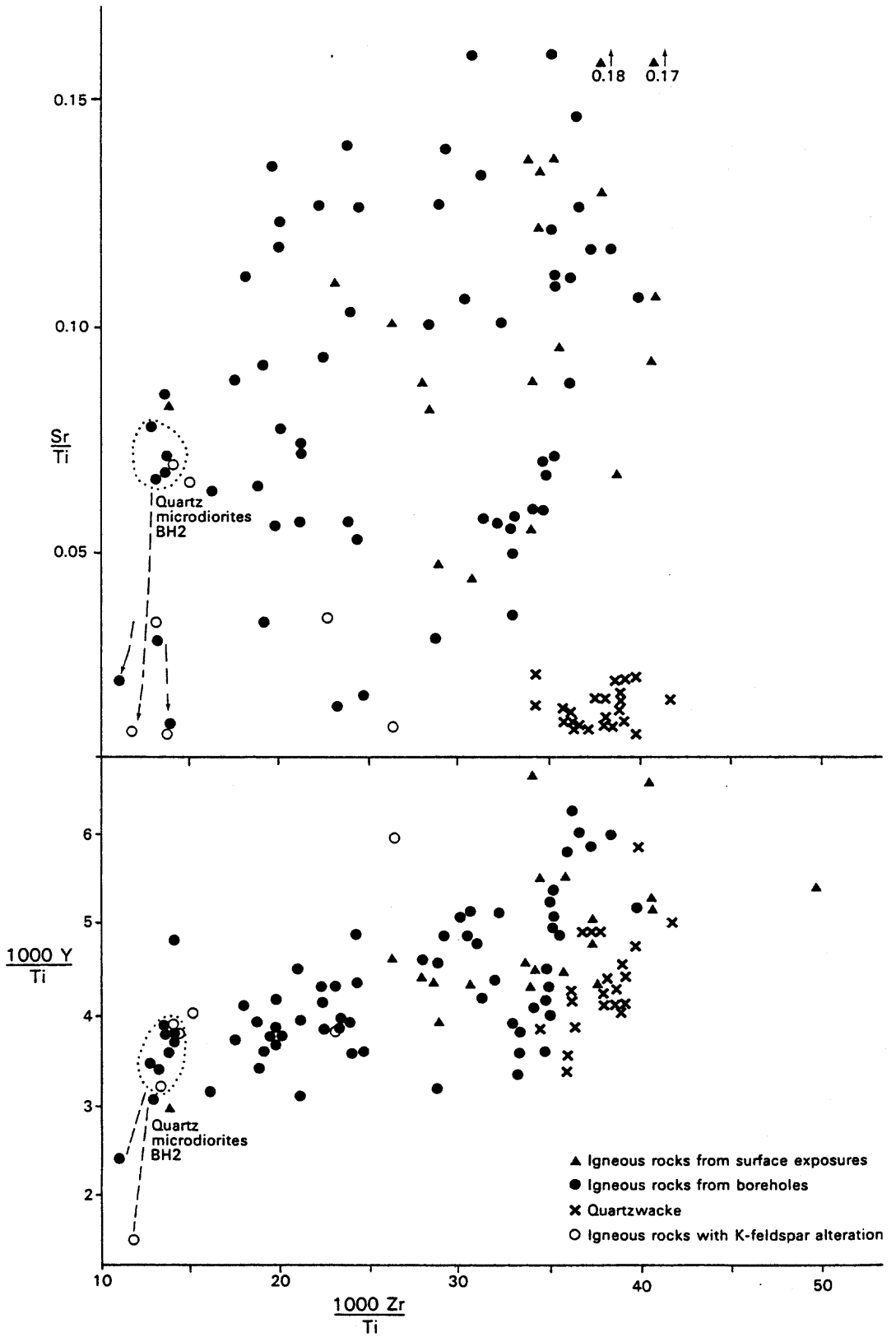

Figure 38 Examples of ratio plots for relatively mobile (Sr) and immobile elements (Zr, Ti and Y)

propylitic alteration, which is concentrated in breccia zones, may be associated with increases in Cu, Zn, Mn and Ca and depletion in Rb and Ba, but the majority of any compositional changes are caused by the accompanying sulphide mineralisation.

Mineralisation, with the exception of a brecciated zone between 105.61 and 106.20 m, is weak in the sedimentary rocks of borehole 8. Cu levels are lower than those in any of the other boreholes with the exception of the lower part of borehole 1. There is no general correspondence of high Cu levels with intrusion breccias. There is no substantial enrichment in any of the other chalcophile elements determined, 45 ppm Pb in a veined magnetite sandstone is the only outlying high result. Some of the highest Fe results in the quartz wackes, for example 8.6% Fe between 99 m and 100 m and 8.1% Fe between 105.61 m and 106.20 m, correspond with zones of relatively heavy pyritisation and intrusion breccias. W levels (up to 9 ppm) are higher in the sedimentary than in the igneous rocks and much higher

than average values quoted for sandstone and slates (Turekian and Wedepohl, 1961). The high results are probably caused by analytical interference from rare earth elements, which are much higher in the sedimentary rocks than the igneous rocks.

It is uncertain whether the relatively weak mineralisation and small changes in LIL elements and their ratios in borehole 8 is a function of alteration zonation or host rock control. Evidence from the borehole is inconclusive. Some of the intrusions intersected appear to show a different type of alteration and enrichment in Cu compared with the adjacent sedimentary rocks, for example the porphyritic quartz microdiorite cut between 45.34 and 46.44 m. Also, ratio plots of the analytical results for borehole 8 intrusives show more scatter than those of the host rocks, although none of the values match the extreme outlying results reported from boreholes 2, 4 and 5. The sedimentary rocks in borehole 8 are not of a type which might be considered particularly resistant to alteration and, in most porphyry systems, host rock lithology has little effect on the intensity of alteration: a comparable example is Coed y Brenin which is emplaced into a very similar sequence of host rocks. It is concluded, therefore, that the sedimentary rocks in borehole 8 were most probably peripheral to the hydrothermal system during the main (propylitic-potassic) phase of hydrothermal activity despite the presence of biotite alteration. The presence of intrusion breccias, a feature of the peripheral areas of porphyry deposits, supports this conclusion.

Regional alteration Surface as well as borehole samples show signs of alteration which has affected the igneous rocks across the whole area. The alkali metals show great variation in the Llandeloy-Middle Mill area as is illustrated using the plot devised by Hughes (1973). On this plot the Llandeloy rocks cut right across the field defined by Hughes as containing most common fresh igneous rocks (Fig. 39). It suggests that many of the rocks collected from available exposures have suffered soda metasomatism and some borehole samples potash metasomatism. Great local variation is expressed by the samples from a small part of the intrusion exposed in Middle Mill quarry. These rocks show quartz-sericite-chlorite-epidote alteration and it is not clear whether the chemical variation here is partly or entirely due to a regional event or hydrothermal alteration associated with the intrusion.

Loss of Na_2O and gain of K_2O is one of the characteristics of the potassic alteration associated with the mineralisation (see above), so on Fig. 39 the borehole rocks define a clear trend extending from the field occupied by soda metasomatised rocks, across the 'igneous spectrum' of Hughes into the potassic field. The rocks with the highest K_2O contents and containing K-feldspar alteration plot in the same sector as mineralised intrusives from Coed y Brenin (Allen and others, 1976) though the Llandeloy rocks are richer in total alkalis. It is likely that these rocks have suffered both potash and soda metasomatism. Na_2O does not show a strong positive correlation with any other element in surface or borehole samples, only a weak association with SiO_2 and Sr, and it is concluded that Na metasomatism was not accompanied by any other element determined.

There is no evidence from the borehole data to equate soda metasomatism with late stage propylitic alteration, although data is insufficient to be certain. On Hughes' diagram (Fig. 39) late stage propylitic alteration shows conflicting trends. One interpretation of the sketchy data indicates that late stage propylitic alteration superimposed on early propylitic alteration increases

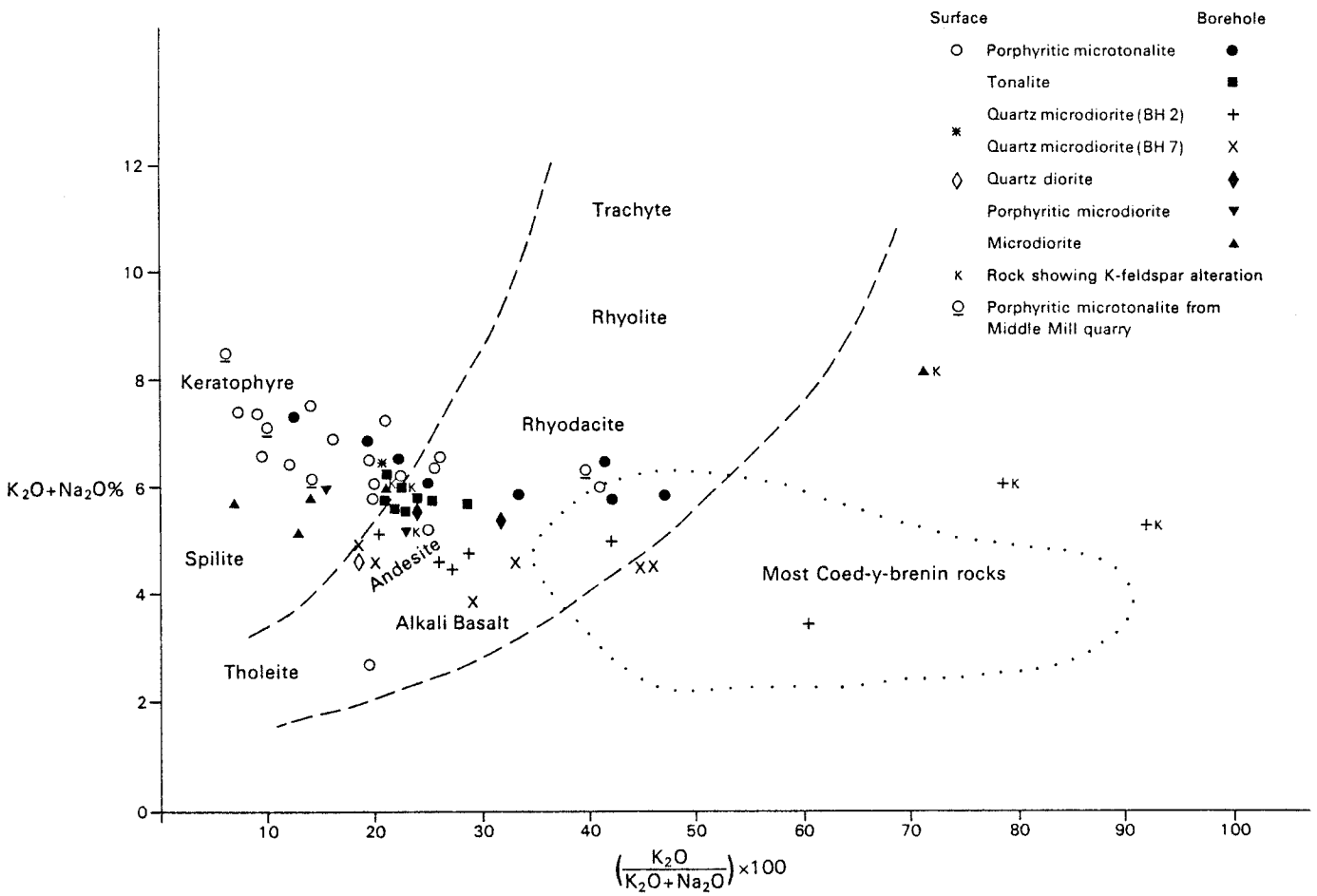

Figure 39 Plot of $(K_2O/K_2O + Na_2O) \times 100$ v $(K_2O + Na_2O)$ showing the fields occupied by common igneous rocks and mineralised Coed y Brenin rocks

potash contents whilst in K-feldspar altered rocks a reduction in potash and increase in soda occurs.

Comparison of surface and borehole rock results From the mineral exploration viewpoint the differences between the surface and borehole results are of great importance, because surface rock sampling gave no clear indication of the disseminated mineralisation intersected by the boreholes.

Precise comparisons between the borehole and surface rock data are hampered by the lack of dioritic rocks in the surface samples, which in itself is significant. The closest chemical comparison that can be obtained is shown in Table 15. Alteration in the borehole samples is dominantly of weak potassic (biotite) type, overprinted with variable intensity by late stage propylitic alteration. In the surface samples alteration is very variable but frequently of quite intense propylitic type with quartz-chlorite-epidote-sericite assemblages developed.

The two groups have virtually the same mean silica content and similar levels of most elements concentrated in basic rocks. Cu is the only element to show a great contrast in the two groups, with the lowest borehole result only slightly less than the highest level recorded in the surface rock group. The borehole samples may also contain higher levels of Pb, Zn, As, Ba and Rb and lower CaO, Na_2O and Zr. As the medians indicate, some of these differences are greatly emphasised by the presence of one or two very high results and the differences may not be significant, but with the exception of Zr, they are changes which might be predicted when moving toward the centre of a porphyry system and changing from propylitic to potassic alteration zones (e.g. Chaffee, 1976). The higher Zr content of the surface samples may be related to weathering.

If the results of the elements and ratios which most clearly show variation in the vicinity of the mineralisation (for example Cu, S, Cu/S, Na/K, Rb/Sr) are plotted out on a regional basis for the surface rocks no clear pattern emerges, and most variables show as great a variation within one outcrop as across the whole area. Only tenuous differences, such as the absence of very high soda in rocks collected in the vicinity of the mineralisation, can be discerned and it is concluded that no regional pattern useful for exploration purposes can be discovered from the surface rock sample results, even with the use of hindsight.

Samples taken closest to the boreholes give no chemical clue to the nearby mineralisation. This is surprising considering the extent of the mineralisation and can only be attributed to chance. The quartz diorite sample taken from Hollybush quarry (Table 2, no. 2) was collected within 200 m of borehole 5 (tonalite at bedrock surface with 300 ppm Cu in drill mud) and contains the highest copper (46 ppm) and Fe (9.05%) content of any surface sample. It also contains low Zr and Na_2O, but these are features entirely consistent with the more basic composition of this lithology compared with other surface rocks. Only a slightly elevated Mo content suggests that it is close to disseminated mineralisation.

It is therefore concluded that inadequate sampling caused by a lack of surface exposure, together with the masking effects of regional alteration and the complicated pattern of alteration associated with the disseminated mineralisation, are the reasons which have prevented the detection of extensive disseminated mineralisation by whole rock analysis of samples from available exposures in this area. It shows that in such an area this type of approach, used in isolation, could be a most misleading prospecting tool.

Table 15 Comparison of surface and borehole analyses of igneous rocks

	Surface Rocks[1]				Borehole Samples[2]			
	Maximum	Minimum	Median	Mean	Mean	Median	Minimum	Maximum
SiO_2	65.21	57.98	61.80	61.58	61.11	60.46	57.49	65.04
Al_2O_3	18.62	15.86	16.99	17.04	16.55	16.50	15.79	17.33
TiO_2	0.62	0.34	0.42	0.43	0.40	0.39	0.35	0.47
Fe_2O_3	7.63	4.57	6.10	6.10	6.14	6.46	4.85	7.06
MgO	4.79	1.78	3.11	3.12	2.71	2.75	2.00	3.17
CaO	9.74	0.29	3.15	3.37	2.81	3.44	0.51	6.03
Na_2O	7.98	2.21	5.24	5.25	4.48	4.35	3.13	6.43
K_2O	2.60	0.52	1.23	1.21	1.65	1.43	0.93	2.80
P_2O_5	0.17	0.12	0.14	0.14	0.14	0.14	0.12	0.16
Cu	42	<6	15	17.7	191	226	36	353
Pb	61	<13	<13	<13	42	<13	<13	376
Zn	111	19	67	66	76	75	54	105
As	16	<2	3	4	13	2	<2	92
Mo	25	<2	<2	2.4	3	3	<2	8
Ni	19	<5	10	9.5	9	7	<5	16
Mn	2120	320	925	966	903	955	510	1080
Ba	893	100	257	327	495	412	229	1841
Rb	91	11	34	35	41	34	25	70
Sr	491	124	287	310	287	291	135	458
Zr	118	80	98	98	87	87	81	96
Nb	7	<2	4	4.5	4	4	3	6
Y	23	12	14	14	13	13	10	15
Ce	33	<21	<21	<21	<21	<21	<21	<21
Th	5	<4	<4	<4	<4	<4	<4	4

Major elements quoted as percent of oxide, trace elements as ppm.

1 Twenty porphyritic microtonalites from outcrops in the Llandeloy-Middle Mill area.
2 Sixteen porphyritic microtonalites and tonalites from boreholes 1, 2 and 5.

Geophysics

Introduction

The main geophysical method employed along all traverse lines was induced polarisation (IP), which is particularly suited to the detection of low-grade disseminated sulphides, but will also respond to more massive deposits. The dipole-dipole electrode array was used throughout with a dipole length (a) of 50 m. For the 600 m spaced reconnaissance traverses a constant dipole separation of n = 2 was used, while along the 200 m spaced infill traverses at Treffynnon an expanding separation from n = 2 to n = 6 was used to provide some depth and dip information. Magnetic measurements were taken on all traverse lines using proton magnetometers. The very low frequency electromagnetic method (VLF-EM) was used in the reconnaissance survey, but artificial conductors are numerous and the method was not helpful.

Cores from the boreholes were subjected to magnetic susceptibility and density measurements and some of the holes were geophysically logged. Aspects of these logs are discussed below, and the detailed logs are held by the Regional Geophysics Group of BGS.

The detailed geophysical results and descriptions are contained in Appendix 2, with the main features described and discussed below.

Induced polarisation

Over most of the area, IP chargeability values remained in the range 5 to 15 milliseconds (ms). Values over 20 ms are considered anomalous, the maximum measured (away from artificial sources) was 50 ms. Two main areas of anomalous chargeability occur (Fig. 40). The smaller lies in the southwest, near the Cambrian-Ordovician boundary mapped by Williams (1933). If the measured maxima are connected between the traverse lines as shown on Fig. 40, the strike of the chargeability anomaly crosses the geological strike at about 40°. Continuity, however, has not been proved between these widely spaced traverses, and the cause of the feature(s) is unknown.

The second area of high chargeability lies east of Treffynnon, where it is accompanied by copper anomalies in soil. Qualitative interpretation of the chargeability pseudosections allows a map of IP sources to be drawn (Fig. 41). The Tetragraptus Shales along the north of the area produced chargeabilities up to 40 ms, and similar values were recorded over the Brunel Beds in the southeast. Both units include dark grey or black mudstones which may contain carbonaceous matter in sufficient quantity to produce these anomalies. In the area of the geochemical anomalies near Treffynnon there occurs a patchy linear chargeability high trending about 065°, with values up to 35 ms. The maximum values apparently lie where this lineation intersects members of a set of weak east-west-trending anomalies (Fig. 40). The boreholes over this feature (2, 3A, 3B, 4 and 5) intersected pyritous altered intrusive rocks under locally thick lacustrine deposits. Detrital magnetite and hematite-coated pyrite occur in these deposits (Allen, 1981) and may be responsible for the IP anomaly. However, under some circumstances clay-bearing rocks can produce IP effects, sometimes equivalent to several percent of sulphides, though by a different mechanism (e.g. Telford and others, 1976). The maximum effects occur in sediments containing perhaps 10 percent clay minerals, well distributed, and a low salinity pore fluid. At Llandeloy the clay content of the lacustrine deposits rises to perhaps 50 percent, but much of this is concentrated into thin clay beds, while the sandy beds approach more closely the conditions described. The downhole IP logs (available for boreholes 1 to 4, figs. 20-24) show that the IP response of these surficial deposits is locally strong, around 30 ms in borehole 3A and rising to 70 ms in borehole 3B. The underlying intrusive rocks produce chargeabilities around 20 ms with peaks up to 50 ms, and it seems likely that both contribute to the IP anomaly measured at the surface. There is good evidence from magnetic (see below) and other data that the lacustrine sediments are composed of weathered bedrock

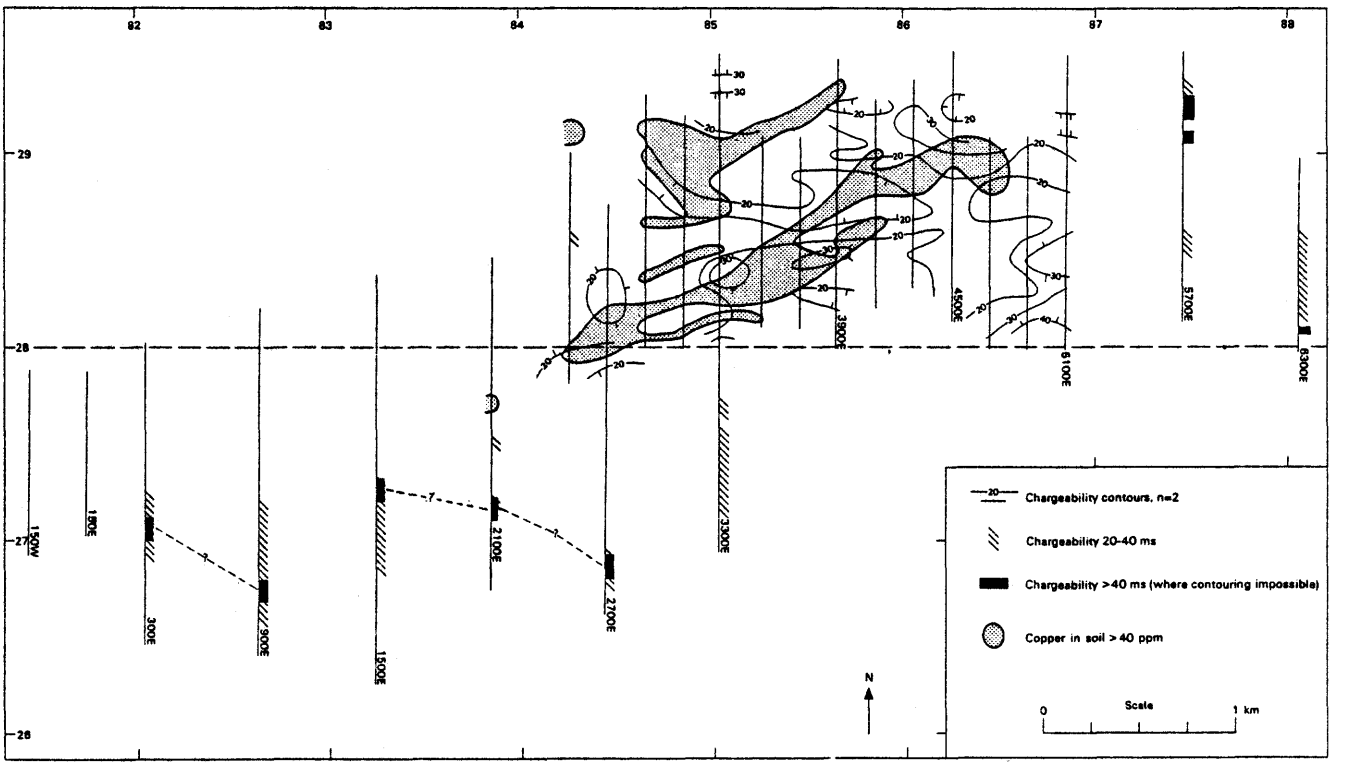

Figure 40 Chargeability anomalies in the Llandeloy area

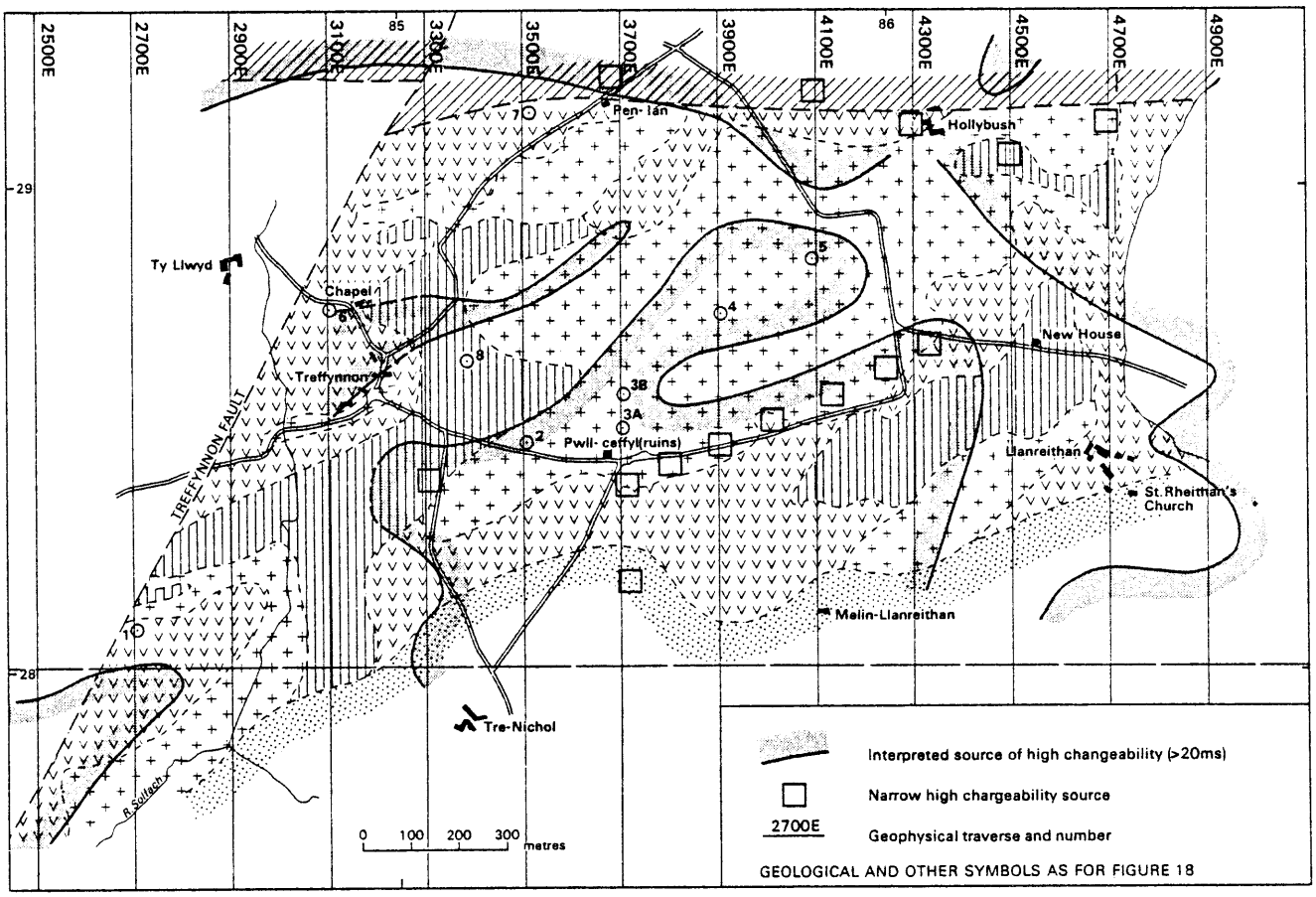

Figure 41 Interpreted induced polarisation sources in the area around the boreholes

material transported only a short distance, perhaps a few hundred metres or less.

Weaker IP anomalies occur over the altered intrusive rocks where the lacustrine sediments are thin or absent. A linear anomaly of 25-35 ms follows the mapped southern margin of the intrusion complex eastwards from Pwll-ceffyl ruin, but it is coincident with a road and may not be geological in origin. The volcanic Treffynnon Group produces moderately high chargeability in parts with values around 10 to 25 ms.

The IP results in the Llandeloy follow-up area, therefore, provide a complicated picture which reflects bedrock lithology and overburden composition. It does not, perhaps as a result of these complications or because only the root zone of the deposit has been preserved, allow evaluation of the mineralised intrusions in terms of a conventional porphyry-copper model.

Resistivity and VLF-EM

Measured apparent resistivities range from 100 to 5000 ohm-metres while VLF horizontal intensity, recorded by the airborne survey and expressed as percentages of the 'normal' intensity, varies from 90 to 115% with one or two larger anomalies due to powerlines. The two quantities are inversely related in a general way: low VLF intensities arise over resistive ground.

The regional maps (Figs. 12 and 13) show that three important linear conductive features enter the Treffynnon area (Figs. 42 and 43). In the north, an east-west fault brings the resistive Cambrian and intrusive rocks which form the core of the horst against conductive Tetragraptus Shales. Resistivities are around 200-300 ohm-metres north of this fault and mostly over 2000 ohm-metres to the south. A second conductive zone, about 200-400 metres wide, passes NNE-SSW through Treffynnon. The pseudosections suggest that the source is a fairly narrow vertical structure near the western side of the anomaly, with surficial low resistivity material extending some way to the east. Magnetic maps discussed below show a marked discontinuity along this line which is therefore confidently interpreted as a fault and named the Treffynnon Fault. Geological indications place this fault somewhat to the west of its geophysical position. The third conductive feature entering the area is the NE-SW trending lineation of Fig. 13 which divides a zone of E-W VLF-EM trends from one of NE-SW trends. This may be the southern fault margin of the horst, but it is nowhere well defined and in the Treffynnon area becomes confused with the low resistivities associated with the lacustrine deposits. These surficial low resistivities occur around the line of boreholes 2 to 5 and to the south and west of Treffynnon. They have been used to provide the estimate of the extent of lacustrine deposits shown on Fig. 19. Attempts to model the conductive overburden mathematically from the dipole-dipole depth information were largely frustrated by lateral variations in resistivity (Appendix 5). One reasonably successful example from the east of the area indicated a 2.5 m layer of overburden of resistivity 1.15% that of the bedrock. Typical values might be 60 ohm-metres for overburden and 5000 ohm-metres for bedrock. The valley of the Solfach, although low-lying and marshy, did not noticeably depress apparent resistivities along the south and west of the area. This may imply that the river has eroded close to bedrock and that the valley is floored by a thin veneer of clean alluvium.

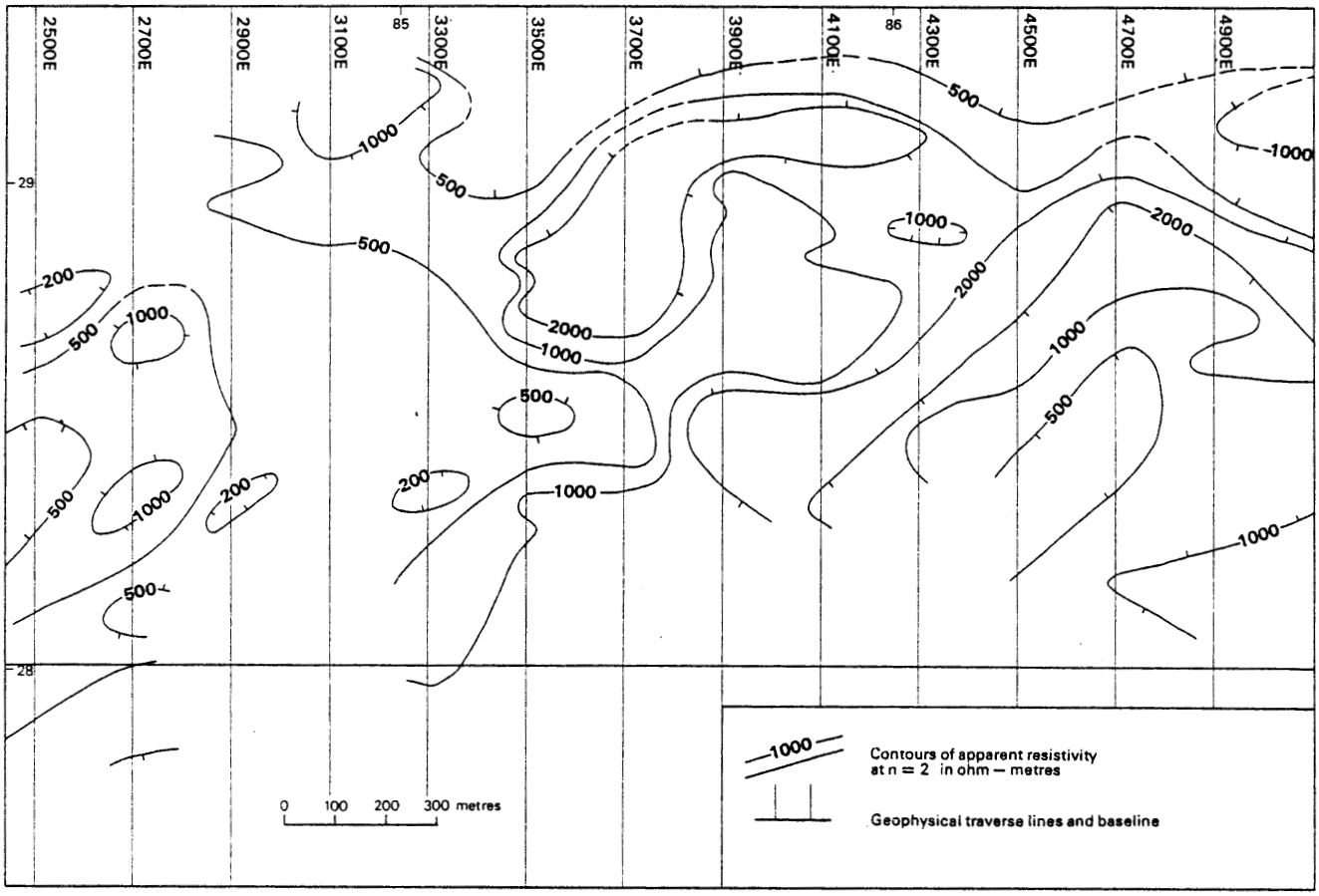

Figure 42 Contour map of apparent resistivity at n=2 in the area around the boreholes

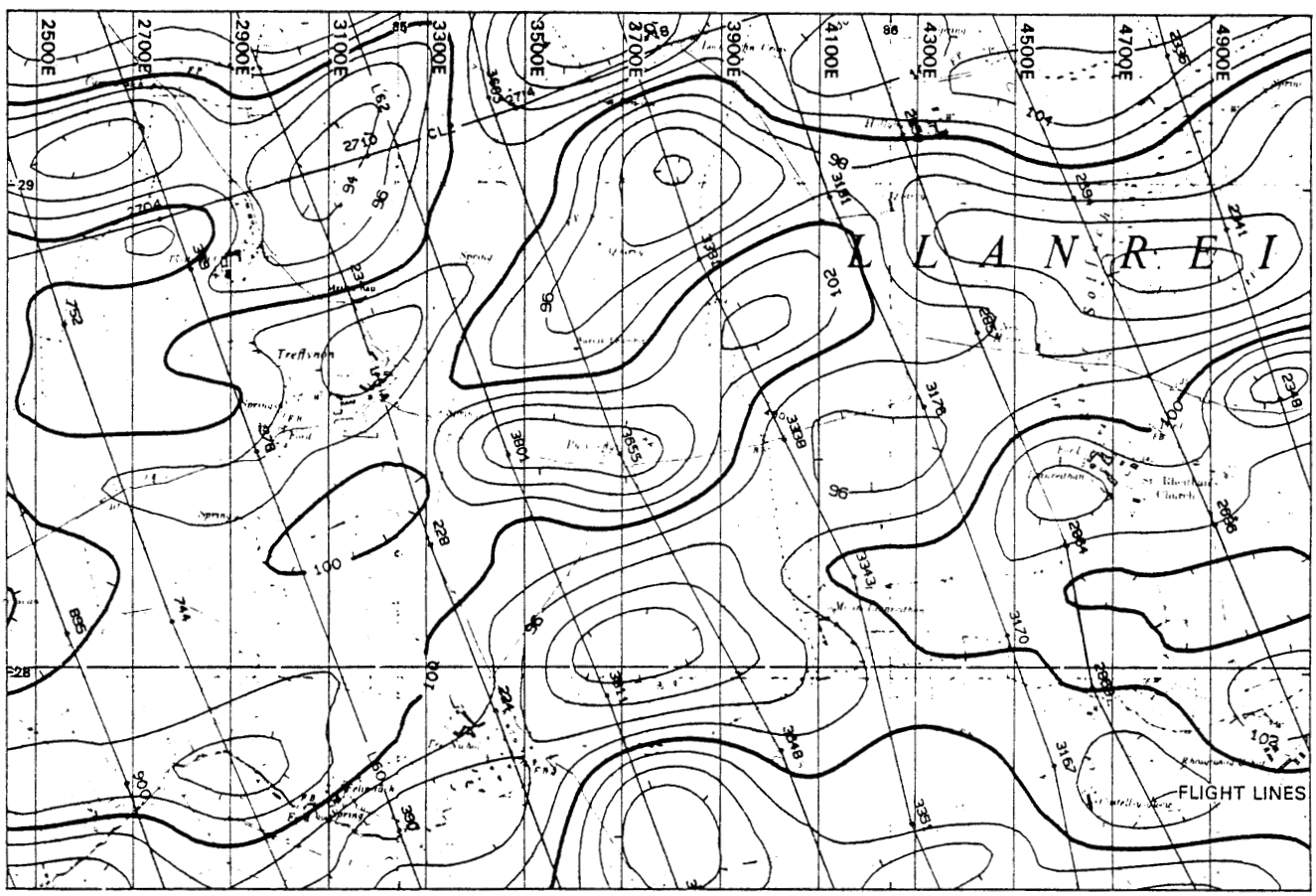

Figure 43 VLF horizontal intensity in the area of the boreholes with contours at 2% intervals

Magnetic surveys

Numerous magnetic anomalies were recorded with maximum amplitudes up to 500 nT on the ground and 200 nT from the detailed airborne survey (Fig. 7). Measurements on borehole cores show that susceptibilities of the magnetic rocks lie generally around 0.6 x 10^{-3} SI units. The magnetic data available for the Llandeloy area provide a picture of considerable complexity, but several useful conclusions can still be drawn. Strong short-wavelength anomalies due to near surface magnetic rocks are superimposed on a broad high indicating an underlying magnetic body of some depth extent. The pattern of aeromagnetic anomalies in the wider area and their interpretation has been discussed in the regional geophysics section.

In the Llandeloy area two groups of short wavelength anomalies occur separated by the line of the Treffynnon Fault (Figs. 44 and 45). To the north-west of the fault lies a roughly triangular group of anomalies with a 250 nT high along the northern edge. There is no geological indication of the source of these anomalies which are not accompanied by high chargeabilities but do coincide in part with weak copper-in-soil anomalies to the north of Ty Llwyd.

To the east of the Treffynnon Fault a roughly linear magnetic high up to 300 nT on the ground runs NE-SW along the line of the major chargeability and geochemical anomalies. The anomaly is not highly peaked, and on one traverse (3700E) becomes noticeably broader. Drilling showed that this effect was due to the lacustrine deposits. Several smaller anomalies occur north of the main high, but to the south the magnetic field falls away quite rapidly. To the west the anomalies of this group end abruptly along a line sub-parallel to the Treffynnon Fault but 200 to 300 metres to its east. A second fault along this line is implied, which could also explain differences in the degree of alteration between boreholes 7 and 8, and the 2 to 5 group. Double or multiple faults with this orientation occur elsewhere in the St David's area, notably southwest of the city.

Table 16 shows the results of the susceptibility measurements and profiles are plotted on the graphic logs (Figs. 20-28). High susceptibilities occur almost exclusively in altered intrusive rocks, but not all members of the intrusion complex are magnetic, and petrographically similar rocks from different boreholes have widely different susceptibilities. Magnetic susceptibility cannot, therefore, be used to distinguish different types of igneous rocks in the complex, different petrographic types having overlapping ranges. This is partly at least because of two secondary factors superimposed on the primary magnetic susceptibility variation. Firstly, there is a general relationship between susceptibility and degree of alteration, the most highly altered rocks of the area intersected by boreholes two to five showing average susceptibility eight times that of the other cores. Secondly, rocks from the weathered zone give lower results. Except for some thin magnetic horizons, low results were also obtained from the shales, sandstones and volcanic rocks. The lacustrine sediments were mostly weakly magnetic but contained some material of moderate susceptibility. If this magnetism arises from detrital magnetite a local source for the sediments is implied, as there is no other magnetic rock within a considerable distance.

There is good evidence, reviewed by Parker (1983) that magnetic susceptibility is distributed log-normally through a rock. Good descriptors of this distribution are the mean and standard deviation of the log-transformed data. Figure 46 shows these quantities calculated for the various lithologies at Llandeloy as well as the frequency histogram of susceptibility on a logarithmic axis. The histogram, constructed from all the data, is clearly polymodal and was split into component populations using cumulative frequency curve analysis (Sinclair,

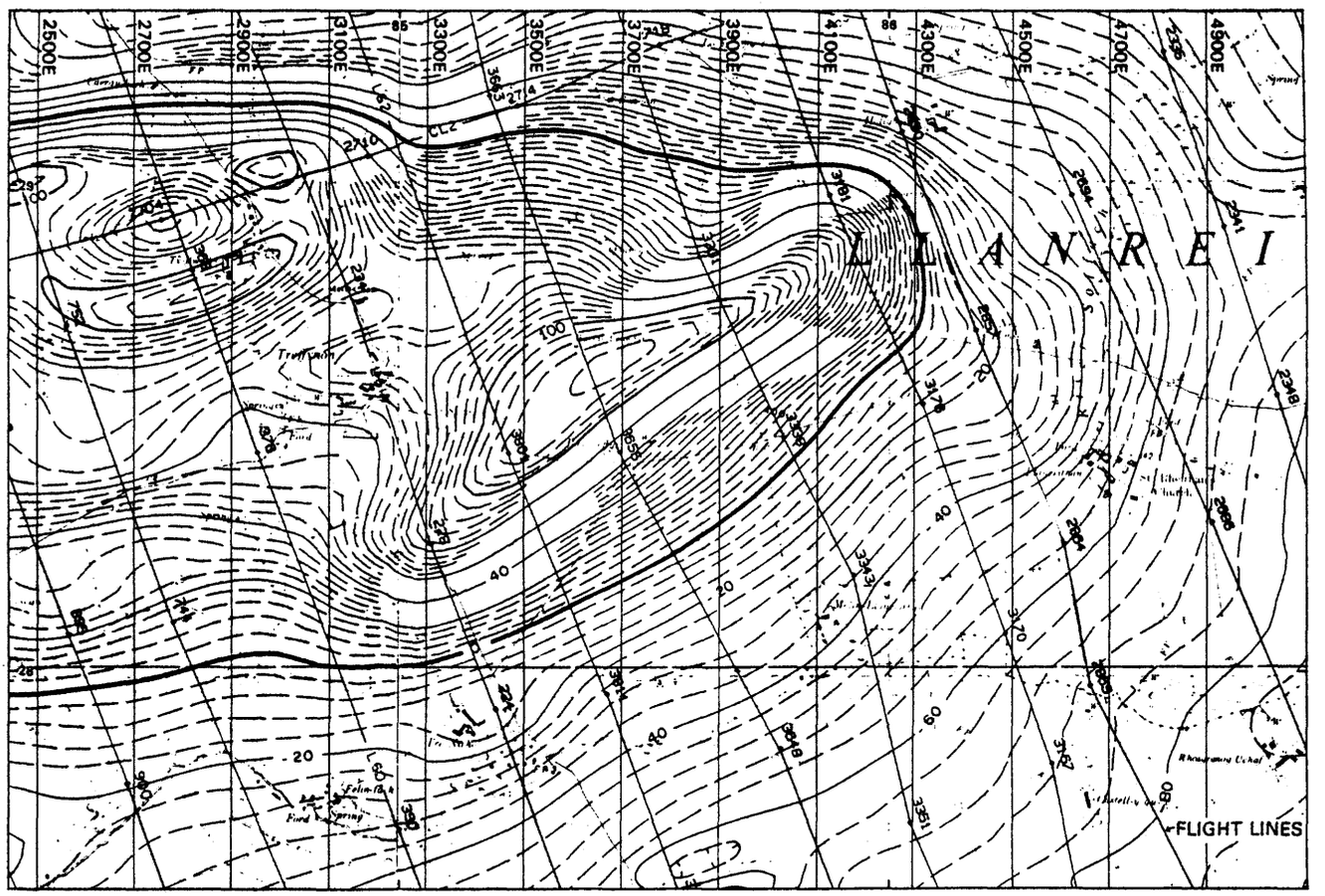

Figure 44 Aeromagnetic anomaly map of the area around the boreholes with contours at 4 nT intervals

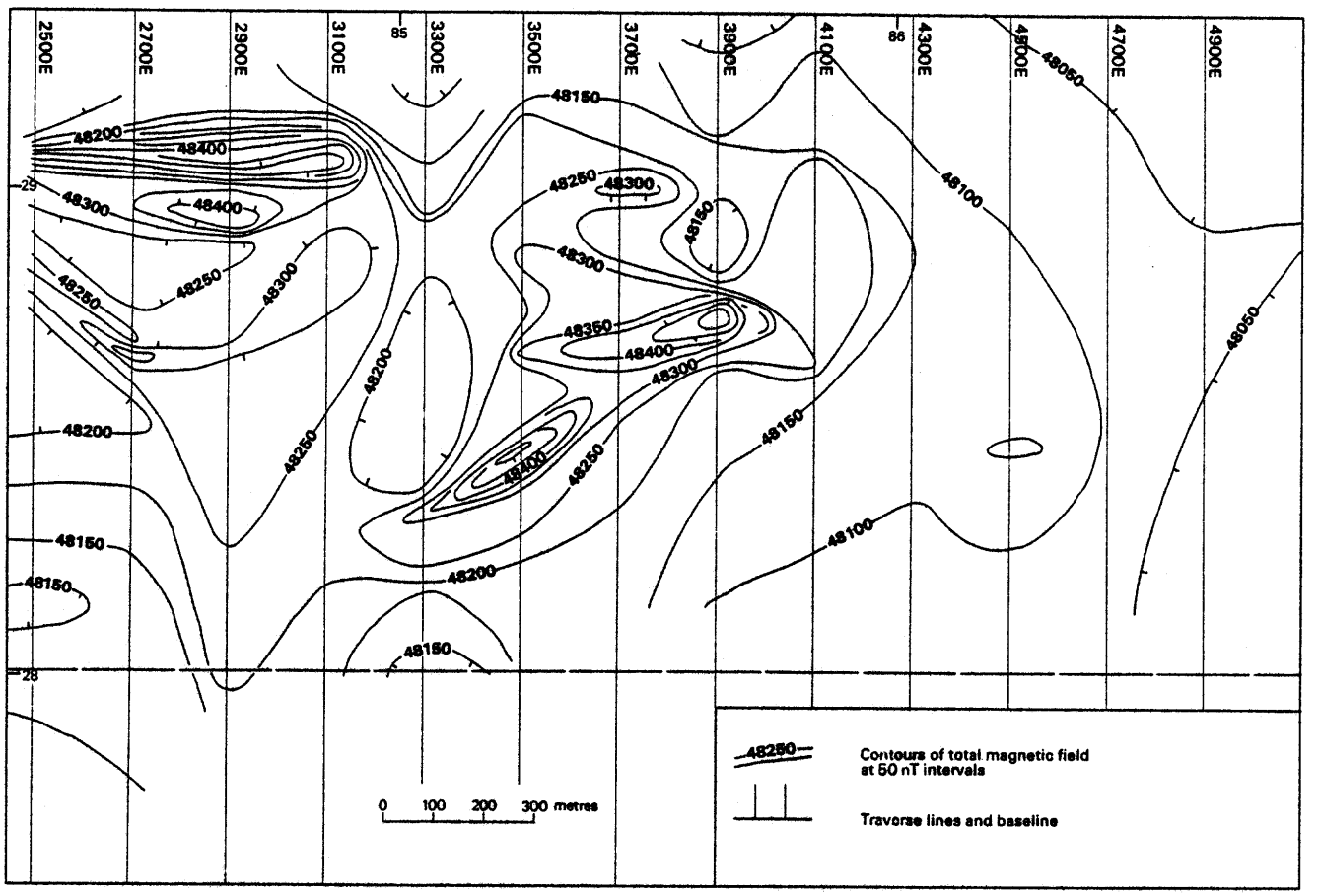

Figure 45 Contour map of total magnetic field from ground survey results in the area around the boreholes

Table 16 Mean ($\bar{K}$) and standard deviation (σ) of magnetic susceptibilities of borehole cores

Rock-type or borehole no.	Code	N	$\bar{K}$ x 10^{-3} SI units	$\overline{\log K}$	$\sigma_{\overline{\log K}}$
Unweathered rocks of BH1		23	0.24		
Unweathered rocks of BH2		23	11.5		
Unweathered rocks of BH4		22	17.7		
Unweathered rocks of BH5		27	5.0		
Unweathered rocks of BH6		15	4.1		
Unweathered rocks of BH7		17	1.02		
Unweathered rocks of BH8		119	1.49		
Lacustrine deposits	C	16	1.76	-0.2	0.73
Weathered rock	W	41	0.56	-0.48	0.46
Volcanics	V	6	0.43	-0.40	0.23
Quartz wackes & siltstones[1]	S	98	1.49	-0.16	0.37
Tonalite	T	24	5.5	0.12	0.82
Porphyritic microtonalite[2]:					
inc. borehole 1	mT	58	3.30	0.043	0.71
excl. borehole 1	mT	38	4.93	0.388	0.61
Quartz-microdiorite:					
borehole 2[3]	QmD	14	13.23	0.68	0.78
borehole 7[3]	QmD	17	1.17	-0.29	0.60
Quartz-diorite	QD	5	8.1	0.52	0.81
Microdiorite	mD	13	23.0	1.18	0.57
Porphyritic microdiorite	mD'	12	8.01	0.12	0.71

1 excluding magnetite bands $\bar{K} = 0.62$
2 $\bar{K}$ for borehole 1 porphyritic microtonalites is 0.21
3 separated on geochemical grounds

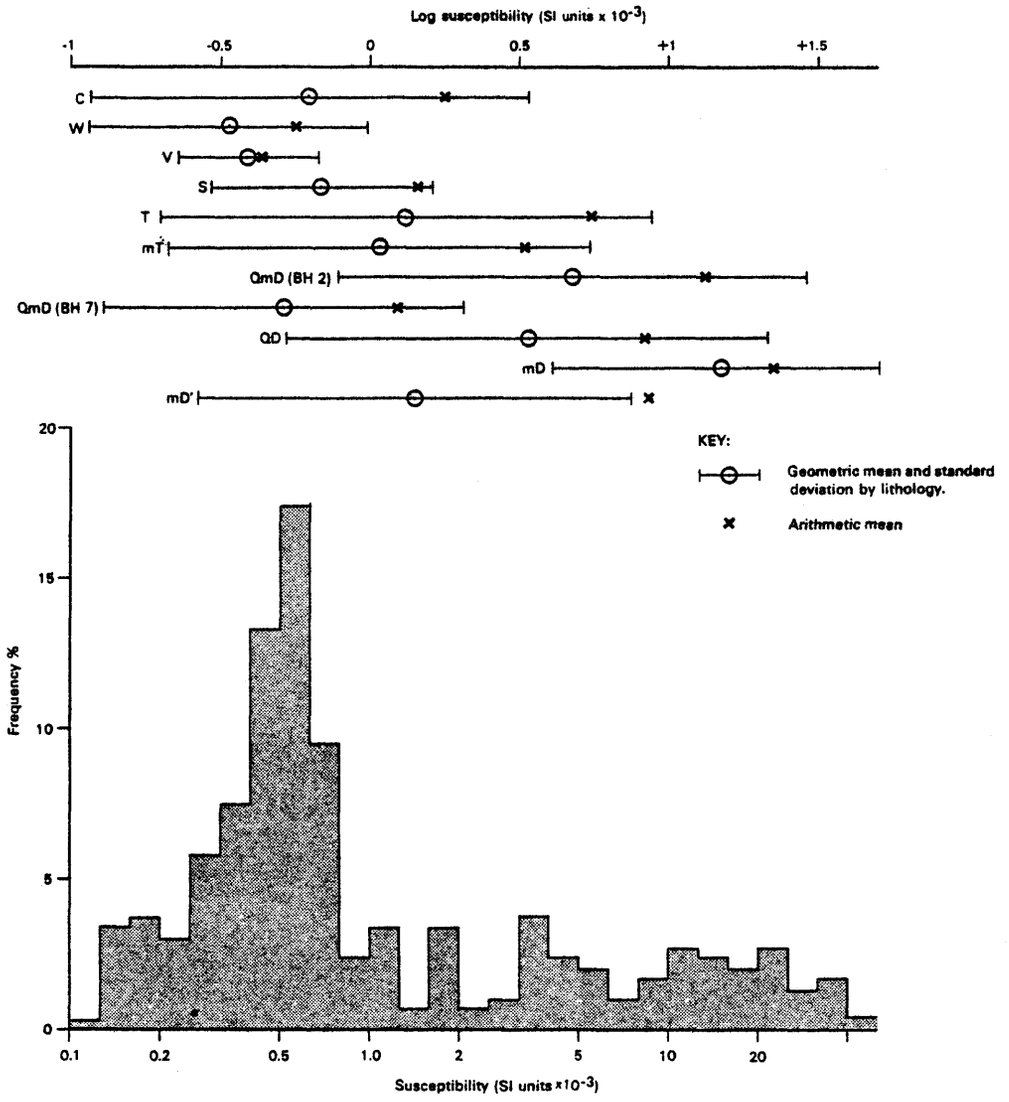

Figure 46 Magnetic susceptibilities of borehole samples

1976). Three component populations with geometric means of 0.22, 0.6 and 17 x 10^{-3} SI units were defined (Fig. 47). The largest population (mean 0.6), consisting of about 75 percent of the sample, can be regarded as the 'primary' background susceptibility of the rocks and probably contains unresolved populations related to different lithologies. The lower population is related to weathered rocks whilst the upper population can be ascribed to rocks containing magnetite generated during late stage propylitic alteration. Magnetic susceptibility may, therefore, be useful in detecting such rocks in boreholes. The magnetic complexity of the area as a whole, however, means that this magnetic signature is of little use on a wider scale because there are at least four modes of occurrence of magnetite here: secondary hydrothermal, primary magmatic, magnetite horizons within sedimentary rocks and detrital magnetite in lacustrine sediments.

The identification of localised highly altered rock as the most magnetic is partly at odds with the interpretation of anomalies in the wider area discussed above. The model of an anticlinal core of magnetic Precambrian rock clearly cannot be adopted without qualification in the Llandeloy area, but the broad magnetic anomaly further west does extend unbroken to Llandeloy, and it is likely that these rocks underlie the area at no great depth. The forms of some of the ground profiles (Appendix 2) certainly suggest some local, near surface effects superimposed on a much deeper seated anomaly. An alternative possibility is that the broader anomaly at Llandeloy is due to a subvolcanic intrusion, perhaps representing the remains of a magma chamber underlying the hypothetical Treffynnon volcano. However, the magnetic source indicated by numerical modelling has sides sloping outwards and a base width of 5 km or more at a depth of about 3 km, not a likely form for a subvolcanic intrusion. The susceptibility used for the models, about 7.5 x 10^{-3} SI units, is much greater than that of the unaltered intrusions at Llandeloy, but more typical of the Precambrian rocks which cause the western part of this anomaly. An anticlinal core therefore provides a more likely explanation of the broad anomaly than a subvolcanic intrusion.

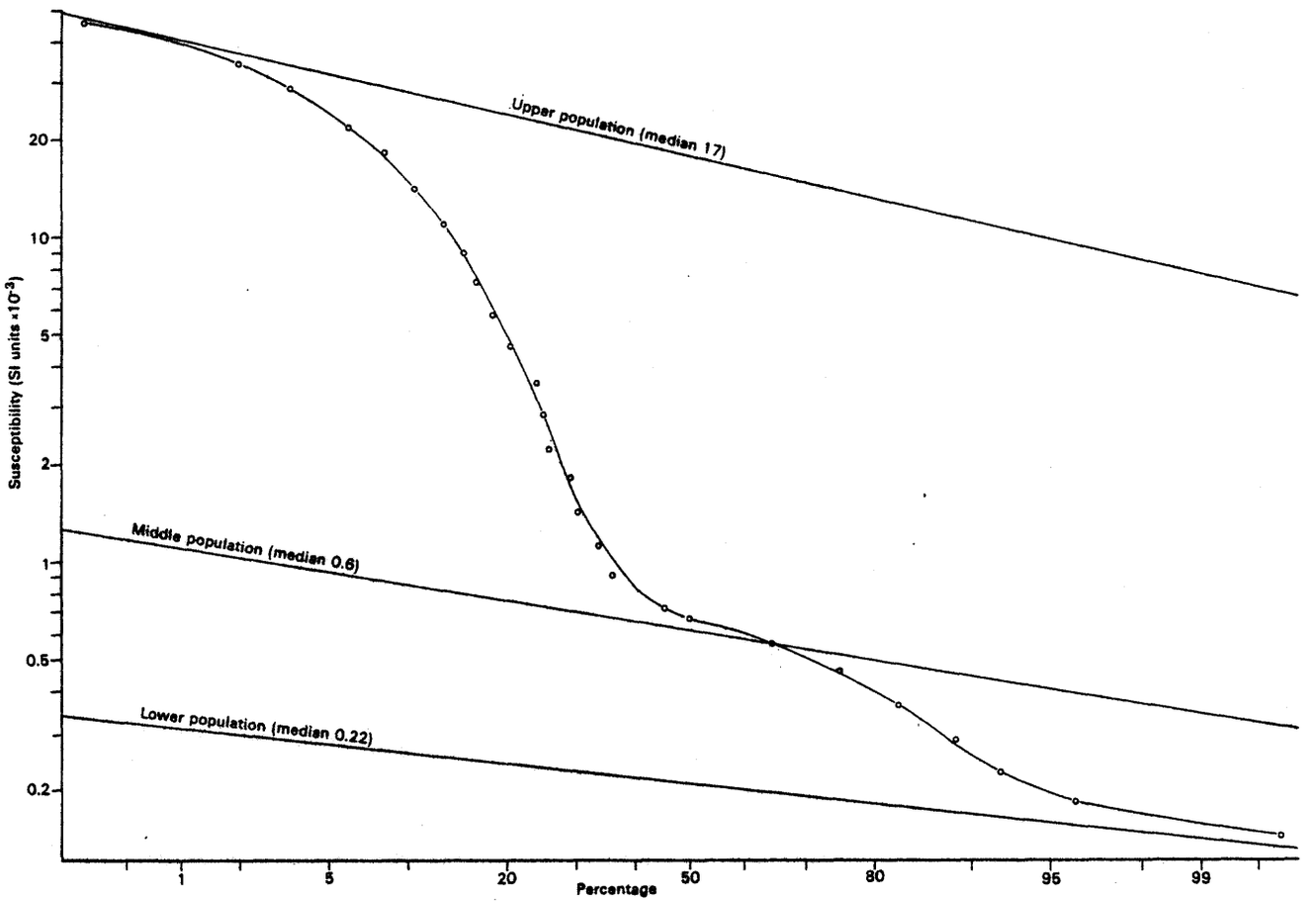

Figure 47 Cumulative frequency plot of magnetic susceptibility data from the Llandeloy area, showing component populations

Gravity survey

Two detailed traverses were made across the Llandeloy survey area in an attempt to resolve some of the questions raised by the magnetic data. Fig. 11 shows the line of the traverses and Fig. 48 the profiles.

The maximum residual anomaly revealed by the profiles is only 0.5 mGal and quite local, implying that no major rock mass of anomalous density underlies the area. The density measurements on borehole cores (Appendix 4) show little variation within the sedimentary rocks, which gave an average of 2.79 g cm^{-3}. Values obtained for intrusive rocks varied considerably, from 2.67 g cm^{-3} for a porphyritic microtonalite to 2.85 g cm^{-3} for a quartz-microdiorite, but average 2.75 g cm^{-3}. If the value obtained for the ?Cambrian quartz wacke and

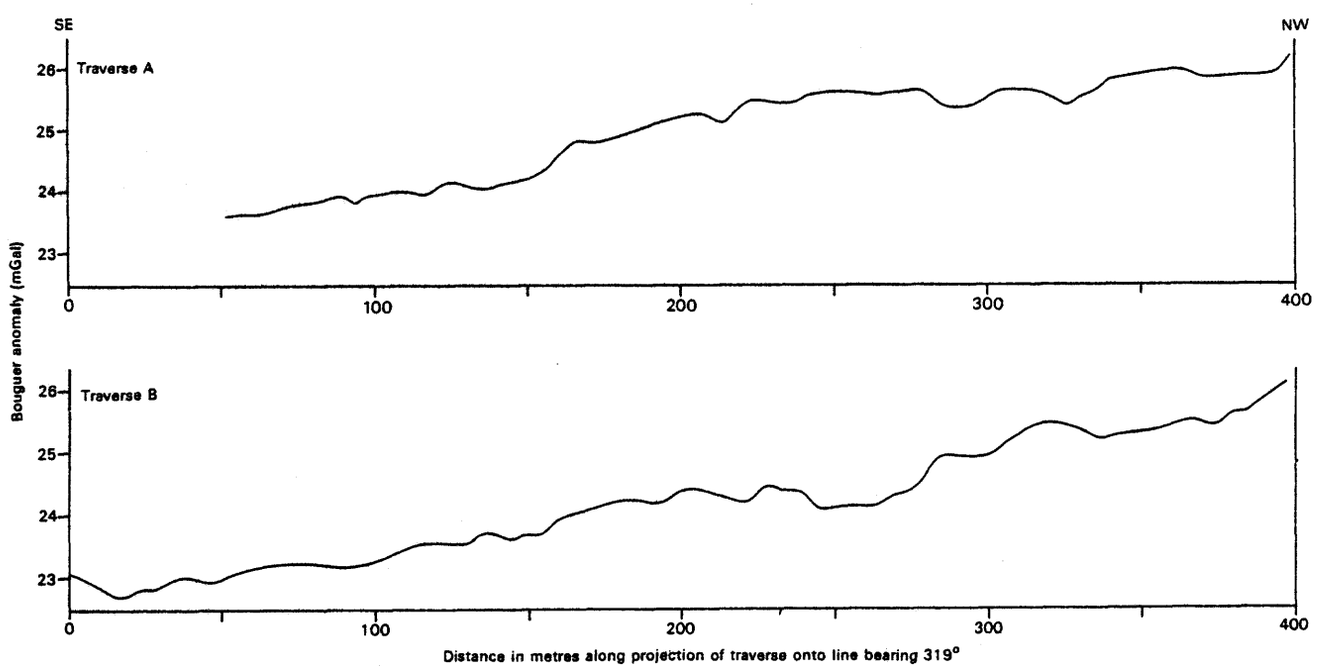

Figure 48 Bouguer anomaly profiles from the Llandeloy area

siltstones is typical of all sedimentary rock in this area, then an intrusion the size of the magnetic sources with a density contrast with its host of -0.04 g cm^{-3} would give a maximum anomaly of about -2 mGal. There is no such anomaly. No density is available for the Pebidian, but around St David's it does not produce a gravity anomaly, implying that its density is close to that of the surrounding rock. The absence of a gravity anomaly at Llandeloy therefore supports the conclusion that the broad magnetic high is caused by an anticlinal core of Precambrian rock, but with the qualifications that the densities of the Llandeloy intrusive rocks are themselves quite variable, and that the measured density of ?Cambrian sedimentary rock is rather high to be representative of other sedimentary rocks in the area.

Discussion

The acid and intermediate rocks penetrated by the boreholes appear to form a single concordant or semi-concordant complex of thin sheets (Treffynnon complex) exposed by a fault-bounded horst or anticlinal structure. The intrusions were emplaced into sedimentary rocks of probable middle Cambrian age and acid volcanic rocks, which may be of Precambrian or lower Ordovician age. Whichever is correct the intrusions, which are not known to penetrate Tetragraptus Shales or Brunel Beds, are most likely to be co-magmetic with the early Arenig Treffgarne andesites and may comprise a sub-volcanic intrusion complex similar to that which hosts the Coed y Brenin copper deposit in North Wales (Rice and Sharp, 1976). The Treffynnon complex consists of two chemically distinct groups of rocks: tonalites (58-65% SiO_2) and diorites (<56% SiO_2). They display common igneous trends which diverge in the diorite group into rocks relatively rich and deficient in the high field strength elements P, Zr, Th and REE. Zn, Mo and Sr also show contrasting concentrations in these two diorite sub groups. The divisions are probably primary features but there is no evidence to indicate that the chemically distinct rock groups are of significantly different age. The composition of all the intrusions is broadly calc-alkaline, they are similar to intrusions associated with porphyry copper deposits in other parts of the world and consistent with emplacement in a volcanic arc setting.

The Cambrian sedimentary, the volcanic and the intrusive rocks have all been subjected to pervasive hydrothermal alteration which seems to have affected neither presumed Tetragraptus Shales to the north nor the Brunel Beds to the south. This hydrothermal event which is inseparable from the sulphide mineralisation, brecciation and veining must, therefore, have been during the end Cambrian or early Arenig.

The hydrothermal alteration and mineralisation which is recognisable over an area of about 1 km^2 in boreholes, is characteristic of a porphyry copper type. Levels of copper are, however, modest, the highest grade intersection being 0.1% Cu over 3.4 m. The mineralisation is concentrated in the intrusion complex, though copper levels in the adjacent sedimentary rocks are high locally.

The alteration associated with the mineralisation is pervasive. The mineral assemblages suggest that early potassic and propylitic alterations were followed by a widespread and locally intense late stage propylitic alteration. Remnants of the highest temperature alteration indicate that K-feldspar formed a stable assemblage with pale green amphibole and biotite. There is a more extensive biotite alteration which is thought to be a lower temperature form of the potassic alteration. The high temperature, K-feldspar, alteration produced significant changes in the bulk chemistry of the rocks and has a distinctive geochemical signature. The alteration is characterised by strong increases in K, K/Na, K/Rb, Rb/Sr, Cu/S and, erratically, Ba and losses of Na, Sr and Ca. Locally the most altered rocks show large increases in K without corresponding increases in Rb resulting in very high K/Rb ratios. The concentration of two so called 'immobile' elements, Y and Nb, is also modified in some rocks within the potassic alteration zone. Rocks displaying biotite alteration show the same chemical trends but only the most altered show appreciable changes in their bulk chemistry. A peculiar feature of rocks showing biotite alteration is their apparent correlation with a high lead content. No chemical features characteristic of the early propylitic alteration could be determined because of the absence of unaltered samples and the effects of late propylitic alteration.

Only a small segment of the hydrothermal alteration system was cut by the boreholes, and biotite alteration was recognised in most intersections. Its absence in borehole 6, where only propylitic alteration was encountered, might suggest a westward decrease, but the pattern of alteration zoning is not simple or fully resolved and is likely to be interrupted by faults. For example, geophysical measurements suggest the presence of a fault between boreholes 2-5 and 8 which may account for the possible alteration hiatus here. Early propylitic alteration was also recognised in boreholes 2, 3A, 4 and 7 and in all cases except 3A, which was a very limited section, it is adjacent to potassic alteration. This might suggest irregular interfingering of alteration zones, but an alternative hypothesis is that the quartz diorite was intruded after the main alteration but before the late stage event. This is because in boreholes 3A and 4 the quartz diorite is only weakly altered and in borehole 4 has a sharp contact (possibly intrusive) against porphyritic microdiorite showing potassic alteration. Borehole 3A, however, intersected no other lithology and is sited close to a major northeast trending geophysical feature which is confidently interpreted as a fault and therefore provides an alternative explanation for the lack of alteration here. Further evidence contrary to this hypothesis comes from Hollybush quarry, where quartz diorite carrying clear signs of biotite alteration overprinted by late stage propylitic alteration was found. Two chemically distinct groups of diorites are recognised but these do not coincide with the early and late intrusive episodes recognised in borehole 4. It is concluded that there are insufficient data available to determine satisfactorily the pattern of early alteration and intrusive events.

The late stage propylitic alteration affected rocks in all boreholes except 3A and gave rise to the dominant alteration assemblage. Characteristically the assemblage contains sericite, chlorite, epidote (clinozoisite), albite, pyrite and magnetite. There is a suggestion of zoning in that magnetite is absent from boreholes 1 and 7, though this could be a function of primary host rock composition. The designation of this alteration as propylitic rather than phyllic takes into account the composition of the total assemblage of alteration minerals, rather than their relative proportions. Sericite and muscovite, for example, are abundant in places and form part of the alteration of amphibole. It is probable, therefore, that this is a phyllic alteration in which the original relatively mafic rock composition has had a strong influence on the final composition of the alteration minerals and the style of alteration. The mafic composition may have also contributed to the production of magnetite as much as any sulphur deficiency, which is sometimes proposed to explain the production of magnetite rather than pyrite. This phase of alteration was not accompanied by any changes in the bulk chemistry of the rocks readily distinguishable from those caused by primary lithological variation except for increases in Fe, S and possibly Mn and Zn. Though evidence is not conclusive, the retrograde effect of this alteration on rocks with potassic alteration may have lowered Rb, Ba, Rb/Sr, K/Na and Cu/S. A regional metasomatism is evident throughout the Llandeloy-Middle Mill area, but there is no strong evidence to link

it to this late propylitic alteration event. Carbonate veining is the last event seen to affect borehole rocks.

Al, P, Zr and Ti are the elements determined which appear to have remained relatively immobile during K-feldspar alteration. Apparent depletion of these elements in the most altered rocks is attributed to dilution. Ce and Th may also be immobile but results are truncated by analytical detection limits. In the propylitic (phyllic) alteration zones only the alkalis, the alkaline earths and chalcophile elements appear to have been affected.

The only metal analysed of economic interest is copper. It is associated with S and Fe and these three elements produce a strong geochemical signature in mineralised rocks. The Mo content of the rocks is generally low (<91 ppm). There are local but very weak enrichments of As, Pb and possibly Zn, though the latter may be a secondary concentration in weathered rocks. All these chalcophile elements show independent behaviour and individual element concentrations are not closely related to each other or, with the possible exception of Pb, to the alteration pattern. Gold has not been determined but, because of the probable tectonic setting of the deposit, it may be present in appreciable amounts. Some chalcopyrite is disseminated but most occurs in veins associated with the late stage propylitic alteration. Such veins occur both earlier and later than pyrite-magnetite veins but the time difference is not considered to be significant. There was, however, an earlier Cu mineralisation associated with the propylitic-potassic alteration. Rocks which show minimal late propylitic alteration are Cu rich and there is a general association of high Cu and particularly high Cu/S with rocks containing evidence of remnant strong potassic alteration. Whether the late stage propylitic alteration was accompanied by an appreciable influx of Cu (as well as Fe and S) or mainly redistributed Cu introduced during the earlier event is uncertain.

The alteration and mineralisation have many features in common with those Hollister (1974) claimed were characteristic of the 'diorite type' of porphyry copper deposit. Recent work by Taylor and Fryer (1980) has led to a refinement of the porphyry alteration models provided by Lowell and Guilbert (1970), Guilbert and Lowell (1974) and Hollister (1974). It is now considered probable that early potassic and propylitic alteration is caused largely be magmatic fluids and that phyllic alteration may be imposed on them when mixing of magmatic fluids with large quantities of meteoric water takes place. At Llandeloy the K/Rb ratios suggest either strong partitioning of Rb into the vapour phase or a minimal involvement of late magmatic fluids in the K-feldspar alteration.

The mineral assemblages characteristic of the alteration at Llandeloy are thought to be influenced by the relatively basic original host rock composition, but they may also be influenced by depth. Little is known about the bottoms of porphyry systems though Sillitoe (1973) and Guilbert and Lowell (1974) amongst others have predicted the probable characteristics of a root zone. Among the predicted features which the Llandeloy rocks share are (i) lack of phyllic (sensu latu) alteration, (ii) low grade of mineralisation, (iii) presence of magnetite and (iv) irregular development of alteration zoning. Further evidence that the root zone of a porphyry system may be exposed at Llandeloy is provided by the overlying lacustrine sediments. These are rich in magnetite, feldspar and Cu and were clearly derived from the erosion of a nearby quartz-poor, magnetite and copper-rich mineralised intrusion complex. Structural inferences from geophysical results, which suggest that the mineralised area lies in the core of an anticline or horst underlain at shallow depth by Precambrian and bounded by faults in the north and southeast, also support the deep level hypothesis.

The drilling did not define the full extent of the mineralised area. Clearly only a small segment of a porphyry system has been examined and the axis of the system may have been considerably modified by post mineralisation earth-movements. The scarce bedding orientation data available suggest that the axis, if perpendicular to bedding, may plunge to the southeast. The disposition of alteration zones in boreholes 4, 6 and 8 may, however, be interpreted in terms of a west or northwesterly tilt of the axis. In either case there is an apparent westward decrease in the intensity of alteration.

Finally, the strong northeast trending geophysical feature near borehole 3A may be interpreted as a fault with a downthrow to the southeast. The ground to the southeast of this line may have relatively high IP but no magnetic anomalies. Tetragraptus Shale is faulted against mineralised rocks in the north and Precambrian is faulted against them on the west. Extensions of the porphyry system may, therefore, be concealed beneath the shales in the north and be at depth southeast of the northeast trending geophysical feature near borehole 3A.

CONCLUSIONS AND RECOMMENDATIONS

1. Disseminated copper mineralisation, believed to be associated with the deep levels of a dioritic copper porphyry system, has been discovered near Llandeloy, southwest Dyfed

2. Because of the deep level of intersection, alteration zonation is imperfectly developed and copper mineralisation is not of economic grade, the best borehole intersection yielding 0.1% Cu over 3.4 m.

3. Alteration and mineralisation was a two phase event in which early propylitic-potassic alteration and accompanying mineralisation was overprinted by a late-stage propylitic event.

4. It is believed that the part of the copper porphyry most likely to have contained ore-grade mineralisation has been eroded away, and that some of the remains are represented by immature, rotted sand and clay deposits beneath boulder clay. These deposits reach 20 m in thickness and contain up to 640 ppm Cu.

5. The geology of the area is still imperfectly understood because of the thick drift deposits, and the possibility exists that, because of tilting and down-faulting, parts of the copper deposit may be concealed in areas to the north and east of the area drilled.

6. The age of the mineralisation is uncertain, but it is reasonable to assume that it is connected with emplacement of intermediate intrusives, which the tenuous evidence suggests was a late Cambrian or early Ordovician event.

7. The style of mineralisation, the chemistry of the associated intrusives and the known geology suggest that mineralisation took place in thin sialic crust, most probably in an island arc type of environment.

8. The deposit was initially located by soil sampling followed by shallow drilling. Drainage sampling and rock sampling of available exposures gave little or no indication of mineralisation in the vicinity. Geophysical measurements (IP, magnetic, VLF-EM) were inconclusive, partly because of the absence of a well-developed pyrite halo and the presence of magnetite from several sources. The thick unconsolidated deposits confused all surface

prospecting techniques because of their high copper, magnetite and clay contents. Resistivity measurements can be used to estimate their extent. Rock geochemistry indicates that high Cu, S and Cu/S ratios provide the most extensive and best lithogeochemical exploration targets, with other chemical changes either confused by the polyphase alteration or confined to highly altered zones. Magnetic susceptibility measurements can provide a useful guide to alteration (late propylitic) zones.

9. It is recommended that other poorly exposed intermediate intrusives of possible late Cambrian-Ordovician age in southwest Wales be examined by soil sampling, deep augering and shallow drilling for indications of this style of mineralisation. Any further exploration at Llandeloy should concentrate on the area immediately to the east and southeast of the area covered by the boreholes. The possibility of accompanying gold mineralisation should be investigated and the mineral potential of the Treffynnon Volcanic Group assessed.

ACKNOWLEDGEMENTS

All sample preparation and analysis was carried out by members of the Analytical Chemistry Research Group, BGS. The authors are grateful in particular to Mr T.K. Smith and Mr A. Davies for XRFS and Beta-probe analyses. The diagrams were all drawn by members of the BGS Drawing Office under the supervision of Mr A.R. Evans and Mr R. Parnaby. Mrs J. Evans and Mrs J. Norman typed the manuscript. We should also like to thank farmers and other landowners in the Llandeloy-Middle Mill area for their co-operation. Finally, editorial work to the geophysical sections by Dr J.D. Cornwell is gratefully acknowledged.

REFERENCES

ALLEN, P.M. 1981. A new occurrence of possible Tertiary deposits in south-western Dyfed. Geol. Mag., Vol. 18, pp. 561-564.

ALLEN, P.M., COOPER, D.C. and SMITH, I.F. 1979. Mineral exploration in the Harlech Dome, North Wales. Mineral Reconnaissance Programme Rep. Inst. Geol. Sci., No. 29.

ALLEN, P.M., COOPER, D.C., REA, W.J. and FUGE, R. 1976. Geochemistry and relationships to mineralisation of some igneous rocks from the Harlech Dome, Wales. Trans. Instn. Mining. Metall. (Sect. B: Applied Earth Sci.), Vol.85, pp.100-118.

ALLEN, P.M. and others. 1981. Copper-bearing intrusive rocks at Cairngarroch Bay, south-west Scotland. Mineral Reconnaissance Programme Rep. Inst. Geol. Sci., No.39.

ARMBRUST, G.A. and GANNICOTT, R.A. 1980. K/Rb ratios as a source indicator of hydrothermal fluids at the Seneca volcanogenic massive sulphide deposit, British Columbia. Econ. Geol., Vol.75, pp.466-477.

ARMBRUST, G.A. 1977. Rubidium as a guide to ore in Chilean porphyry copper deposits. Econ. Geol., Vol.72, pp.1086-1100.

BEESON, R. 1980. The relationship of siltstone geochemistry to sedimentary environment and uranium mineralisation in the Beaufort Group, Cape Province, South Africa. Chem. Geol., Vol.30, pp. 81-107.

BESWICK, A.E. and SOUCIE, G. 1978. A correction procedure for metasomatism in an Archean greenstone belt. Precambrian Research, Vol.6, pp.235-248.

BRADLEY, R.I., RUDEFORTH, C.E. and WILKINS, C. 1978. Distribution of some chemical elements in the soils of north-west Pembrokeshire. Jl. Soil Sci., Vol.29, pp.258-270.

CHAFFEE, M.A. 1976. The zonal distribution of selected elements above the Kalamazoo porphyry copper deposit, San Manuel district, Pinal County, Arizona. Jl. Geochem. Explor., Vol.5, pp.145-165.

CONDIE, K.C. and SNANSIENG, S. 1971. Petrology and geochemistry of the Duzel (Ordovician) and Gazelle (Silurian) Formations, Northern California. Jl. Sediment. Petrol., Vol.41, pp.741-751.

CORNWELL, J.D. and CAVE, R. (in press). An airborne geophysical survey of part of west Dyfed, South Wales, and some related ground surveys. Mineral Reconnaissance Programme Rep. Brit. Geol. Surv.

COX. A.H., GREEN, J.F.N., JONES, O.T. and PRINGLE, J. 1930. The geology of the St Davids district, Pembrokeshire. Proc. Geol. Assoc., Vol.41, pp.274-289.

DAVIES, J.F. 1980. K-Rb patterns in an Archean "porphyry-type" copper deposit, Timmins, Ontario, Canada. Econ. Geol., Vol.75, pp.760-770.

DAVIES, J.F., GRANT, R.W.E. and WHITEHEAD, R.E.S. 1979. Immobile trace elements and Archean volcanic stratigraphy in the Timmins mining area, Ontario. Canada. Earth Sci., Vol.16, pp. 305-311.

EL BOUSEILY, A.M. and EL SOKKARY, A.A. 1976. The relationship between Rb, Ba and Sr in granite rocks. Quart. Jl. Geol. Min. Metall. Soc. India, Vol.47, pp.103-116.

FINLOW-BATES, T. and STUMPFL, E.F. 1981. The behaviour of so-called immobile elements in hydrothermally altered rocks associated with volcanogenic submarine exhalative ore deposits. Mineral Deposita, Vol.16, pp.319-328.

FLOYD, P.A. and WINCHESTER, J.A. 1978. Identification and discrimination of altered and metamorphosed volcanic rocks using immobile elements. Chem. Geol., Vol.21, pp.291-306.

FORD, J.H. 1978. A chemical study of alteration at the Panguna porphyry copper deposit, Bougainville, Papua New Guinea. Econ. Geol., Vol.73, pp.703-720.

GUILBERT, J.M. and LOWELL, J.D. 1974. Variations in zoning patterns in porphyry ore deposits. CIM Bull., Vol.67, pp.99-109.

HALL, G.W. 1971. Metal Mines of Southern Wales. Westbury on Severn, G.W. Hall. 95pp.

HAWKES, D.D. and LITTLEFAIR, M.J. 1981. An occurrence of molybdenum, copper and iron mineralisation in the Argentine Islands, West Antarctica. Econ. Geol., Vol.76, pp.898-904.

HOLLISTER, V.F. 1974. An appraisal of the nature and source of porphyry copper deposits. Minerals Sci. Engng., Vol.7, pp.225-233.

HUGHES, C.J. 1973. Spilites, keratophyres and the igneous spectrum. Geol Mag., Vol.109, pp.513-527.

IMPERIAL COLLEGE, 1978. The Wolfson geochemical atlas of England and Wales. Clarendon Press, Oxford.

INSTITUTE OF GEOLOGICAL SCIENCES, 1980. 1:250 000 series, aeromagnetic anomaly map Lundy sheet, 51°N -6°W. London: Institute of Geological Sciences.

KESLER, S.E., JONES, L.E. and WALKER, R.L. 1975. Intrusive rocks associated with porphyry copper mineralisation in island arc areas. Econ. Geol., Vol.70, pp.515-526.

KOKELAAR, B.P. 1979. Tremadoc to Llanvirn volcanism on the south east side of the Harlech Dome (Rhobell Fawr), N. Wales. In: Harris, A.L., Holland, C.H. and Leake, B. E. (Eds.) The Caledonides of the British Isles -Reviewed. Geol. Soc. Lond. Spec. Pub. No.8, pp.591-596.

KOKELAAR, B.P. and others, 1984. The Ordovician marginal basin in Wales. In: Kokelaar, B.P. and Howells, M.F. (Eds.) Marginal basin geology. Geol. Soc. Lond. Spec. Pub. No.16, pp.245-269.

LOWELL, J.D. and GUILBERT, J.M. 1970. Lateral and vertical alteration - mineralisation zoning in porphyry copper deposits. Econ. Geol., Vol.65, pp.373-408.

LEPELTIER, C. 1969. A simplified statistical treatment of geochemical data by graphical representation. Econ. Geol., Vol.64, pp.538-550.

NUTT, M.J.C. and SMITH, E.G. 1981. Transcurrent faulting and the anomalous position of pre-Carboniferous Anglesey. Nature, Vol.290, pp.492-494.

OLADE, M.A. 1977. Major element haloes in granitic Wall rocks of porphyry copper deposits. Guichon Creek batholith, British Columbia. Jl. Geochem. Explor., Vol.7, pp.59-71.

OLADE, M.A. and FLETCHER, W.K. 1976. Trace element geochemistry of the Highland Valley and Guichon Creek Batholith in relation to porphyry copper mineralisation. Econ. Geol., Vol.71, pp.733-748.

ONDRICK, C.W. and GRIFFITHS, J.C. 1969. Frequency distribution of elements in Rensselaer greywacke, Troy, New York. Geol. Soc. Amer. Bull., Vol.80, pp.509-518.

PARKER, M.E. 1983. Statistical treatment of susceptibility data. Unpublished report, Applied Geophysics Unit Inst. Geol. Sci. No. 147.

PARSLOW, G.R. 1974. Determination of background and threshold in exploration geochemistry. J. Geochem. Explor., Vol.3, pp.319-336.

PATCHETT, P.J. and JOCELYN, J. 1979. U-Pb zircon ages for late Precambrian igneous rocks in South Wales. Jl. Geol. Soc. Lond., Vol.136, pp.13-19.

PEARCE, J.A. and GALE, G.H. 1977. Identification of ore deposition environment from trace element geochemistry of associated igneous host rocks. In: Volcanic processes in ore genesis. Geol. Soc. Lond. Spec. Publ., No.7, pp.14-24.

PEARCE, J.A. and NORRY, M.J. 1979. Petrogenetic implications of Ti, Zr, Y and Nb variations in volcanic rocks. Contrib. Mineral. Petrol., Vol.69, pp.33-47.

PRICE, N.B. 1963. The geochemistry of the Menevian rocks of Wales. Unpublished Ph.D. thesis, University of Wales, 233 pp.

READ, D. 1983. Rare earth element behaviour during sub-aerial weathering. Unpublished Ph.D. thesis, University of London, 355 pp.

RICE, R. and SHARP, G. 1976. Copper mineralisation in the forest of Coed-y-brenin, Wales. Trans. Instn. Mining Metall. (Sect. B: Appl. Earth Sci.), Vol.85, pp.1-13.

RIVALENTI, G. and SIGHINOLFI, G.P. 1969. Geochemical study of greywackes as a possible starting material for para-amhibolites. Contrib. Mineral. Petrol., Vol.23, pp.173-188.

RUDEFORTH, C.C. and BRADLEY, R.I. 1972. Soils, land classification and land use in west and central Pembrokeshire. Spec. Surv. No.6, Soil Surv., Harpenden.

RUSHTON, A.W.A. 1974. The Cambrian of Wales and England. In: Holland, C.H. Cambrian of the British Isles, Norden and Spitzburgen. J. Wiley, London, pp.43-121.

SAUNDERS, A.D., TARNEY, J. and WEAVER, S.D. 1979. Transverse geochemical variations across the Antarctic Peninsula: implications for the genesis of calc-alkaline magmas. Earth Planet Sci. Lett., Vol.46, pp.344-369.

SILLITOE, R.H. 1973. The tops and bottoms of porphyry copper deposits. Econ. Geol., Vol.68, pp.799-815.

SINCLAIR, A.J. 1976. Applications of probability graphs in mineral exploration. Assoc. Explor. Geochemists Spec. Vol.4.

STEAD, J.T.G. and WILLIAMS, B.P.J. 1971. The Cambrian rocks of north Pembrokeshire. In: Bassett, D.A. and Bassett, M.G. (Eds.) Geological excursions in South Wales and the Forest of Dean. Geol. Assoc. of South Wales, Cardiff, pp.180-198.

TAYLOR, R.P. and FRYER, B.J. 1980. Multiple-stage hydrothermal alteration in porphyry copper systems in northern Turkey: the temporal interplay of potassic, propylitic and phyllic fluids. Canad. Jl. Earth Sci., Vol.17, pp.901-926.

TELFORD, W. and others. 1976. Applied Geophysics. Cambridge University Press, Cambridge.

THOMAS, H.H. and COX, A.H. 1924. The volcanic series of Trefgarn, Roch and Ambleston (Pembrokeshire). Quart. Jl. Geol. Soc. Lond., Vol.80, pp.520-548.

THORPE, R.S. 1970. The origin of Pre-Cambrian diorite-granite plutonic series from Pembrokeshire (Wales). Geol. Mag., Vol.107, pp.491-499.

THORPE, R.S. 1972. Possible subduction zone origin for two Precambrian calc-alkaline plutonic complexes from southern Britain. Geol. Soc. Amer. Bull., Vol.83, pp.3663-3668.

TUREKIAN, K.K. and WEDEPOHL, K.H. 1961. Distribution of elements in some units of the earth's crust. Geol. Soc. Amer. Bull., Vol.72, pp.175-192.

WEBER, J.N. and MIDDLETON, G.V. 1961. Geochemistry of the turbidites of the Normanskill and Charny Formations. Geochem et Cosmochim Acta., Vol.22, pp.206-243.

WEDEPOHL, K.H. 1969. Handbook of geochemistry. Springer-Verlag, Berlin.

WILLIAMS, T.G. 1933. The Pre-Cambrian and Lower Palaeozoic rocks of the eastern end of the St Davids Pre-Cambrian area, Pembrokeshire. Quart. Jl. Geol. Soc. Lond., Vol.90, pp. 32-75.

APPENDIX 1

ABBREVIATED BOREHOLE LOGS FROM LLANDELOY

The complete logs have been lodged with the Welsh Office of BGS, Llanfarian, Aberystwyth. All boreholes were drilled using a JKS 300 rig. Boreholes 1-7 were vertical and BQ core was retrieved throughout. Borehole 8 was inclined 60° to 180° (True); BQ core was retrieved to 72.26 m, AQ below. All measurements of inclination given below relate to the length of the core.

BOREHOLE 1 Registration Number SM 82NW/1

Grid Reference SM 8446 2809
Height above O.D. 89.77 m
Casing to 8.38 m

Description of strata	Thickness(m)	Depth(m)
OPEN HOLE		3.66
?Cambrian		
VOLCANIC BRECCIA: angular fragments quartzose sandstones, volcanic rocks up to 3 cm. Beds coarse tuff up to 33 cm thick. Network veinlets quartz; some sericite veinlets. Pyrite sparsely disseminated	1.70	5.36
QUARTZ:	0.58	5.94
MICROTONALITE, porphyritic: deeply weathered, with white altered feldspar phenocrysts 3 mm, sparse amphibole phenocrysts. Xenoliths volcanic rock at 6.70. Network fractures below 6.97; breccia veinlet at 7.28. Pyrite sparse, disseminated; totally hematised in hair fractures	1.51	7.45
VOLCANIC BRECCIA: As above	0.23	7.68
MICROTONALITE, porphyritic: as above; less weathered. Sharp upper contact 30°, basal contact irregular, sharp. Some quartz veinlets, sericite and chlorite in fractures. Pyrite sparse and disseminated	1.36	9.04
ACID VOLCANIC: fine-grained with small feldspar phenocrysts, crude banding. Brecciated and veined by quartz, chlorite	0.28	9.32
MICROTONALITE, porphyritic: as above. Flames penetrate upper unit; xenoliths at top. Network fracturing, plentiful quartz veinlets, some 35°-40°. Pyrite sparse, disseminated	1.14	10.46
CRYSTAL TUFF: weathered. Quartz veinlets; quartz-chlorite vein 3 cm, 40°. Network fractures	0.62	11.08
QUARTZ: anastomosing veins with crystal tuff	0.40	11.48
ACID VOLCANIC: as above	0.05	11.53
CLAY GOUGE:	0.10	11.63
MICROTONALITE, porphyritic: as above. Quartz veins with pyrite 2-30 mm. Pyrite disseminated, sparse, increasing downwards	1.07	12.70
ACID VOLCANIC: as above. Brecciated at top. Network fractures, sericitised. Pyrite sparsely disseminated, hematised in 1 cm vein at 21.91	0.53	13.23
VOLCANIC BRECCIA: clasts mudstone, sandstone, sericitised, 4 cm long. Veinlets quartz, chlorite. Pyrite sparse disseminated, local concentrations, hematised in network fractures	1.10	14.33

	Thickness(m)	Depth(m)
CRYSTAL TUFF: as above	0.15	14.48
VOLCANIC BRECCIA: as above	0.03	14.51
CLAY GOUGE:	0.20	14.71
VOLCANIC BRECCIA: as above	0.07	14.78
MICROTONALITE, porphyritic, as above. Pyrite sparse, disseminated	0.37	15.15
SILTSTONE: thin beds, sandy and pebbly	0.47	15.62
MICROTONALITE, porphyritic: as above	1.96	17.58
CLAY GOUGE: with lost core		17.58
MICROTONALITE, porphyritic: as above, unweathered below 26.91. Phenocrysts feldspar 8 mm, amphibole, rare quartz in greyish-green matrix. Upper contact sharp, horizontal. Quartz veins at intervals. Pyrite sparse, disseminated with concentrations below 26.92	10.02	27.60
MICROTONALITE, porphyritic: as above, sharp upper contact 50°. Network fractures at top, below 28.60, 29.28-29.64 with quartz veinlets, chlorite. Pyrite abundant disseminated to 28.00, 29.28-29.64 and elsewhere, also veins. Veins porphyritic microdiorite below 29.80 richly pyritic	2.64	30.24
MICRODIORITE, porphyritic: phenocrysts feldspar up to 8 mm, amphibole to 1 cm in green matrix. Sharp upper contact. Pyrite plentiful, disseminated and in hair fractures	0.41	30.65
QUARTZ-MICRODIORITE: sparse phenocrysts feldspar, amphibole in medium-grained feldspathic rock. Some xenoliths sedimentary rocks, diorite. Upper contact broken. Grain-size reduces below 33.19; rock is porphyritic to 33.93, fine-grained non-porphyritic to base. Pyrite disseminated and in fractures with chlorite, locally abundant especially 31.80-32.47	3.50	34.15
MICROTONALITE, porphyritic: as above, variable concentration phenocrysts. Network fractures, breccia with chlorite veinlets at intervals 35.09-38.27, 42.97-44.91. Quartz veinlets, rare carbonate. Epidote below 43.27. Pyrite disseminated, concentrated in fracture zones		
END HOLE	11.57	45.72

BOREHOLE 2 Registration Number SM 82NE/3

Grid Reference SM 8526 2847
Height above O.D. 112 m
Casing to 3.35 m

Description of strata	Thickness(m)	Depth(m)
Pleistocene		
CLAY WITH PEBBLES:	0.91	0.91
?Tertiary		
FELDSPAR SAND AND CLAY: deeply weathered	2.44	3.35
?Cambrian		
MICROTONALITE, porphyritic: deeply weathered. Variable content phenocrysts feldspar to 3 mm, amphibole and uncommon quartz, biotite in very fine-grained groundmass. Quartz veinlets sparse	2.05	5.40
CLAY GOUGE:	0.01	5.41
MICROTONALITE, porphyritic: as above. First fresh rock at 5.57, greenish grey. Xenoliths below 6.05. Quartz veinlets rare. Pyrite sparse in fractures	4.39	9.80
QUARTZ: with epidote, chlorite, hematite, pyrite	0.34	10.14
MICROTONALITE, porphyritic: as above. Some xenoliths porphyritic quartz-microdiorite. Veinlets quartz, pink feldspar rare. Epidote with carbonate, chlorite below 14.02. Pyrite in network fractures, veins, disseminated, locally abundant. Chalcopyrite in quartz-carbonate vein 17.00	9.61	19.75
QUARTZ-MICRODIORITE: medium grained, feldspathic with sparse phenocrysts 3 mm plagioclase, hornblende. Upper contact sharp, 45°. Small xenoliths below 20.73. Quartz veins uncommon. Veinlets chlorite, quartz-chlorite, quartz-carbonate occur throughout. Epidote with pyrite veins 19.75-22.38, 23.90-24.42, 27.50. Intense epidotization 25.00. Pyrite disseminated, veins locally abundant. Chalcopyrite in veins with pyrite, 19.80, 22.77, 22.98. ?Autoclastic brecciation, 22.80-28.07	8.32	28.07
QUARTZ-MICRODIORITE: as above. Some veins carbonate, quartz. Pyrite sparse disseminated and veinlets. ?Autoclastic breccia zone 29.27-29.70	1.63	29.70
QUARTZ-MICRODIORITE: as above. Upper contact nearly parallel core. Network fracturing and breccia veins locally. Pyrite in veinlets common below 29.60. Chalcopyrite at 29.65, 30.07	0.91	30.61
QUARTZ-MICRODIORITE: as above. Sharp upper contact. Brecciation at intervals. Pyrite sparsely disseminated; veinlets with quartz, chlorite, carbonate and some chalcopyrite		
END HOLE	2.31	32.92

BOREHOLE 3A Registration Number SM 82NE/4

Grid Reference SM 8546 2850
Height above O.D. 116.2 m
Casing to 8.93 m

Description of strata	Thickness(m)	Depth(m)
Recent		
SOIL:	0.25	0.25
Pleistocene		
CLAY WITH PEBBLES:	0.75	1.00
CLAY: silty with layers pebbly clay and gravel	0.75	1.75
?Tertiary		
FELDSPAR SAND AND CLAY: deeply weathered; gravel beds between 3.05-4.88, 14.63-16.46	18.83	20.58
?Cambrian		
QUARTZ-DIORITE: coarse-grained, plagioclase, hornblende, interstitial quartz, minor biotite. Some xenoliths sedimentary rocks. Deeply weathered; much core lost. Some epidote veinlets	1.98	22.56
CLAY GOUGE:	0.02	22.58
QUARTZ-DIORITE: as above. Minor pyrite cubes; sparse quartz, epidote veins		
END HOLE	4.25	26.83

BOREHOLE 3B Registration Number SM 82NE/5

Grid Reference SM 8546 2857
Height above O.D. 118.5 m
Casing to 9.45 m

Description of strata	Thickness(m)	Depth(m)
Recent		
SOIL:	0.53	0.53
Pleistocene		
CLAY: sandy, pebbly, massive heterolithic	1.09	1.62
CLAY: silty, sandy	0.15	1.77
GRAVEL:	0.06	1.83
?Tertiary		
CLAY: silty, bedded with thin gravel beds	1.52	3.35
FELDSPAR SAND AND CLAY: deeply weathered feldspar sand with white clay laminae up to 4 mm	0.31	3.66
GRAVEL:	0.06	3.72
FELDSPAR SAND AND CLAY: deeply weathered, regular alternation 1.3-2.0 cm sand and 0.2-0.4 cm clay to 5.94. Thickness variation below this	10.91	14.63
GRAVEL: heterolithic, waterworn pebbles above 8 cm lithic sand layer	0.20	14.83
CLAY: retrieved with small pebbles 17.48-17.68 only	?5.17	20.00
SILT: sludge only		
END HOLE	1.95	21.95

BOREHOLE 4 Registration Number SM 82NE/6

Grid Reference SM 8566 2874
Height above O.D. 123.7 m
Casing to 8.23 m

Description of strata	Thickness(m)	Depth(m)
Recent		
SOIL:	0.40	0.40
Pleistocene		
CLAY WITH PEBBLES:	1.77	2.17
?Tertiary		
FELDSPAR SAND AND CLAY: deeply weathered, regular alternation of sand 1-2.5 cm, clay 0.3-1.0 cm to 2.23; irregular below	?0.93	?3.10
GRAVEL: heterolithic	?0.28	3.38
FELDSPAR SAND AND CLAY: regular bedding as above. Some beds gravel with diorite pebbles only. Thick clay beds below 7.77	7.58	10.96
?Cambrian		
MICRODIORITE: medium grained, feldspathic with sparse phenocrysts, feldspar and amphibole up to 5 mm. Deeply weathered to 15.24. Quartz veins up to 2 cm at intervals with some adjacent silicification. Chlorite veinlets between 22.00-24.00; epidote veinlets mainly below 22.00; some epidotisation 17.30, 22.00. Pyrite disseminated and in fractures moderately abundant 11.36-11.50, minor below, but in veins with gangue at intervals. Chalcopyrite below 22.00	14.44	25.40
MICRODIORITE: as above. Sharp, irregular intrusive contact 30° at top. Porphyritic marginal phase to 25.59. Carbonate alteration, some epidote veinlets. Quartz veins with pyrite and chalcopyrite 25.75-25.85. Also disseminated pyrite	0.58	25.98
MICRODIORITE: as above. Sharp upper contact 45°, porphyritic to 26.40. Patchy texture below 27.31, mainly due to recrystallization. Sparse veining. Pyrite rare disseminated, in veinlets with epidote 27.31-27.85. Chalcopyrite at 27.84	3.44	29.42
MICRODIORITE, porphyritic: fine-medium grained, greyish-green with phenocrysts feldspar 2 mm, hornblende 5 mm. Patchy carbonate alteration. Xenoliths up to 6 cm at 29.64, 31.78. Pyrite sparsely disseminated; commonly in veins with quartz, feldspar, chlorite, epidote to 32.80 only	3.77	33.19
QUARTZ-DIORITE: coarse-grained, feldspathic; sparsely porphyritic with plagioclase to 2 mm, hornblende to 5 mm increasing in proportion downwards. Sharp irregular upper contact with upward penetrating flames. Basic xenoliths at intervals; pegmatitic patch 34.15. Quartz veins rare, Epidote, chlorite, quartz, carbonate, feldspar veins more common; local epidotisation. Patchy recrystallization and textural variation. Pyrite in veinlets and disseminated only at 34.65, 35.90, 37.85-38.02		
END OF HOLE	4.83	38.02

BOREHOLE 5 Registration Number SM 82NE/7

Grid Reference SM 8585 2885
Height above O.D. 128.05 m
Casing to 14.32 m

Description of strata	Thickness(m)	Depth(m)
Recent		
SOIL:	0.23	0.23
Pleistocene		
CLAY WITH PEBBLES: heterolithic, structureless. Buff clay passes down into yellow brown clay with smaller pebbles	1.60	1.83
?Tertiary		
FELDSPAR SAND AND CLAY: deeply weathered feldspar sand beds up to 5 cm alternate with brown clay up to 5 mm; plentiful pebbles rotted diorite	3.20	5.03
SAND AND SILT: sludge only	4.11	9.14
?Cambrian		
TONALITE: coarse-grained feldspathic rock with hornblende, interstitial quartz. Deeply weathered with some fresh rock to 20.57. Patchy recrystallization below 20.57. Quartz veins at intervals. Epidote veinlets below 14.50 with some epidotisation. Chlorite veinlets along irregular fractures 14.63, 18.60-19.44, 20.55 with silicification. Pyrite sparsely disseminated to 14.63, mainly in fractures below 19.04, abundant 20.23-20.57	12.67	21.81
MICRODIORITE, porphyritic: fine-grained, greenish-grey with pseudomorphs after amphibole phenocrysts 7 mm long, plagioclase 2 mm. Sharp contact and chilled margin against tonalite above. Xenoliths tonalite 22.06-22.12. Intrusion breccia vein at 22.74, 5 cm thick. Clay lined fractures 21.95, 22.18. Pyrite disseminated, in blebs and veinlets locally plentiful	1.55	23.36
TONALITE: as above. Quartz in veins up to 1 cm with pyrite at intervals. Epidotization at 24.32 and below at intervals associated with local brecciation. Chlorite veinlets at irregular intervals. Breccia veins at 24.74, 33.78. Network fractures below 26.82. Pyrite abundant disseminated and in veinlets 24.16-24.87, at intervals 26.15-31.46; in fractures 32.52-33.28, 37.54-38.01. Malachite in quartz-pyrite veins 24.87, 25.98; on joints 26.66, 26.90; breccia vein 24.74	14.65	38.01
TONALITE: as above. Sharp upper contact; chilled margin, fine-grained to 38.20. Network fracturing with intense pyritization near upper margin and below 39.83. Veinlets quartz, epidote, chlorite mainly below 38.20, most numerous 39.83-41.75. Some carbonate veins. Local epidotisation; many veinlets 39.83-41.75. Pyrite disseminated and veinlets to 39.83; disseminated only 41.57-42.14 m. Chalcopyrite in quartz veins 39.41, 39.83-41.75	4.13	42.14
MICRODIORITE, porphyritic: as above. Sharp contact 45° crossed by quartz veins. Brecciated with abundant pyrite	0.17	42.31

	Thickness(m)	Depth(m)
TONALITE: as above, with sparse feldspar and amphibole phenocrysts, local recrystallization. Crackle breccia; minor veining, but abundant disseminated and veinlet pyrite. Rose quartz vein 43.00	0.69	43.00
MICRODIORITE, porphyritic: as above. Chilled upper and lower contacts. Abundant pyrite. Chalcopyrite in quartz-chlorite vein	0.08	43.08
TONALITE: as above. Minor network fracturing; abundant quartz and chlorite veins. Pyrite abundant in fractures, disseminated	1.87	44.95
MICRODIORITE, porphyritic: as above. Sharp irregular contact. Abundant pyrite; minor quartz veins		
END HOLE	0.17	45.12

BOREHOLE 6 Registration Number SM 82NW/2

Grid Reference SM 8486 2875
Height above O.D. 99.4 m
Casing to 9.75 m

Description of strata	Thickness(m)	Depth(m)
Recent		
SOIL:	0.60	0.60
Pleistocene		
CLAY WITH PEBBLES: buff, structureless sandy clay with subangular pebbles to 0.83; horizontal streaky lamination and increased silt content below	1.17	1.77
?Tertiary		
CLAY: thinly laminated brown clay and silty clay with rare pebbles passes down into massive clay. Below 2.00 regular alternation, brown clay 2-5 mm, blotchy greyish-orange sandy feldspathic clay 0.5-2.0 cm	0.38	2.15
GRAVEL: interbedded with lithic sand	0.13	2.28
FELDSPAR SAND AND CLAY: regularly interbedded clay and feldspathic sandy clay as above to 3.50; irregular below Downward increase in feldspar content. Clay bed 0.37 m thick at 4.33. Rotted diorite pebble gravel beds	6.56	8.84
?Cambrian		
ACID LAVA: porphyritic with feldpar 3 mm, smaller quartz phenocrysts in greenish-grey fine-grained groundmass. Feldspar orientation 20° to 35° below 11.00. Local brecciation	3.00	11.84
CLAY:	0.03	11.87
ACID LAVA: as above. Rare pyrite	2.93	14.80
CLAY:	0.01	14.81
ACID LAVA: as above. Rare veinlets quartz, chlorite	3.04	17.85
QUARTZITE: greenish grey, poorly sorted, badly fractured, minor pyrite	0.37	18.22
ACID LAVA: as above. Top 10 cm shows contorted bedding. Minor quartz-chlorite veins, 4 cm breccia vein at 22.45. First fresh rock at 20.98	5.72	23.94
MICROTONALITE, porphyritic: deeply weathered to 30.46. Plagioclase 3 mm, pseudomorphs after hornblende, minor quartz phenocrysts in fine-grained matrix. Minor quartz, chlorite and epidote veining. Breccia vein 33.06. Sparse pyrite cubes		
END HOLE	10.16	34.10

BOREHOLE 7 Registration Number SM 82NE/8

Grid Reference SM 8527 2915
Height above O.D. 123.7 m
Casing to 8.23 m

Description of strata	Thickness(m)	Depth(m)
Recent		
SOIL:	0.23	0.23
Pleistocene		
CLAY WITH PEBBLES: brown sandy clay, structureless with mainly black shale pebbles to 1.07; laminated and silty with sparse pebbles below with pebbly band 1.22-1.30	1.29	1.52
?Tertiary		
CLAY: regularly alternating brown-clay 2-3 mm, greyish mottled clay 1.1-1.5 cm with local irregularities. Beds coarse lithic muddy sand below 1.83. Gravel bed ?0.36 cm thick at 4.94	3.42	4.94
?Cambrian		
QUARTZ-MICRODIORITE: deeply weathered with sparse plagioclase, amphibole phenocrysts	0.55	5.49
ACID LAVA: deeply weathered, badly broken core, much lost	2.43	7.92
QUARTZ-MICRODIORITE: medium-grained with sparse plagioclase and hornblende phenocrysts. Deeply weathered. Network fracturing 12.75-14.83 and locally elsewhere. Quartz veins up to 1 cm at intervals, some with pyrite. Quartz-feldspar, epidote and chlorite veinlets uncommon. Locally epidote-pyrite veins. Pyrite, disseminated and in veinlets is locally abundant; especially 15.74, 16.96-18.28	11.26	19.18
CLAY GOUGE:	0.10	19.28
QUARTZ-MICRODIORITE: as above. Xenoliths microdiorite and other rocks in upper parts. Glomeroporphyritic below 21.00. Patchy carbonate alteration. Network fractures throughout. Quartz veinlets common. Pyrite abundant in veinlets and disseminated, locally with quartz-chlorite veinlets. Local carbonate, epidote veinlets and silicification	2.87	22.15
QUARTZ-MICRODIORITE: as above. Sharp intrusive upper contact. No xenoliths. Downward increase in porphyricity. Numerous epidote veinlets, quartz veinlets not common. Pyrite mainly in fractures 23.00-24.08, 24.47-24.94	2.79	24.94
QUARTZ-MICRODIORITE: as above. Sharp intrusive upper contact, xenolithic. Network fractures in places. Abundant veinlets quartz, carbonate, chlorite 27.30-27.47. Intense epidotization locally 25.48 to base. Pyrite abundant disseminated and in fractures 25.68-26.02	2.88	27.82
CLAY GOUGE:	0.06	27.88
QUARTZ-MICRODIORITE: as above. Epidotization increases downwards. Pyrite veins and disseminated		
END HOLE	2.00	29.88

BOREHOLE 8 Registration Number SM 82NE/9

Grid Reference SM 8514 2864
Height above O.D. 115 m
Casing to 12.5 m

Description of strata	Thickness(m)	Depth(m)
OPEN HOLE		9.45
Cambrian		
SILTSTONE: greenish-grey, thinly interlaminated with muddy fine sandstone in places; some laminated beds spotted mudstone. Bedding 70°. Brecciated 9.53-10.24, 10.88-11.37 and below with chlorite veinlets and pyrite disseminated, in quartz veinlets and fractures	?4.59	12.21
SANDSTONE: fine-grained, greenish-grey, massive	0.44	12.65
SILTSTONE: as above. 5 cm breccia vein at 12.95. Chlorite in fracture, 1 cm carbonate vein. Pyrite disseminated throughout, rich in breccia vein	0.72	13.37
SANDSTONE: as above, thickly bedded. Pyrite cubes and finely disseminated and in veins below 13.52	0.96	14.33
MAGNETITE SAND: thinly interbedded black and white sandstone	0.11	14.44
SILTSTONE: as above. Network fracturing and breccia veins 15.62-17.04. Pyrite sparse except 16.43-17.04, mainly in fractures	3.37	17.81
SANDSTONE: as above, locally interlaminated with silty mudstone, mudstone. Bedding 70°. Brecciation, network fractures below 19.53. Minor chlorite-quartz veins. Abundant chlorite veinlets 21.24-21.39. Pyrite disseminated and veinlets to 19.25, abundant 21.24-21.39	3.82	21.63
MAGNETITE SAND: as above	0.06	21.69
SANDSTONE: as above. Minor pyrite	1.78	23.47
SILTSTONE: as above. Breccia 23.97-24.33. Pyrite abundant, especially in breccia	0.86	24.33
SANDSTONE: as above, with laminae and beds of silty mudstone and spotted mudstone at intervals to 35.58. Below this is a sharp increase in abundance of argillaceous component. Bedding 80°. Network fracturing with chlorite at intervals 25.35-28.20. Intrusion breccias 28.13-28.20, 35.25, 36.37. Veinlets chlorite, quartz, calcite, epidote throughout. Pyrite disseminated and veinlets mostly 29.27-35.58, associated with epidotisation 35.58-36.55	12.22	36.55
MICRODIORITE, porphyritic: dark green, feldspar and pseudomorphs after amphibole phenocrysts 1.5 mm. Sharp intrusive chilled contacts 20°. Abundant disseminated pyrite with local concentrations. Minor quartz, chlorite, carbonate veinlets	1.98	38.53

	Thickness(m)	Depth(m)
SANDSTONE: greenish-grey, muddy with laminae silty mudstone, mostly above 39.69 and below 43.90, but wispy mudstone throughout and several thin beds spotted mudstone, below 44.61. Bedding 70°. Network fractures with chlorite to 39.10 and at intervals to 42.80. Breccia at 41.03. Minor quartz-chlorite, epidote veins. Pyrite disseminated and in fractures moderately abundant, locally rich associated with epidotisation. Chalcopyrite in quartz veinlet 43.00	6.81	45.34
QUARTZ-MICRODIORITE, porphyritic: dark greenish-grey, abundant 2 mm plagioclase phenocrysts, fewer amphibole. Chilled contacts approx 80°. Carbonate veinlets and alterations	1.10	46.44
SANDSTONE: as above. Magnetite bearing laminae at 49.51; sparse silty mudstone between 49.51-54.10. Pyrite in veinlets, disseminated and in nodules moderately abundant to 47.85 and 54.80-55.33. Local concentrations only between. Network fractures with chlorite at intervals 52.45-55.14	9.09	55.53
ARKOSE: coarse-grained, dark grey, graded bed. Plentiful pyrite below 55.74	0.26	55.79
SANDSTONE: grey with muddy laminae	0.30	56.09
SANDSTONE, quartzose: medium-grained massive, graded beds. Intrusion breccia at 56.66. Abundant disseminated pyrite, some in fractures	0.71	56.80
ARKOSE: as above. Pyrite	0.19	56.99
SANDSTONE, quartzose: as above. Network fractures, mostly pyritic at base	0.36	57.35
SANDSTONE: fine, grey, muddy, laminated to thickly bedded. Abundant silty mudstone laminae 57.62-58.81 and 62.30-66.00, 69.35-69.58, 70.13-81.30 with spotted mudstone and tuffitic mudstone beds. Magnetite sand laminae at 82.16. Bedding 70°. Chlorite veinlets fairly common. Epidotisation only between 57.49-57.57, 74.04-74.32. Breccias 57.89-57.99, 66.19, 66.42, 66.45, 70.27-70.57 and narrow zones to 81.78. Pyrite disseminated, veinlets and fractures locally abundant, especially in breccia zones with chlorite to 62.30, 66.95-69.35 and 70.27-82.12	24.92	82.27
ARKOSE: as above. Pyrite moderately abundant. Intrusion breccia 82.35	0.51	82.78
FAULT:		82.78
ARKOSE: as above, silty mudstone laminae at top and below 83.26	2.25	85.03
MICROTONALITE, porphyritic: chilled upper contact 90°. Pyrite in fractures with chlorite, calcite	1.50	86.53
SANDSTONE: as above. Breccia 87.44-87.55. Pyrite in fractures	1.18	87.71
MICROTONALITE, porphyritic: as above. Intrusion breccias 88.64, 91.98, 95.66-95.81. Network fractures with abundant pyrite 92.60 to base. Quartz, epidote, calcite veining minor	8.10	95.81

	Thickness(m)	Depth(m)
SANDSTONE: as above	0.31	96.12
CLAY GOUGE:	0.01	96.13
SANDSTONE: as above. Laminated to thickly bedded. Wispy laminae, thin beds silty mudstone generally uncommon to common, but abundant 100.18-100.83, 102.89-105.61, 108.70-109.22. Purple and green banded sandstone 98.49; magnetite sand laminae 102.32 and 108.92. Bedding 70°. Network fractures and breccias with chlorite veining at intervals throughout. Pyrite disseminated, in veinlets and veins up to 1 cm, locally abundant. Calcite, quartz and epidote veinlets variable. Chalcopyrite 96.40-97.44	16.63	112.76
SANDSTONE: bluish-grey, massive, medium grained to 114.17; coarse-grained, graded, quartzose below. 1 cm mudstone with magnetite laminae at 114.17. Minor pyrite	1.76	114.52
MICROTONALITE, porphyritic: as above. Upper contact 45°. Xenolithic. Pyrite not abundant	3.97	118.49
MICROTONALITE, porphyritic: as above. Sharp irregular upper contact; 10 cm chilled zone. Pyrite moderately abundant in veinlets, disseminated and irregular fractures. Epidote veinlets common, quartz less so. Chalcopyrite and ?galena in quartz vein 122.47	5.63	124.12
END HOLE		

APPENDIX 2

GEOPHYSICAL MEASUREMENTS IN THE LLANDELOY AREA

Line-by-line descriptions are given of pseudosections measured along traverse lines only in the area of detailed investigations around Treffynnon. A subjective interpretation has been made of the pseudosections shown in A2.1-A2.9 (see Fig. 41 for locations). Near-surface anomalies are assigned in the text to the dipole positions at which they are estimated to occur, while deeper anomalies have been identified as such.

Line 2500E
Resistivity is low to moderate on most of the line, and generally lower at the surface than at depth. Narrow lows occur at about 720N and probably off the end of the line at about 350S. At about 620N and 75N lie narrow resistivity highs. Chargeability is moderate on much of the line, but the north end has a lower, and the south end a higher IP response. A narrow maximum occurs at about 600N.

Line 2900E
Again low to moderate resistivities are seen, increasing generally with depth. Near surface values are rather higher between 400 and 450N, and at about 1100N. Four narrow resistivity lows occur, at 1120N, 850N, 670N and 370N approximately, of which the last is the strongest. Low resistivity material extends to greater depth to the south of 370N than to the north. Chargeability is moderate except for a high at the northern end of the traverse. A narrow high at 1000N coincides with a road, and a possible high lies at depth below about 150N.

Line 3100E
Low resistivity occurs to depth on the whole traverse except the northern end, where values are moderate to high. The two sections are separated by a narrow minimum at 720N. Most of the line also has low chargeability, but highs occur at 500 to 720N and north of 1200N. The former occurs where the line passes Treffynnon village.

Line 3500E
Resistivity on this line is generally moderate to high, although some surficial lows occur, notably at 300 to 600N. At the northern end of the line, however, resistivity is low to depth. A narrow low lies at about 320N. Chargeability is high on the southern part of the traverse, with a maximum at 720N, and a broader high southwards from 450N.

Line 3700E
Most of this line seems to be underlain by high resistivity material at shallow depth (probably <20 m) except for the far north, where moderately low values extend to depth. A zone of low resistivity surficial material between 350 and 370N separates two blocks of nearly outcropping high resistivity rock. A narrow low occurs at about 550N. Chargeability is high on much of the traverse with maxima at 170N, and (possibly) 370N and 1170N. Shallow lows lie at 900-1150N, 650-850N and at about 230N.

Line 4100E
Two high resistivity zones (950-1200N, and 600N southwards) are separated by a zone of moderately low values. A surficial low resistivity zone lies between 600 and 850N, and narrow lows occur at 920N and 1220N. Almost the whole line gives a high IP response, although minima occur at about 600 to 700N and 900 to 950N.

Line 4300E
This is a confused line with many interfering narrow features, and a very strong artificial IP anomaly caused by Hollybush farm buildings. The north end of the line has low resistivity extending to depth. The rest of the line has moderate to high resistivity except at about 450 to 500N, where a narrow low occurs. There may be other narrow lows at about 1150N and 920N. Chargeability is high in the south, with a narrow maximum lying at 650N. From 700N to Hollybush farm chargeability is low.

Line 4700E
Resistivity is generally moderate, with surficial low values on much of the line (200 to 750N). Low resistivities probably occur to depth north of 1100N and south of 50N. The northern half of the line has a high IP response, reaching a maximum at 1070N. There is a high at the southern end of the traverse, probably southwards from 200N.

Line 4900E
Most of the line has moderate resistivity, with surficial lows 200 to 750N. From 1050N northwards, resistivity is probably low to depth. Chargeability is high south of 180N, from 400 to 550N (with a maximum at 420N), at 620N and between 770 and 830N.

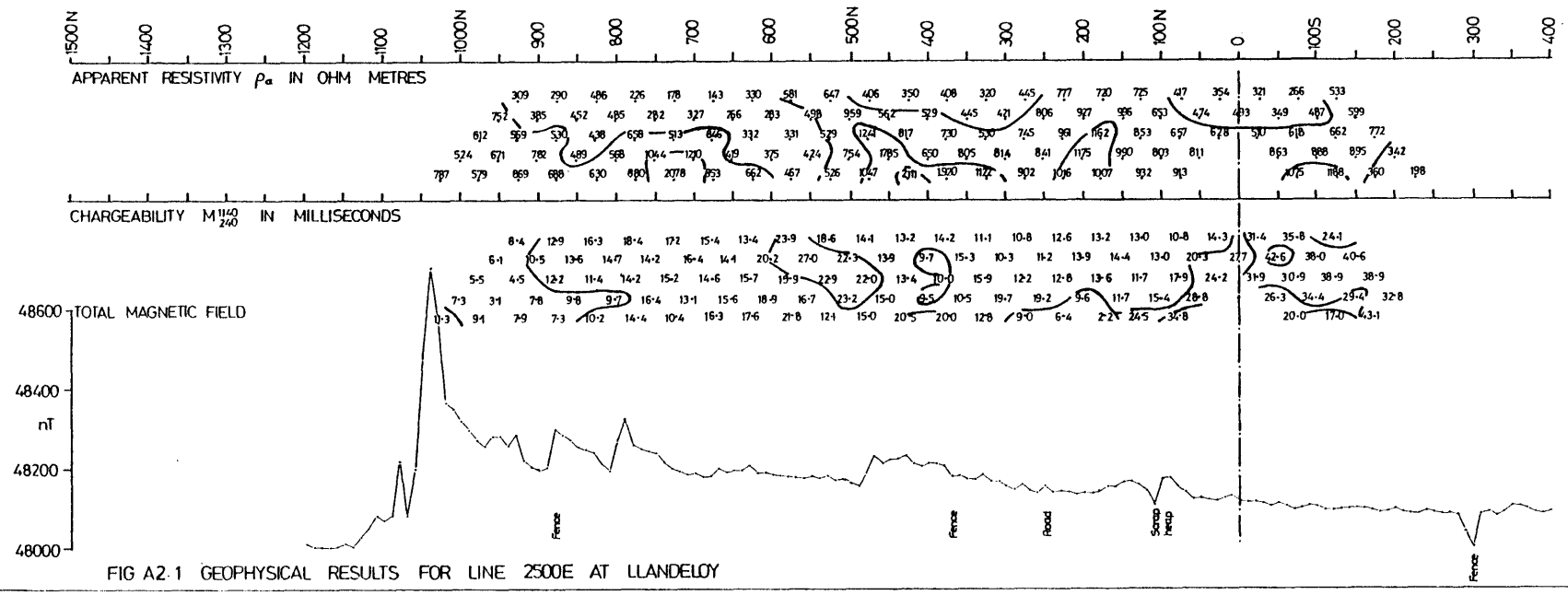

FIG A2.1 GEOPHYSICAL RESULTS FOR LINE 2500E AT LLANDELOY

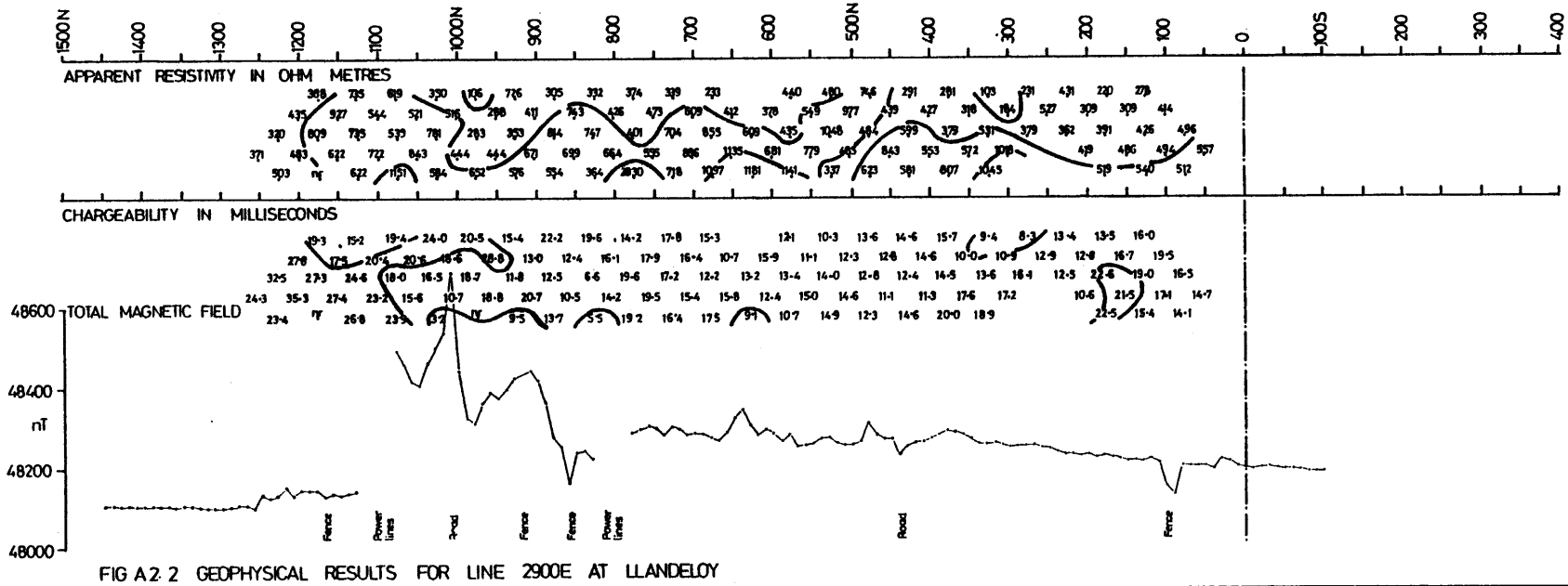

FIG A2.2 GEOPHYSICAL RESULTS FOR LINE 2900E AT LLANDELOY

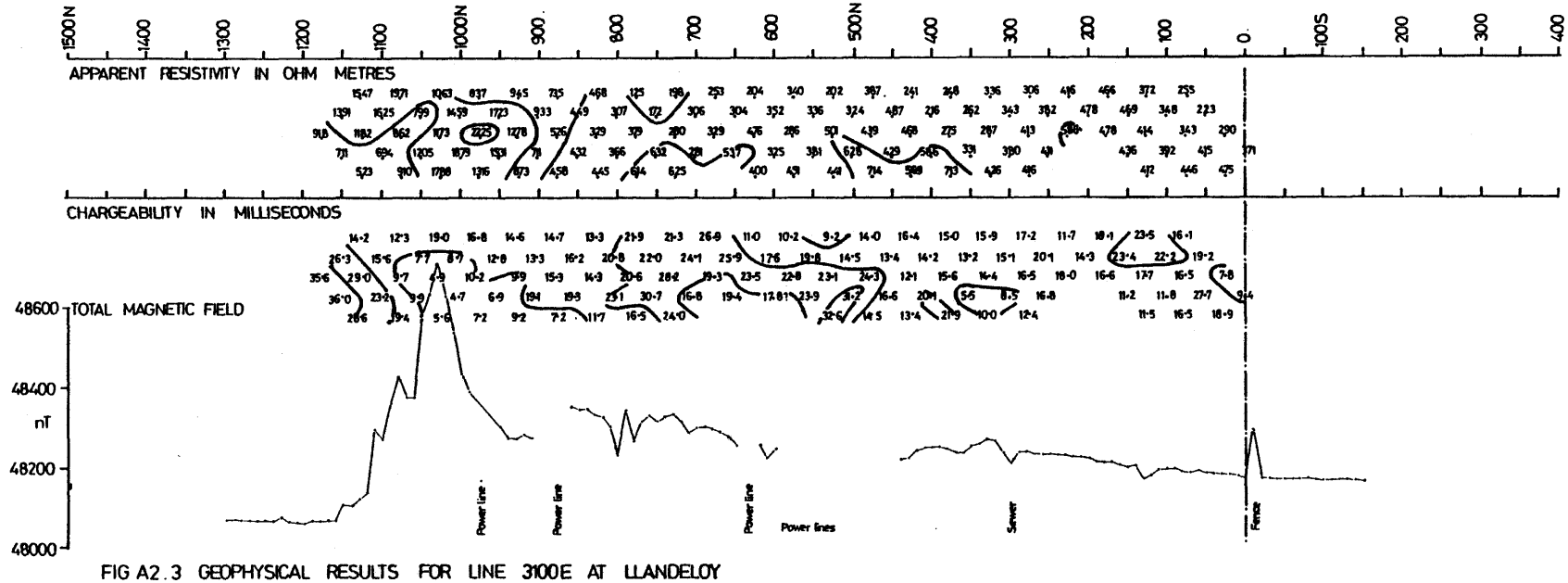

FIG A2.3 GEOPHYSICAL RESULTS FOR LINE 3100E AT LLANDELOY

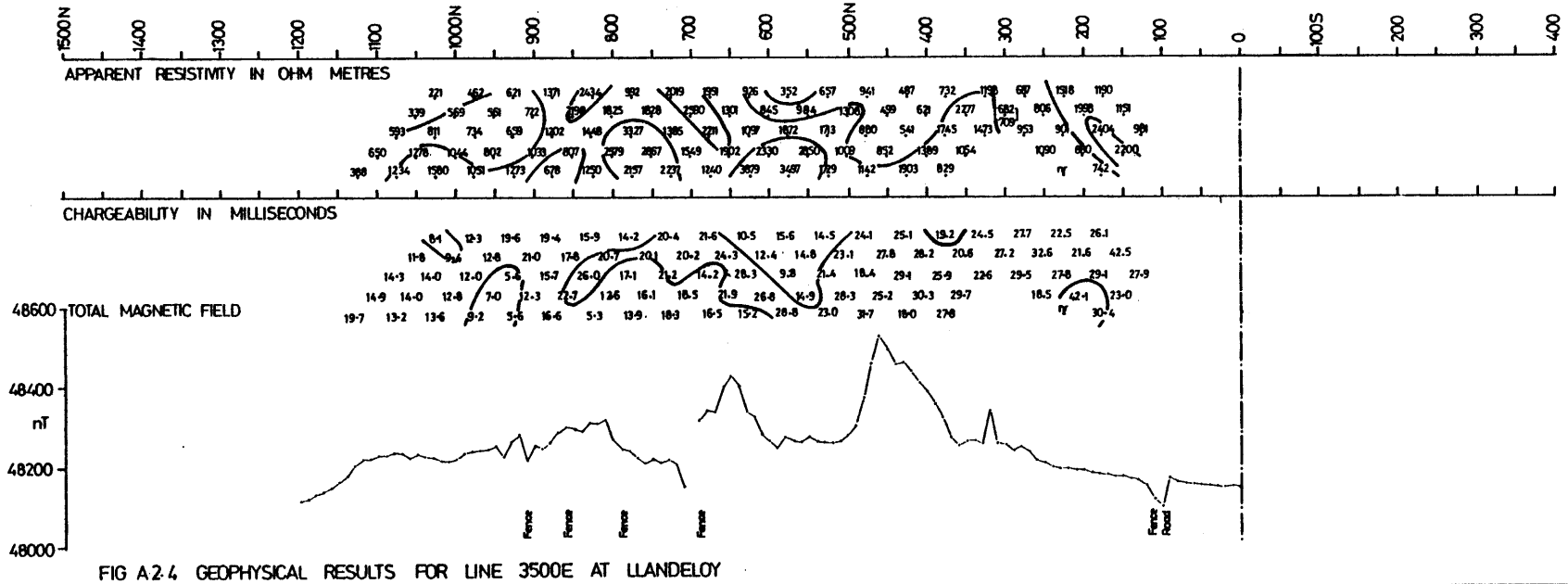

FIG A.2.4 GEOPHYSICAL RESULTS FOR LINE 3500E AT LLANDELOY

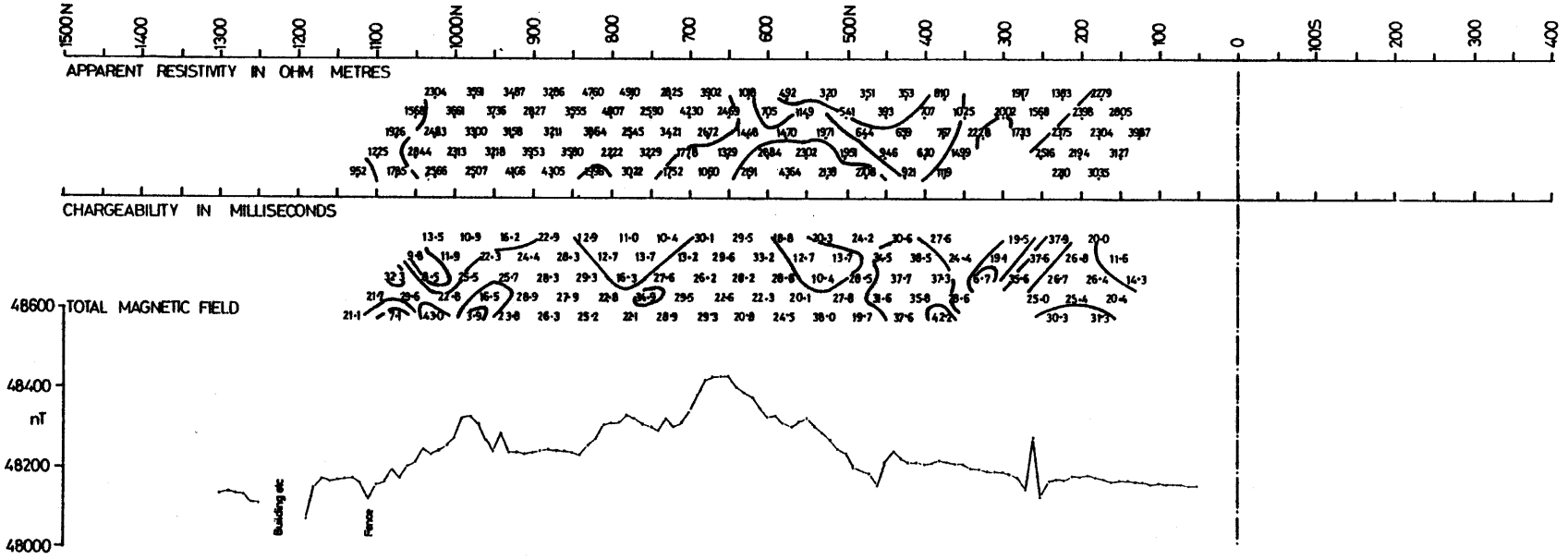

FIG A2.5 GEOPHYSICAL RESULTS FOR LINE 3700E AT LLANDELOY

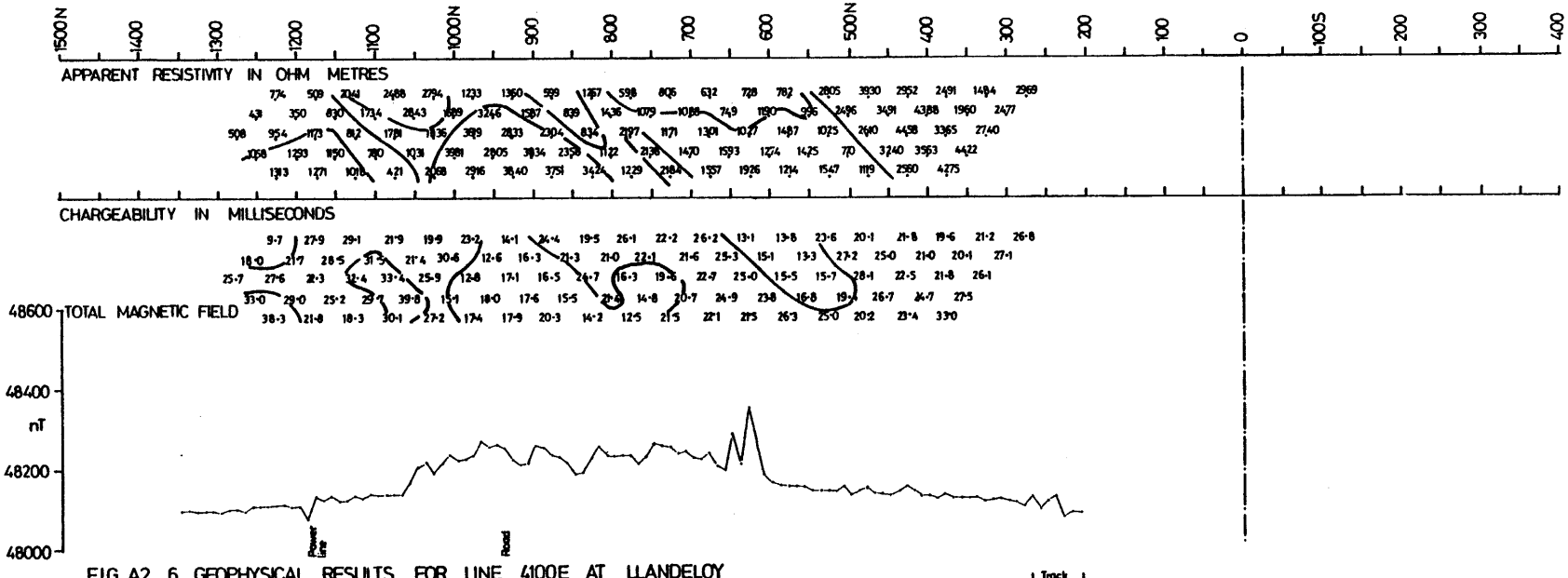

FIG A2.6 GEOPHYSICAL RESULTS FOR LINE 4100E AT LLANDELOY

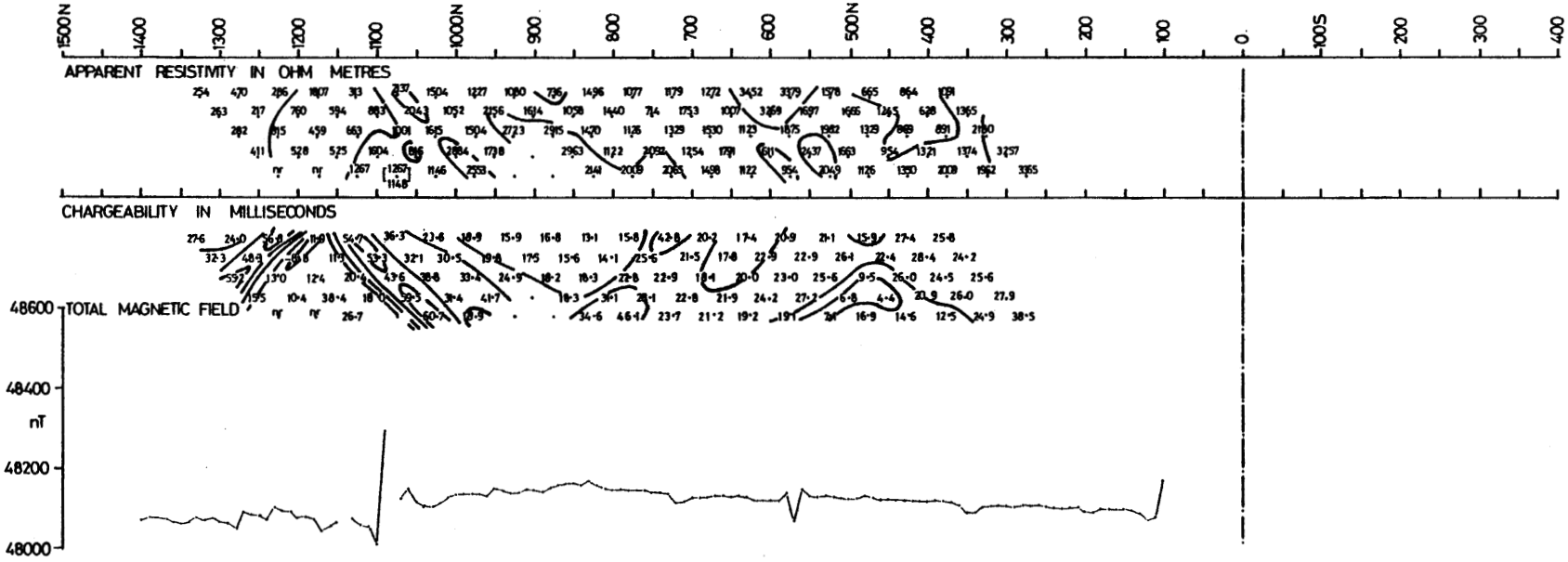

FIG A2.7 GEOPHYSICAL RESULTS FOR LINE 4300E AT LLANDELOY

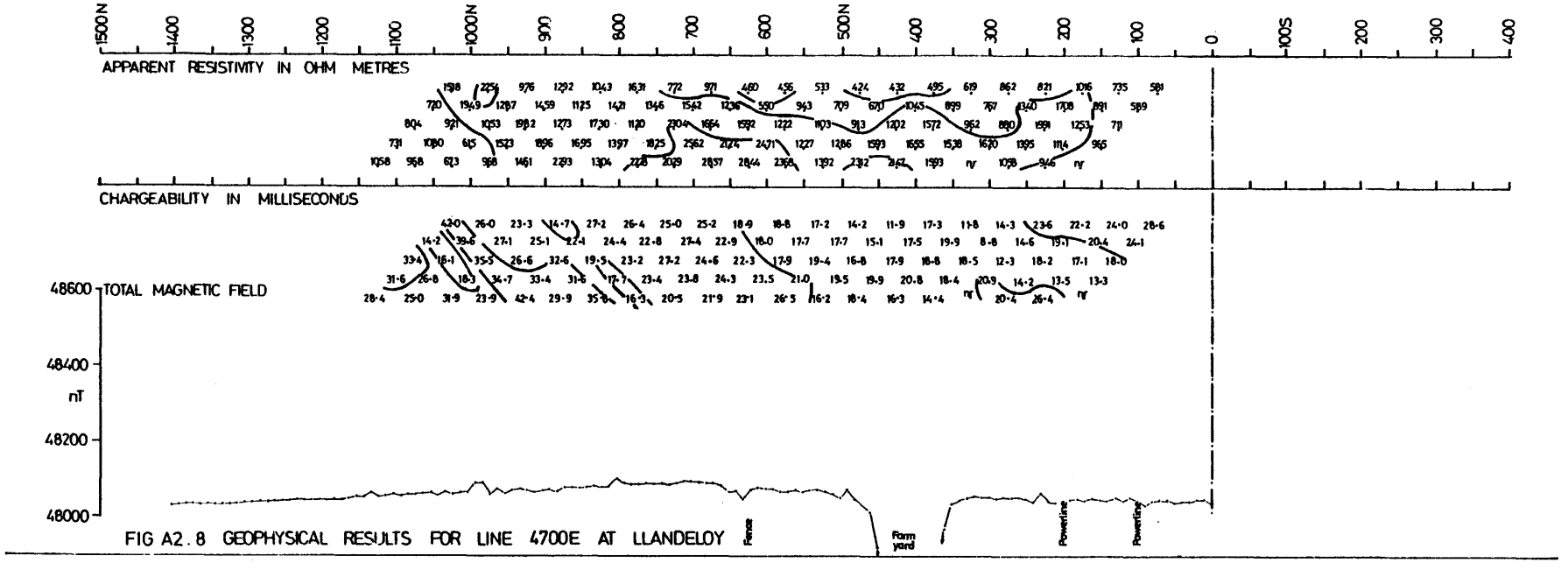

FIG A2.8 GEOPHYSICAL RESULTS FOR LINE 4700E AT LLANDELOY

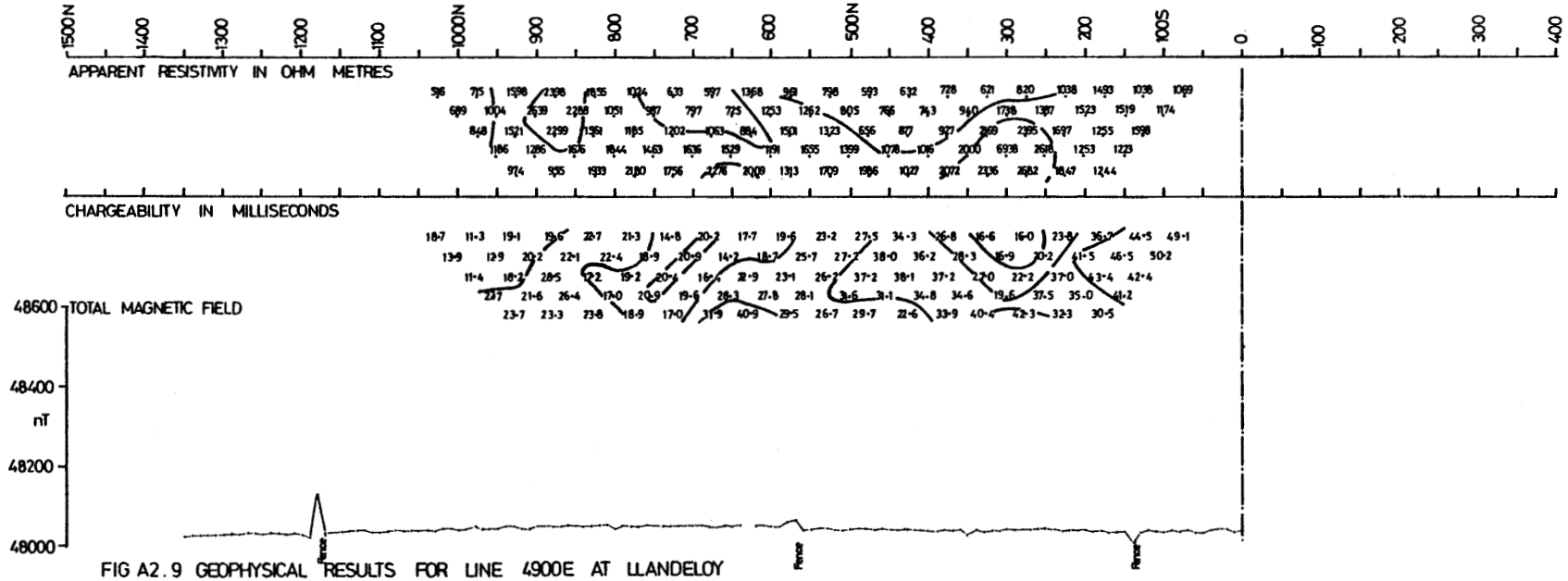

FIG A2.9 GEOPHYSICAL RESULTS FOR LINE 4900E AT LLANDELOY

APPENDIX 3

GEOPHYSICAL RESULTS FROM THE MIDDLE MILL AREA

The results are displayed on figures A3.1 to A3.6, line numbers refer to Fig. 16. As in Appendix 2, a subjective interpretation of the pseudosections has been made.

Line 150W
Severe artificial interference was encountered on this line, and many readings were completely unobtainable. There are two zones of high chargeability, both apparently artificial is origin. At its northern end, the line runs close to a road for 400 m, giving a complex pattern of very high, low and even negative chargeabilities. At the southern end of the line very high chargeabilities arise from dipole positions near buildings and a water pipe. The apparent resistivity also shows interference. Values are generally 600-900 ohm metres but slightly lower values obtained at 100N and higher values at about 350-450N may be significant above noise. The magnetic profile shows only man-made anomalies.

Line 150E
On this traverse artificial interference was a severe problem again, making many readings unobtainable. The chargeability pseudosection shows one feature which is probably due to bedrock geology, values to the south of about 150S being generally higher than those to the north. Two strong IP anomalies are almost certainly due to artificial sources: the high along the roadside at the north of the line and the narrow high across a farm lane and buried services at about 150S. The negative IP effect occurring just north of the baseline has no obvious artificial source. Resistivity, like chargeability, is higher south of about 150S than on the rest of the line. A broad resistivity low extends northwards from 150S to about 200N, where values become somewhat higher. The magnetic profile has minor peaks (about 50nT amplitude) in the area of the low resistivities and negative IP effects.

Line 450E
This traverse also suffers from artificial interference. Chargeabilities are generally 7 to 17 ms, with a minor high lying at the south end of the line giving values up to 25 ms. Otherwise high chargeability occurs only in areas of interference: the airfield perimeter at the northern end of the line and the farmyard at 150-300S. Variations on the resistivity pseudosection probably reflect bedrock variations. High resistivity occurs at 800N-500N; low values at 500N to 50N, with a minimum at about 100-200N: moderately high values recur between 50N and 200S, and values are again low from 200S to the housing estate at 500S. Other than aritificial anomalies there is little structure on the magnetic profile.

Line 750E
Line 750E had to be offset 100 m to the west at its northern end to avoid the quarry (Fig. 16). For most of its length it runs along or close to the steep slope of the Solfach river gorge. The line has three chargeability anomalies, of which two are likely to be artificial in origin. A minor IP high occurs at about 100N, where it may be related to a small intrusion. The main feature on this line is a double anomaly centred at 700-850N on the offset part of the line, immediately west of the quarry, where chargeability rises to 60 ms. In pseudosection, the anomaly has a core of low values, indicative either of an artificial conductor at about 725N or of a shallow flat-lying slab-like source less than 100 m wide. The absence of a coincident low resistivity anomaly tends to support a geological origin for this feature, but its position, between the quarry and the end of the airfield where strong anomalies were obtained on the previous line, strongly suggest an artificial source. A resistivity feature of interest on this traverse is the low at about 400N, where a fault has been mapped.

Line 1050E
Three chargeability anomalies occur, of which one is probably due to electrical noise from Middle Mill village at about 600N, and another to a large watermain at 700S. The third anomaly is the weakest but probably has a geological source. It is a diffuse near-surface feature on the baseline. Resistivity varies considerably, with narrow lows at about 275S and 500N. The magnetic profile shows nothing of interest.

Line 1350E
All four chargeability anomalies on this line are probably artificial in origin, the sources being farms at 400S and 600N, cables at 900N and fences at 1150N. The first three also give low resistivity anomalies. The last could have a geological source, however. All but the weakest magnetic anomalies are artificial.

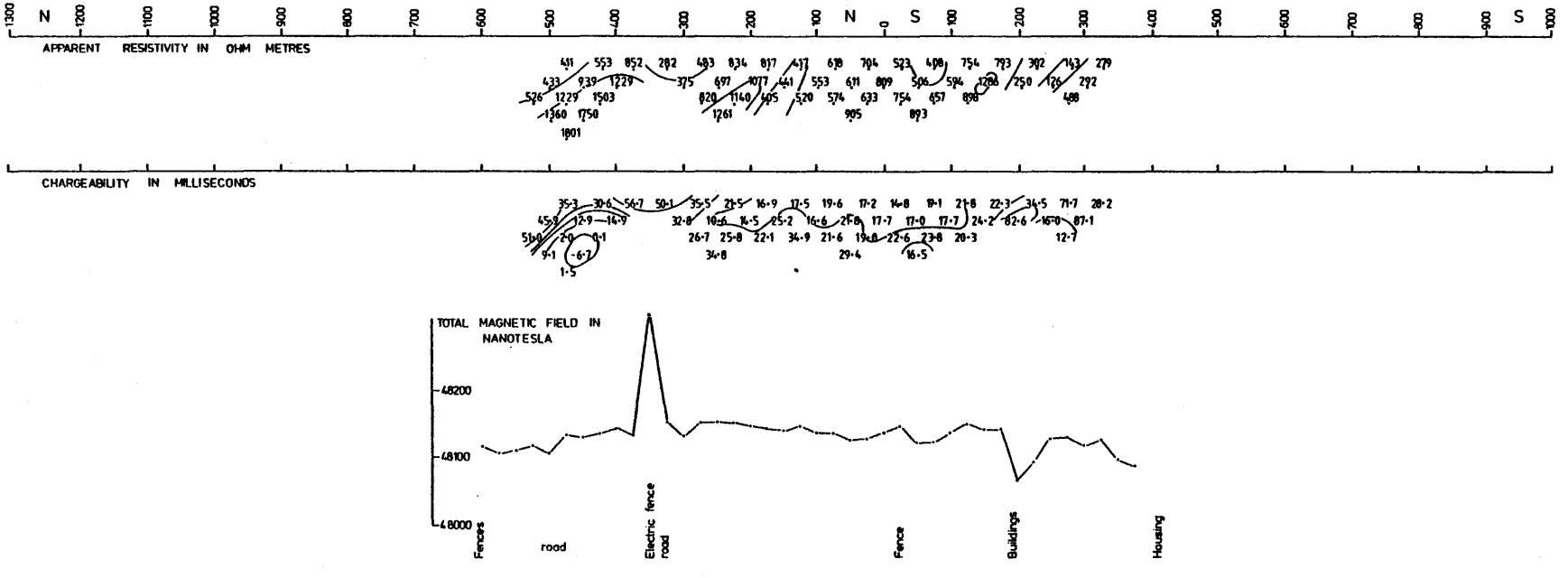

FIG A3·1 GEOPHYSICAL RESULTS FOR LINE 150W AT MIDDLE MILL

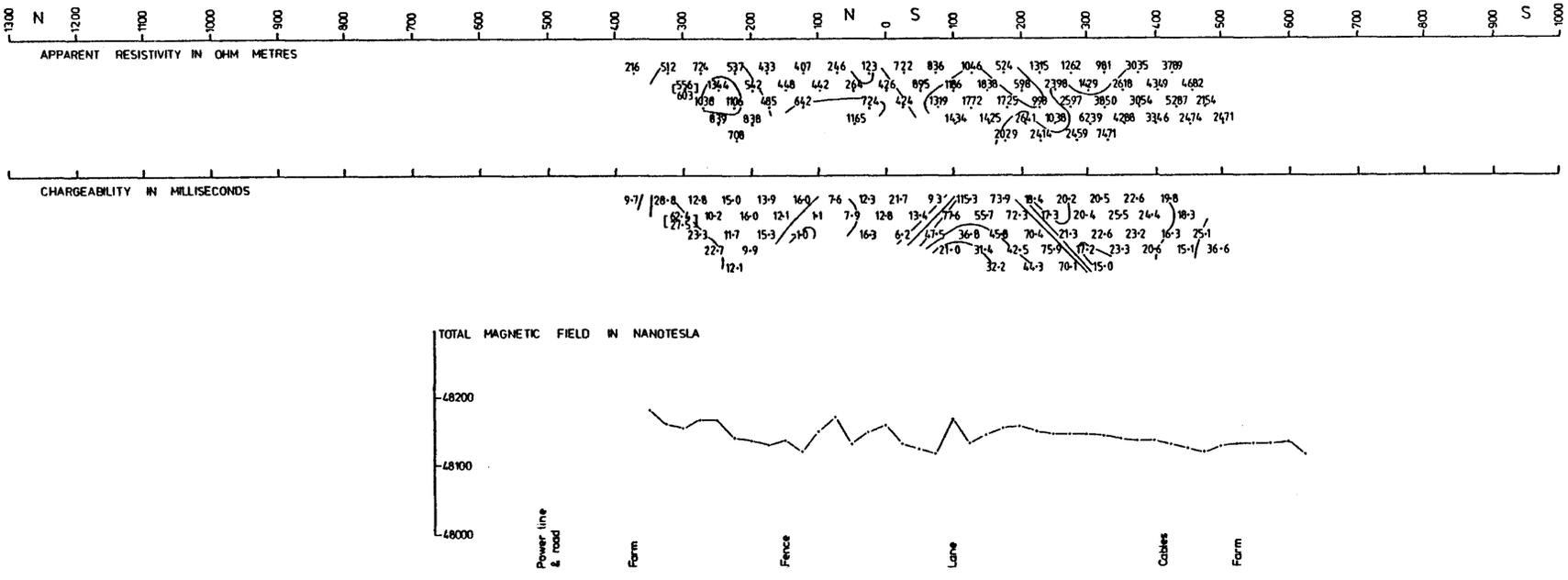

FIG. A3·2 GEOPHYSICAL RESULTS FOR LINE 150E AT MIDDLE MILL

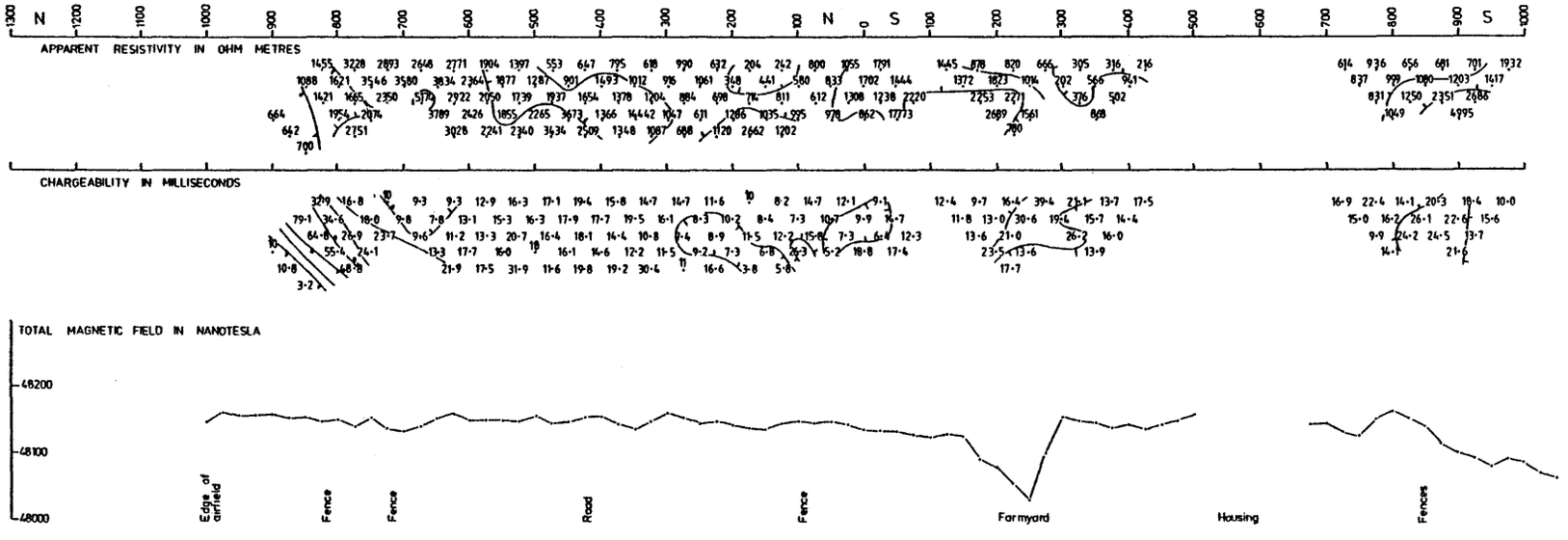

FIG A3·3 GEOPHYSICAL RESULTS FOR LINE 450E AT MIDDLE MILL

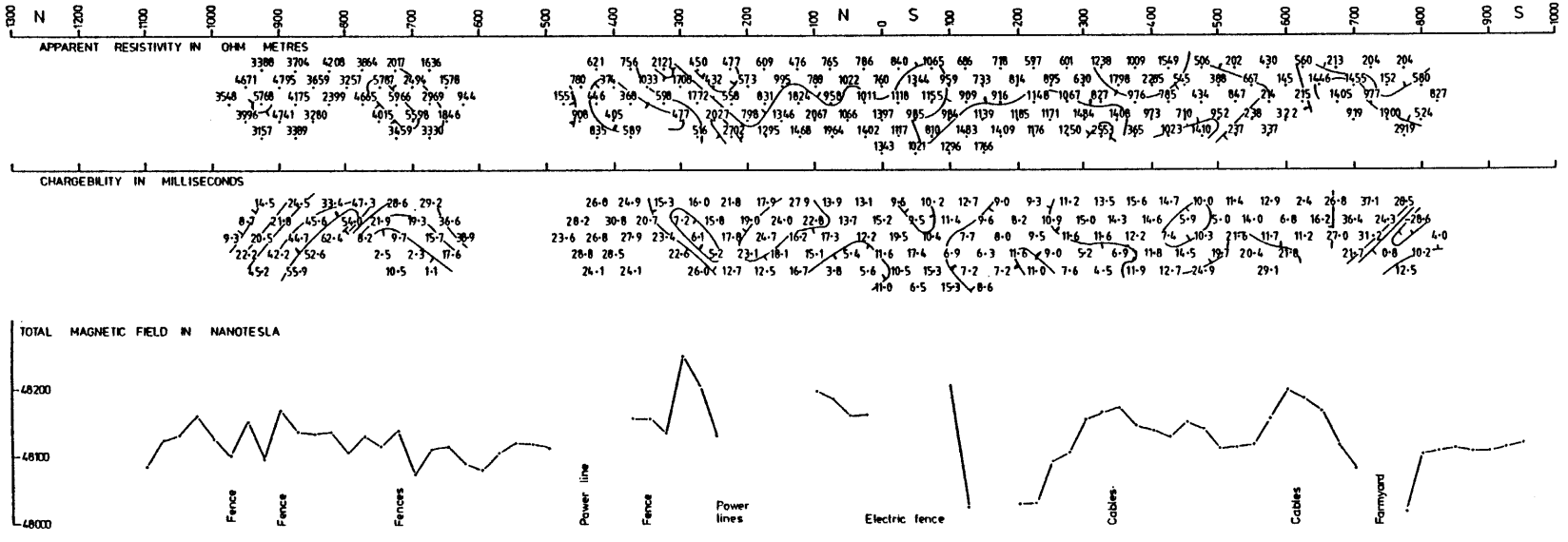

IG A34 GEOPHYSICAL RESULTS FOR LINE 750E AT MIDDLE MILL

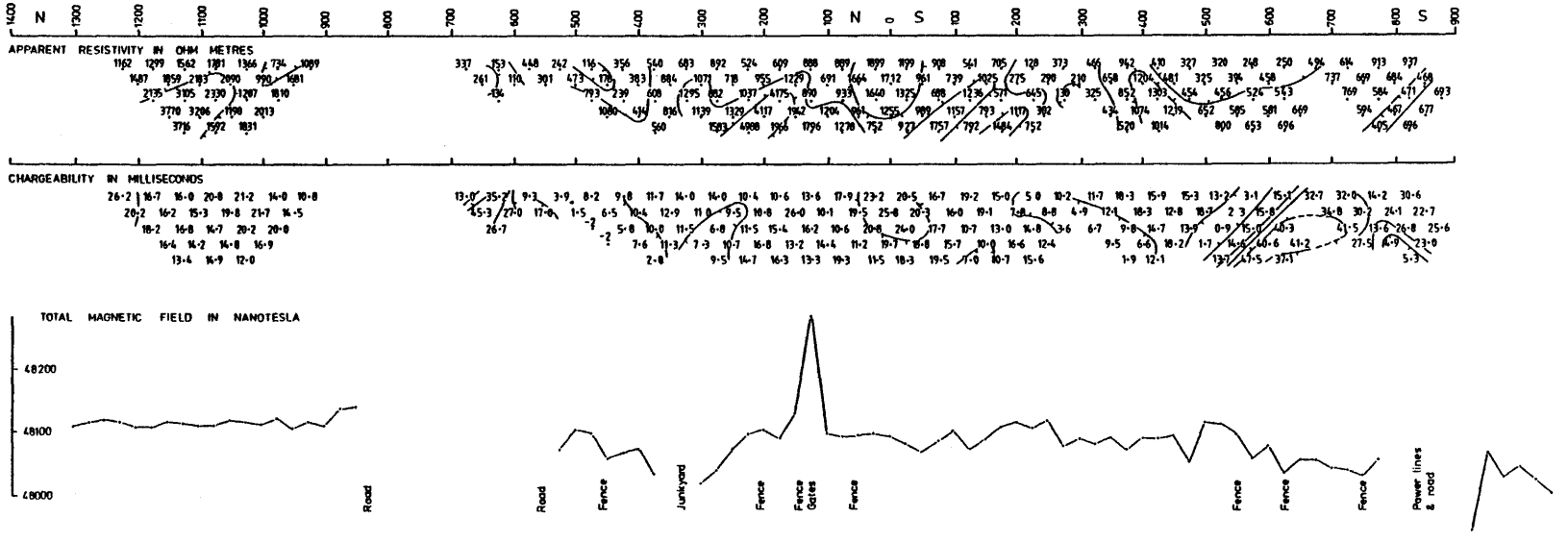

FIG. A3·5 GEOPHYSICAL RESULTS FOR LINE 1050E AT MIDDLE MILL

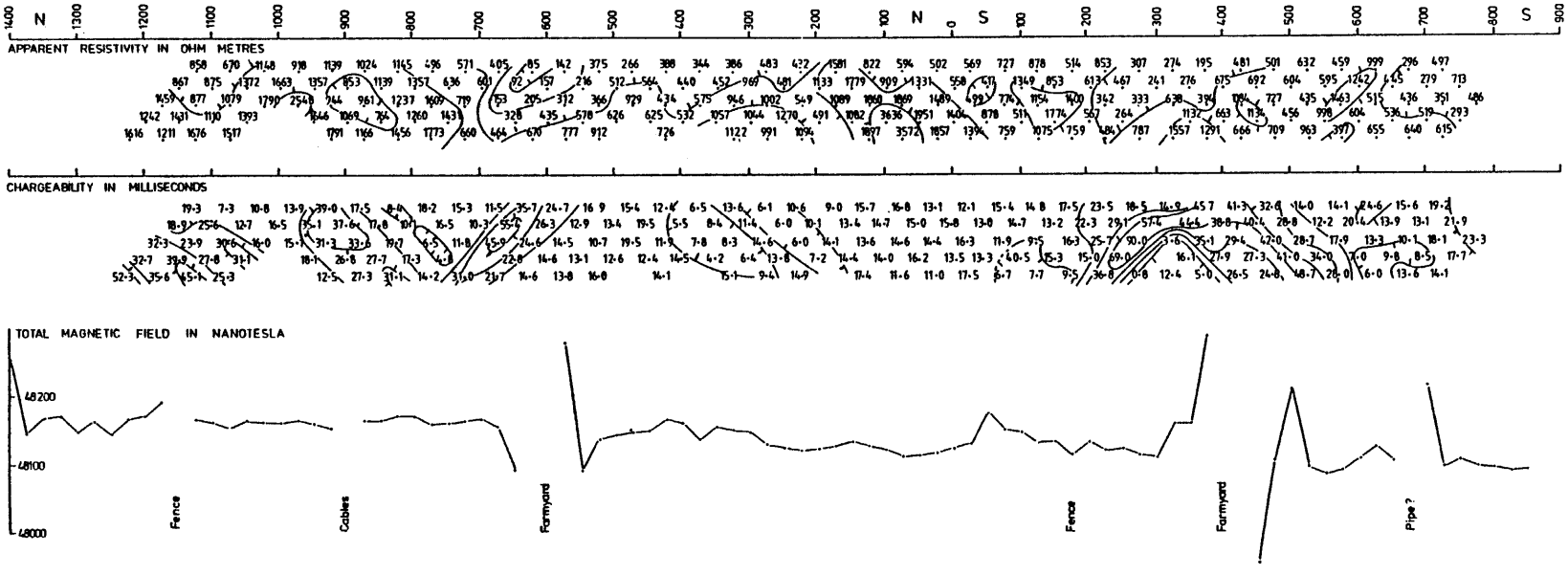

FIG. A3·6 GEOPHYSICAL RESULTS FOR LINE 1350E AT MIDDLE MILL

APPENDIX 4

PHYSICAL PROPERTY MEASUREMENTS ON BOREHOLE CORES

Magnetic susceptibility

Apparent susceptibility was measured with a 'Kappameter' at intervals of about one metre along the cores. Segments tested were unsplit and at least 100 mm long. True susceptibility was obtained by application of a factor dependent on core diameter. For accuracy better than 5% the diameter should be greater than 60 mm but at Llandeloy most core was either 50 or 25 mm in diameter, so somewhat greater errors are likely particularly in the higher susceptibility values.

The detailed results are given in Table A4.1

Density

Fourteen lengths of core were chosen to represent the main rock-types roughly in proportion to their occurrences in the eight boreholes. Each core was broken into 2 or 3 samples to provide a check. The samples were saturated with water under vacuum for 24 hours, then weighed in water (W_w) and in air (W_a). After drying in an oven for 48 hours, they were weighed in air again (W_d). Then:

Saturated density	$P_s = W_a/(W_a - W_w)$
Dry density	$P_d = W_d/(W_a - W_w)$
Grain density	$P_g = W_d/(W_d - W_w)$
Effective porosity	$= (W_a - W_d)/(W_a - W_w)$

The results are presented in Table A4.2

Table A4.1:
Magnetic Susceptibilities of Borehole Cores from Llandeloy, Dyfed

Depths in metres
Susceptibilities (K) in SI Units x 10^{-3}

Borehole 1 (diameter of core 50 mm)

Depth	K
3.88	0.01
4.46	0.36
4.90	0.18
6.83	0.29
7.96	0.76
9.20	0.50
10.74	0.18
12.00	0.32
13.05	0.32
13.60	0.22
14.95	0.36
16.20	0.26
16.95	0.14
17.98	0.14
19.00	0.18
20.75	0.14
21.50	0.04
22.40	0.14
23.50	0.22
24.32	0.22
25.50	0.18
26.50	0.07
27.50	0.18
28.50	0.18
28.84	0.18
29.87	0.32
30.40	0.54
31.40	0.43
32.50	0.25
33.80	0.43
34.40	0
35.50	0.14
36.45	0.29
37.90	0.32
38.60	0.29
39.70	0.14
40.70	0.29
41.60	0.32
42.80	0.18
43.50	0.14
44.36	0.25
45.60	0.29

Borehole 2 (diameter of core 50 mm)

Depth	K
3.75	0.47
6.03	1.12
8.45	0.23
10.13	0.50
11.85	9.18
12.84	15.66
13.83	10.08
14.90	12.42
15.85	0.18
17.05	14.94
17.90	1.26
18.80	1.80
19.70	3.24
20.73	24.12
21.70	24.84
22.75	20.16
23.90	2.70
24.78	5.22
25.55	43.20
26.50	22.32
27.25	15.30
28.40	1.08
29.45	0.36
30.54	0.54
31.80	24.30
32.80	0.54

Borehole 3A (diameter of core 50 mm)

Depth	K
20.70	2.74
24.10	0.43
24.50	1.40
26.80	0.25

Borehole 3B (diameter of core 65 mm)

Depth	K
2.90	0.63
4.00	1.11
7.65	0.15
8.80	1.05

Borehole 4
(diameter of core: 0-11 m, 65 mm; 11-40 m, 50 mm)

Depth	K
2.40	7.20
3.40	3.45
11.20	0.50
14.74	0.47
16.76	33.30
17.95	36.00
19.35	31.50
20.43	8.10
21.56	24.30
22.30	27.00
23.20	0.90
24.10	35.10
25.00	18.90
25.96	0.90
27.36	16.92
28.20	32.04
29.23	34.20
30.10	18.72
30.90	15.30
31.80	9.54
32.60	6.12
33.70	16.74
34.70	10.62
35.66	12.24
36.49	0.54
37.50	0.36

Borehole 5
(diameters of core 0-9 m, 65 mm; 9-46 m, 50 mm)

Depth	K
2.33	0.21
3.66	0.24
4.88	0.12
10.73	0.32
14.46	3.67
15.85	0.29
19.28	1.62
20.55	23.04
21.56	10.80
22.00	0.43
22.80	0.32
24.10	5.04
24.87	6.12
26.20	15.66
27.20	1.80
28.17	18.90
29.60	26.10
30.20	0.36
31.25	0.25
32.16	12.60
33.15	0.36
34.18	7.56
35.05	0.25
36.40	0.36
37.40	0.04
38.40	0.36
39.50	0.23
40.38	0.36
41.28	0.58
41.98	0.47
42.82	0.40
43.62	0.36
44.34	0.43
45.07	0.61

Borehole 6
(diameters of core: 0-9 m, 65 mm; 9-34 m, 50 mm)

Depth	K
3.35	5.49
3.85	1.32
4.60	4.35
7.50	2.55
10.05	0.50
11.38	0.65
12.35	0.61
13.15	0.72
14.53	0.40
17.46	0.14
18.27	0.61
19.66	0.40
21.10	0.54
22.05	0.43
23.20	0.47
24.33	5.76
25.46	3.88
26.50	3.60
27.50	3.67
29.10	9.00
30.40	1.80
31.50	4.86
32.46	10.44
33.40	15.84

Borehole 7
(diameters of core: 0-5 m, 65 mm; 5-30 m, 50 mm)

Depth	K
2.35	0.03
3.40	0.18
4.00	0.09
5.55	0.07
9.56	0
11.25	0.14
12.35	0.47
14.00	0.50
15.10	0.61
15.65	0.61
16.90	0.86
17.80	0.72
18.90	0.22
19.95	0.44
20.95	0.50
22.00	0.07
23.12	0
24.41	0.61
25.37	0.58
26.36	0.65
27.13	0.79
28.00	0.72
28.80	4.54
29.68	4.86

Borehole 8
(diameters of core 9-72 m, 50 mm; 72-124 m, 25 mm)

Depth	K
9.70	0.25
10.10	0.40
11.05	0.36
12.10	0.58
12.95	0.40
14.03	0.65
15.60	0.40
16.30	0.32
17.20	0.29
18.15	0.76
19.15	0.61
20.15	0.47
20.80	0.65
21.40	0.58
22.00	0.61
23.05	0.72
23.70	0.58
24.60	0.40
25.25	0.65
26.25	0.50
27.23	0.50
28.30	1.15
29.45	0.83
30.05	0.58
31.00	0.61
31.97	0.65
33.15	0.58
33.98	0.40
35.00	0.61
35.60	0.68
37.10	0.76
38.00	0.65
39.00	0.50
40.00	0.40
41.00	0.54
42.05	0.61
42.90	0.58
44.10	0.50
45.00	0.65
45.30	1.04
46.86	0.43
47.35	0.40
48.20	0.54
49.13	0.32
50.25	0.40
51.20	0.61
52.10	0.61
53.20	0.43
54.23	0.40
55.06	1.66
55.65	4.79
56.50	30.24
57.48	0.76
58.15	0.72
59.05	3.35
59.92	8.82
60.99	0.61
62.15	0.65
63.35	0.50
64.58	0.29
65.50	0.54
66.40	0.65
67.30	0.47
68.22	0.50
69.00	0.58
70.05	0.47
71.15	0.61
71.96	0.50
73.00	0.48
73.90	0.53
74.87	0.45
75.95	0.45
76.90	0.40
77.84	0.48
78.74	0.68
79.70	0.56
80.86	0.65
81.75	1.21
82.70	19.18
83.93	0.61
84.92	0.85
86.25	0.48
87.90	0.45
88.88	3.48
90.00	3.43
91.05	1.77
91.90	11.51
93.05	0.25
94.15	0.16
94.90	0.33
96.00	0.40
96.90	0.45
97.80	0.65
98.70	1.62
99.70	20.19
100.85	0.65
101.70	0.68
102.85	0.36
104.35	0.53
105.03	0.33
106.35	0.25
106.90	0.56
108.20	0.93
109.10	1.66
109.85	0.73
111.05	3.31
112.00	0.73
112.90	1.23
113.80	1.69
114.70	2.10
115.70	13.13
116.85	1.97
118.24	0.61
119.00	4.72
119.95	2.02
121.25	0.28
121.95	0.40
122.90	4.69
123.82	7.47

Table A4.2

Density and Porosity Determinations on Core Samples

Rock Type	Borehole No.	Depth m.	N	Satd. Dens. g cm^{-3}	Dry Dens. g cm^{-3}	Grain Dens. g cm^{-3}	Eff. Poros. %
Porphyritic microtonalite	1	35.80	3	2.71	2.69	2.75	2.35
Porphyritic microtonalite	1	43.01	3	2.67	2.66	2.70	1.24
Porphyritic microtonalite	6	33.30	2	2.71	2.69	2.74	1.81
Mean			3	2.70	2.68	2.73	1.80
Tonalite	5	23.79	3	2.77	2.76	2.77	0.44
Tonalite	5	40.58	3	2.75	2.74	2.76	0.59
Mean			2	2.76	2.75	2.77	0.51
Quartz microdiorite	2	20.69	3	2.85	2.85	2.86	0.53
Quartz microdiorite	2	32.39	3	2.76	2.75	2.79	1.54
Mean			2	2.81	2.80	2.83	1.04
Mean of intrusive rocks			7	2.75	2.75	2.77	1.21
Acid volcanic[1]	6	23.24	3	2.73	2.70	2.78	3.01
Sandstone	8	19.76	2	2.79	2.78	2.80	0.59
Sandstone	8	30.25	3	2.81	2.81	2.81	0.18
Sandstone	8	42.47	3	2.78	2.77	2.78	0.35
Sandstone	8	53.47	2	2.79	2.79	2.80	0.18
Siltstone/sandstone	8	35.54	2	2.79	2.79	2.80	0.26
Siltstone	8	23.52	3	2.78	2.78	2.79	0.41
Mean of sedimentary rocks			6	2.79	2.79	2.80	0.33

[1] All volcanic rock samples were from the weathered zone

APPENDIX 5

COMPUTER MODELLING OF AEROMAGNETIC AND RESISTIVITY DATA

Aeromagnetic anomaly

Three profiles from the aeromagnetic map (Fig. 7) were subjected to computer interpretation. The IGS Applied Geophysics Unit Program GAM2D2 was used (Lee, 1979). Profiles were taken from the contour map and sampled at 250 m intervals. The Llandeloy magnetic anomaly lies within the influence of two larger anomalies to the south: that due to the rocks in the core of the Hayscastle anticline, and that which extends along the south coast of Wales. The mutual interference of these anomalies made it impossible to define the regional field accurately. A value of 2nT km^{-1} was used though there are indications for a gradient of up to 5nT km^{-1} negative northward.

At Llandeloy, the width and gentle flanks of the anomaly indicate a source extending to some depth. The base of the model was therefore set at 3 km, and the shape of the top surface and the susceptibility were adjusted to give the best possible fit of calculated to observed anomalies, while permitting the body to be exposed at the surface where appropriate. The susceptibility which gave the best fit within these limitations was 7.5 x 10^{-3} cgs units, which is close to the average value for acid to intermediate igneous rocks often given in the literature.

The shape provided for the interpreted sources are all generally similar. A steep southern margin dips southwards at 60-70° from the surface just south of the maximum anomaly. The northern margin, corresponding at the surface with the steepest gradient, has dips as little as 20° and is therefore somewhat concave on two of the three profiles. The individual profiles and their interpretations are presented below (Figs. A5.1 to A5.5). For profile two, an iterative interpretation method was also used, which adjusts the length of prisms (extending to infinity at right angles to the paper) above a base, which was again assumed to be 3 km. The two bodies from the automatic iterative process and the manual polygon process correspond closely to one another.

Thickness of conductive overburden

An attempt was made to model the resistivity vertical profile at two points using data from the pseudosections. The dipole-dipole array is not well suited to this use however, because it is very sensitive to lateral variations, and because the relatively large dipole length makes for poor resolution of the shallower layers. The two sites chosen were 3700E/500N where borehole 3 intersected over 20 m of lacustrine sediments, and 4100E/675N, where the pseudosection indicated freedom from lateral effects. It was not possible to produce a realistic model for the former site, suggesting that lateral variations are predominant here. The model for the more easterly site is shown on Fig. A5.6. Even with this relatively thin overburden, the maximum measured resistivity will be only half the true resistivity of the bedrock.

MAGNETIC INTERPRETATION . . . ANOMALY IN NANOTESLA

RMS RESID = 7.26

FLD PT	ELEV	OBS ANOM	CALC ANOM	RESID
0.000	60.000	0.00	0.19	-0.19
0.250	60.000	0.50	1.91	-1.41
0.500	60.000	3.00	4.17	-1.17
0.750	60.000	6.50	7.14	-0.64
1.000	60.000	9.00	11.00	-2.00
1.250	60.000	22.50	16.05	6.45
1.500	60.000	33.00	22.65	10.35
1.750	60.000	36.50	31.37	5.13
2.000	60.000	46.00	43.15	2.85
2.250	60.000	61.50	59.80	1.70
2.500	60.000	85.00	85.82	-0.82
2.750	60.000	136.50	139.85	-3.35
3.000	60.000	220.00	224.81	-4.81
3.250	60.000	185.50	182.16	3.34
3.500	60.000	161.00	153.17	7.83
3.750	60.000	82.50	51.03	31.47
4.000	60.000	23.00	26.12	-3.12
4.250	60.000	17.50	14.53	2.97
4.500	60.000	14.00	7.71	6.29
4.750	60.000	8.50	3.42	5.08
5.000	60.000	4.00	0.28	3.72
5.250	60.000	-1.50	-2.59	1.09
5.500	60.000	-5.00	-5.57	0.57
5.750	60.000	-8.50	-8.69	0.19
6.000	60.000	-12.00	-11.88	-0.12
6.250	60.000	-12.50	-15.05	2.55
6.500	60.000	-13.00	-18.12	5.12

Fig. A5·1

RESULTS OF POLYGON INTERPRETATION

LLANDELOY MAGNETIC ANOMALY 1 (COARSE)

FOR EACH POLYGON :
DENS = DENSITY CONTRAST IN G/CC
AZF = AZIMUTH OF PROFILE DIRECTION W.R.T MAG NORTH
DIPF = INCLINATION OF EARTHS FIELD (+VE DOWN)
AZM = AZIMUTH OF MAGNETISATION VECTOR W.R.T PROFILE
DIPM = INCLINATION OF MAGNETISATION VECTOR (+VE DOWN)
AMAG = INTENSITY OF MAGNETISATION (NANOTESLA)

DEPTHS IN KM (+VE DOWN), ELEVS IN METRES (+VE UP), ANGLES IN DEGS

POLYGONS

1 DENS = 0.000 AZF = 4.0 DIPF = 70.0
AZM = 4.0 DIPM = 70.0 AMAG = 31.000

X	Z
2.900	0.000
1.860	3.000
7.500	3.000
7.500	2.000
4.700	0.900
3.600	0.000

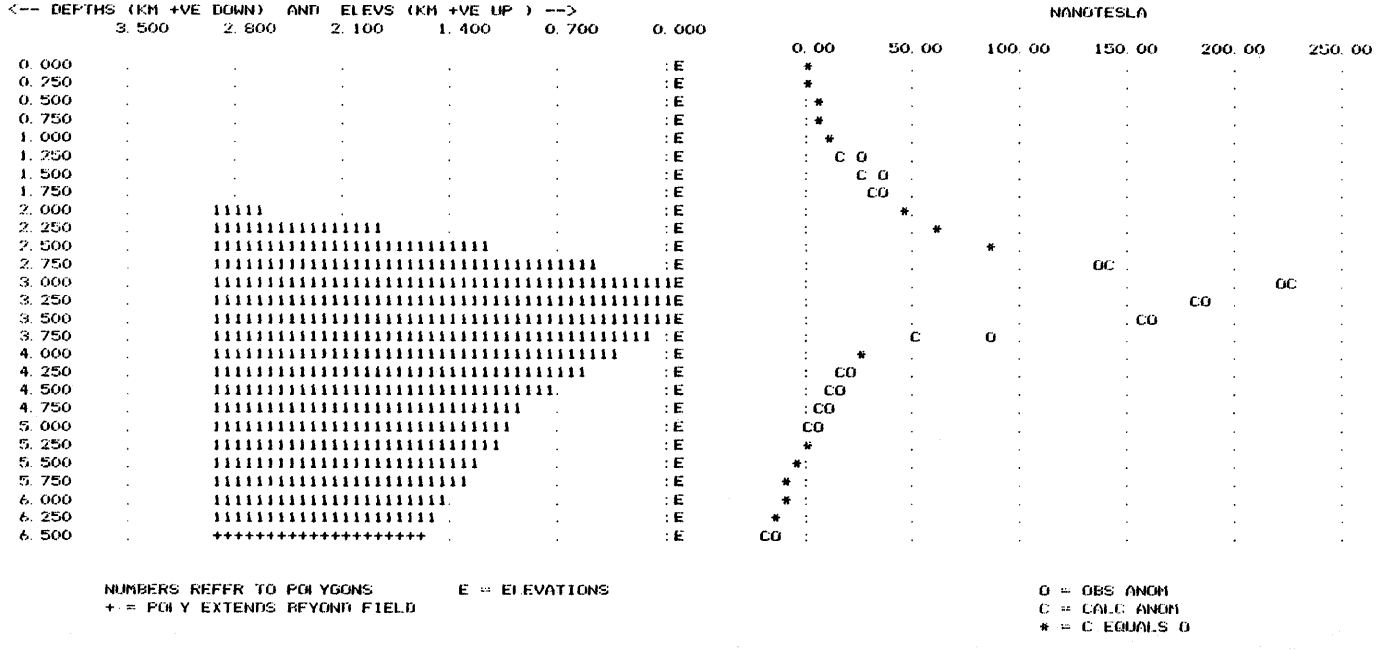

NUMBERS REFFR TO POLYGONS E = ELEVATIONS
+ = POLY EXTENDS BEYOND FIELD

O = OBS ANOM
C = CALC ANOM
* = C EQUALS O

MAGNETIC INTERPRETATION. . . . ANOMALY IN NANOTESLA

Fig. A5·2

RMS RESID = 12.70

FLD. PT	ELEV	OBS ANOM	CALC ANOM	RESID
0.000	60.000	74.00	64.02	9.98
0.050	60.000	77.09	68.64	8.45
0.100	60.000	82.18	73.74	8.43
0.150	60.000	88.26	79.43	8.84
0.200	60.000	94.35	85.82	8.53
0.250	60.000	101.44	93.13	8.32
0.300	60.000	111.53	101.60	9.92
0.350	60.000	122.62	111.68	10.94
0.400	60.000	135.71	124.03	11.67
0.450	60.000	150.79	139.85	10.95
0.500	60.000	175.88	161.31	14.57
0.550	60.000	194.97	191.85	3.12
0.600	60.000	218.06	226.36	-8.30
0.650	60.000	226.15	234.42	-8.28
0.700	60.000	225.24	224.81	0.43
0.750	60.000	220.32	213.68	6.64
0.800	60.000	213.41	203.91	9.50
0.850	60.000	205.50	195.59	9.91
0.900	60.000	196.59	188.43	8.16
0.950	60.000	187.68	182.16	5.51
1.000	60.000	186.76	176.55	10.22
1.050	60.000	184.85	171.34	13.51
1.100	60.000	179.94	166.22	13.73
1.150	60.000	165.03	160.61	4.42
1.200	60.000	153.12	153.17	-0.05
1.250	60.000	144.21	139.83	4.37
1.300	60.000	131.29	111.94	19.36
1.350	60.000	116.38	80.42	35.96
1.400	60.000	97.47	61.96	35.51
1.450	60.000	71.56	51.03	20.53
1.500	60.000	53.65	43.54	10.11
1.550	60.000	44.74	37.85	6.88
1.600	60.000	34.82	33.27	1.55
1.650	60.000	29.91	29.42	0.49
1.700	60.000	28.00	26.12	1.88

RESULTS OF POLYGON INTERPRETATION

LLANDELOY MAGNETIC ANOMALY PROFILE 1 (DETAIL)

FOR EACH POLYGON :
DENS = DENSITY CONTRAST IN G/CC
AZF = AZIMUTH OF PROFILE DIRECTION W.R.T MAG NORTH
DIPF = INCLINATION OF EARTHS FIELD (+VE DOWN)
AZM = AZIMUTH OF MAGNETISATION VECTOR W.R.T PROFILE
DIPM = INCLINATION OF MAGNETISATION VECTOR (+VE DOWN)
AMAG = INTENSITY OF MAGNETISATION (NANOTESLA)

DEPTHS IN KM (+VE DOWN), ELEVS IN METRES (+VE UP), ANGLES IN DEGS

POLYGONS

1 DENS = 0.000 AZF = 4.0 DIPF = 70.0
AZM = 4.0 DIPM = 70.0 AMAG = 31.000

X	Z
0.600	0.000
-0.440	3.000
5.200	3.000
5.200	2.000
2.400	0.900
1.300	0.000

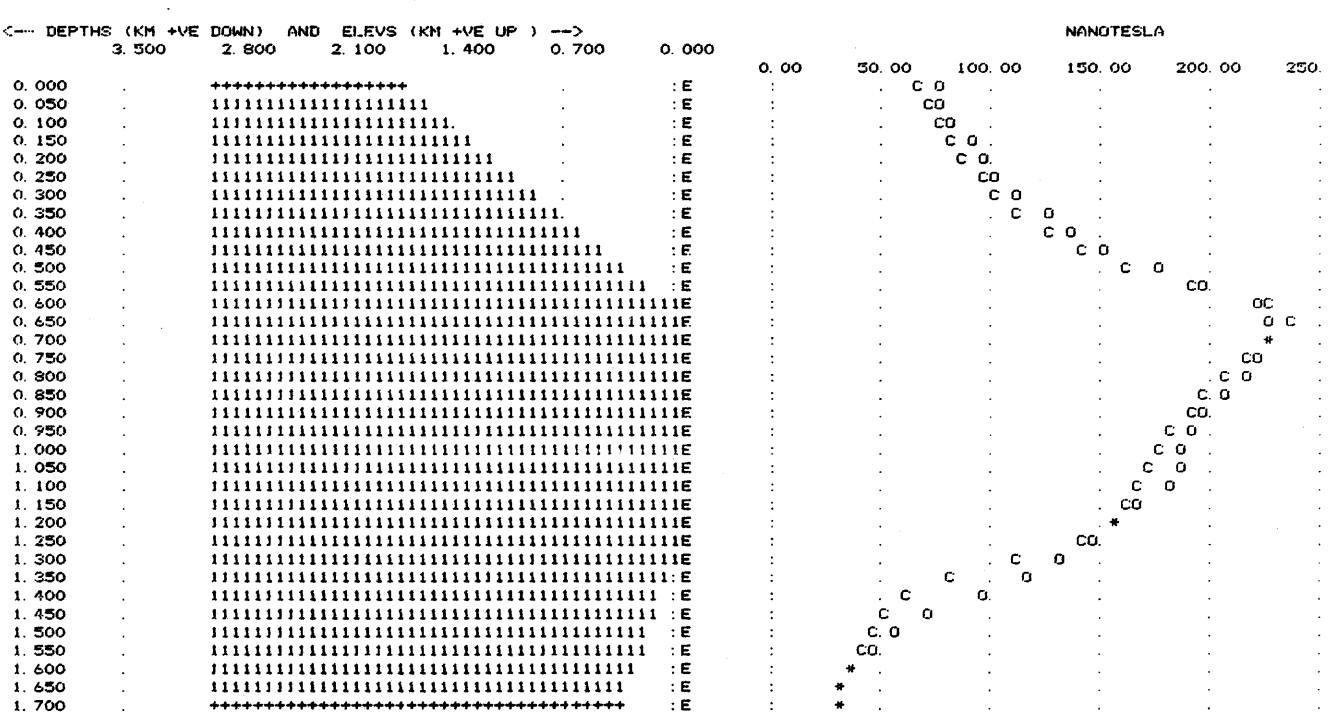

NUMBERS REFER TO POLYGONS
+ = POLY EXTENDS BEYOND FIELD

E = ELEVATIONS

O = OBS ANOM
C = CALC ANOM
* = C EQUALS O

MAGNETIC INTERPRETATION . . . ANOMALY IN NANOTESLA

RMS RESID = 6.53

FLD. PT	ELEV	OBS ANOM	CALC ANOM	RESID
0.000	60.000	0.00	3.16	-3.16
0.250	60.000	0.50	5.21	-4.71
0.500	60.000	5.00	7.82	-2.82
0.750	60.000	7.50	11.11	-3.61
1.000	60.000	14.00	15.25	-1.25
1.250	60.000	27.50	20.44	2.06
1.500	60.000	32.00	26.92	5.08
1.750	60.000	41.50	35.04	6.46
2.000	60.000	50.00	45.33	4.67
2.250	60.000	66.50	58.72	7.78
2.500	60.000	89.00	77.07	11.93
2.750	60.000	121.50	105.44	16.06
3.000	60.000	160.00	168.27	-8.27
3.250	60.000	198.50	196.59	1.92
3.500	60.000	155.00	147.51	7.49
3.750	60.000	27.50	23.43	4.07
4.000	60.000	-3.00	-2.22	-0.78
4.250	60.000	-4.50	-10.72	6.22
4.500	60.000	-10.00	-15.27	5.27
4.750	60.000	-15.50	-18.01	2.51
5.000	60.000	-22.00	-19.85	-2.15
5.250	60.000	-24.50	-21.26	-3.24
5.500	60.000	-29.00	-22.43	-6.57
5.750	60.000	-32.50	-23.40	-9.10
6.000	60.000	-34.00	-24.14	-9.86

Fig.A5·3

RESULTS OF POLYGON INTERPRETATION

LLANDELOY MAGNETIC PROFILE 2

FOR EACH POLYGON :
DENS = DENSITY CONTRAST IN G/CC
AZF = AZIMUTH OF PROFILE DIRECTION W.R.T MAG NORTH
DIPF = INCLINATION OF EARTHS FIELD (+VE DOWN)
AZM = AZIMUTH OF MAGNETISATION VECTOR W.R.T PROFILE
DIPM = INCLINATION OF MAGNETISATION VECTOR (+VE DOWN)
AMAG = INTENSITY OF MAGNETISATION (NANOTESLA)

DEPTHS IN KM (+VE DOWN), ELEVS IN METRES (+VE UP), ANGLES IN DEGS

POLYGONS

1 DENS = 0.000 AZF = 8.0 DIPF = 70.0
AZM = 8.0 DIPM = 70.0 AMAG = 30.000

X	Z
3.100	0.000
1.500	3.000
7.000	3.000
7.000	2.750
4.600	1.250
3.650	0.000

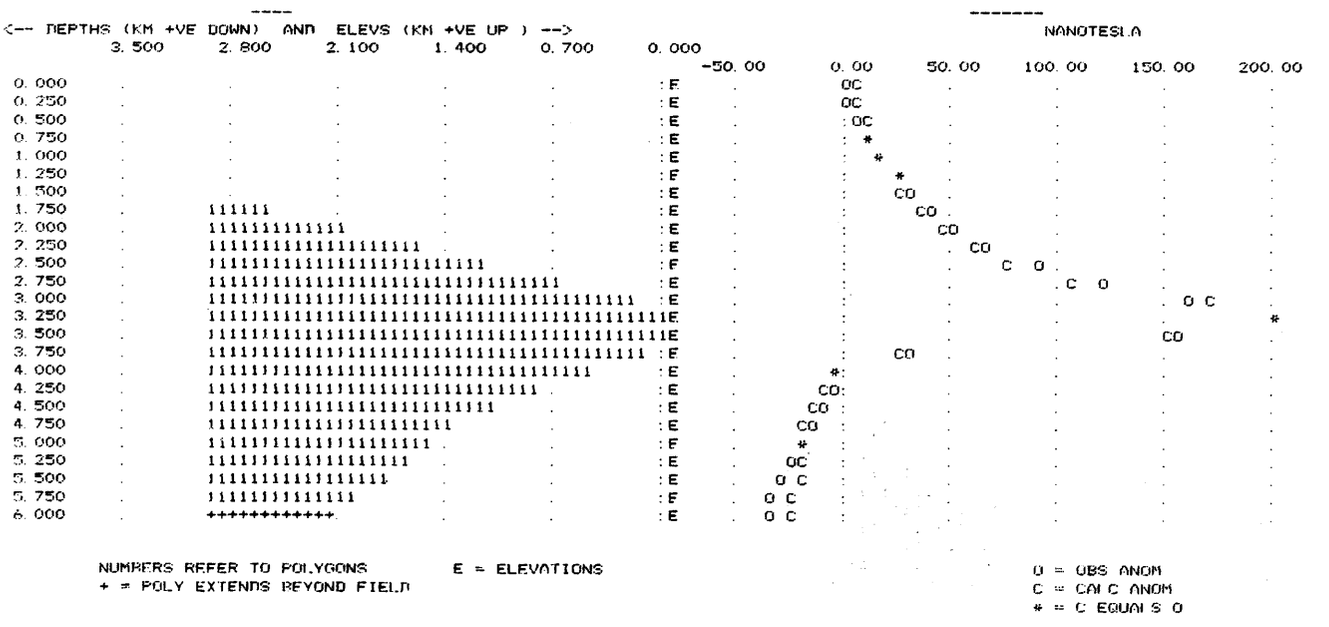

NUMBERS REFER TO POLYGONS E = ELEVATIONS
+ = POLY EXTENDS BEYOND FIELD

O = OBS ANOM
C = CALC ANOM
* = C EQUALS O

MAGNETIC INTERPRETATION. . . . ANOMALY IN NANOTESLA

Fig. A5·4

ITERATION NO. = 13 RMS RESID = 8.14

FLD. PT	ELEV	OBS ANOM	FIX Z	VAR Z	CALC ANOM	RESID
0.000	60.000	0.00			5.12	-5.12
0.250	60.000	0.50			7.71	-7.21
0.500	60.000	5.00			10.93	-5.93
0.750	60.000	7.50			14.93	-7.43
1.000	60.000	14.00			19.87	-5.87
1.250	60.000	22.50			25.99	-3.49
1.500	60.000	32.00	3.000	2.214	33.64	-1.64
1.750	60.000	41.50	3.000	2.014	43.36	-1.86
2.000	60.000	50.00	3.000	1.699	56.12	-6.12
2.250	60.000	66.50	3.000	1.265	73.64	-7.14
2.500	60.000	89.00	3.000	0.746	98.35	-9.35
2.750	60.000	121.50	3.000	0.318	127.68	-6.18
3.000	60.000	160.00	3.000	0.164	153.96	6.04
3.250	60.000	198.50	3.000	0.004	193.64	4.86
3.500	60.000	155.00	3.000	0.000	139.19	15.82
3.750	60.000	27.50	3.000	0.145	38.29	-10.79
4.000	60.000	-3.00	3.000	0.360	10.98	-13.98
4.250	60.000	-4.50	3.000	0.433	-5.69	1.19
4.500	60.000	-10.00	3.000	0.832	-20.90	10.90
4.750	60.000	-15.50	3.000	1.267	-29.86	14.36
5.000	60.000	-22.00	3.000	1.627	-33.53	11.53
5.250	60.000	-24.50	3.000	1.893	-34.70	10.20
5.500	60.000	-29.00	3.000	2.064	-34.72	5.72
5.750	60.000	-32.50	3.000	2.146	-34.18	1.68
6.000	60.000	-34.00	3.000	2.151	-33.33	-0.67

RESULTS OF ITERATIVE INTERPRETATION

LLANDELOY MAGNETIC PROFILE 2

DENSITY CONTRAST = 0.000 G/CC
AZF (AZIMUTH OF PROFILE DIRECTION W.R.T MAG NORTH) = 8.0
DIPF (INCLINATION OF EARTHS FIELD (+VE DOWN)) = 70.0
AZM (AZIMUTH OF MAGNETISATION VECTOR W.R.T PRFILE) = 8.0
DIPM (INCLINATION OF MAGNETISATION VECTOR (+VE DOWN)) = 70.0
AMAG (INTENSITY OF MAGNETISATION IN NANOTESLA) = 30.000

DEPTHS IN KM (+VE DOWN), ELEVS IN METRES(+VE UP), ANGLES IN DEGS

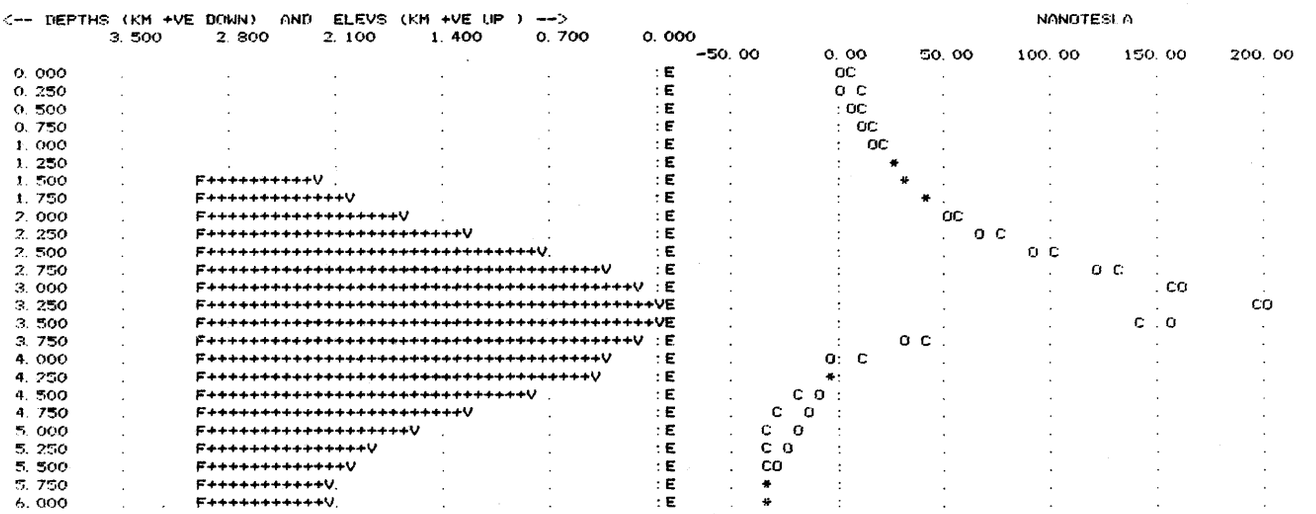

F = FIXED SURFACE
V = VARIABLE SURFACE
\+ = BODY

E = ELEVATIONS

O = F AND V COINCIDE

O = OBS ANOM
C = CALC ANOM
* = C EQUALS O

Fig. A5·5

MAGNETIC INTERPRETATION . . . ANOMALY IN NANOTESLA

RMS RESID = 4.14

FLD. PT	ELEV	OBS ANOM	CALC ANOM	RESID
0.000	60.000	14.00	19.13	-5.13
0.250	60.000	17.48	22.06	-4.58
0.500	60.000	22.96	25.09	-2.13
0.750	60.000	26.44	28.20	-1.76
1.000	60.000	31.92	31.43	0.49
1.250	60.000	36.40	34.85	1.55
1.500	60.000	38.88	38.58	0.30
1.750	60.000	45.36	42.78	2.58
2.000	60.000	48.84	47.62	1.22
2.250	60.000	52.32	53.31	-0.99
2.500	60.000	56.80	60.00	-3.20
2.750	60.000	65.28	67.75	-2.47
3.000	60.000	73.76	76.39	-2.63
3.250	60.000	86.24	84.93	1.31
3.500	60.000	92.72	89.89	2.83
3.750	60.000	90.20	83.29	6.91
4.000	60.000	65.68	63.10	2.58
4.250	60.000	38.16	40.60	-2.44
4.500	60.000	14.64	21.89	-7.25
4.750	60.000	-0.88	7.21	-8.09
5.000	60.000	-10.40	-4.11	-6.29
5.250	60.000	-17.92	-12.63	-5.29
5.500	60.000	-23.44	-18.83	-4.61
5.750	60.000	-28.96	-23.21	-5.75
6.000	60.000	-31.48	-26.14	-5.34
6.250	60.000	-32.00	-27.95	-4.05

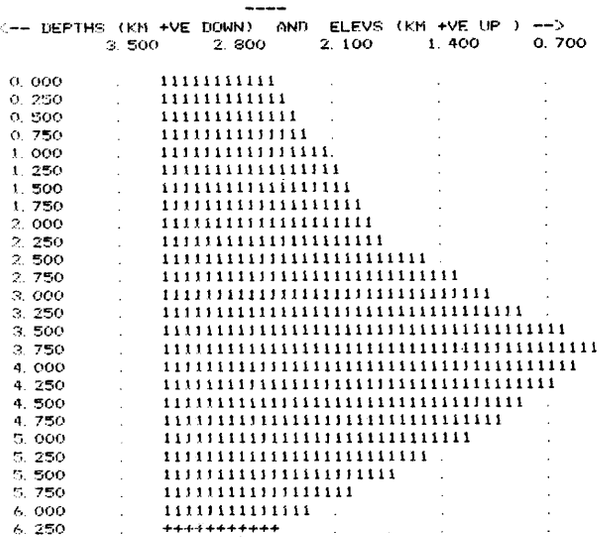

RESULTS OF POLYGON INTERPRETATION

LLANDELOY MAGNETIC ANOMALY 3

FOR EACH POLYGON :
DENS = DENSITY CONTRAST IN G/CC
AZF = AZIMUTH OF PROFILE DIRECTION W.R.T MAG NORTH
DIPF = INCLINATION OF EARTHS FIELD (+VE DOWN)
AZM = AZIMUTH OF MAGNETISATION VECTOR W.R.T PROFILE
DIPM = INCLINATION OF MAGNETISATION VECTOR (+VE DOWN)
AMAG = INTENSITY OF MAGNETISATION (NANOTESLA)

DEPTHS IN KM (+VE DOWN), ELEVS IN METRES (+VE UP), ANGLES IN DEGS

POLYGONS

1 DENS = 0.000 AZF = 12.0 DIPF = 70.0
AZM = 12.0 DIPM = 70.0 AMAG = 31.000

X	Z
3.750	0.400
2.250	1.750
0.000	2.500
0.000	3.250
6.500	3.250
6.500	2.750
4.750	1.000

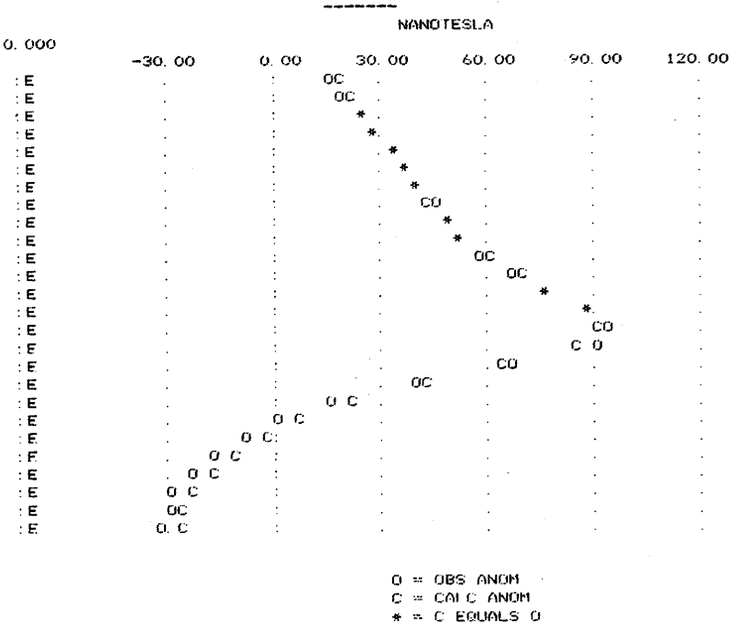

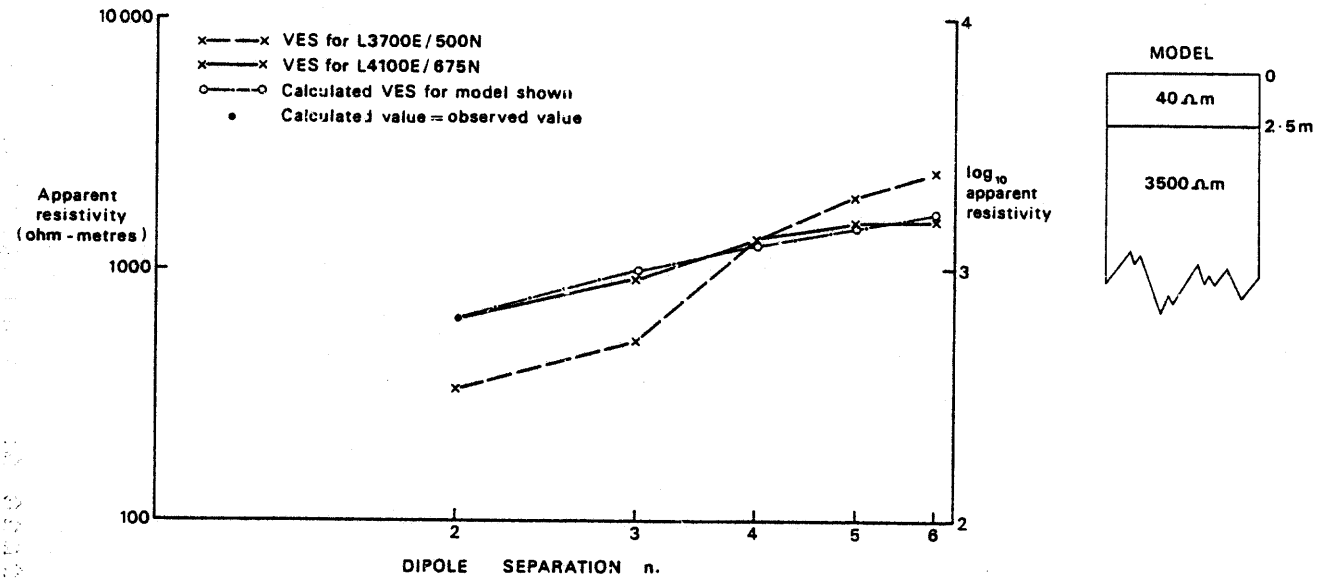

Fig. A5.6 Resistivity soundings

APPENDIX 6

ANALYSES OF BOREHOLE CORES: TRACE ELEMENTS, Ti, Fe, Mn and Ca

Sample No	Borehole depth From	To	Cu	Pb	Zn	Fe	As	Mo	Ni	Mn	Ti	Ba	Rb	Sr	Zr	Ca	Th	W	Nb	Y	Ce
Borehole 1																					
6	15.84	17.07	123	265	116	50390	7	3	19	1020	2820	339	61	85	93	2040	<4	<3	4	11	<21
7	17.07	20.12	153	138	104	48130	9	<2	17	930	2880	432	69	108	96	2550	<4	3	4	11	<21
8	20.12	23.16	168	<13	91	49200	12	<2	17	810	2860	496	55	172	99	4670	<4	<3	6	12	<21
9	23.16	26.21	309	15	72	49740	18	<2	15	850	2790	579	46	202	96	4840	<4	<3	5	10	<21
10	26.21	27.13	211	<13	61	50880	33	<2	14	740	2710	544	65	160	90	3190	<4	<3	4	9	<21
11	27.13	27.79	60	<13	64	48640	77	2	16	770	2750	560	60	202	96	4320	<4	3	4	11	<21
12	27.79	29.26	91	<13	68	49900	92	<2	16	850	2720	499	65	135	90	2480	<4	<3	5	10	<21
13	29.26	32.31	82	<13	118	69170	58	<2	12	1600	3850	548	76	137	87	2720	<4	<3	5	15	<21
14	32.31	35.36	18	<13	111	63740	24	<2	10	1320	3650	451	64	193	88	4130	<4	<3	3	16	<21
15	35.36	38.40	53	<13	75	56140	33	<2	15	1040	2640	433	70	158	90	3160	<4	<3	4	11	<21
16	38.40	41.45	81	<13	72	55320	<2	<2	15	920	2760	399	52	158	90	3440	4	4	4	11	<21
17	41.45	44.50	36	<13	63	53500	<2	<2	14	910	2630	281	38	155	82	4380	<4	<3	5	11	<21
18	44.50	45.72	49	23	67	51780	<2	4	15	790	2690	445	46	153	86	3600	<4	3	4	12	<21
Borehole 2																					
19	3.35	5.49	322	71	104	61680	3	6	17	1080	3550	648	62	69	88	1980	<4	5	5	13	<21
20	5.49	8.53	335	41	96	68610	<2	<2	17	780	3990	578	72	65	92	2000	<4	<3	7	15	<21
21	8.53	9.19	716	61	76	114850	<2	18	7	560	3110	953	101	99	89	3660	4	3	3	10	<21
22	9.19	11.58	197	67	49	54280	<2	<2	<5	710	1860	696	49	448	65	19910	<4	<3	4	9	<21
23	11.58	14.63	150	72	58	53530	<2	2	7	620	2740	858	39	312	96	11150	<4	<3	5	14	<21
24	14.63	17.68	120	65	54	48540	<2	<2	<5	530	2570	583	26	293	90	15490	<4	4	5	13	<21
25	17.68	19.75	330	54	57	43090	<2	4	<5	510	2570	1841	30	416	90	18870	<4	3	4	14	<21
26	19.75	20.73	173	<13	81	79340	<2	<2	17	1520	4360	410	32	300	59	39830	<4	<3	4	16	<21
27	20.73	22.60	252	<13	78	80990	<2	2	26	1510	4580	419	37	364	58	33780	<4	<3	3	16	<21
28	22.60	23.77	781	<13	78	72470	<2	91	19	1310	4170	383	28	295	57	39940	<4	<3	4	15	<21
29	23.77	25.25	239	<13	81	80650	2	3	20	1390	4370	456	25	289	58	40100	<4	<3	4	15	<21
30	25.25	26.82	696	<13	93	137690	<2	6	20	2300	4090	499	43	89	46	21200	<4	<3	<2	10	<21
31	26.82	27.80	158	<13	90	78590	<2	2	19	1480	4540	902	47	317	64	33760	<4	3	<2	17	<21
32	27.80	29.56	56	<13	89	67110	<2	2	16	2440	3710	320	56	42	52	63670	<4	3	<2	18	<21
33	29.56	30.18	1388	<13	92	77430	<2	<2	18	1350	4550	258	49	45	55	7410	<4	<3	<2	7	<21
34	30.18	30.46	3515	<13	56	62400	2	6	36	1810	3080	67	38	32	42	37950	<4	<3	3	12	<21
35	30.46	32.92	690	<13	86	86590	<2	4	20	1910	4630	973	48	160	60	25540	<4	<3	4	15	<21
Borehole 3A																					
36	23.77	24.07	73	<13	196	63090	3	<2	39	920	4080	405	34	379	76	30070	<4	5	4	16	<21
37	26.37	26.83	152	<13	69	72890	<2	<2	39	980	4530	287	29	393	78	20300	<4	<3	3	17	<21
Borehole 4																					
38	11.58	16.13	257	<13	174	79340	<2	<2	28	1230	4700	371	30	300	78	16310	<4	<3	4	15	<21
39	16.13	17.68	171	<13	95	70220	<2	<2	25	1380	3970	309	23	464	79	26810	<4	6	3	15	<21
40	17.68	20.73	419	<13	148	74210	<2	3	23	1150	4050	315	21	265	76	19270	<4	<3	5	14	<21
41	20.73	22.00	366	<13	86	81230	<2	4	21	1290	4390	221	14	248	86	7940	<4	3	4	16	<21
42	22.00	23.78	302	<13	117	81710	<2	5	22	1430	3550	231	10	261	75	36870	<4	3	4	14	<21
43	23.78	25.20	872	<13	84	93980	<2	3	24	1430	3630	866	22	264	77	23830	<4	4	4	11	<21
44	25.20	26.82	294	<13	88	66260	<2	11	22	1410	3310	264	18	410	65	34210	<4	<3	3	14	<21
45	26.82	29.87	260	<13	95	75260	<2	6	29	1510	4160	958	32	274	63	36740	<4	4	3	17	<21
46	29.87	32.92	127	<13	106	72790	<2	5	28	1530	4150	562	33	356	56	40530	<4	3	4	16	<21
47	32.92	35.97	122	<13	72	60340	<2	2	18	1000	3580	580	33	402	65	35310	<4	3	5	15	<21
48	35.97	38.02	316	<13	105	70550	<2	5	11	1430	3450	536	50	267	69	20990	<4	4	<2	13	<21
Borehole 5																					
49	20.81	21.81	337	376	84	59680	<2	4	8	1000	2860	565	32	458	87	18600	<4	<3	4	14	<21
50	21.81	23.36	566	31	110	86920	<2	3	23	1370	5680	278	25	175	74	8850	<4	<3	6	18	<21
51	23.36	26.82	269	55	92	61030	<2	<2	7	1070	3090	358	26	435	89	19670	<4	3	4	15	<21
52	26.82	29.87	269	31	76	55240	<2	2	6	1080	2880	353	31	427	87	25350	<4	5	4	15	<21
53	29.87	32.92	304	<13	90	60180	<2	8	6	1000	2840	292	31	367	81	21090	<4	4	4	13	<21
54	32.92	35.98	353	<13	105	58640	<2	5	7	1020	2980	320	29	303	84	21190	<4	<3	4	14	<21
55	35.98	37.98	238	<13	79	50060	<2	3	6	910	2680	229	25	362	82	32250	<4	<3	6	13	<21
56	37.98	39.01	249	<13	88	54290	<2	3	5	990	2690	424	53	279	86	17170	<4	<3	4	14	<21
57	39.01	42.14	214	<13	82	51500	<2	4	5	1060	2700	339	36	289	81	25120	<4	5	3	14	<21
58	42.14	45.12	131	<13	120	66250	<2	3	9	1810	3330	176	42	37	88	15490	<4	<3	5	20	<21

Sample No	Borehole depth From	To	Cu	Pb	Zn	Fe	As	Mo	Ni	Mn	Ti	Ba	Rb	Sr	Zr	Ca	Th	W	Nb	Y	Ce
Borehole 6																					
59	29.87	32.91	181	<13	37	54770	<2	<2	5	520	2620	259	29	448	91	18980	<4	<3	4	14	<21
60	32.91	34.10	86	<13	40	52720	<2	<2	5	480	2610	296	39	399	93	16060	<4	<3	3	13	<21
Borehole 7																					
61	11.58	14.63	312	<13	77	92440	<2	6	26	880	4720	317	51	165	90	5920	4	<3	3	17	<21
62	14.63	17.67	215	<13	51	79460	<2	6	22	850	4250	272	34	539	102	21550	4	<3	<2	15	35
63	17.67	19.10	281	<13	48	72530	<2	52	20	810	4280	308	50	451	102	20090	<4	<3	4	17	23
64	19.10	22.15	303	<13	50	66210	<2	20	22	1060	3750	409	55	351	84	34010	5	5	3	16	29
65	22.15	24.94	151	<13	50	67860	<2	20	24	910	4040	258	24	556	95	27360	4	3	6	16	27
66	24.94	26.83	153	<13	72	73780	<2	3	41	1210	4370	288	26	554	96	30950	<4	3	<2	18	22
67	26.83	29.88	120	<13	60	71900	<2	69	40	1110	4250	347	29	579	83	31470	5	3	6	16	26
Borehole 8																					
71	17.81	20.42	54	<13	79	67610	7	2	33	1900	6540	304	135	75	242	6450	9	8	15	32	74
72	20.42	23.47	64	<13	76	70210	2	<2	31	1660	6360	425	109	111	254	6430	9	4	17	25	53
73	23.47	26.52	31	<13	68	66180	<2	<2	33	1210	6520	610	147	65	256	3640	13	<3	14	31	52
74	26.52	29.57	21	<13	62	66360	<2	3	29	1170	5790	558	146	72	222	8680	11	<3	15	25	51
75	29.57	32.61	33	<13	66	62810	2	<2	34	1220	6570	527	135	82	241	7890	12	8	16	32	68
76	32.61	35.66	38	<13	67	71460	3	2	30	1240	6110	437	113	76	232	4580	10	8	15	26	56
77	35.66	36.55	42	<13	45	59410	2	<2	35	790	6510	486	119	158	222	7540	10	3	14	25	54
78	36.55	38.53	58	<13	77	102830	<2	<2	9	1450	4400	179	40	249	93	8950	<4	6	6	20	26
79	38.53	41.76	36	<13	67	68990	<2	<2	31	1100	6420	497	133	75	245	3750	13	<3	15	28	42
80	41.76	45.34	29	<13	67	64570	2	<2	31	1130	6550	551	126	83	235	4680	11	5	14	23	43
81	45.34	46.44	194	<13	56	62710	<2	<2	12	1100	3720	337	35	212	89	15140	<4	3	5	18	30
82	46.44	49.37	67	<13	39	57050	2	4	29	920	6240	530	94	121	237	13430	9	7	14	26	59
83	49.37	49.47	80	<13	54	84980	<2	11	27	1120	5530	318	48	281	219	33140	8	7	13	33	70
84	49.47	53.00	55	<13	56	75090	5	<2	32	1220	6480	422	46	97	235	7450	7	3	14	28	65
85	53.00	55.79	37	<13	45	68080	<2	4	32	980	6510	461	114	83	234	4370	8	4	12	22	32
86	55.79	57.35	68	<13	34	67910	2	7	30	810	4740	481	88	75	182	8690	8	5	11	20	48
87	57.35	60.46	54	<13	48	73460	<2	2	36	1100	6520	515	121	125	245	9820	10	7	16	32	67
88	60.46	63.09	47	<13	65	74430	3	<2	30	1150	6200	357	91	93	224	6810	8	5	14	26	52
89	63.09	66.14	40	<13	58	63500	5	<2	25	1020	5630	500	110	100	280	6710	13	6	13	31	63
90	66.14	69.19	96	15	53	65880	<2	2	25	1040	5330	327	82	101	224	8880	8	4	11	27	47
91	69.19	72.24	54	<13	59	65380	7	<2	32	1110	5930	478	136	83	349	4110	13	6	18	39	65
92	72.24	75.29	66	<13	54	66830	<2	2	29	1080	6190	414	99	119	258	5990	10	5	16	29	59
93	75.29	78.33	79	<13	60	63570	5	3	29	1070	6220	453	114	108	279	7340	12	6	15	30	68
94	78.33	81.38	51	<13	55	59940	<2	<2	31	1050	6510	498	108	124	317	7590	12	9	17	38	73
95	81.38	85.03	53	<13	60	66240	<2	3	34	1220	6940	579	123	108	238	7290	9	7	17	27	64
96	85.03	86.53	58	<13	39	58010	<2	2	11	800	2870	354	70	193	99	14380	<4	3	4	13	<21
97	86.53	87.71	49	<13	57	64690	<2	<2	29	1100	6790	474	82	124	233	7560	10	9	15	26	36
98	87.71	90.54	55	<13	46	46030	<2	3	5	820	2520	357	47	223	91	18320	<4	<3	6	16	21
99	90.54	93.57	77	<13	38	42920	<2	2	<5	490	2410	429	54	281	89	18850	4	<3	4	14	<21
100	93.57	95.81	124	<13	37	44120	<2	2	<5	540	2330	373	40	273	89	19670	<4	4	6	14	22
101	95.81	99.00	56	<13	48	59150	<2	3	28	880	6190	532	149	71	225	6240	9	4	16	24	45
102	99.00	100.00	54	<13	49	86530	2	4	35	1040	5790	333	83	168	215	12170	11	9	14	26	52
103	100.00	102.20	63	<13	50	67620	<2	3	31	980	6240	418	117	145	240	8370	9	7	13	26	59
104	102.20	102.34	75	<13	47	97090	2	<2	29	1490	4780	319	108	189	168	40990	7	3	11	28	67
105	102.34	105.61	79	<13	44	61230	<2	2	28	740	6080	449	133	79	236	7370	10	5	13	25	51
106	105.61	106.20	794	<13	59	80770	<2	3	28	1200	5130	276	70	124	202	10520	7	5	10	30	52
107	106.20	108.81	222	<13	48	60190	2	3	30	980	6300	291	97	128	242	9690	10	9	15	26	62
108	108.81	111.86	154	45	45	58960	<2	2	30	970	5610	305	108	145	216	27510	9	3	13	22	49
109	108.95	111.66	97	<13	49	57820	<2	5	28	910	6360	281	91	146	247	11100	10	5	14	28	58
110	111.86	114.17	61	<13	49	69130	<2	<2	32	940	6190	384	119	104	239	7420	11	5	14	28	54
111	114.17	114.52	108	<13	48	122030	2	3	24	1460	3810	338	37	301	159	37070	7	<3	10	23	42
112	114.52	117.96	156	<13	32	44960	<2	3	9	450	2860	338	39	305	114	20540	4	4	5	15	21
113	117.96	121.01	144	<13	37	49120	<2	2	5	400	2480	342	34	320	91	19680	<4	<3	6	15	<21
114	121.01	124.05	75	<13	48	47540	<2	5	6	570	2580	360	43	283	93	15010	<4	<3	5	15	23

All analytical results in ppm
Borehole depths in metres

APPENDIX 7

ANALYSES OF BOREHOLE CORES: MAJOR ELEMENTS AND SULPHUR

Sample	BH	Depth (m) From	To	Total	SiO_2	Al_2O_3	TiO_2	Fe_2O_3*	MgO	CaO	Na_2O	K_2O	P_2O_5	S
11	1	27.13	27.79	96.81	64.17	16.77	0.38	5.52	2.72	0.85	3.96	2.00	0.12	0.32
12	1	27.79	29.26	96.90	65.00	16.11	0.37	5.93	2.68	0.51	3.13	2.80	0.13	0.24
15	1	35.36	38.40	96.25	63.55	16.35	0.36	6.52	2.84	0.66	3.36	2.48	0.12	0.01
16	1	38.40	41.45	96.95	63.35	16.62	0.37	6.32	2.85	0.69	3.84	2.67	0.13	0.11
17	1	41.45	44.50	96.78	64.01	16.29	0.35	5.77	2.67	0.83	5.10	1.46	0.12	0.18
18	1	44.50	45.72	97.09	65.04	15.86	0.36	5.94	2.76	0.71	4.63	1.54	0.12	0.13
24	2	14.63	17.68	96.62	61.03	17.11	0.37	5.33	2.00	3.00	6.43	0.93	0.16	0.26
25	2	17.68	19.75	96.19	60.56	17.33	0.38	4.85	2.21	3.68	5.54	1.35	0.15	0.14
26	2	19.75	20.73	94.45	50.52	15.82	0.68	9.78	5.18	7.45	3.30	1.27	0.13	0.32
27	2	20.73	22.60	95.93	52.19	16.44	0.72	9.61	5.56	6.40	3.42	1.44	0.13	0.02
28	2	22.60	23.77	94.28	51.93	15.15	0.65	8.75	4.92	7.41	3.45	1.24	0.11	0.67
29	2	23.77	25.25	93.50	49.00	15.86	0.66	10.05	5.05	7.29	4.07	1.04	0.13	0.35
30	2	25.25	26.82	95.56	45.95	14.70	0.58	17.75	6.24	4.00	1.37	2.13	0.11	2.73
31	2	26.82	27.80	95.54	51.79	17.08	0.70	9.22	5.20	6.42	2.89	2.10	0.13	0.01
32	2	27.80	29.56	89.72	42.79	14.69	0.56	9.17	4.86	12.00	0.39	4.94	0.10	0.22
33	2	29.56	30.18	95.73	55.18	16.47	0.66	9.69	5.27	1.57	1.30	4.86	0.11	0.62
42	4	22.00	23.78	94.74	50.50	15.21	0.54	10.07	4.07	6.67	5.31	0.41	0.12	1.84
43	4	23.78	25.20	96.68	51.77	15.21	0.55	11.45	3.98	4.57	4.95	0.84	0.13	3.23
44	4	25.20	26.82	95.07	56.33	14.94	0.50	7.63	4.06	6.31	4.42	0.68	0.13	0.07
45	4	26.82	29.87	93.73	49.86	16.19	0.62	8.69	5.45	6.67	4.78	1.30	0.13	0.04
46	4	29.87	32.92	95.04	51.13	16.13	0.65	8.75	5.18	7.38	4.09	1.26	0.13	0.34
47	4	32.92	35.97	95.10	54.81	16.69	0.55	7.02	3.98	6.16	4.23	1.39	0.15	0.12
48	4	35.97	38.02	95.80	55.19	17.09	0.49	8.43	3.96	4.05	3.67	1.76	0.15	1.01
49	5	20.81	21.81	97.47	60.36	17.33	0.44	6.74	2.52	3.53	4.92	1.33	0.16	0.14
50	5	21.81	23.36	95.01	52.76	17.99	0.83	10.21	5.42	1.62	5.09	0.92	0.16	0.01
51	5	23.36	26.82	96.53	59.34	17.05	0.47	6.84	2.88	3.71	4.65	1.22	0.16	0.21
52	5	26.82	29.87	96.68	58.67	16.84	0.44	6.64	2.83	4.79	4.43	1.30	0.16	0.58
53	5	29.87	32.92	96.16	58.65	16.35	0.43	7.06	3.04	4.11	4.28	1.34	0.14	0.76
54	5	32.92	35.98	95.22	58.09	16.67	0.44	6.60	3.17	3.85	4.69	1.35	0.15	0.21
55	5	35.98	37.98	94.73	57.49	16.00	0.41	5.93	2.65	6.03	4.28	1.40	0.14	0.40
56	5	37.98	39.01	95.26	59.73	16.39	0.39	6.40	2.80	3.34	4.00	1.71	0.14	0.36
57	5	39.01	42.14	94.58	58.80	15.79	0.39	5.92	2.74	4.69	4.37	1.51	0.13	0.24
58	5	42.14	45.11	94.18	50.26	17.25	0.45	8.59	5.01	3.11	2.32	5.96	0.15	1.08
62	7	14.63	17.67	97.60	55.80	17.44	0.65	9.99	3.98	4.20	3.11	1.54	0.21	0.68
63	7	17.67	19.10	95.69	55.46	17.55	0.65	8.92	4.14	3.85	2.44	2.09	0.20	0.39
64	7	19.10	22.15	94.98	51.89	16.40	0.57	8.42	4.39	6.66	2.50	2.03	0.20	1.92
65	7	22.15	24.94	95.90	55.04	16.77	0.61	8.23	4.24	5.00	4.01	0.88	0.21	0.91
66	7	24.94	26.83	95.73	52.80	16.92	0.68	8.88	5.18	5.60	3.65	0.94	0.20	0.88
67	7	26.83	29.88	95.96	55.22	15.81	0.67	8.49	5.32	5.84	2.81	1.17	0.19	0.44

* Total iron reported as Fe_2O_3

APPENDIX 8

ANALYSES OF STREAM SEDIMENT, PANNED CONCENTRATE AND WATER SAMPLES FROM THE SOLFACH CATCHMENT

Stream Sediments

No	East	North	Cu	Pb	Zn	Be	B	V	Cr	Mn	Fe	Co	Ni	Y	Zr	Ba	As
1	18648	22869	20	30	110	2.3	74.4	107	99	3110	36500	19	31	37	555	359	10
2	18690	22830	25	40	110	2.3	98.0	116	101	3319	38100	13	27	40	494	460	9
3	18535	22786	15	30	90	2.5	69.7	140	114	2392	38300	<10	26	35	259	659	<2
4	18476	22714	40	30	210	3.0	72.1	153	118	20546	67500	104	77	42	446	657	<2
5	18470	22911	15	40	120	2.2	65.2	125	116	2668	42600	11	29	34	550	434	15
6	18470	22782	15	20	90	1.3	51.9	96	285	2363	23500	<10	16	26	791	323	7
7	18426	22754	20	40	160	2.2	55.1	103	80	4453	38900	14	28	30	481	443	10
8	18429	22746	15	30	140	2.7	54.7	116	114	3334	44100	55	35	38	348	491	8
9	18525	22719	15	40	140	2.5	59.1	103	87	1971	41400	35	25	28	613	445	10
10	18348	22910	15	30	80	1.6	65.3	115	114	3453	38400	10	20	41	535	393	<2
11	18330	22838	15	40	150	2.1	77.8	115	119	2889	37200	<10	20	78	534	584	6
12	18365	22748	15	30	140	2.0	48.7	136	117	3638	48300	20	24	32	447	424	10
13	18299	22757	15	30	140	1.8	66.0	98	154	4390	32600	12	20	39	546	444	7
14	18306	22748	15	30	120	2.5	70.7	110	109	4389	46000	23	25	32	515	491	9
15	18211	22722	20	30	170	2.5	83.0	109	111	4955	39500	22	28	42	441	508	18
16	17994	22672	45	40	110	2.4	82.1	112	124	2623	49600	10	17	31	439	344	<2
17	18030	22660	15	60	140	2.6	65.5	119	105	4341	50400	17	28	36	443	577	10
18	18042	22606	15	30	130	5.0	79.1	92	123	4644	39700	19	21	30	394	744	8
19	18072	22544	20	40	160	6.7	89.6	141	121	6236	56800	27	27	40	293	880	11
20	18122	22800	10	20	70	4.1	128.9	85	158	4520	24600	15	22	51	502	457	7
21	18076	22794	15	30	130	5.1	101.4	136	180	18303	50900	28	38	38	495	640	14
22	18117	22690	15	30	120	5.1	74.5	95	119	3802	43400	16	29	26	397	676	10
23	18110	22692	20	40	190	5.6	76.6	121	191	11646	57600	16	26	40	596	622	12
24	18090	22467	25	30	150	6.1	87.4	126	175	5622	54200	21	25	36	310	755	9
26	18351	22554	25	30	80	6.0	88.1	154	207	2743	42700	14	26	42	292	625	10
27	18346	22500	25	20	70	7.8	102.3	118	234	867	38900	12	22	61	581	654	10
28	18320	22488	30	40	170	6.0	103.6	139	171	4117	60700	31	31	37	277	494	18
29	18296	22420	50	50	250	8.7	138.2	148	243	1392	65300	23	33	40	292	724	9
30	18288	22427	30	30	140	7.4	124.5	157	191	2403	69800	22	29	41	237	668	21
31	18345	22421	30	50	190	5.1	87.1	147	165	3018	61200	89	58	36	231	462	26
32	18029	22386	35	40	200	3.9	78.4	116	121	4671	52800	22	30	32	410	497	15
33	18217	22402	40	40	160	3.0	87.7	171	97	3280	52700	36	33	31	263	436	17
35	18176	22440	40	40	160	6.2	98.5	135	174	4576	55000	23	30	33	361	611	22
36	18148	22590	20	40	90	3.8	77.2	127	155	993	39900	<10	15	19	583	634	<2
39	18108	22433	30	30	210	5.7	82.7	123	143	5241	53100	35	34	33	307	569	20

All results in ppm

Panned Concentrates

No	Ce	Ba	Sn	Cu	Pb	Zn	Ca	Ni	Fe	Mn	Ti	Th	Mo	As
1	1335	113	513	7	74	28	3120	10	25020	740	5950	28	6	29
2	464	151	<9	7	18	37	3370	9	28750	960	8380	12	<2	19
3	906	50	36	15	<13	24	3510	6	22470	840	7920	17	5	27
4	1489	34	16	7	28	29	10540	13	36880	1410	8230	28	4	20
5	356	59	13	<6	<13	27	2290	7	19610	1080	5300	11	4	29
6	394	133	<9	<6	42	33	2580	7	28580	570	5310	12	<2	21
7	919	84	22	<6	13	31	5330	7	24880	1030	8690	20	5	27
8	361	144	10	<6	<13	56	2360	9	33010	540	5710	18	<2	19
9	1099	83	68	<6	19	58	5980	16	53130	900	9200	26	3	25
10	999	84	17	9	26	42	19040	13	47740	1890	17780	22	<2	18
11	608	109	28	<6	14	35	3630	8	24660	890	7640	17	4	23
12	682	93	41	<6	<13	34	3710	5	27700	600	4540	18	<2	20
13	212	126	14	<6	<13	35	2780	6	21480	720	5440	10	<2	24
14	1049	63	28	<6	<13	33	4450	11	28120	810	8090	22	2	19
15	251	107	16	<6	18	32	2400	6	22910	520	3080	8	2	28
16	630	95	689	214	5877	160	4200	85	127760	4820	40350	37	6	57
17	613	169	49	<6	14	49	3190	14	37050	1450	9950	13	<2	29
18	353	98	34	7	18	38	3020	8	31830	1450	15890	10	7	20
19	47	274	21	7	16	75	9730	12	46850	960	3650	5	<2	21
20	450	68	26	<6	<13	18	4540	6	22860	1330	17840	10	4	21
21	1453	34	58	<6	27	99	7090	23	98150	11880	121220	35	6	21
22	492	164	11	33	<13	41	2990	10	80570	890	9370	15	<2	20
23	705	68	101	<6	173	124	6420	26	111890	17180	161090	15	7	20
24	47	237	<9	<6	16	56	6900	8	32410	690	3140	2	<2	24
26	198	126	<9	6	<13	31	1890	9	31040	700	9190	10	5	27
27	206	114	12	<6	<13	18	1620	5	22700	560	8560	7	3	23
28	39	203	16	29	29	95	1880	18	62070	680	3830	6	5	28
29	26	174	9	10	<13	70	860	9	29740	180	2580	6	3	21
30	119	426	<9	26	23	75	1700	33	70050	510	6730	10	<2	32
31	58	274	<9	11	<13	85	940	21	41180	450	3810	5	5	19
32	32	211	11	31	67	93	2680	14	39850	1160	7190	3	6	32
33	224	251	18	42	98	88	2800	22	76650	1690	15600	10	3	41
35	1086	177	188	129	377	114	6560	44	131500	1910	25130	24	6	48
36	35	176	<9	7	<13	83	2490	11	32240	830	5170	5	<2	19
39	218	381	22	77	126	181	7230	27	77970	2400	23970	9	3	28

All results in ppm.

All results for Sb in panned concentrate <11 ppm except:

1 34 ppm
16 58 ppm

Streamwater

All results for Cu and Zn in water ≤ 0.02 ppm except:

24 Zn 0.06 ppm
27 Zn 0.37 ppm

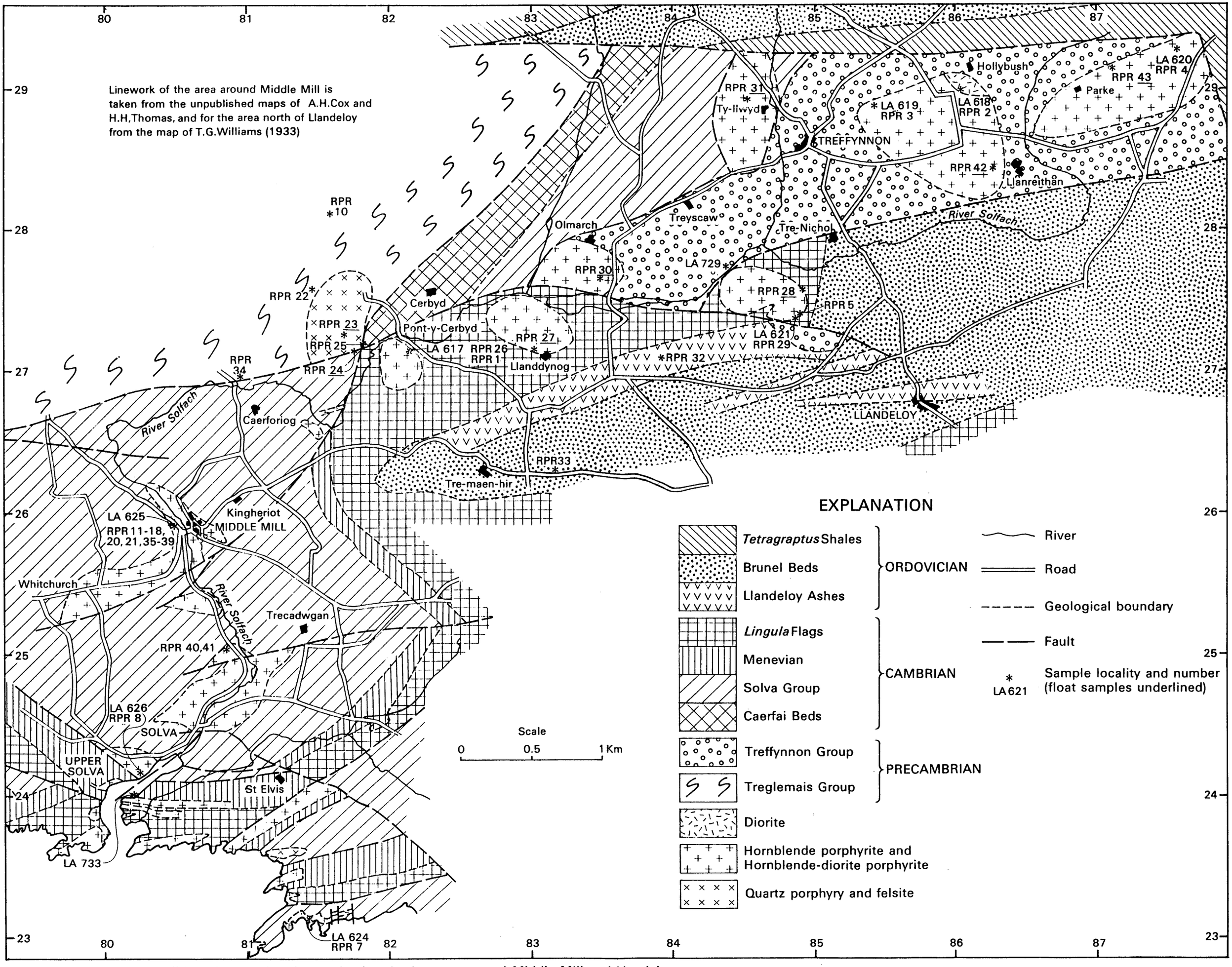

Fig.2. Map showing the solid geology and rock sample sites in the area around Middle Mill and Llandeloy.

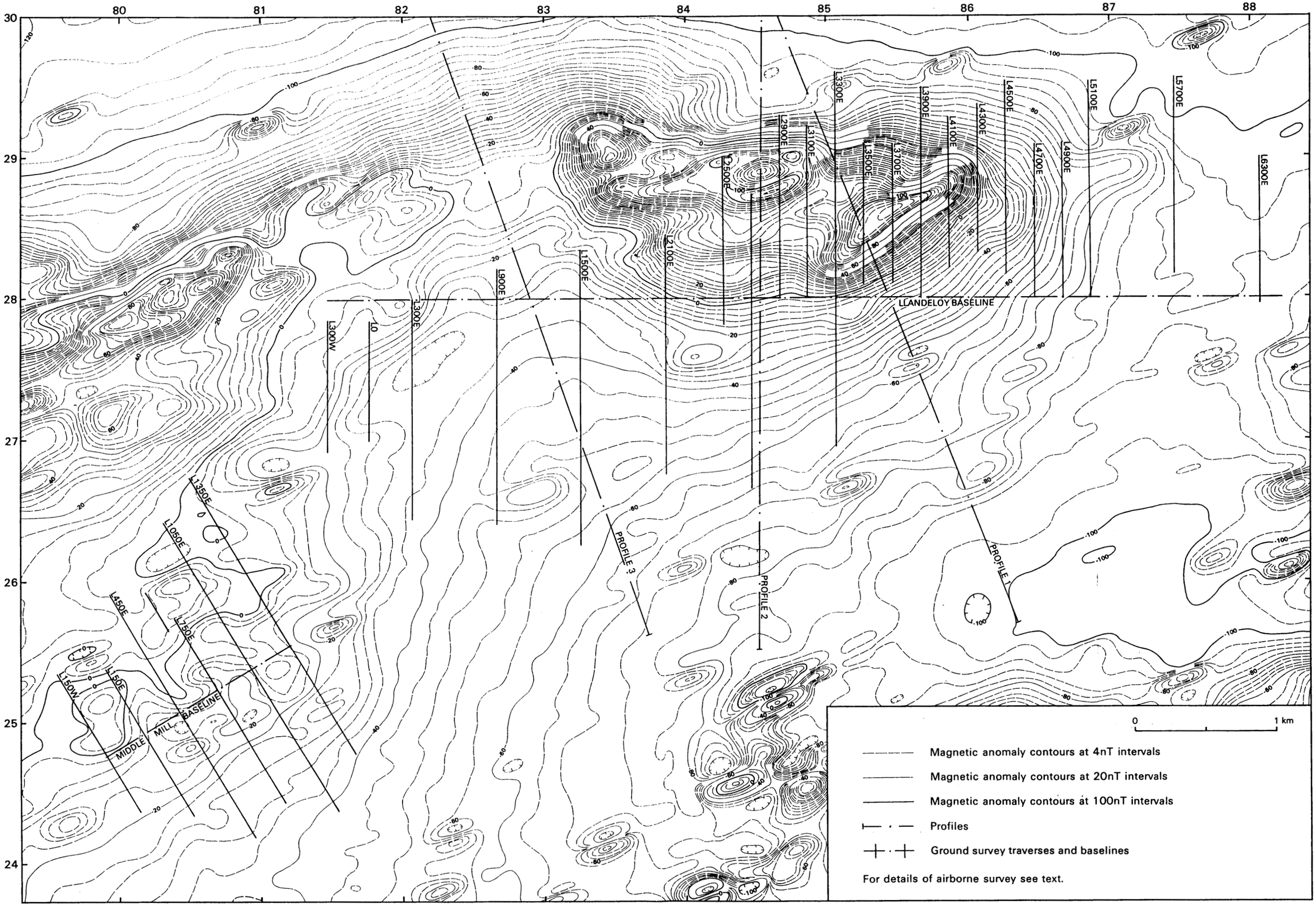

Fig.7 Aeromagnetic anomaly map of the Llandeloy-Middle Mill area.

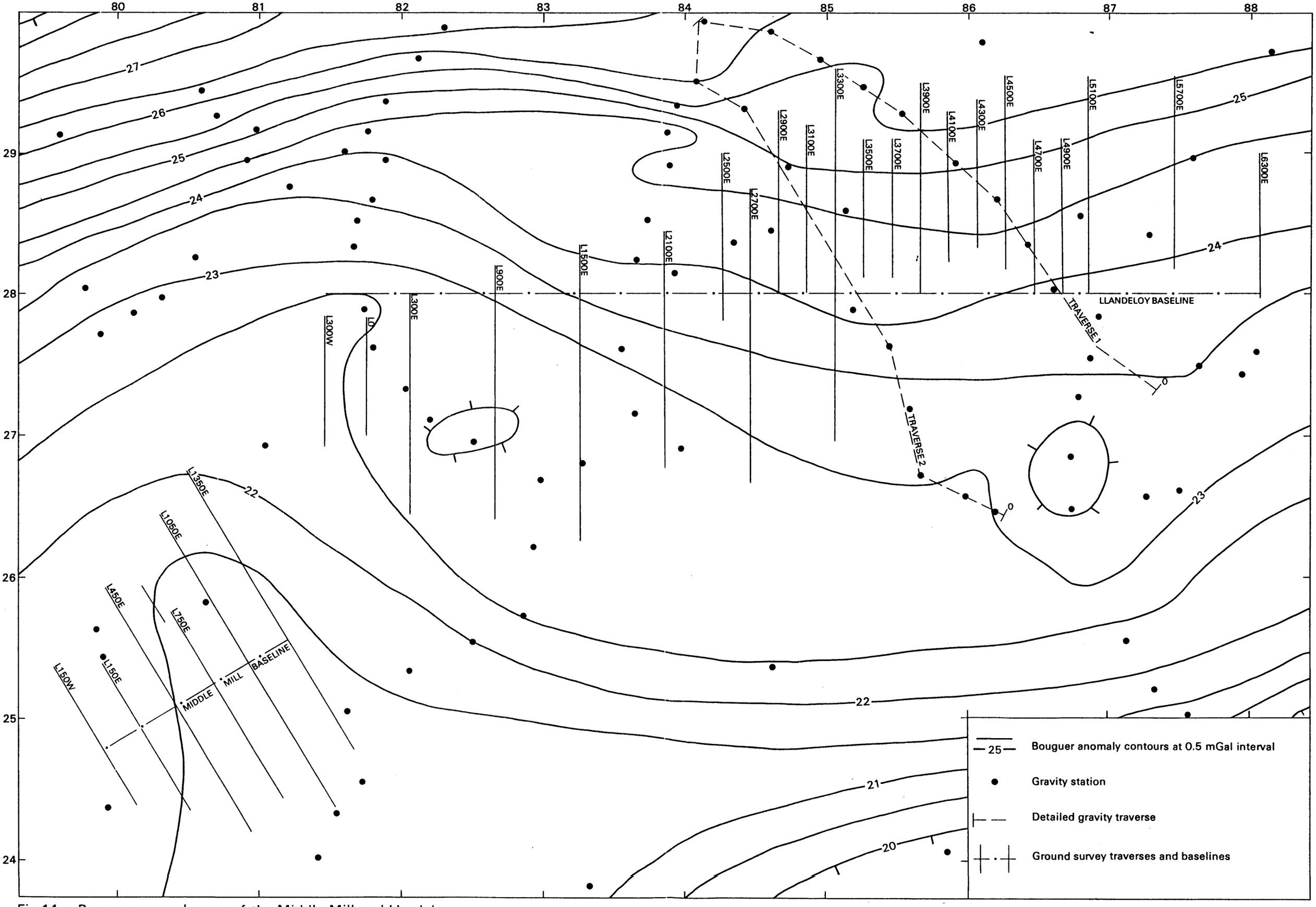

Fig.11. Bouguer anomaly map of the Middle Mill and Llandeloy areas.

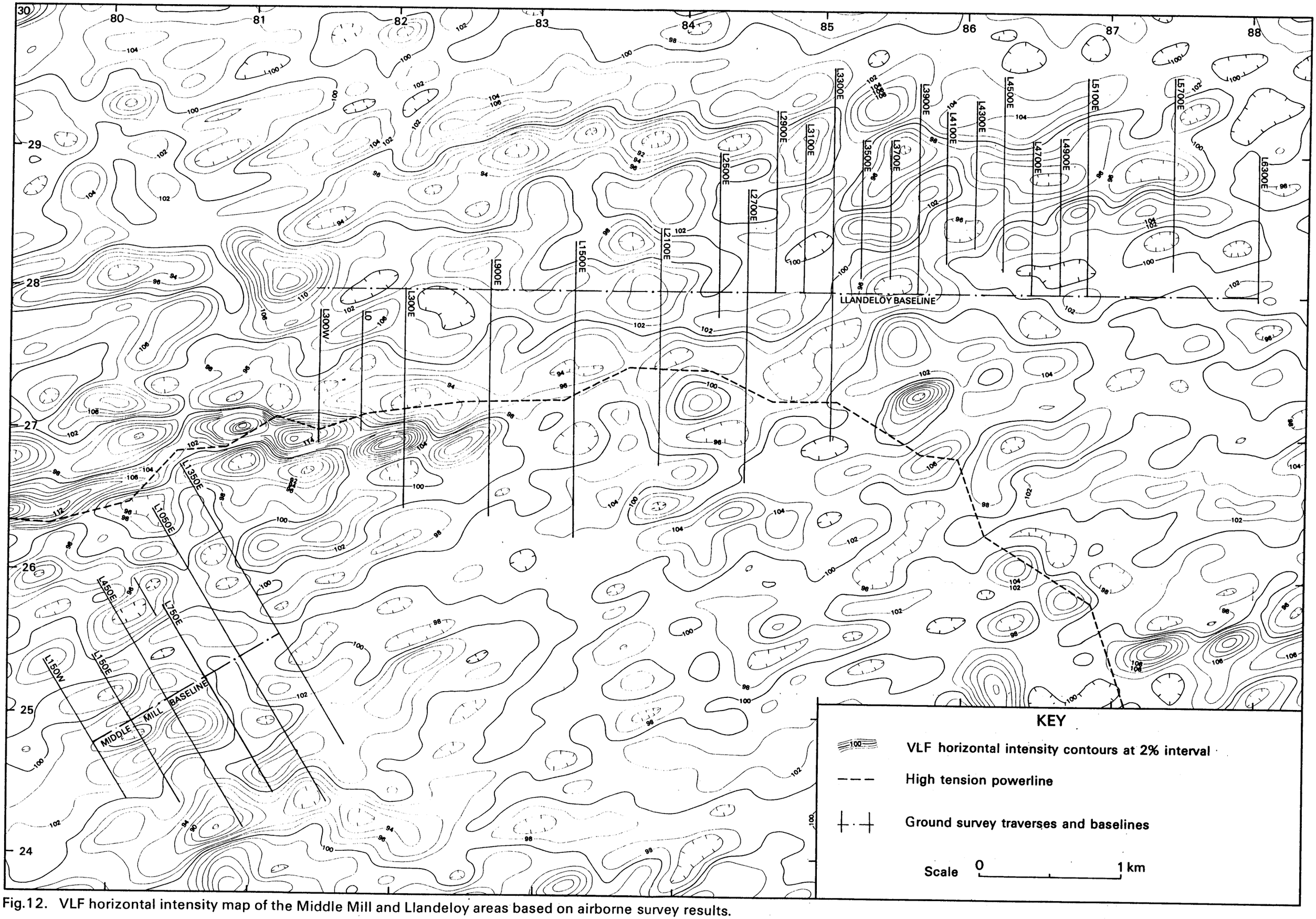

Fig.12. VLF horizontal intensity map of the Middle Mill and Llandeloy areas based on airborne survey results.

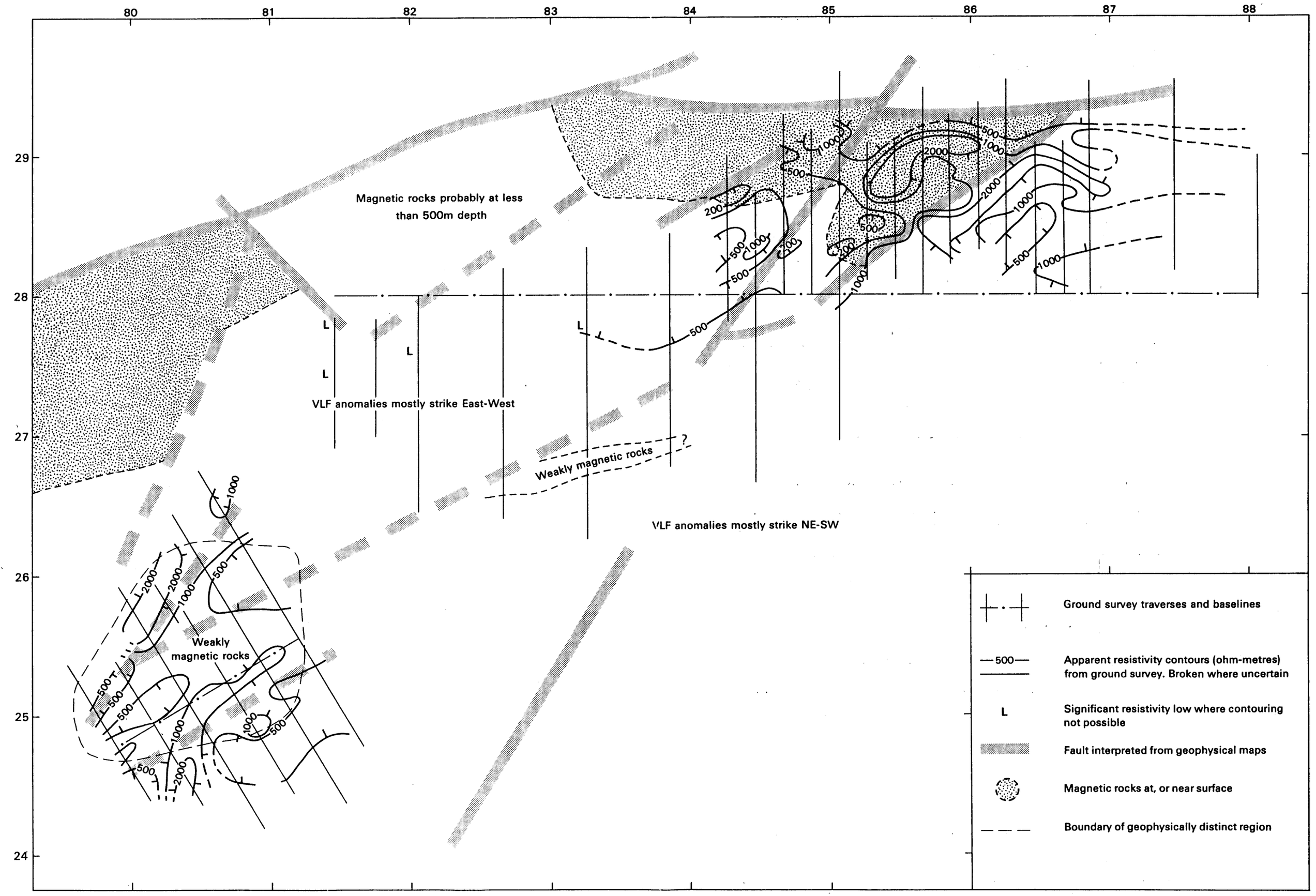

Fig.13. Compilation map of resistivity at Middle Mill and Llandeloy, showing summary of geophysical results.

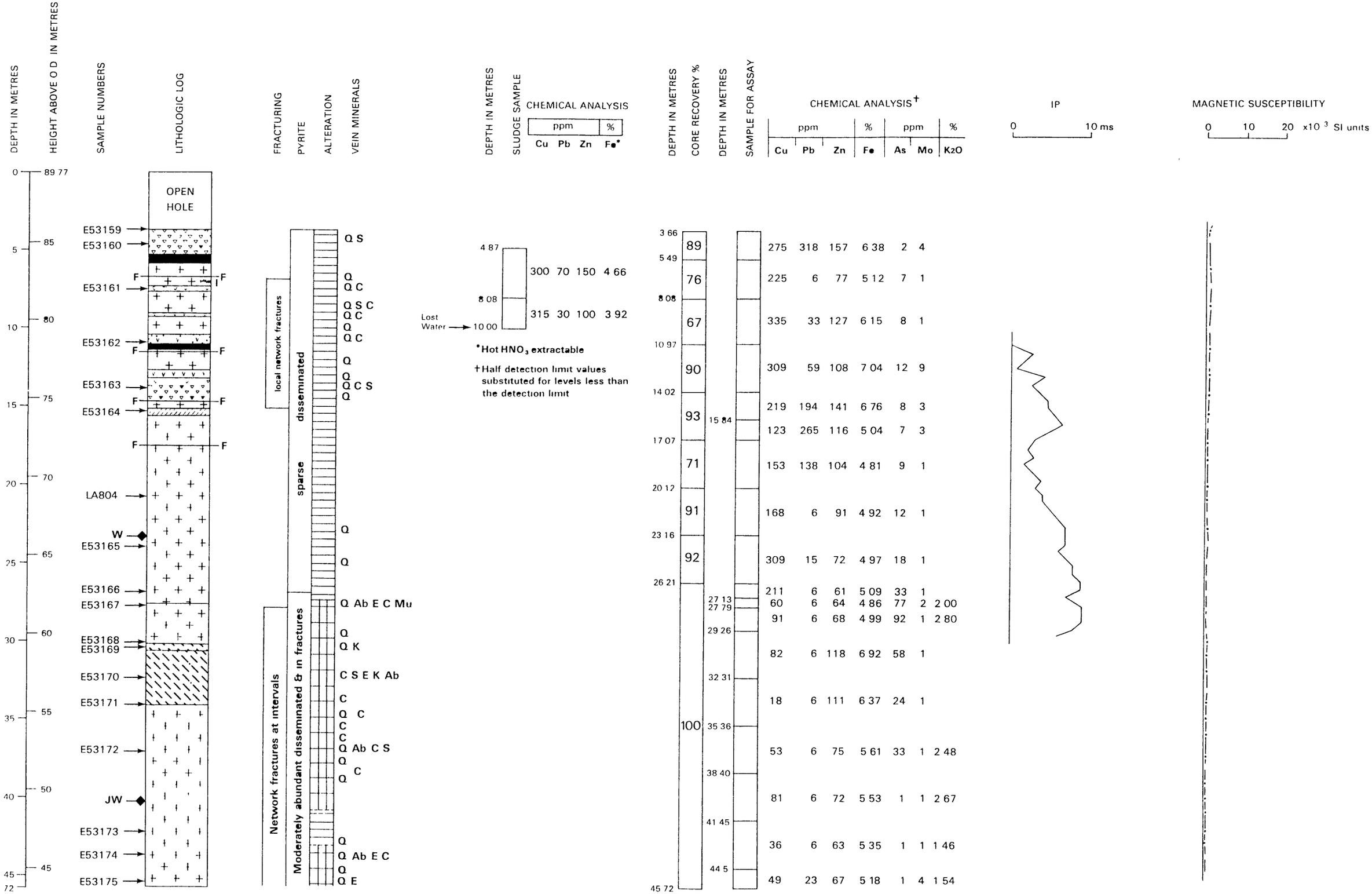

Quartz vein
Acid tuff
Volcanic breccia
Crystal tuff
Siltstone
Porphyritic microtonalite
Quartz-microdiorite
Porphyritic microdiorite
W — Base of weathered zone
F — Probable fault
I — Intrusion breccia vein
JW — Base of zone with weathering along joints

Q Quartz
C Chlorite
Ab Albite
S Sericite
Mu Muscovite
E Epidote
K K-feldspar

sericite-chlorite-biotite
Sericite-chlorite (rare clinozoisite)

Fig.20.

BOREHOLE 1

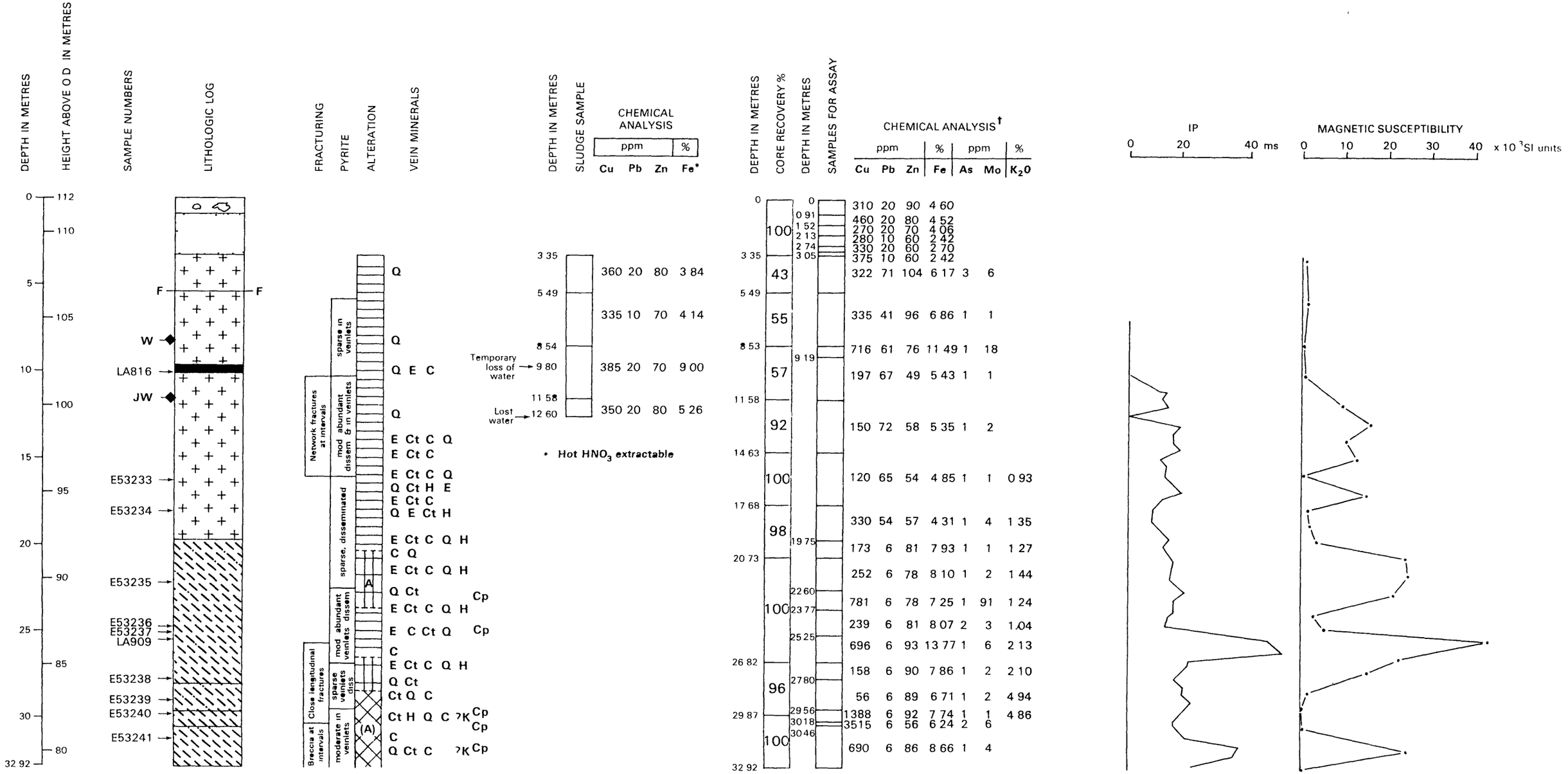

Fig.21

BOREHOLE 2

Drift deposits
Feldspar sand and clay
Quartz vein
Porphyritic microtonalite
Quartz microdiorite

W — *Base of weathered zone*
F — *Probable fault*
JW — *Base of zone of weathering along joints*

Q *Quartz*
E *Epidote*
C *Chlorite*
H *Hematite*
Ct *Carbonate*
Cp *Chalcopyrite*
K *K-feldspar*

sericite-chlorite-biotite with rare minor epidote
sericite-chlorite
sericite-chlorite-magnetite with biotite in places

A *fresh amphibole*
(A) *relict amphibole*

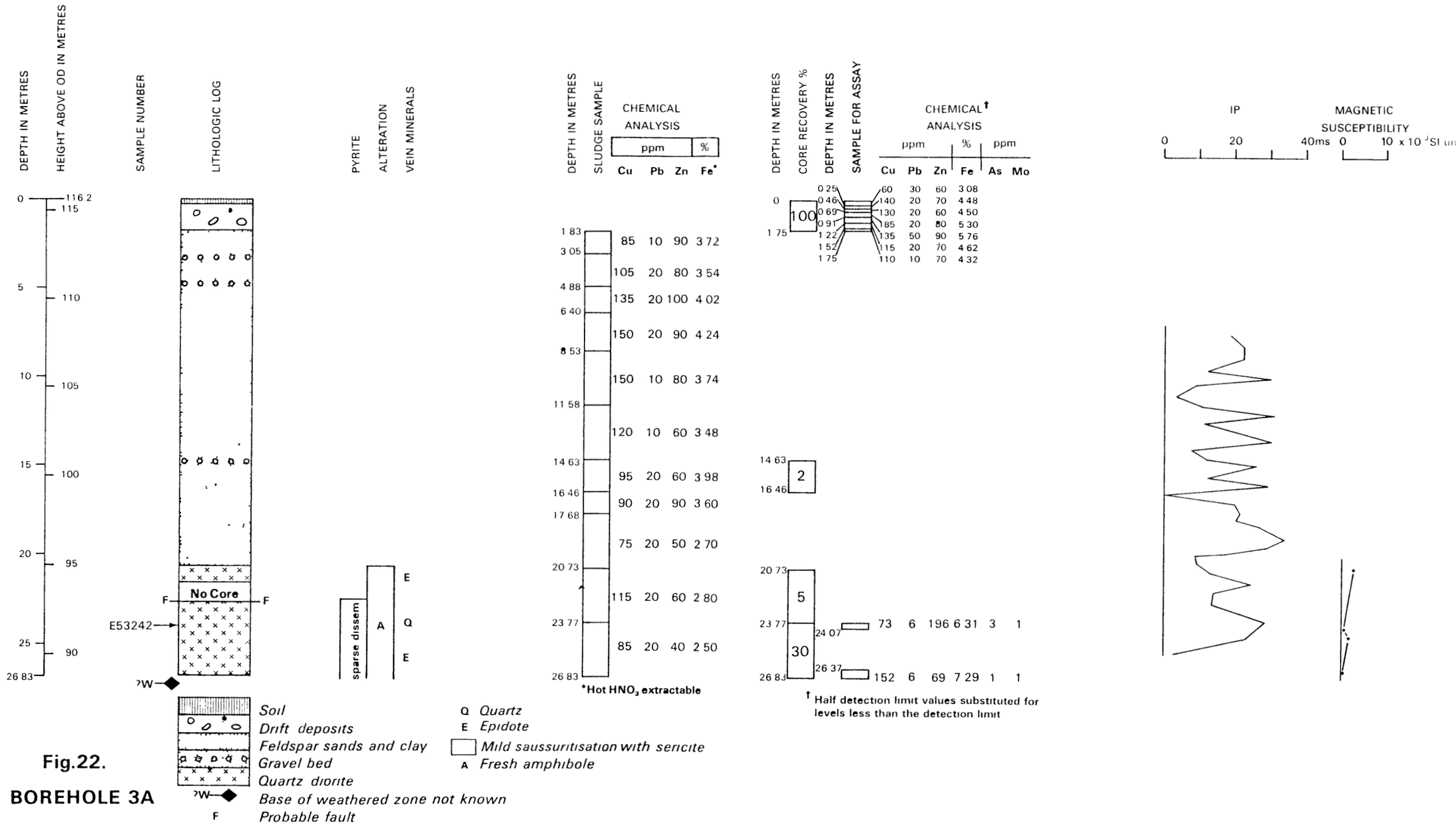

Fig.22.

BOREHOLE 3A

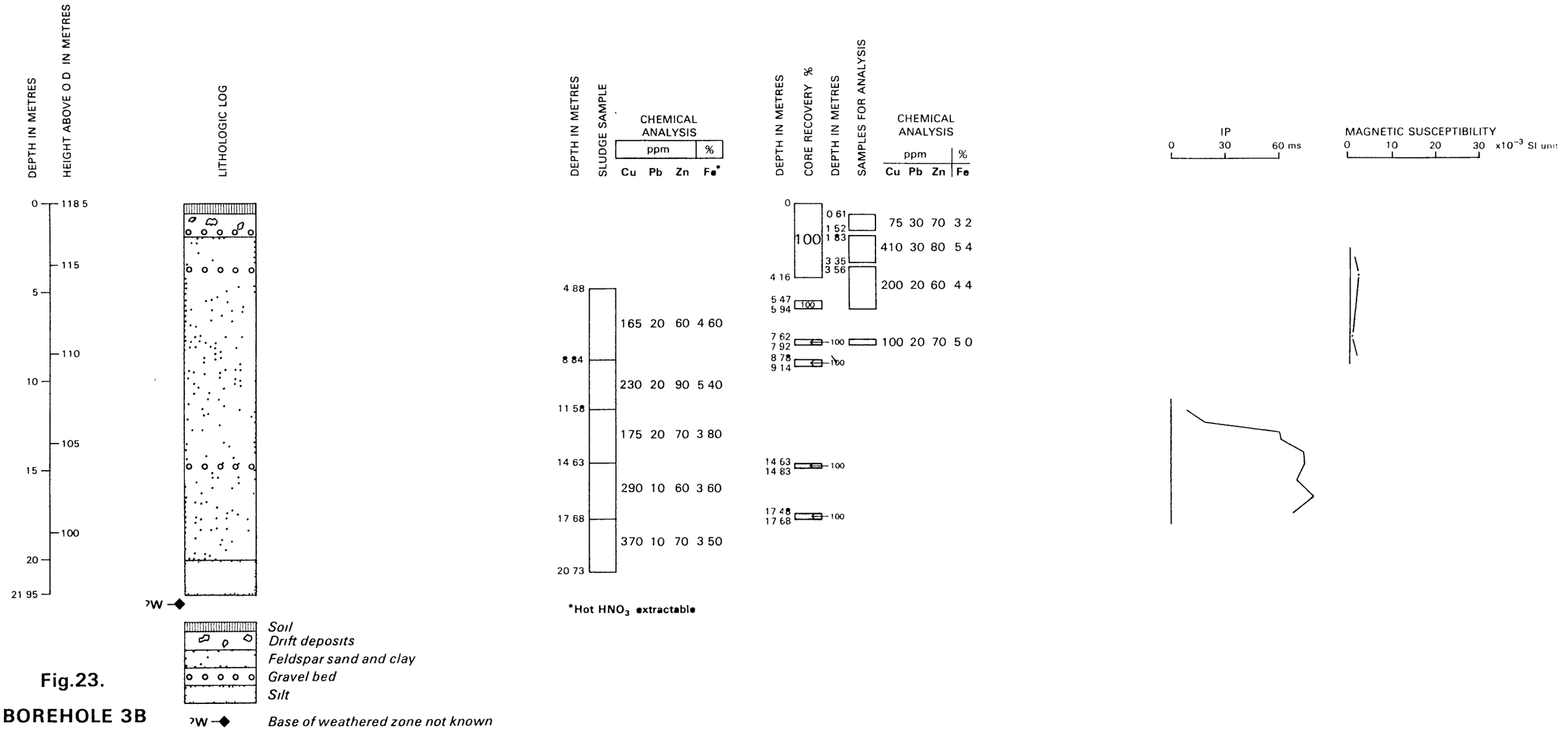

Fig.23.

BOREHOLE 3B

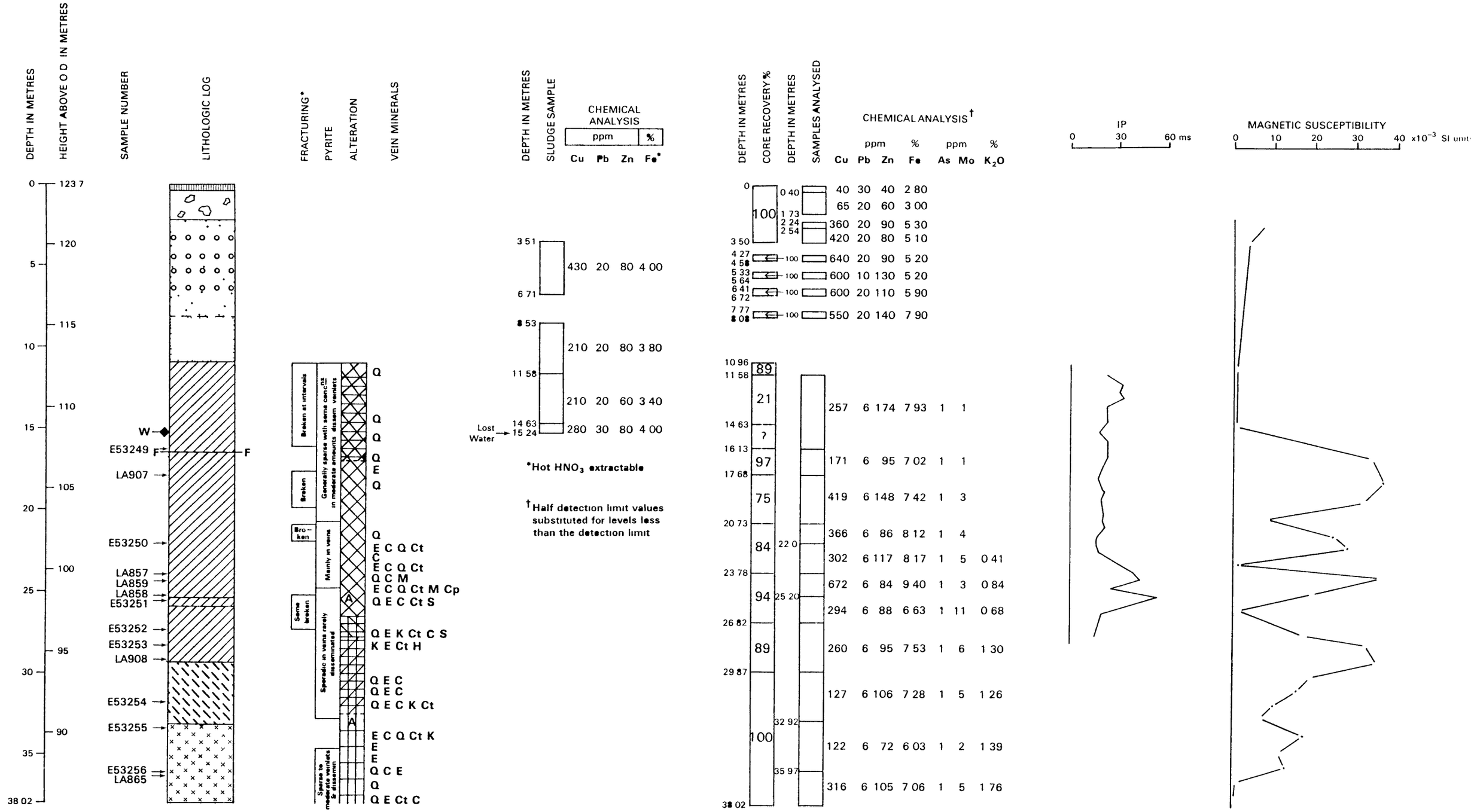

Soil
Drift deposits
Feldspar sand and clay
Gravel bed
Silt
Microdiorite
Porphyritic microdiorite
Quartz diorite

W—◆ Base of weathered zone

F Probable fault

Q Quartz
C Chlorite
Ct Carbonate
E Epidote
K K-feldspar
S Sericite
H Hematite
M Magnetite
Cp Chalcopyrite

Sericite–chlorite–amphibole

Sericite–chlorite–magnetite

Sericite–chlorite–biotite–K-feldspar

Sericite–chlorite–magnetite–amphibole–K-feldspar

Sericite–chlorite with rare epidote

A Fresh amphibole

*FRACTURING–Broken core may conceal lengths of network or other fracturing

Fig.24.

BOREHOLE 4

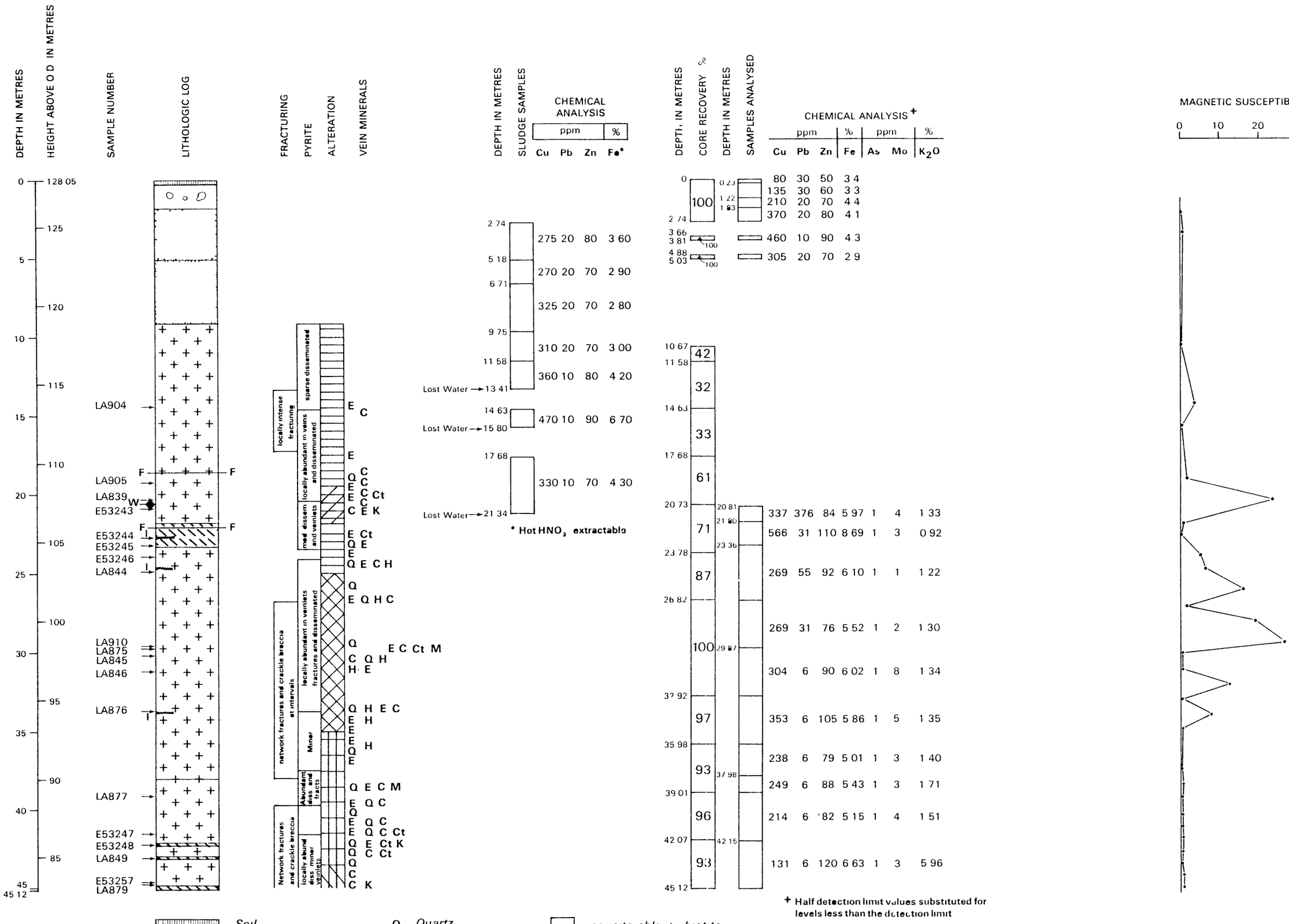

Soil
Drift deposits
Feldspar sand and clay
Silt and sand
Tonalite
Porphyritic microdiorite
Base of weathered zone
Probable fault
Intrusion breccia vein

Q Quartz
E Epidote
C Chlorite
Ct Carbonate
K K- feldspar
H Hematite
M Magnetite

sericite-chlorite-biotite with some epidote
sericite-chlorite-magnetite amphibole-K feldspar-epidote
sericite-chlorite-magnetite
sericite-chlorite
sericite-chlorite-K feldspar

Fig.25
BOREHOLE 5

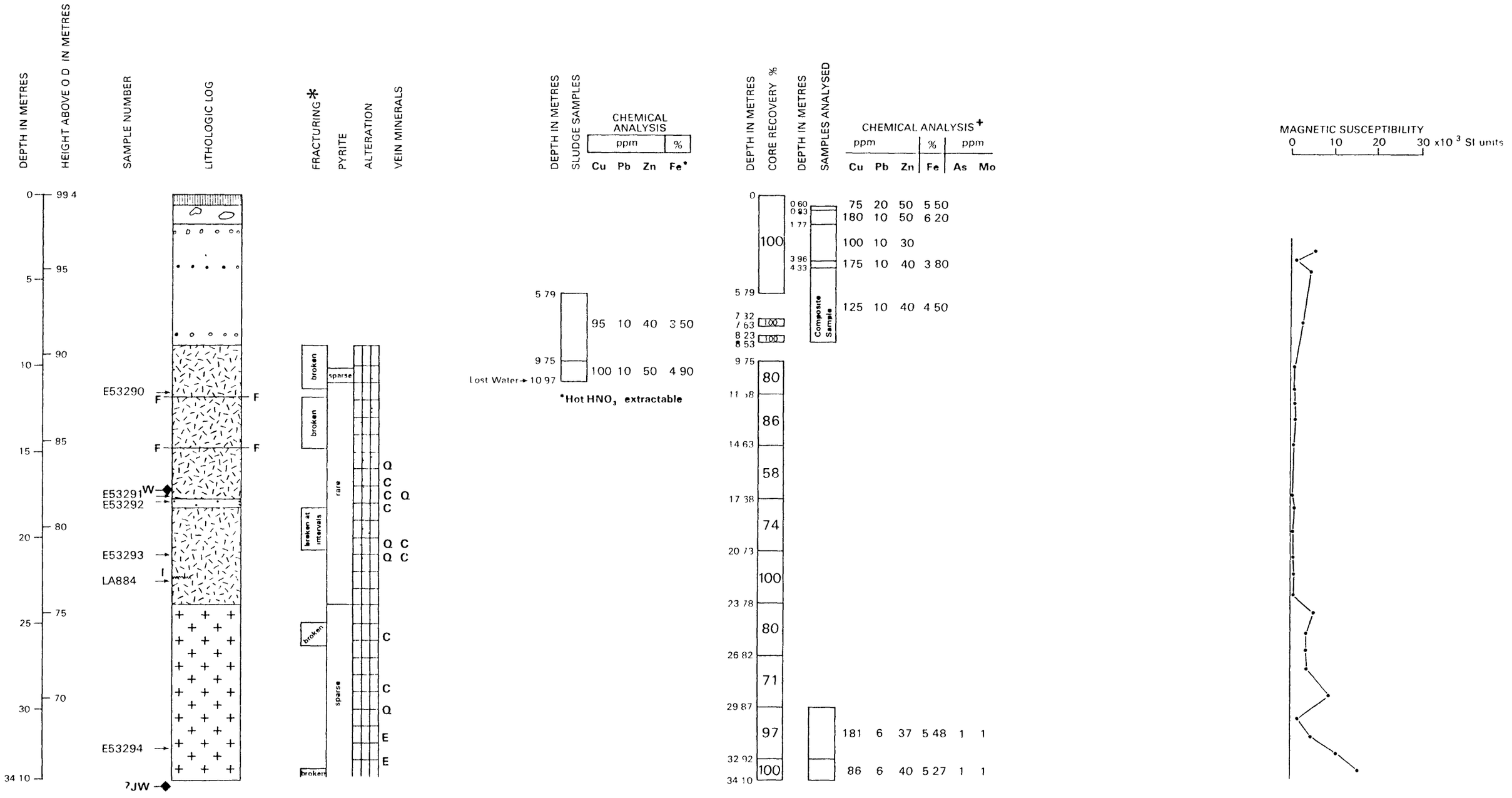

+ Half detection limit values subsituted for levels less than the detection limit

Fig.26.

BOREHOLE 6

* FRACTURING In this borehole badly broken core may conceal lenghts of network or other fracturing

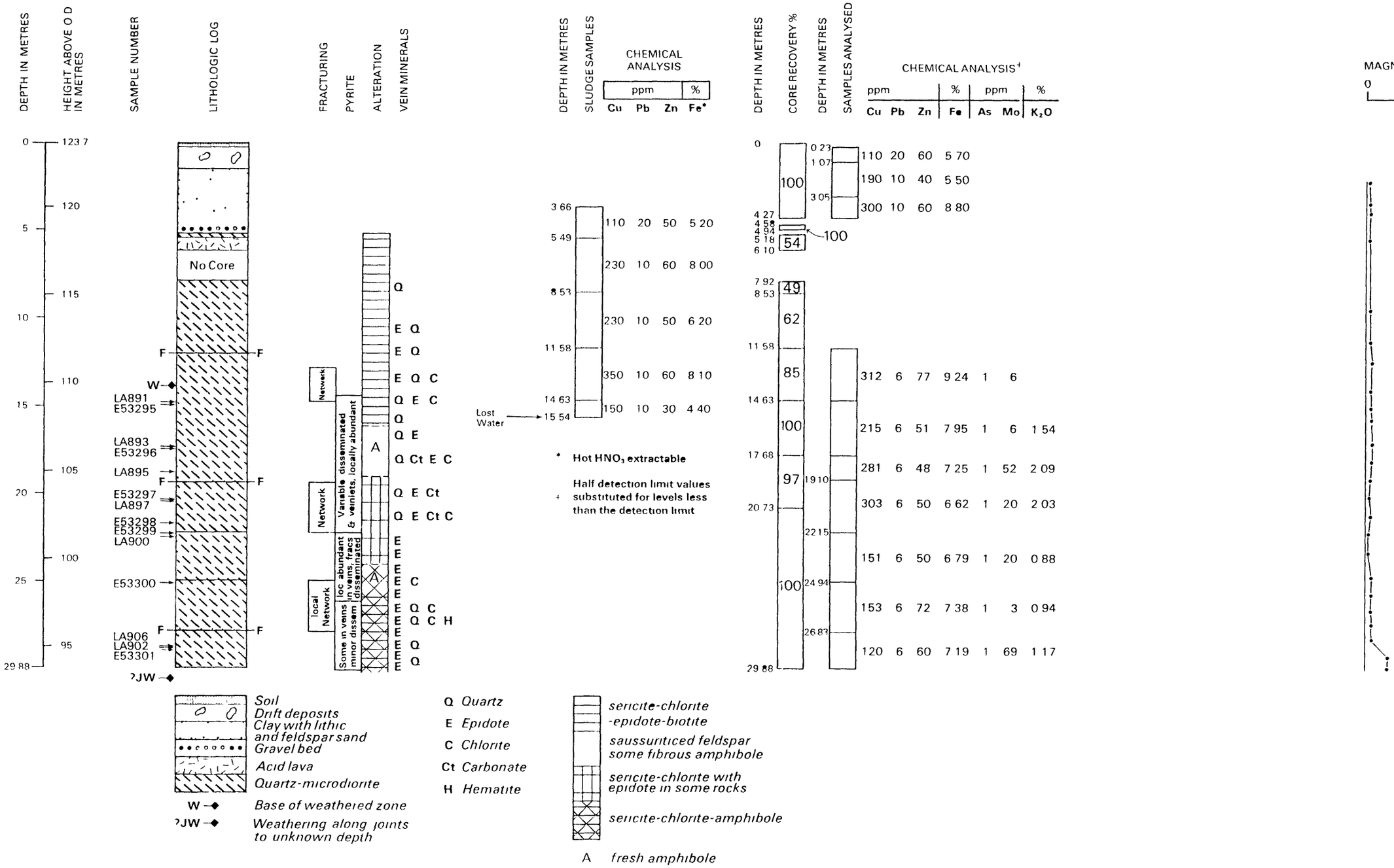

Fig.27

BOREHOLE 7

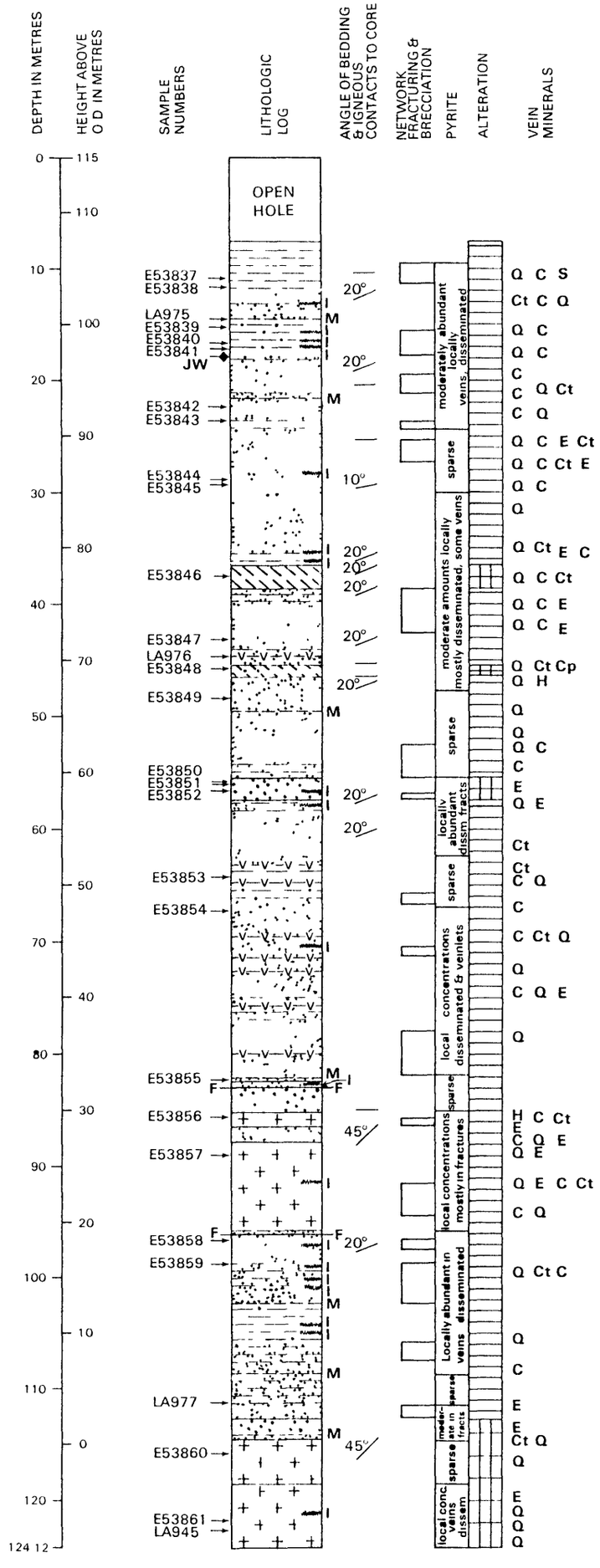

* Hot HNO_3 extractable

\+ Half detection limit values substituted for levels less than the detection limit

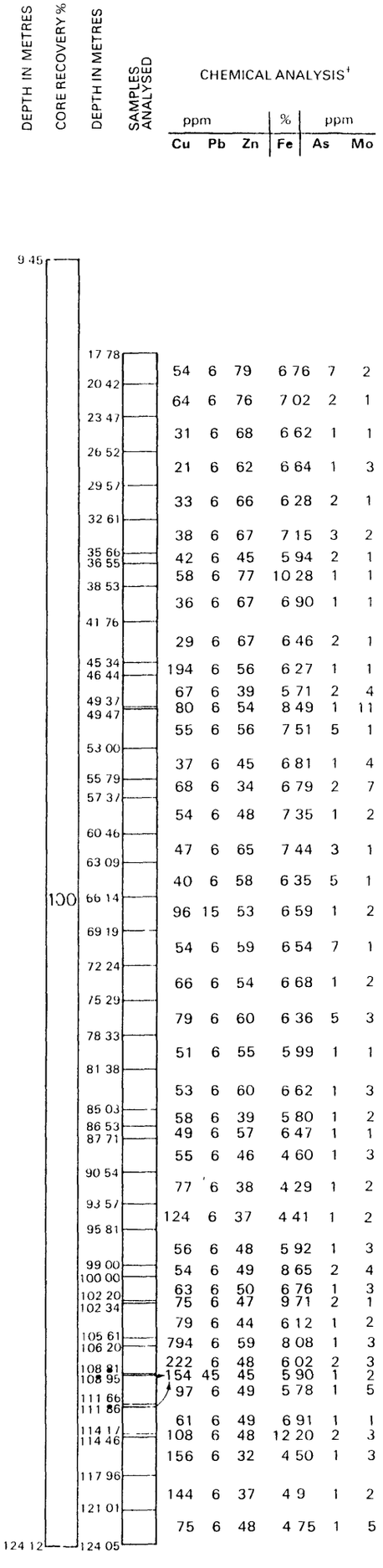

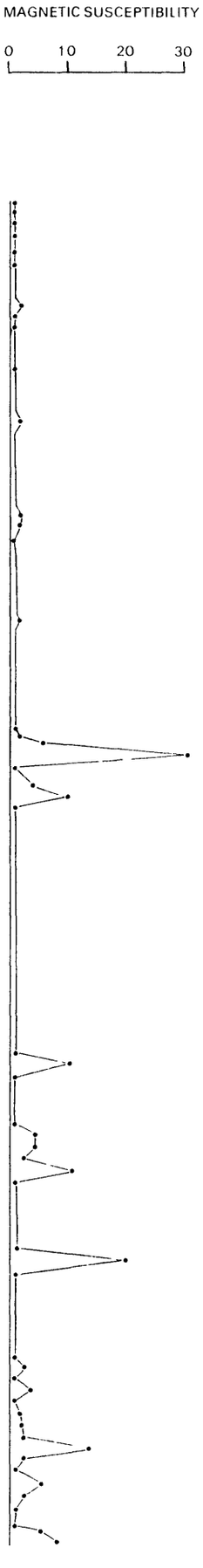

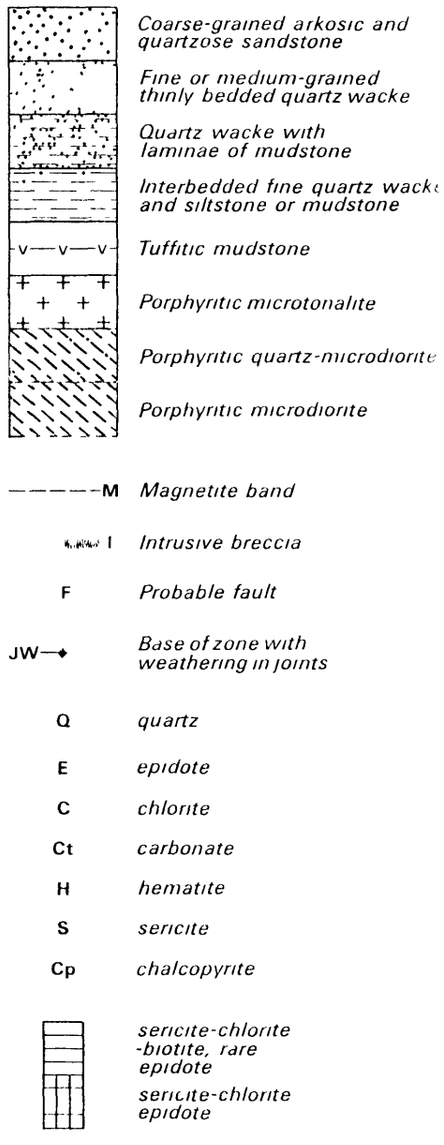

Fig.28.

BOREHOLE 8

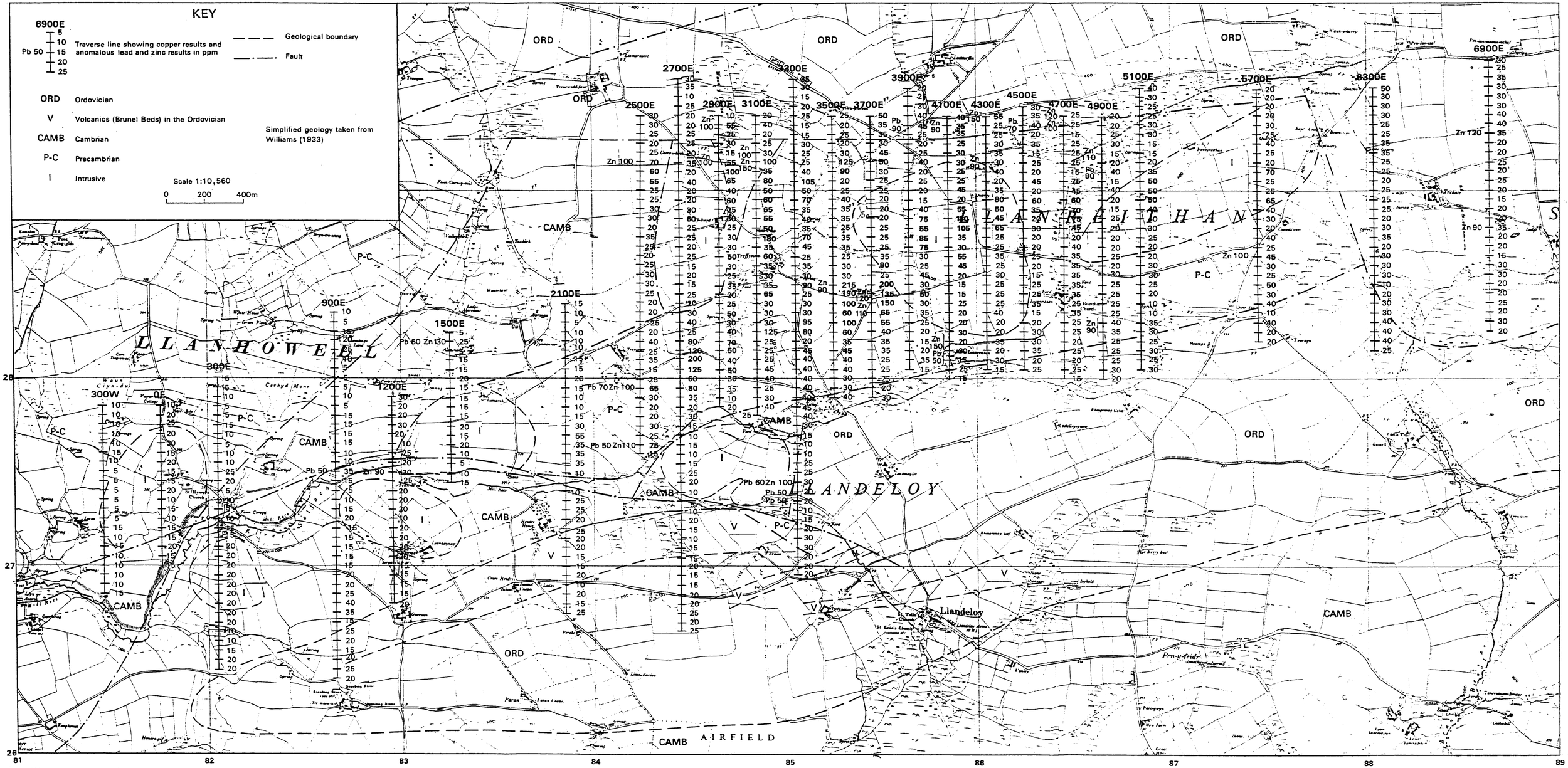

Fig.30. : Location of copper, lead and zinc anomalies in soil samples collected around Llandeloy.